Exploring expression of neurodevelopmental susceptibility genes in the foetal human thalamus and other related structures

Maznah Alhesain

180587230

Thesis submitted for the degree of Doctor of Philosophy at Newcastle University

08 November 2024

Supervisors

Dr Gavin Clowry

Dr Fiona LeBeau

Biosciences Institute

Table of contents

Acknowledgments

After an intensive and stressful five years, today is the day to express my heartfelt gratitude in the final touch to my thesis. This experience has been a profound educational journey for me, not only in terms of scientific learning but also in personal growth. Pursuing a PhD and writing this thesis has had a crucial impact on my development. I would like to reflect on the people who have stood by me and supported me throughout this journey.

First and foremost, I wish to express my sincere gratitude to the Kingdom of Saudi Arabia for granting me this exceptional opportunity and for steadfastly supporting my academic pursuits through the scholarship I received. I am also deeply appreciative of the unwavering assistance provided by Qassim University throughout my doctoral studies. A special acknowledgment is due to Dr. Saleh Al-Damgh for his invaluable guidance and mentorship, which have been instrumental in shaping my academic journey. Additionally, I would like to thank Dr. Hamad and Dr. Abdulelah for their support in matters concerning my scholarship.

I am immensely thankful to my esteemed doctoral supervisor, Dr. Gavin Clowry, for his consistent support before and after my arrival in the UK. I never felt like a foreigner here, thanks to his encouragement and emotional support throughout my PhD studies at Newcastle University. He is not only a mentor but also a figure I aspire to emulate. His character has inspired my love for science and education, and he has helped me discover my identity and make my name prominent. He has motivated me to strive for excellence and has transformed me in ways I never thought possible. I will always cherish his support; he has been more like a father than just a supervisor. Thank you from the depths of my heart; I will never forget this great man.

Many thanks are also due to my co-supervisor, Dr. Fiona LeBeau, for her guidance and mentorship throughout my PhD studies at Newcastle University. She is a great and wonderful person who has supported me immensely during this period, helping me grow as both an educator and a researcher. I would like to extend my heartfelt thanks to my progress panel, Dr. Evelyne Sernagor and Dr. Marc Woodbury, for their advice and support throughout my 4-year meetings. Also, I am grateful to the dedicated staff at the Biomedical Imaging Lab, particularly David Bulmer, Glyn Nelson and Emma Foster, for their exceptional training and assistance, which helped me achieve my PhD project.

My colleagues have been pillars of strength during this period, and I wish to especially mention Dr. Faye McLeod, Dr. Connie Mackenzie-Gray Scott, Dr. Adrian Rees, Dr. Bas Olthof, and Dr. Sasha Gartside, who made me never to hesitate to ask them for any helping information. I also extend special thanks to Dr. Amrita Benoy for being beside me during the writing of my thesis and for always offering her help and encouragement to finish my thesis writing. Also, I would like to extend my gratitude to Natalie for her help and support. They have both been supportive to me emotionally, particularly during my father's illness. I also extend my thanks to Dr Fiez who supported me during this challenging time. Many thanks for Ross Laws who helped and trained me with 3 models programme and stood by me all the time to achieve the models.

I am deeply thankful for my family here: Dr. Ibtisam, Lauren, Dr. Anastasia, Dr. Bethany Dennis, Aysha and Dr. Daipayan. My deepest thanks go to my parents, especially my mother who took care of my children in my absence, and siblings, especially Majidah, Khulud, and Fatimah, who have taken care of my children, and to my husband, Sulman, who has been incredibly patient and supportive. I am especially grateful to my oldest daughter, Sulaf and my son Saleh for their unwavering support during my studies. I also appreciate my friends Salwa own, Asma Alshahrani for their steadfast presence and encouragement. Special recognition goes to Omar Al-Kharraz and my aunt Fatimah, whose continuous assistance has been invaluable in my journey; I believe I could not have completed my PhD without them.

As I conclude my doctoral studies, I ask God to bless me in this endeavour. I have learned so much and met incredible people, and I will miss them dearly.

Conference presentations

Federation of European Neuroscience Societies Forum (virtual) July 2020. Poster. Mapping gene expression during development of the human thalamus.

North-East Postgraduate Student Conference (Newcastle upon Tyne City, The UK) November 2023. Poster. Neurexin expression in developing human forebrain.

North-East Postgraduate Student Conference (Newcastle upon Tyne City, The UK) November 2022. Poster. Expression of the schizophrenia associated gene FEZ1 in the early developing foetal human forebrain

NUBI LIVE INSITUTE Newcastle upon Tyne City, The UK) (November 2023). Poster. Neurexin expression in early developing human forebrain.

Federation of European Neuroscience Societies Forum (France, Paris) July 2022. Poster. Expression of the schizophrenia associated gene FEZ1 in the early developing foetal human forebrain.

Neuroscience North East Conference Durham (12 December 2022). Oral presentation. Expression of the schizophrenia associated gene FEZ1 in the early developing foetal human forebrain.

Anatomical Society winter meeting in Nottingham (January 2023). Poster and Oral Presentation. Expression of the schizophrenia associated gene FEZ1 in the early developing foetal human forebrain.

Anatomical Society summer meeting Edinburgh (July 2024). Poster. CNTNAP2 expression in early developing human forebrain.

British Neuroscience Association in Brighton (April 2023). Poster. Neurexin 1 expression in early developing human forebrain.

British Neuroscience Association in Brighton (April 2025) CNTNAP2 expression in early developing human forebrain.

Publications

Expression of the schizophrenia associated gene FEZ1 in the early developing foetal human forebrain, Frontiers in Neuroscience, 08-09-2023 | Journal article.

Contributors: Maznah Alhesain; Hannah Ronan; Fiona E. N. LeBeau; Gavin J. Clowry

DOI: 10.3389/fnins.2023.1249973

Part of ISSN: 1662-453X

Development of the early fetal human thalamus; from protomap to emergent thalamic nuclei. Frontiers in Neuroscience, 07-02-2025 | Journal article.

Contributors: Maznah Alhesain, Ayman Alzu'bi, Niveditha Sankar, Charles Smith, Janet Kerwin, Ross Laws, Susan Lindsay, Gavin J Clowry.

DOI. 10.3389/fnana.2025.1530236

Part of ISSN: 1662-453X

Abstract

The thalamus is a brain region consisting of neuronal clusters and with a large number of connections which are responsible for several important functions including cognitive functions. It serves as a major relay centre, transmitting and modulating information between the cerebral cortex and subcortical structures. Given its involvement in higher-order cognitive functions, abnormalities in thalamic development have been implicated in various neurodevelopmental disorders, including schizophrenia and autism spectrum disorders. However, the developmental process of these nuclei in the human brain is still unknown. Understanding the developmental trajectory of the thalamus in humans is essential for several reasons. Firstly, while rodent models have provided insights into thalamic development, there are significant species-specific differences in the timing, organization, and molecular regulation of thalamic nuclei formation. These differences necessitate direct investigation of human developmental processes to bridge the gap between animal models and human neurodevelopment. Secondly, delineating how thalamic nuclei emerge during early foetal development may provide critical information on the origins of functional specialization within the thalamus, shedding light on how distinct neuronal populations are specified and how their connectivity is established. Finally, by identifying molecular markers and gene expression patterns specific to early thalamic development, we can gain a deeper understanding of the genetic and cellular mechanisms that may contribute to neurodevelopmental disorders, potentially informing future diagnostic and therapeutic approaches.

This study aims to investigate gene expression patterns in the human thalamus, extending from 8 to 21 PCW, in order to track the development of each thalamic nucleus. Additionally, we focus on 14 PCW to identify distinct thalamic nuclei based on the expression of a unique combination of transcription factors and other genes/proteins. We also aim to investigate the expression of susceptibility genes linked to neurological diseases such as *FEZ1, NRXN1* regarding their expression in specific thalamic nuclei.

The methods we used are immunostaining and RNAscope in situ hybridisation, including double staining methods for multiple markers. Sections were taken from human early foetal brains (ethically sourced and supplied by the Human Developmental Biology Resource), in all planes and covering the extent of the diencephalon. Sections taken at 14 PCW were aligned with 3-D maps of the forebrain collected by structural MRI scanning. The expression of

combinations of markers were localised to particular regions of the thalamus. We also analysed open source scRNAseq data with the aim of identifying clusters of cells grouped by shared gene expression patterns. We also investigated the expression of neurodevelopmental disease susceptibility genes in specific nuclei and cell types of the thalamus and telencephalon.

This study provides significant insights into the early development of the human thalamus and telencephalon. The study highlights distinct gene expression patterns and the emergence of thalamic nuclei from a protomap. Our findings demonstrate that different transcription factors and molecular markers define specific thalamic regions, reinforcing the concept that a structured thalamic map begins to emerge by 14 PCW. Furthermore, we identified 15 distinct groups of cells with functional characteristics, supporting the notion that thalamic differentiation is an intricate and highly regulated process. It also implicates that neurogenesis and extensive cellular migration are critical processes during this crucial period.

The differential expression of neurodevelopmental disease susceptibility genes in the thalamus further underscores the importance of studying early thalamic development in the context of neurological disorders. The high expression of *FEZ1* in progenitor cells, transitioning to glutamatergic neurons, and the elevated presence of *NRXN1* in the thalamus suggest potential roles in neuronal connectivity and function. These findings may provide critical clues for understanding the etiology of conditions such as schizophrenia, where thalamic dysfunction has been implicated.

Overall, this study bridges a crucial gap in our knowledge of human thalamic development, and lay the foundation for future research into the molecular mechanisms underlying thalamic organization. Further investigations, including functional studies and longitudinal analyses, will be essential for uncovering how early developmental events shape thalamic function and its implications for neurodevelopmental and neuropsychiatric disorders.

List of figures:

List of tables

List of abbreviations

4',6-diamidino-2-phenylindole (DAPI)
Abnormal spindle-like microcephaly-associated protein (ASPM)
Achaete-scute family BHLH transcription factor 1 (ASCL1)
Actin-related protein 2/3 complex subunit 1B (ARPC1B)
Adhesion G-protein coupled receptor gene 1 (ADGRG1)
A-kinase anchoring protein 9 (AKAP9)
Aldolase, fructose-bisphosphate C (ALDOC)
Alexa Fluor 488 (AF488)
Allograft inflammatory factor 1 (AIF1)
Alpha globin (HBA1)
Alpha globin (HBA2)
Alpha hemoglobin stabilizing protein (AHSP)
Alpha neurexins (αNRXNs)
Alpha synuclein (SNCA)
Alpha-2-macroglobulin (A2M)
3-aminolevulinate synthase 2 (ALAS2)
Amygdala (Ag)
Anterior (A)
Anterior nucleus (AN)
Anterior pulvinar (PulA)
Anterodorsal AD
Anteroventral nucleus (AV)
Antigen Kiel-67 (Ki67)
Apolipoprotein D (APOD)
Apolipoprotein E (APOE)
Aquaporin 4 (AQP4)
Aqueous (aq)
Arp2/3 complex protein 2 (ARPP2)
Astrocytes (AS)
Attention deficit hyperactivity disorder (ADHD)
Autism spectrum disorders (ASD)

Autism, susceptibility to, type 15 (AUTS15)

Axis Inhibition Protein 2 (*Axin2*)

Basic helix-loop-helix (bHLH)

Bcl-2-like protein 1 (BCL2L1)

Bervican core protein (BCAN)

Beta globin (HBB)

Beta neurexins (βNRXNs)

Biglycan (BGN)

Cytochrome b-245 alpha chain (CYBA)

Fibronectin 1 (FN1)

Biliverdin reductase B (BLVRB)

Bone morphogenetic proteins (BMPs)

T-box brain 1 (TBR1)

Brain abundant membrane attached signal protein 1 (BASP1)

Calbindin 1 (CALB1)

Calbindin 2 (CALB2)

Calcium/calmodulin-dependent serine protein kinase (CASK)

Caldesmon 1 (CALD1)

Calmodulin 2 (CALM2)

Calponin 3 (CNN3)

Carboxypeptidase E (CPE)

Carboxypeptidase E (CPE)

Cathepsin B (CTSB)

Caudal ganglionic eminence (CGE)

Caudal ganglionic eminences (CGE)

Caudal thalamic progenitor domain (pTh-C)

Caudal thalamus (cTh-C)

Caudate (Ca)

Caudodorsal (MDcd)

C-C motif chemokine ligand 3-like 3 (CCL3L3)

C-C motif chemokine ligand 4-like 2 (CCL4L2)

Cell division cycle 20 (CDC20)

Central lateral nucleus (CL)

Central medial nucleus (CeM)

Central nervous system (CNS)

Centrolateral nucleus of the PuI (PuI_{cl})

Centromedial (PuI_{cm})

Centromedian (CM)

Centromedian nucleus (CM)

Centromere protein A (CENPA)

Centromere protein F (CENPF)

Cerebral development expression viewer (CoDEx)

Cervical flexure (CF)

Chemokine ligand 3 (CCL3)

Chicken ovalbumin upstream promotor-transcription factor 1/2 (COUP-TF 1/2)

Choroid plexus (ch P)

Chromosome 1 open reading frame 54 (C1orf54)

Chromosome 1 open reading frame 61 (C1orf61)

Claudin-5 (CLDN5)

Claustrum (Cl)

Cluster of differentiation 20 (CD20)

Cluster of differentiation 24 (CD24)

Cluster of differentiation 83 (CD83)

Collagen, type IV, alpha 1 (COL4A1)

Collagen, type IV, alpha 2 (COL4A2)

Colony stimulating factor 1 (CSF1)

Complement C3b/C4b receptor 1 like (CR1L)

Interferon-induced protein tetratricopeptide repeats 1B (IFIT1B)

Contactin alpha (CNTNA)

Contactin-associated protein-like 2 (CNTNAP2)

Cornu Ammonis 1 (CA1)

Cortex (CRX)

Cortex (Crx)

Cortical development expression viewer (CoDEx)

Cortical dysplasia-focal epilepsy (CDFE)

Cortical plate (CP)

Corticothalamic (CT)

Coxsackievirus and adenovirus receptor (CXADR)

CUGBP, Elav-like family member 2 (CELF2)

Cyanine fluorescent dye 3 (cy3)

Cyclin A2 (CCNA2)

Cyclin B1 (CCNB1)

Cyclin B2 (CCNB2)

Cyclin dependent kinase 1 (CDK1)

Cyclin-dependent kinase inhibitor 2 (CDKN2)

Cyclin-dependent kinase regulatory subunit 2 (CKS2)

Cystatin 3 (CST3)

Cytoskeleton-associated protein 2 (CKAP2)

Cytoskeleton-associated protein 2 (CKAP2)

C-X3-C motif chemokine receptor 1 (CX3CR1)

Dedicator of cytokinesis 6 (DOCK6)

Deleted in liver cancer 1 (DLC1)

Delta like protein A (*DeltaA*)

Diaminobenzidine (DAB)

Diazepam binding inhibitor (DBI)

Dibutylthalate polystyrene xylene (DPX)

Diencephalic/telencephalic boundary (DTB)

Diencephalon (D)

Disrupted in schizophrenia 1 (DISC1)

DNA binding domain (DBD)

Docking protein 5 (DOK5)

Dorsal (Dor)

Dorsal lateral geniculate thalamic nuclei (dLGN)

Dorsomedial nucleus of the Pul (Pul_{dm})

Doublecortin (DCX)

Doublecortin-expressing (DCX+)

Drosophila distal-less homeobox 1 (DLX1)

Drosophila distal-less homeobox 5 (DLX5)

Early growth response protein 1 (EGR1)

Embryonic day (E)

Endothelin receptor type B (EDNRB)

Epidermal growth factor-like (EGF-like)

Epithalamus (Epith)

Eukaryotic translation elongation factor 1 beta 2 (EEF1B2)

Eva-1 homolog B (EVA1B)

Family with sequence similarity 210 member B (FAM210B)

Solute carrier family 40 member 1 (SLC40A1)

Fasciculation and elongation protein zeta-1 (FEZ1)

Fasciculation and elongation protein zeta-2 (FEZ2)

Fatty acid binding protein 5 (FABP5)

Fatty acid binding protein 7 (FABP7)

Fc receptor of IgG, receptor, transporter, alpha chain (FCGRT)

Ferric chelate reductase 1 (FRRS1)

Ferritin heavy chain 1 (FTH1)

Ferritin light chain (FTL)

Ferrochelatase (FECH)

Fibroblast growth factors (FGFs)

Fibrogen growth factor receptor 3 (*Fgfr3*)

First order (FO)

Forkhead box protein (FOXP)

Forkhead box protein 1 (FOXP1)

Forkhead box protein 2 (FOXP2)

Forkhead box protein G1 (FOXG1)

Fos proto-oncogene (FOS)

Gamma-Aminobutyric acid (GABA)

Ganglionic eminence (GE)

Gap junction alpha-1 protein (GJA1)

Gastrulation Brain Homeobox 2 (GBX2)

Gestation week (GW)

Glial fibrillary acidic protein (GFAP)

Globus pallidus (GP)

Glutamate decarboxylase 1 (GAD1)

Glutamate decarboxylase 2 (GAD2)

Glutamate decarboxylase 67 (GAD67)

Glutamate dehydrogenase 1 (GLUD1)

Glutamate receptor-interacting protein 2 (GRIP2)

Glycophorin A (GYPA)

Glycophorin C (GYPC)

Glycoprotein M6B (GPM6B)

Growth arrest and DNA damage inducible beta (GADD45B)

Growth associated protein 43 (GAP43)

GTPase of the immune-associated nucleotide-binding protein 1 (GIMAP1)

Guanine nucleotide-binding protein, gamma 3 (GNG3)

H3.3 histone B (H3F3B)

Chemokine ligand 14 (CXCL14)

Habenula (Ha)

Haematoxylin and eosin (H&E)

Hairy and enhancer of split homolog-1 (HES1)

Hairy and enhancer of split homolog-5 (HES5)

Hairy-like factor 6 (*Her6*)

Heart (Ht)

Haemogen (HEMGN)

Haemoglobin subunit alpha 1 (HBA1)

Haemoglobin subunit gamma-1 (HBG1)

Haemoglobin subunit gamma-2 (HBG2)

Haemoglobin subunit Mu (HBM)

Haemoglobin subunit theta-1 (HBQ1)

Hey-related bHLH Transcription Factor (*HELT*)

Higher order (HO)

High-mobility group protein 2 (HGMP2)

Hippocampus (Hipp)

Histone deacetylase (HDAC11)

Histone deacetylase 9 (HDAC9)

Homeobox B4 (HOXB4)

Homeodomain-only protein (HOPX)

Horseradish peroxidase (HRP)

Human Developmental Biology Resource (HDBR)

Human induced pluripotent stem cells (hiPSCs)

4-hydroxy-3-methylglutaryl CoA synthase 1 (HMGCS1)

Hypothalamus (HyTH)

Hypothalamus golgi apparatus expressed 19 kDa protein (HMP19)

Hypoxia-inducible domain containing protein B (HIGDIB)

Immediate early response 3 (IER3)

Immunofluorescence (IF)

Immunohistochemistry (IHC)

Inferior pulvinar (PulI)

Inferior pulvinar (PulI)

Inhibitor of DNA binding (*Id*)

Inhibitor of DNA binding 2 (ID2)

Inner fiber layer (IFL)

Insulin-like growth factor 1 (IGF1)

Insulin-like growth factor binding protein 7 (IGFBP7)

Integral membrane protein 2B (ITM2B)

Inter-alpha-trypsin inhibitor heavy chain 5 (ITIH5)

Intercellular adhesion molecule 2 (ICAM2)

Interferon-induced transmembrane protein 3 (IFITM3)

Intermediate zone (IZ)

Internal capsule (IC)

Intramedullary nucleus (IMN)

Iroquois-type transcription factor (IRX3),

Isopentenyl-diphosphate delta isomerase 1 (IDI1)

Jun proto-oncogene (JUN)

Karyopherin subunit alpha-2 (KPNA2)

Keratin 1 (KRT1)

Kilo Dalton (kDa)

Kinesin family member 11 (KIF11)

Kinesin family member 2 C (KIF2C)

Kinesin light chain 1 (KLC1)

Knockout (KO)

Lateral dorsal (LD)

Lateral dorsal nucleus (LD)

Lateral ganglionic eminence (LGE)

Lateral geniculate nucleus (LGN)

Lateral geniculate nucleus dorsal (LGNd)

Lateral geniculate thalamic nuclei (LGN)

Lateral mediodorsal nuclei (MDI)

Lateral posterior nucleus (LP)

Lateral pulvinar (PulL)

Lateral pulvinar nucleus (PulL)

Lateral PuM ($PulM_l$)

Leucine zipper protein 2 (LUZP2)

Ligand binding domain (LBD)

Retinoic acid response element (RARE)

Ligand-neutralizing sequence (LNS)

LIM domain only 1 (LMO1)

LIM Homeobox (LHX)

LIM Homeobox 1 (LHX1)

LIM Homeobox 2 (LHX2)

LIM Homeobox 5 (LHX5)

LIM Homeobox 9 (LHX9)

Limbic system associated membrane protein (LSAMP)

Liver (Li)

Long intergenic non-protein coding RNA 152

Lung (Lg)

Lymphocyte antigen 6 family member H (LY6H)

Lymphoid enhancer binding factor 1 *(Lef1*)

Lysosomal-associated protein transmembrane 5 (LAPTM5)

Magnetic resonance (MR)

Magnetic resonance imaging (MRI)

Magnocellular (MDmc)

Makorin ring finger protein 1 (MKRN1)

MARCKS like-1 (MARCKSL1)

Marginal zone (MZ)

Marker of proliferation Ki 67 (MKI67)

Maternally expressed gene 3 (MEG3)

Medial caudal ganglionic eminences (mCGE)

Medial dorsal (MD)

Medial ganglionic eminences (MGE)

Medial geniculate nucleus (MGN)

Medial geniculate nucleus ventral (MGNv)

Medial mediodorsal nucleus (MDm)

Medial pulvinar (PulM)

Medial pulvinar nucleus (PulM)

Median geniculate nucleus (MGN)

Mega base pair (Mbp)

Membrane palmitoylated protein 1 (MPP1)

Mesencephalon (M)

Metallothionein 1E (MT1E)

Metallothionein 2A (MT2A)

Metallothionein 3 (MT3)

Microsomal glutathione S-transferase 1 (MGST1)

Microtubule-associated protein Tau (MAPT)

Mid diencephalic organizer (MDO)

Midgut (Mg)

Milk fat globule-EGF factor 8 protein (MFGE8)

MIS18 binding protein 1 (MIS18BP1)

Mitogen activated protein 1B (MAP1B)

Mitogen activated protein 2 (MAP2)

Mitogen activated protein kinase 3/Phosphoinositide 3-kinase (MAPK/PI3K)

Mitogen-activated protein kinase kinase-3 (MAP2K3)

N-myc downstream regulated gene 2 (NDRG2)

Myocardial infarction associated transcript (MIAT)

Myocyte enhancer factor 2 C (MEF2C)

Myosin light chain 12A (MIL12A)

NADH dehydrogenase (ubiquinone) 1 alpha subcomplex, 4-like 2 (NDUFA4L2)

Neural stem cells (NSCs)

Neurexin (NRXN)

Neurexin 1 (NRXN1)

Neurexin 1-alpha (NRXN1α)

Neurexin 1-beta (NRXN1β)

Neurexin 1-gamma (NRXN1γ)

Neurexin 2 (NRXN2)

Neurexin 3 (NRXN3)

Neurexin 4 alpha (NRXN4)

Neurexin alpha (NRXNα)

Neurexin beta (NRXNβ)

Neurexin-1 alpha (NRXN1)

Neurexin-2 alpha (NRXN2)

Neurexins *(NXRN)*,

Neuritin 1 (NRN1)

Online Mendelian Inheritance in Man (OMIM)

Olfactomedin 1 (OLFM1)

Neurocan (NCAN)

Neurodevelopmental disorders (NDDs)

Neurofilament light chain (NEFL)

Neurogenic differentiation 4 (NEUROD4)

Neurogenic differentiation 6 (NEUROD6)

Neurogenin 1 (NGN1)

Neurogenin 2 (NGN2)

Neuroligin/neurexin (NLGN/NRXN)

Pertaining to or affecting the neurotransmitter gamma-aminobutyric acid (GABAergic)

Neuroligins (NLGNs)

Neuronal membrane glycoprotein M6B (GPM6B)

Jun proto-oncogene B (JUNB)

Neuropeptide Y (NPY)

Neuroscience Multi-Omic Analytics (NEMO)

Neurotrimin (NTM)

Neurotrophic tyrosine receptor kinase 2 (NTRK2)

Nitric oxide synthase 3 (NOS3)

NK2 Homeobox 2 (*NKX2.2*)

Normalized reads per kilobase of exon per million mapped reads (RPKM)

Nova alternative splicing regulator 1 (NOVA1)

Nuclear enriched abundant transcript 1 (NEAT1)

Nuclear factor 1-A type (NF1A)

Nuclear factor 1-B type (NF1B)

Nuclear Receptor Family1/ 2 NR2F1/2

Nuclear Receptor Subfamily 2 Group F Member 2 (NR2F2)

Nuclear Receptor Subfamily 4 Group A Member 2 (NR4A2)

Nuclear ubiquitous casein and cyclin-dependent kinases substrate 1 (NUCKS1)

Nucleolar and associated protein 1 (NUSAP1)

Oligodendrocyte precursor cells (OPC)

Oligodendrocyte transcription factor 1 (OLIG1)

Oligodendrocyte transcription factor (OLIG2)

Oligodendrocyte Transcription factor 3 (*OLIG3*)

Orthodenticle homeobox 2 (OTX2)

Outer subventricular zone (oSVZ)

Paired box 6 (PAX6)

Paired box gene 2 (PAX2)

Paracentral nucleus (Pc)

Parafascicular nucleus (PF)

Paratenial nucleus (Pt)

Parvalbumin (PVALB)

Parvocellular (MDpc)

Paternally expressed gene 10 (PEG10)

Peripheral myelin protein 2 (PMP2)

Pertaining to or affecting the neurotransmitter gamma-aminobutyric acid (GABAergic)

Phosphate buffer saline (PBS)

Phosphoglucomutase 2 (PGM2)

Phosphoglucomutase 2 like 1 (PGM2L1)

Phosphohydroxythreonine aminotransferase (PSAT)

Phospholipid phosphatase 3 (PLPP3)

Pim-1-proto-oncogene, serine/threonine kinase (PIM1)

Pitt-Hopkins-like syndrome-1 (PTHSL1)

Platelet-derived growth factor receptor A (PDGFRA)

Pleiotrophin (PTN)

Pleiptrophin-protein tyrosine phosphatase receptor type Z (PTN-PTPRZ1)

Pontine fexure (PF)

Post synaptic density protein, Drosophila disc large tumour suppressor, and Zonula-occludens-1 protein (PDZ)

Post-conception weeks (PCW)

Posterior (Pos)

Posterior medial (PM)

Posteroventral PV

Potassium-calcium activated channel 3 (KCNN3)

Prefrontal cortex (PFC)

Presubplate (pSP)

Prethalamus (PTh)

Pretectum (PTc)

Principle component analysis (PCA)

Profilin 1 (PFN1)

Prosencephalon (P)

Prospero homeobox 1 (PROX1)

Protein kinase C, delta binding protein (PRKCDBP)

Protein regulator of cytokinesis 1 (PRC1)

Protein tyrosine phosphatase receptor zeta 1 (PTPRZ1)

Prothymosin alpha (PTMA)

Protocadherin 10b (*pcdh10b*),

Pulvinar (Pul)

Pulvinar medial subnucleus ($PulM_m$)

Pulvinar region (Pulv)

Purkinje cells (PCs)

Putamen (Pu)

Quantitative polymerase chain reaction (qPCR)

Radial glial (RG)

Radial glial-like (RGL)

Ras-homolog gene family B (RHOB)

Ras-related C3 botulinum toxin substrate 3 (RAC3)

Reads per kilo base of transcript per million mapped reads (RPKM)

Reads per kilobase of exon per million mapped reads (RPKM)

Receptor activity modifying protein 1 (RAMP1)

Receptor activity modifying protein 2 (RAMP2)

Regulator of G-protein signaling 10 (RGS10)

Reticular formation (RF)

Reticular nucleus (Re)

Reticulon 1 (RTN1)

Retinoic acid (RA)

Reuniens nucleus (MV-re)

Rhombencephalon (R)

Ribosomal protein L10 (RPL10)

Ribosomal protein L13 (RPL13)

Ribosomal protein L13A (RPL13A)

Ribosomal protein L19 (RPL19)

Ribosomal protein L21 (RPL21)

Ribosomal protein L23 (RPL23)

Ribosomal protein L24 (RPL24)

Ribosomal protein L30 (RPL30)

Ribosomal protein L32 (RPL32)

Ribosomal protein L37A (RPL37A)

Ribosomal protein L39 (RPL39)

Ribosomal protein lateral stalk subunit protein 1 (RPLP1)

Ribosomal protein S8 (RPS8)

Ribosomal protein S11 (RPS11)

Ribosomal protein S12 (RPS12)

Ribosomal protein S13 (RPS13)

Ribosomal protein S14 (RPS14)

Ribosomal protein S15 (RPS15)

Ribosomal protein S15A (RPS15A)

Ribosomal protein S18 (RPS18)

Ribosomal protein S19 (RPS19)

Ribosomal protein S27 (RPS27)

Ribosomal protein S27A (RPS27A)

Ribosomal protein S29 (RPS29)

RNA binding protein Quaking (QKI)

RNA sequencing (RNAseq)

RNAScope, 2.5 HD detection Reagent (RED)

Roof plate-specific spondin-3 (RPSO3)

Rostral thalamic progenitor domain (pTh-R)

Rostral thalamus (cTh-R)

S100 calcium binding protein A13 (S100A13)

S100 calcium binding protein B (S100B)

Ribosomal protein L41 (RPL41)

Saline sodium citrate (SSC)

Schizophrenia (SZ)

Semaphorin 3F (SEMA3F)

Serine replaced by cysteine at 704 (Ser704Cys)

Serpin family E member 2 (SERPINE2)

Serpin family H member 1 (SERPINH1)

Serum paraoxonase 2 (PON2)

Shootin 1 (SHTN1)

Shugoshin 1 or Shugoshin-like 1 (SGOL1)

Sine Oculis Homeobox Homolog 3 (SIX3)

Sine Oculis Homeobox Homolog 3 (SIX3)

Single cell Omics in Low-throughput (SOLO)

Single cell RNA sequencing (scRNAseq)

Sodium chloride (NaCl)

Sodium voltage-gated channel alpha subunit 2 (SCN2A)

Sodium/potassium transporting ATPase interacting 4 (NKAIN4)

Sodium/potassium-transporting ATPase subunit alpha-2 (ATP1A2)

Soluble-N-ethylmaleimide-sensitive component attachment protein 25 (SNAP25)

Soluble-N-ethylmaleimide-sensitive component attachment protein receptor (SNARE)

Solute carrier family 17 (SLC17)

Solute carrier family 17 member 6 (SLC17A6)

Solute carrier family 17 member 6/Vesicular glutamate transporter 2 (SLC17A6/vGLUT2)

Solute carrier family 2 member 1 (SLC2A1)

Solute carrier family 2 member 3 (SLC2A3)

Solute carrier family 3 member 2 (SLC3A2)

Solute carrier family 6 member 11 (SLC6A11)

Solute carrier family 7 member 5 (SLC7A5)

Solute carrier family 25 member 37 (SLC25A37)

Solute carrier family 38 member 5 (SLC38A5)

Sonic Hedgehog (SHH)

SP zinc finger transcription factor gene family member 8 (SP8)

SPARC/osteonectin, Cwcv and Kazal-like domains proteoglycan (SPOCK)

Sparc-related modular calcium-binding protein 1 (SMOC1)

Specificity protein 8 (SP8)

Spermidine/spermine N1-acetyltransferase 1 (SAT1)

Spindle component 25 (SPC25)

Src homology 2 domain containing E protein (SHE)

Src like adaptor (SLA)

SRY-box 2 (SOX2)

SRY-box 9 (SOX9)

SRY-box transcription factor 14 (SOX14)

SRY-Box Transcription Factor 2 (*SOX2*)

SRY-box transcription factor 28 (SOX28)

Stathmin 1 (STMN1)

Stathmin 4 (STMN4)

STE20 related adaptor beta (STRADB)

Stratum oriens (SO)

Stratum pyramidalis (SP)

Subplate (SP)

Subventriclar zone (SVZ)

Subventricular zone (SVZ)

Supraoptic layer (SP)

Surface protein 1 (S1)

Synaptoporin (SYNPR)

Stearoyl-CoA desaturase 5 (SCD5)

Syntaxin binding protein 1 (STXBP1)

Targeting protein for Xklp2 (TPX2)

T-distributed stochastic neighbour embedding (t-SNE)

Telencephalon (T)

Temporal cortex (Temp Crtx)

Tenascin-R (TNR)

TGF-beta stimulated clone 22 domain family member 4 (TSC22D4)

Thalamic eminence (ThEm)

Thalamic reticular nucleus (TRN)

Thalamocortical (TC)

Thalamocortical axons (TCA)

Thalamus (Th)

Thymosin beta 10 (TMSB10)

Tissue factor pathway inhibitor (TFPI)

Tongue (Tn)

Transcription factor 7-like (TCF7L)

Transcription factor 7-like 2 (TCF7L2)

Tris-buffered saline (TBS)

Tubulin alpha-1 A (TUBA1A)

Tubulin beta-2 A (TUBB2A)

Tubulin beta-4 B (TUBB4B)

Tweety-homolog 1 (TTYH1)

Tyramide Signal Amplification (TSA)

TYRO protein tyrosine kinase binding protein (TYROBP)

Tyrosine-protein kinase (KIT)

Ubiquitin B (UBB)

Ubiquitin carboxyl-terminal hydroxylase L1 (UCHL1)

Umbilical cord (UC)

Uncoordinated 76 (UNC-76)

Uniform Manifold Approximation and Projection (UMAP)

Ventral (Ven)

Ventral caudal ganglionic eminences (vCGE)

Ventral lateral (VL)

Ventral lateral anterior nucleus (VLa)

Ventral lateral geniculate thalamic nuclei (vLGN)

Ventral lateral posterior nucleus (VLp)

Ventral medial (VM);

Ventral posterior (V)

Ventral posterior (VP)

Ventral posterolateral (VPL)

Ventral posteromedial (VPM)

Ventral thalamus (vTH)

Ventral-anterior (VA)

Ventral-lateral (VL)

Ventricular zone (VZ)

Ventro lateral (VL)

Ventroanterior (VA)

Ventromedial nucleus (VM)

Ventroposteriolateral (PVM).

Ventroposteriolateral (VPL)

Vesicular glutamate transporter 2 (vGLUT2)

Vessicle-associated membrane protein 2 (VAMP2)

Vessicle-associated membrane protein 5 (VAMP5)

Vimentin (VIM)

Visinin-like protein 1 (VSNL1)

Wingless/integrated (WNT)

ZFP36 ring finger like protein 1 (ZFP36L1)

Zic family member 4 (ZIC4)

Zic family member 4 (ZIC4)

Zinc finger homeobox 3 (ZFHX3)

Zinc finger protein 804 A (ZNF804A)

Zona limitans (ZL)

Zona Limitans Intrathalamica (ZLI)

1 Chapter 1. Introduction

In recent years, significant progress has been made in understanding the development of the human forebrain, particularly the telencephalon. The telencephalon, which gives rise to the cerebral cortex, hippocampus, and basal ganglia, has been thoroughly examined due to its direct role in higher cognitive functions, voluntary motor control, and sensory processing (Monuki, 2022). Nevertheless, the thalamus, an essential structure within the diencephalon, and study of the thalamus has been relatively neglected, despite its essential role in brain function and development.

This thesis therefore focuses on the thalamus, a structure that has co-evolved with the cerebral cortex in primates and humans in particular, establishing complex reciprocal connections essential for sensory integration, cognition, and awareness. The thalamocortical system is essential for the processing and transmission of information in the brain, acting as a nexus that connects subcortical areas to the cerebral cortex. Due to its pivotal function in regulating and conveying sensory, motor, and cognitive information, disruptions in thalamic development can significantly impact brain function.

The aberration or impairment of the thalamus has been associated with several neurodevelopmental and neuropsychiatric illnesses, such as autism spectrum disorder (ASD), schizophrenia, and attention-deficit hyperactivity disorder (ADHD) (Krol et al., 2018). Irregularities in thalamocortical connections are thought to lead to cognitive impairments, sensory processing abnormalities, and disturbances in consciousness. Nonetheless, our comprehension of thalamic development, its interaction with the cortex, and its role in higher-order cognitive tasks is still inadequate.

This thesis seeks to address the information deficit about thalamic and telencephalic development by investigating the genetic, molecular, and cellular factors that regulate its formation and integration with the cerebral cortex. This study will also investigate the role of the thalamus and the telencephalon with regards to its impact on developmental disturbances in neurodevelopmental diseases. This study aims to further the understanding of forebrain development and its relevance to human cognition and disease by concentrating on this generally overlooked but essential brain component.

1.1 Early Human Brain Development

Prenatal age is defined as postfertilization age, although menstrual weeks are frequently employed in obstetrics for convenience, they may not accurately reflect true age. The phrase "gestational age" should be avoided because of its vagueness, as it can denote three distinct starting points: the last menstrual period, fertilization, or implantation. I have used the term "postconceptional weeks" (PCW) to precisely denote both the postfertilization and postovulation age. Prenatal development is divided into three main subdivisions: the fertilization, embryo, and foetus periods. The first period, fertilization (conception), is the first 3 PCW of prenatal development, from fertilization to the formation of the blastocyst (Schoenwolf et al., 2014). The embryonic stage, which begins at 3 PCW following conception and lasts until 8 PCW, and the foetal period start from 9 PCW to birth (Stiles, 2008, O'rahilly and Müller, 2010, Stiles and Jernigan, 2010). The human embryonic period can be divided into 23 stages, known as the Carnegie stages (Figure 1.1). Each Carnegie stage can be represented by a corresponding time in PCW (Table 1.1) (O'Rahilly and Müller, 1987).

The embryo then advances to the next stage and is referred to as a ‘foetus’. This is the foetal period of prenatal development, which is associated with further significant changes in the brain. This stage of development begins in the 9 week post-conception and lasts until the baby is born (Stiles and Jernigan, 2010).The formation of the human brain begins in the 3 and 4 PCW, namely the embryonic stage, with the differentiation of the neural progenitor cells through a process of neurulation (Li et al., 2023). Normal brain development depends on both the expression of genes and input from the surrounding environment; any interruption to either of these processes can alter the neural results significantly (Sadler, 2005). The initial stage of neurulation is marked by the emergence of a longitudinal mid-line structure in the embryo’s top layer, known as the ‘primitive streak’, which helps to define the body’s axis: cranial-caudal, dorsal-ventral, and medial-lateral. The cranial end of the primitive streak is expanded as the primitive node (Schoenwolf et al., 2020). The epiblast cells detach from the embryo’s top layer and depart the primitive streak. Some invade the hypoblast and the three primary germ layers form, namely the ectoderm, mesoderm, and endoderm. Human brain development begins when the primitive node starts to induce the overlying ectoderm to form the neural plate, which begins to fold to form the neural tube. This tube is broad cranially and tapered caudally. The expanded cranial portion engenders the forebrain, midbrain, and hindbrain. The narrower caudal portion of the neural plate engenders the spinal cord (Copp et al., 2003, Sadler, 2005).

As the neurulation process commences formation of the brain in 5 PCW, the three primary brain vesicles in the anterior neural tube, namely the prosencephalon, the mesencephalon, and the rhombencephalon (forebrain, midbrain, and hindbrain, respectively), convert to five secondary brain vesicles, the prosencephalon divides into the telencephalon (cerebral hemispheres) and diencephalon (thalamus and hypothalamus). The Rhombencephalon (hindbrain) divided into metencephalon (pons and cerebellum) and myelencephalon (medulla). The cavity of the diencephalon is the third ventricle and the cavity of the telencephalon is the lateral ventricle (Figure 1.2) (Schoenwolf, 2021).

The four major morphogens, wingless/integrated (WNT), Sonic Hedgehog (SHH), bone morphogenetic proteins (BMPs), and fibroblast growth factors (FGF), act in a concentration dependent manner, and induce different cell fates in the prosencephalon (Dessaud et al., 2008). The spatio-temporal distribution of the different morphogens during the early developmental stages constitutes a crucial step for neural fate specification and brain morphogenesis. In the prosencephalon, these morphogens impart positional information to the different cell types distributed in the compartments along the neural tube wall (Puelles and Rubenstein, 2003). The neural tube is dorsalized by the surface ectoderm secreting WNT and BMPs, which causes the formation of the roof plate of the neural tube. The neural plate is ventralized by the signals received from the notochord and induces the floor plate to secrete SHH. This engenders the secretion of SHH from the floor plate and the notochord (Figure 1.3) (Schoenwolf et al., 2014).

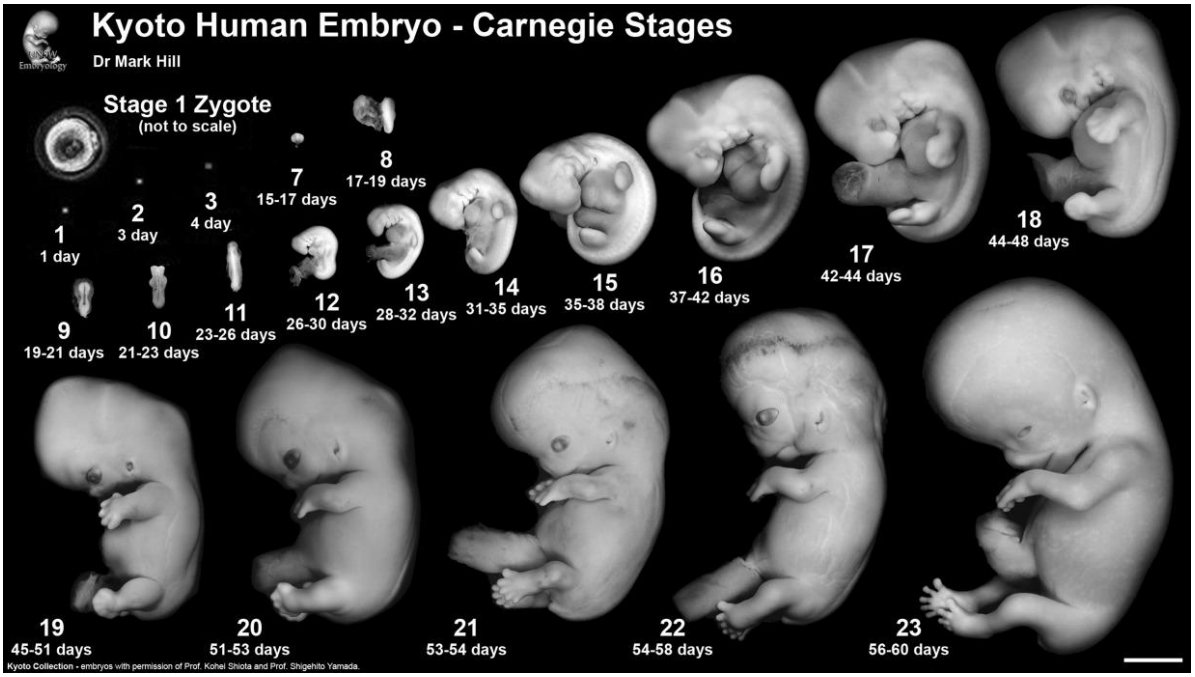

Figure 1.1 Left lateral view of human embryos. This image illustrates the Carnegie stages of human embryonic development, depicting morphological changes from the zygote stage Stage 1 to Stage 23 over a period of 1 to 60 days. Stage 1: Zygote (Day 1), Stages 2-6: Early cell division and implantation (Days 2-14), Stages 7-8: Gastrulation and early neural development (Days 15-19), Stages 9-13: Formation of the neural tube, somites, and early limb buds (Days 19-32), Stages 14-17: Development of brain vesicles, limb differentiation, and facial structures (Days 31-44), Stages 18-23: Continued organogenesis, limb elongation, and facial feature refinement (Days 44-60) Scale bar is 5 mm. (Source: the Kyoto Collection of Human Embryos, provided by Kohei Shiota, Kyoto) (Hill, 2018).

Table 1.1 Carnegie stages 23, the embryo transitions into the foetal stage (week 8) (O'Rahilly and Müller, 1987).

Carnegie Stage	PCW (post-Conception Weeks)
Stage 1	Week 1 (Day 1)
Stage 2	Week 1 (Days 3)
Stage 3	Week 1 (Days 4)
Stage 4	Week 1 (Days 5-6)
Stage 5	Week 2 (Days 7–12)
Stage 6	Week 2 (Days 13)
Stage 7	Week 3 (Days 15-17)
Stage 8	Week 3 (Days 17-19)
Stage 9	Week 3 (Days 19-21)
Stage 10	Week 4 (Days21- 23)
Stage 11	Week 4 (Days 23-26)
Stage 12	Week 4 (Days 26-30)
Stage 13	Week 5 (Days 28-32)
Stage 14	Week 5 (Days 31-35)
Stage 15	Week 5 (Days 35-38)
Stage 16	Week 6 (Days 37-42)
Stage 17	Week 6 (Days 42-44)
Stage 18	Week 6 (Days 44-48)
Stage 19	Week 7 (Days 45–51)
Stage 20	Week 7 (Days 51–53)
Stage 21	Week 8 (Days 53-54)
Stage 22	Week 8 (Days 54-58)
Stage 23	Week 8 (Days 56–60)

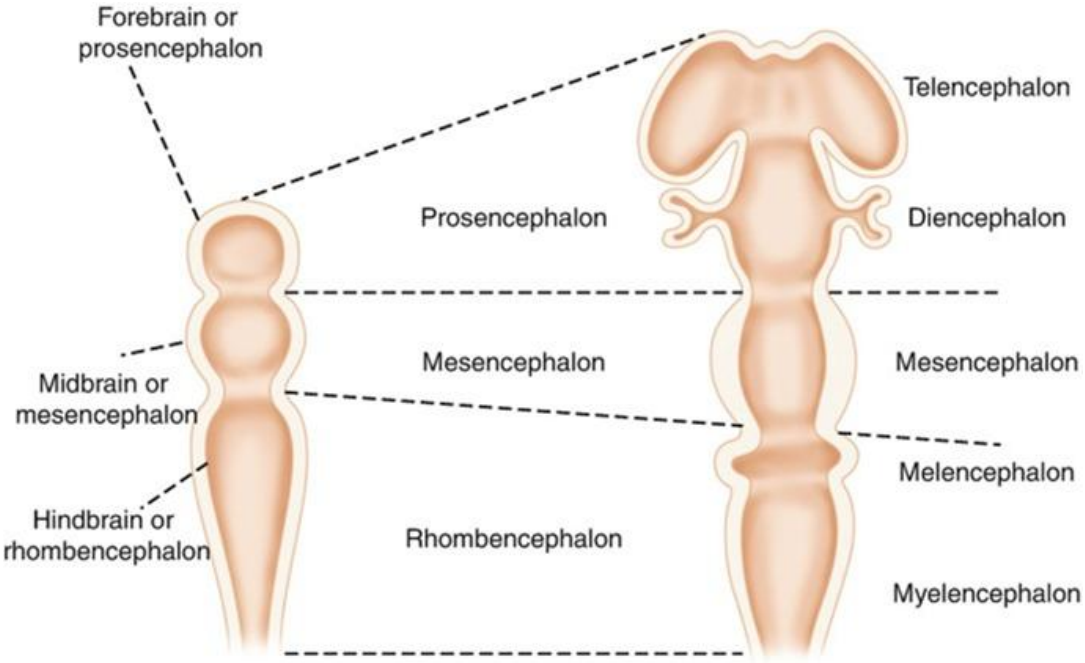

Figure 1.2 The development of the brain. Three primary vesicle including prosencephalon (Forebrain), mesencephalon (midbrain) and Rhombencephalon (hindbrain). Three brain vesicles differentiate into 5 secondary vesicles, prosecephalon divide into (telencephalon and diencephalon), rhombencephalon divide into (melecephalon and myelencephalon) (Carachi and Doss, 2019).

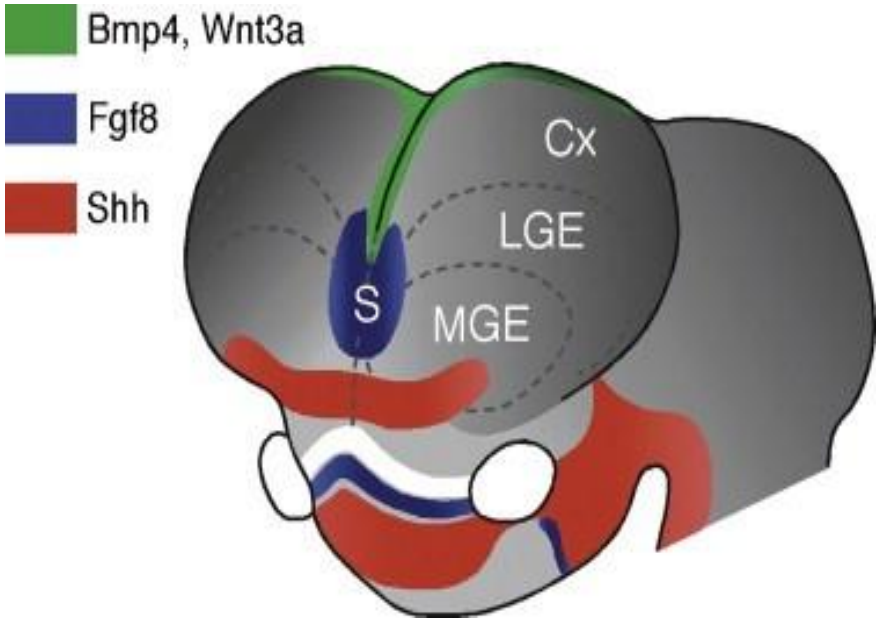

Figure 1.3 The four distinct signalling centres of the forebrain. A rostral patterning centre (RPC) (blue) situated within the anlage of the septum (S) that secretes fibroblast growth factors (Fgfs); a caudodorsal centre (green) known as the cortical hem that secretes wingless/integrated (Wnts) and bone morphogenetic proteins (BMPs); a ventral centre (red) that secretes sonic hedgehog (Shh). Abbreviations: Cortex (CX), Lateral ganglionic eminence (LGE), Medial ganglionic eminence (MGE), Septum (S) (Source: (Hoch et al., 2009)).

1.2 Early development of the telencephalon

The anterior neural plate develops into the prosencephalon, which is later partitioned into the telencephalon and the diencephalon (Hébert and Fishell, 2008). The embryonic telencephalon generates a variety of neuronal and glial cells that follow complex migration patterns to attain their definitive locations in the mature cerebral cortex and basal ganglia (Schuurmans and Guillemot, 2002). The telencephalon is divided into ventral subpallium and dorsal pallium regions which give rise to basal ganglia and cerebral cortex respectively. The dorsal telencephalon generates primarily glutamatergic neurons and can be divided into the following: the dorsal pallium (DP), which is the anlage of the neocortex; the lateral pallium (LP), which produces the olfactory cortex; the ventral pallium (VP), which produces the claustroamygdaloid complex; and the medial pallium (MP), which gives rise to the archicortex, including the hippocampus. Each of these pallial domains develops into a specific region of the mature brain. The ventral telencephalon comprises two separate progenitor domains: the lateral ganglionic eminence (LGE) and the medial ganglionic eminence (MGE) (Figure 1.4) (Puelles et al., 2000, Hébert and Fishell, 2008).

In rodents, the pallium and subpallium are primarily distinguished by the characteristic expression of certain transcription factors in each region, with their expression regulated by gradients of soluble morphogens (FGF, SHH, BMP) released from forebrain signalling centres. The pallium is distinguished by the expression of PAX6, EMX1, EMX2, and TBR1, whereas transcription factors such as GSH, DLX, and NKX are only expressed in the subpallium (Anderson et al., 1997, Pabst et al., 2000, Monuki et al., 2001). The graded expression of dorsally and ventrally expressed transcription factors in the pallium and subpallium further subdivides these into numerous progenitor domains that give rise to a large diversity of unique neuronal subtypes.

The subpallium proliferative zone is categorised into several regions known as ganglionic eminences (GE), which correlate to their anatomical positions: MGE, LGE, and CGE. Gene expression and fate mapping studies have demonstrated that three subpallial domains can be further partitioned into smaller domains, hence enhancing the neuronal variety generated in these locations (Wonders and Anderson, 2006, Flames et al., 2007). In contrast to the pallium, the GE serves as a source of neural types that occupy not only subpallial regions such as the striatum, globus pallidus, and portions of the amygdala, but also give rise to several GABAergic neuron subtypes that migrate tangentially into the cortex and olfactory bulb. The

MGE is recognised as the source of projection neurones in the globus pallidus and is also a major source of cortical GABAergic neurones (Lavdas et al., 1999, Anderson et al., 2001, Wonders and Anderson, 2006). Whereas the LGE serves as the origin of projection neurones in the striatum and interneurons in the olfactory bulb (Stenman et al., 2003). Although the CGE is characterised solely as caudal extensions of the MGE and LGE, numerous investigations have established that the CGE possesses its own distinct identity and serves as a source of neuronal types that are discrete from those produced in the MGE and LGE (Nery et al., 2002, Corbin et al., 2003, Wonders and Anderson, 2006).

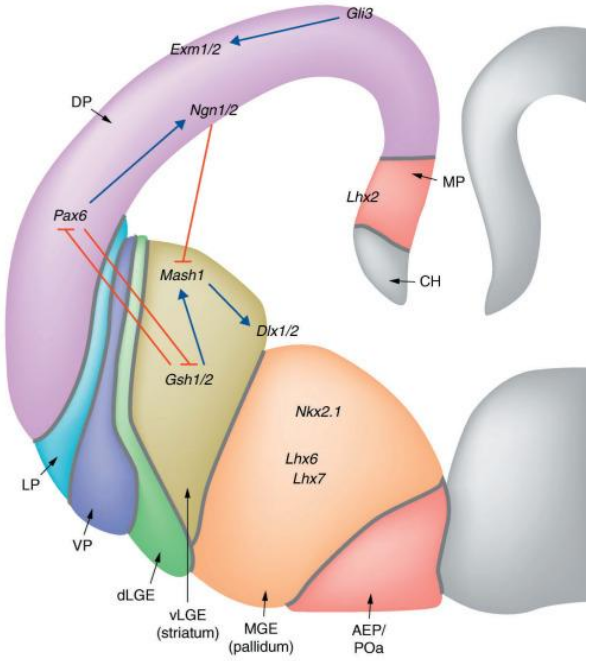

Figure 1.4 The subdivision of the telencephalon. Schematic coronal section illustrating the subdivision of the telencephalon as indicated by the expression of specific transcription factors. The pallium is partitioned into medial, dorsal, lateral, and ventral pallial regions. The subpallium is separated into the medial and lateral ganglionic eminences. Abbreviation medial pallium (MP), dorsal pallium (DP), lateral pallium (LP), ventral pallium (VP), cortical hem (CH), dorsal lateral ganglionic eminence (dLGE), ventral lateral ganglionic eminence (vLGE), medial ganglionic eminence (MGE), Anterior entopeduncular (AEP) (Evans et al., 2012).

1.3 Development of the Diencephalon

During early embryogenesis, the diencephalon originates from the prosencephalon (Kiral et al., 2023). The prosencephalon is subdivided into the telencephalon anteriorly, and the diencephalon posteriorly. The diencephalon is divided into four major neuroepithelial domains: the pretectum, thalamus, epithalamus, and prethalamus (Jessell and Sanes, 2000, Colas and Schoenwolf, 2001, Puelles and Rubenstein, 2003). The orientation of the diencephalic structures can be explained by two contrasting models: the columnar and the prosomeric models. According to the columnar model, the diencephalon can be divided dorsoventrally into the epithalamus, the dorsal and ventral thalamus, and the hypothalamus (Figure 1.5 A) (Herrick, 1910, Kuhlenbeck, 1973, Nakagawa, 2019). However, according to the prosomeric model (Puelles and Rubenstein, 2003), it is possible to draw a rostrocaudal axis that follows the curvatures observed in the developing brain: prosomeres, prosomere 1 (p1/pretectum); prosomere 2 (p2/thalamus); and prosomere 3 (p3/prethalamus). The dorsal and ventral thalamus were renamed the thalamus and the prethalamus, respectively (Figure 1.5 B) (Martinez-Ferre and Martinez, 2012). The zona limitans intrathalamic (ZLI) is a narrow strip of cells that separates the prethalamus and the thalamus(Kuhlenbeck, 1937). The thalamus and epithalamus are derived from the p2, and the prethalamus from the p3 (Nakagawa, 2019).

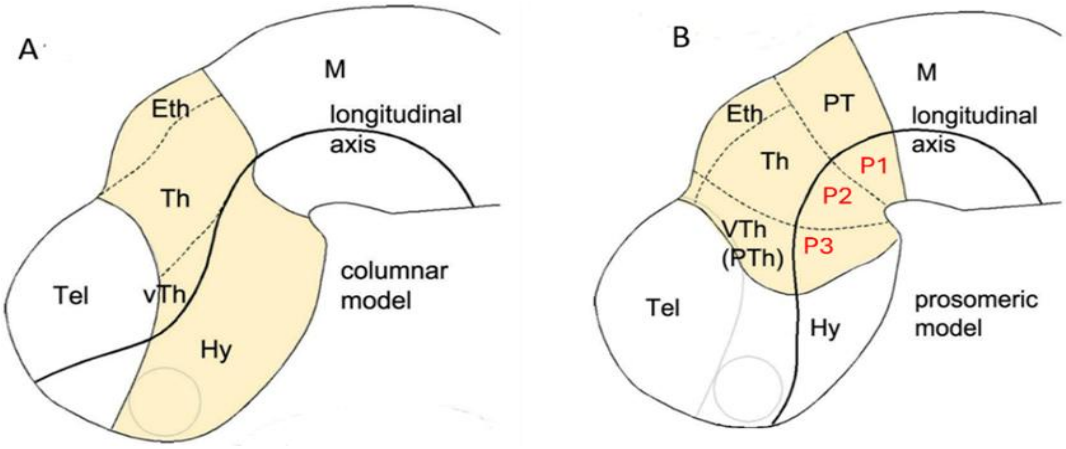

Figure 1.5. Schematic representation of the diencephalon in a mouse, embryonic day (E10) lateral view. (A) The columnar model divides the diencephalon into four distinct regions: the epithalamus, thalamus, ventral thalamus, and hypothalamus. In contrast, (B) the prosomeric model classifies the diencephalon into three prosomeres: prosomere 1 (P1), which corresponds to the pretectum; prosomere 2 (P2), which includes the epithalamus and thalamus; and prosomere 3 (P3), which consists of the ventral thalamus, also known as the prethalamus. The following abbreviations are used: Tel for telencephalon, Hy for hypothalamus, vTH for ventral thalamus, Eth for epithalamus, PT for pretectum, PTh for prethalamus, Th for thalamus, and (M) for mesencephalon. (Source: (Martinez-Ferre and Martinez, 2012)).

1.4 Development of the Thalamus and Epithalamus (p2)

The epithalamus engenders the pineal gland, an endocrine organ that secretes melatonin, is involved with circadian rhythm, and is responsible for puberty, along with the habenula (Ha) nuclei, which connect with the limbic system (Donnelly, 2011), and the stria medullaris (Hikosaka, 2010). The Ha nuclei are involved in motor and cognitive actions, as well as emotional responses (Hikosaka, 2010).

The thalamus, the largest part of the diencephalon, is a bulb-shaped structure that lies on top of the brain stem, on either side of the third ventricle, and between the cerebral cortex and the mid-brain (Vinod Jangir Kumar, 2017). It plays a central role as a relay centre for processing sensory and motor information, and regulates sleep, alertness, consciousness, and cognition (Sherman and Guillery, 2002, Sherman and Guillery, 2006, Sherman and Guillery, 2011). The processing of sensory information from different inputs requires different subsets of neurons that perform specific functions, and are clustered to form higher and first order thalamic nuclei. Understanding the development of thalamic nuclei is important for elucidating the origins of behaviour (Nakagawa, 2019). The progenitor cells that are responsible for the formation of different sets of neurons in the thalamus receive patterning signals from nearby tissues, and divide along the third ventricle in the ventricular zone (VZ) (Nakagawa and Shimogori, 2012). Postmitotic neurons from the thalamic progenitor cells, from the ventricular epithelium, migrate towards the mantle layer and form thalamic nuclear aggregates (Nakagawa and Shimogori, 2012). The transcription factor Pax6 is essential for the development of the diencephalon at the earliest stage; it is later progressively downregulated in these progenitors and is not expressed in postmitotic thalamic neurons (Walther and Gruss, 1991, Mastick et al., 1997, Kiecker and Lumsden, 2004), Pax6 is also very important for developing thalamocortical axons (TCAs) which connect the thalamus to the cortex (Kawano et al., 1999, Pratt et al., 2000, Jones et al., 2002, Hevner et al., 2002). The homeodomain transcription factor, gastrulation brain homeobox-2 (GBX2), maintains the neuronal identity in the thalamus (Bulfone et al., 1993, Puelles and Rubenstein, 1993). GBX2 is excluded from the VZ of the thalamus (Bulfone et al., 1993, Nakagawa and O'Leary, 2001), becoming restricted to the postmitotic neurons (Chen et al., 2009).

The thalamic complex is divided into the rostral and the caudal-thalamus (pTh-R and pTh-C), according to two different neuronal populations. The pTh-R lies close to the MDO/ZLI, and contains GABAergic inhibitory neurons. The caudal thalamus lies away from the MDO/ZLI,

and contains glutamatergic projection neurons (Vue et al., 2009; Hagemann and Scholpp, 2012). Two different thalamic progenitor domains have been delineated by gene expression and fate mapping studies. Rostral thalamus progenitor domain can be expressed by marker genes such as Achaete-scute family bHLH transcription factor 1 (ASCL1) and NK2 homeobox 2 (NKX2.2), while the caudal thalamic progenitor domain (pTh-C) expresses the glutamatergic neuronal markers, Neurogenin1/2 (NGN1) and (NGN2), gastrulation brain homeobox-2 (GBX2), oligodendrocyte transcription factor 3 (OLIG3), and SRY-box transcription factor 2 (SOX2) (Vue et al., 2007, Jeong et al., 2011, Nakagawa and Shimogori, 2012). In contrast, the oligodendrocyte transcription factor (OLIG3), which belongs to the basic helix-loop-helix (bHLH) transcription factor family, is localised throughout the thalamic ventricular layer, and belongs to two distinct domains (Figure 1.6) (Vue et al., 2007).

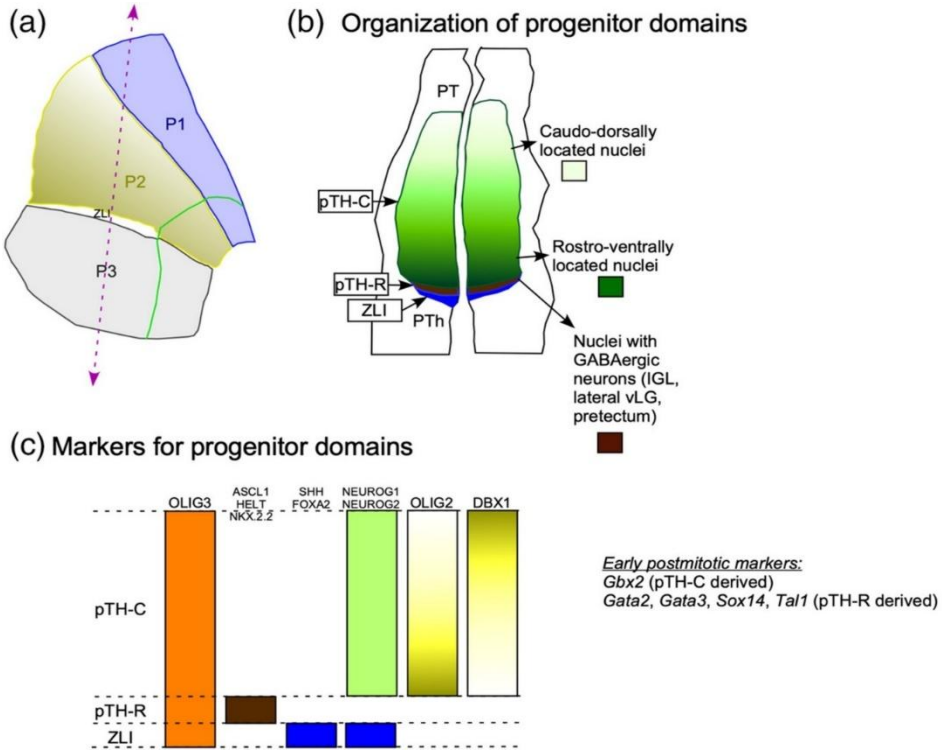

Figure 1.6 The diencephalon progenitor domains and instances of transcription factor expression patterns in mice. (A) Schematic, parasagittal view of the diencephalon based on the prosomeric model which divided into Prosomere 1(P1), prosomere 2 (P2), prosomere3(P3). (B) shows the organization of progenitor domains, which include pretectum, the thalamus is anatomically structured into two distinct regions: the caudal-posterior progenitor domain (pTH-C; green), the rostral-anterior progenitor domain (pTH-R; brown) and zona limitans (ZLI; blue), and last progenitor domains is prethalamus. (C) Marker expression in thalamic progenitor domains, OLIG3 expressed in the whole progenitor domain, DBX1, OLIG2, NEUROG1, NEUROG2 expressed in pTH-C, SHH, FOXA2 expressed in ZLI and ASCL1, HELT and NKX2.2 expressed in Pth-R. Abbreviations: pretectum (PT), prethalamus (PTh), and zona limitans intrathalamica (ZLI). (Source:(Nakagawa, 2019)).

1.5 SHH, FGF, and WNT During Thalamus Development

1.5.1 SHH and ZLI

The ZLI acts as central boundary of the thalamus that divides the prethalamus and the thalamus during neural tube development. The cells within the ZLI are known as the 'mid-diencephalic organizer' (MDO) and express three signalling molecules (SHH, WNT, FGF). These proteins released are linked to local organizing activity in other regions of the brain (Hagemann and Scholpp, 2012). SHH is an important protein that plays an essential role in development and cause neurodevelopmental disorders attributed to thalamic dysfunction (Nakagawa and Shimogori, 2012). Previous studies that used mice suggested that SHH is an essential signalling molecule for the growth of the thalamus (Ishibashi and Mcmahon, 2002). This *Shh* expression initiates at the ZLI ventral edge and extends to the surface along the diencephalic alar plate in chick embryo (Vieira et al., 2005). In addition, *Shh* also controls the expression of several transcription factors and genes involved in the regionalization of the diencephalon and thalamic cell fate determination, including its own regulation, such as *Olig2, Olig3, Ngn, Sox14, Pax6, Nkx2.2* and SIX Homeobox 3 (*Six3)* (Nakagawa, 2019). A study conducted in chicks showed that the ectopic production of the SHH protein in the caudal diencephalon and mesencephalon causes the upregulation of the *Gbx2* gene and the downregulation of the *Pax6* gene (Kiecker and Lumsden, 2004, Vieira et al., 2005).

The differentiation processes of these neurons in the thalamus are highly dependent on the morphogen activity of *Shh*. In high concentrations, *Shh* causes the development of the rostral thalamus, while in low concentrations it causes the development of the caudal thalamus (Vue et al., 2009, Jeong et al., 2011). This conclusion was supported by experiments that used different animal models and showed that a blockage of the *Shh* pathway causes a reduction of the caudal thalamus. However, the establishment of the distinct boundary between the rostral and the caudal thalamus is the result of the interplay of several other factors. For example, the expression of hairy-like factor 6 (*Her6)* determines the neuronal identity. The presence of *Shh* in the rostral region activates Ascl1 in cells expressing *Her6*, and in the caudal region activates Ngn1 expression in cells with a minimal expression of *Her6* (Hagemann and Scholpp, 2012). The differentiation of the glutamatergic neurons and the GABAergic neurons is dependent on the expression of the two genes, *Ngn1* and *Ascl1*, by their respective progenitor cells (Figure 1.7 B).

1.5.2 FGF

The role of FGF signalling, along with SHH and WNT signalling, in the development of the diencephalon has been known for a long time (Hébert, 2011). Specifically, FGF15 and FGF19, which act downstream of SHH, play a crucial role in the development of the thalamus (Miyake et al., 2005). These proteins secreted from the prosencephalon act as morphogens by forming gradients, and influence the development and patterning of the embryo. Previous studies reported that the blockage of *Fgf19* expression, or of its receptor *Fgfr3*, causes the downregulation of production of prethalamic GABAergic inhibitory neurons, and *Ascl1* positive GABAergic neurons in the rostral thalamus, respectively (Miyake et al., 2005, Kataoka and Shimogori, 2008). In contrast, increased FGF signalling broadens the rostral thalamic area, causing a shift in the position of the sensory nuclei of the caudal thalamus (Kataoka and Shimogori, 2008). This suggests that FGF signalling plays an essential role in the GABAergic neuron development in the prethalamus, and in the rostral thalamus (Figure 1.7 C). Furthermore, FGF signalling also influences glutamatergic neuron development in the caudal thalamus. The reduction of *Fgf8* activity in the diencephalon was shown to be linked to dosage-dependent changes in the epithalamus. Specifically, the Ha nuclei and pineal gland are either reduced or lacking in Fgf8 hypomorphic mice, the study of which revealed the presence of reduced *Gbx2* expression in the thalamic neuroepithelium of the caudal thalamus in *Fgf8* mutants at E11.5 (Martinez-Ferre and Martinez, 2009). It is known that the dorsal part of the diencephalon shows a predominant expression of *Fgf8*, specifically in the dorsal tip of the MDO, and in the epithalamus, while *Fgf-15* and *Fgf-19* are seen only in the ventral area of the thalamus. The role of FGFs and FGFRs, other than FGFR3, in the development of the human brain is not known, and the individual molecular mechanisms regulating the diencephalic patterning are yet to be clearly understood.

1.5.3 WNT

Previous research suggested that WNT signalling plays a crucial role in the development of the thalamus (Bluske et al., 2009). Several studies also demonstrated that WNT induces differentiation of the posterior forebrain, while its absence causes differentiation of the anterior forebrain (Braun et al., 2003). This conclusion was supported by the induction of Iroquois-type transcription factor (IRX3), and the suppression of SIX3 transcription factors by WNT in the chick embryonic caudal diencephalon (Braun et al., 2003). During ZLI formation, WNT

signalling is required for *Shh* expression towards the dorsal side, between the thalamus and the prethalamus (Martinez-Ferre and Martinez, 2012). Specifically, WNT continues to be expressed in the thalamus during patterning and neurogenesis, even during the late stages (Quinlan et al., 2009, Hagemann and Scholpp, 2012). Meanwhile, LIM Homeobox (LHX) transcription factors, along with GBX2 and neurogenin (NGN), are among the few transcription factors that are expressed in the thalamus and have been characterised. Therefore, WNT and LHX factors work together to form mature postmitotic thalamic neurons (Figure 1.7 A and E) (Hagemann and Scholpp, 2012). This was supported in the study by Zhou et al. (2004) where a mutation in the WNT co-receptor Lrp6 resulted in defects in the expression of Lef1. In addition, the upregulation of WNT activity, along with its target genes, *Axin2* and *Pcdh10b*, was observed in *Lhx2/Lhx9* morphant embryos in the VZ of the thalamic neuroepithelium, while *Lef1* was downregulated. This suggested that WNT signalling occurs in phases, and that the second phase is required for thalamic neuronal differentiation in the mantle zone, revealing the interdependence of WNT, SHH, and FGF signalling pathways and transcription factors (Peukert et al., 2011), although further studies are required to understand their influence on one another during thalamus development.

Some previous studies suggested that Lhx2/Lhx9 is important for the completion of neurogenic development in the thalamus. This was highlighted by a study that showed a high expression of delta-like protein A (*DeltaA*), Ngn1, and protocadherin 10b (*pcdh10b*), and no expression of Inhibitor of DNA Binding 2 (Id2) and lymphoid enhancer binding factor 1 (Lef1) in zebra fish morphant embryos. Thus, although neuronal progenitors were formed, their differentiation ceased in the later stages (Hagemann and Scholpp, 2012). It is important to note that *Pcdh10b*, which is expressed in the ventricular zone and is regulated by LHX proteins, and Id and Lef1 are activated by WNT signalling in the thalamus (Figure 1.7 A and E) (Jones and Rubenstein, 2004, Peukert et al., 2011).

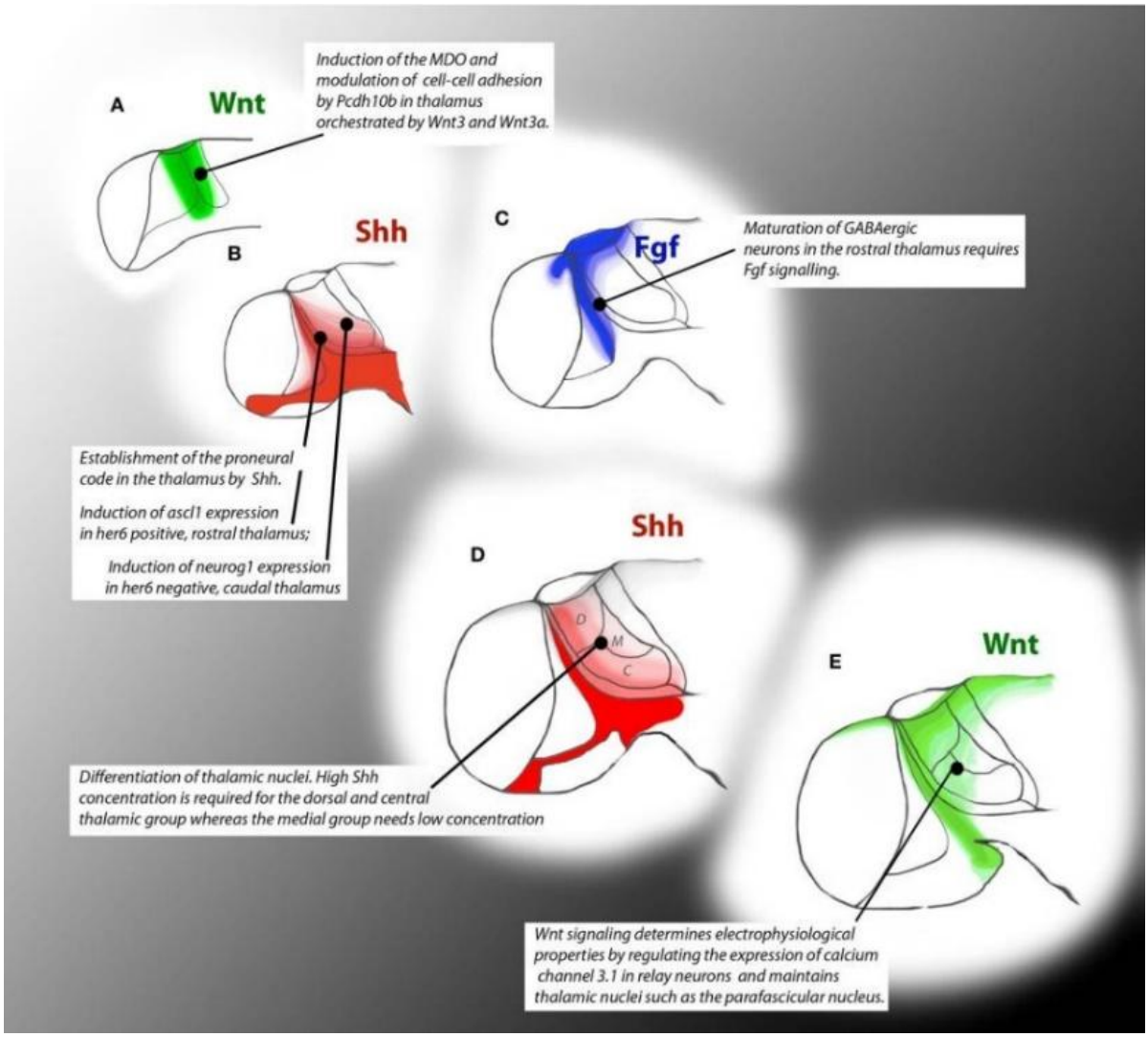

Figure 1.7 Schematic chronology of signalling events throughout the development of the thalamus in zebrafish embryos. The coloured patterns indicate the specific regions of impact of the signalling pathways shown. (A) Wnt signals from the caudal forebrain are necessary to initiate the MDO, and to facilitate the division of the thalamus. (B) Shh signalling is necessary to initiate neurogenesis by activating the proneural genes. (C) Fgf signalling affects the development of GABAergic neurones. (D) Shh signal delineates precisely the region of the thalamic nuclei. (E) Wnt signalling coordinates neurogenesis at 48 hours post-fertilization by modulating post-mitotic features of thalamic neurones (Source: (Hagemann and Scholpp, 2012)).

1.6 Thalamic Nuclei

Discrete groups of cells are recognizable in histological sections of the thalamus and these are termed ‘nuclei’. The thalamic nuclei are classified according to i) their position in the thalamus, ii) their afferent and efferent connections, and iii) their functions. More than 40 distinct nuclei have been identified in the thalamus, according to their cell structure, anatomical connections, gene expression, and functions (Puelles et al., 2012a). In mice, thalamic nuclei are not clearly distinguished at embryonic day 12.5 (E12.5), only becoming distinct by E16.5 (Nakagawa and O'Leary, 2001). The first nuclei to form are the anterior nucleus (AN) of the thalamus, which is divided into anterodorsal (visual memory, spatial navigation), anteroventral (episodic memory), and anteromedial (emotional, cognitive, and executive functions) (Child and Benarroch, 2013, Perry and Mitchell, 2019) (Figure 1.8). These are separated from other nuclei by the anterior portion of internal medullary lamina, located between the arms of the Y shapes lamina (Jones, 2007).These AN regulate alertness, learning, and memory modulation in the mature brain (Puelles et al., 2012a). Meanwhile, the ventral-anterior and ventral-lateral nuclei (VA, VL, respectively) are involved in motor function. The ventral posterior nucleus (VP), which is also known as the ‘ventrobasal complex’, is located towards the caudal region in the thalamus. It is composed of a ventral posterolateral (VPL) and posteromedial (VPM) nucleus, and is located in both the lateral and medial parts of the thalamus. The VP nucleus is associated with the somatosensory systems, whereas the medial dorsal (MD) thalamic nuclei (Gauthier et al., 2011) are associated with emotional arousal, memory, and feelings of pleasure (Warren et al., 2017). The intramedullary (IMN) (central medial, CeM; central lateral, CL; paracentral, Pc; centromedian, CM; parafascicular, Pf) play a crucial role in arousal and alertness by regulating the excitability levels in the cerebral cortex (Jang et al., 2014), and are also synchronized with the circadian rhythms. The posterior nuclear group consists of the lateral geniculate nucleus (LGN), medial geniculate nucleus (MGN) (Lee, 2013), and the lateral and inferior pulvinar (PulL, PulI) (Baldwin et al., 2017) (Figure 1.8). Auditory information ascends to the inferior colliculus of the midbrain through the cochlear nuclei and the superior olivary complex of the brainstem. This information then arrives in the medial geniculate nucleus in the thalamus and is transmitted to the primary auditory cortex, while the visual inputs from the retina are guided primarily towards the dorsal lateral geniculate thalamic nuclei (dLGN), and reach the visual centres of the cerebral cortex (Vertes et al., 2015, Giraldo-Chica and Woodward, 2017). LGN acts as the first step in the initial visual processing of information (Covington and Al Khalili, 2019). In all, two major regions have been identified in the LGN: the dorsal (dLGN) and ventral

LGN (vLGN). The dLGN receives inputs from the retina, and relays information to the visual cortex, while the vLGN is involved in several functions, including processing and integration from other regions, such as the retina and superior colliculus, and connections to other thalamic nuclei (Figure 1.9) (Nakagawa and Shimogori, 2012). The reticular nucleus is a thin, shell-like structure that surrounds the thalamus. It plays a role in regulating the flow of information between the thalamus and the cortex (Pinault, 2004). This nucleus sends projections to the anterior, dorsal, intralaminar, posterior, and ventral thalamic nuclei (Guillery and Harting, 2003).

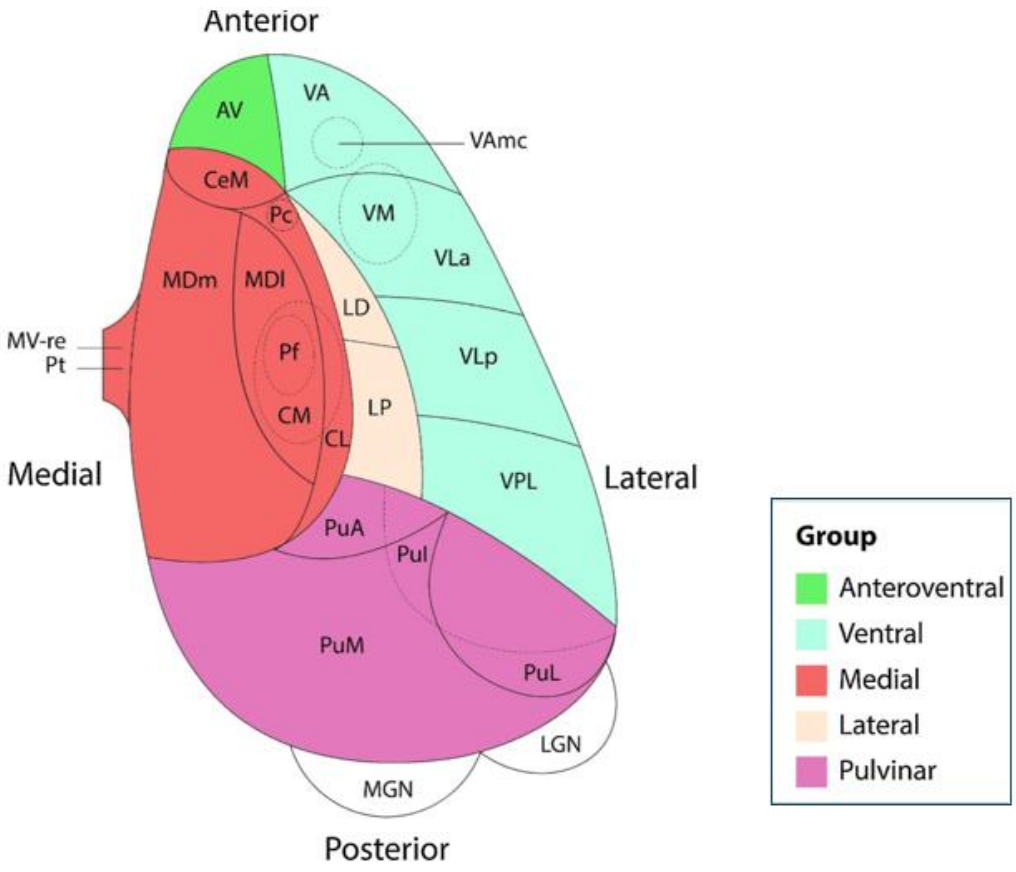

Figure 1.8. Classification of thalamic nuclei in human, showing several nuclei and their positions. Abbreviations: anteroventral nucleus (AV), ventral anterior nucleus (VA), ventromedial nucleus (VM), ventral lateral anterior nucleus (VLa), ventral lateral posterior nucleus (VLp), ventral posterolateral nucleus (VPL), lateral dorsal nucleus (LD), lateral posterior nucleus (LP), central medial nucleus (CeM), paracentral nucleus (Pc), lateral mediodorsal nucleus (parvocellular) (MDl), medial mediodorsal nucleus (magnocellular) (MDm), parafascicular nucleus (PF), centromedian nucleus (CM), central lateral nucleus (CL), reuniens nucleus (MV-re), paratenial nucleus (Pt), anterior pulvinar nucleus (PuA), inferior pulvinar nucleus (PuI), lateral pulvinar nucleus (Pul), medial pulvinar nucleus (PuM), lateral geniculate nucleus (LGN), medial geniculate nucleus (MGN) (Source: (Keun et al., 2021).

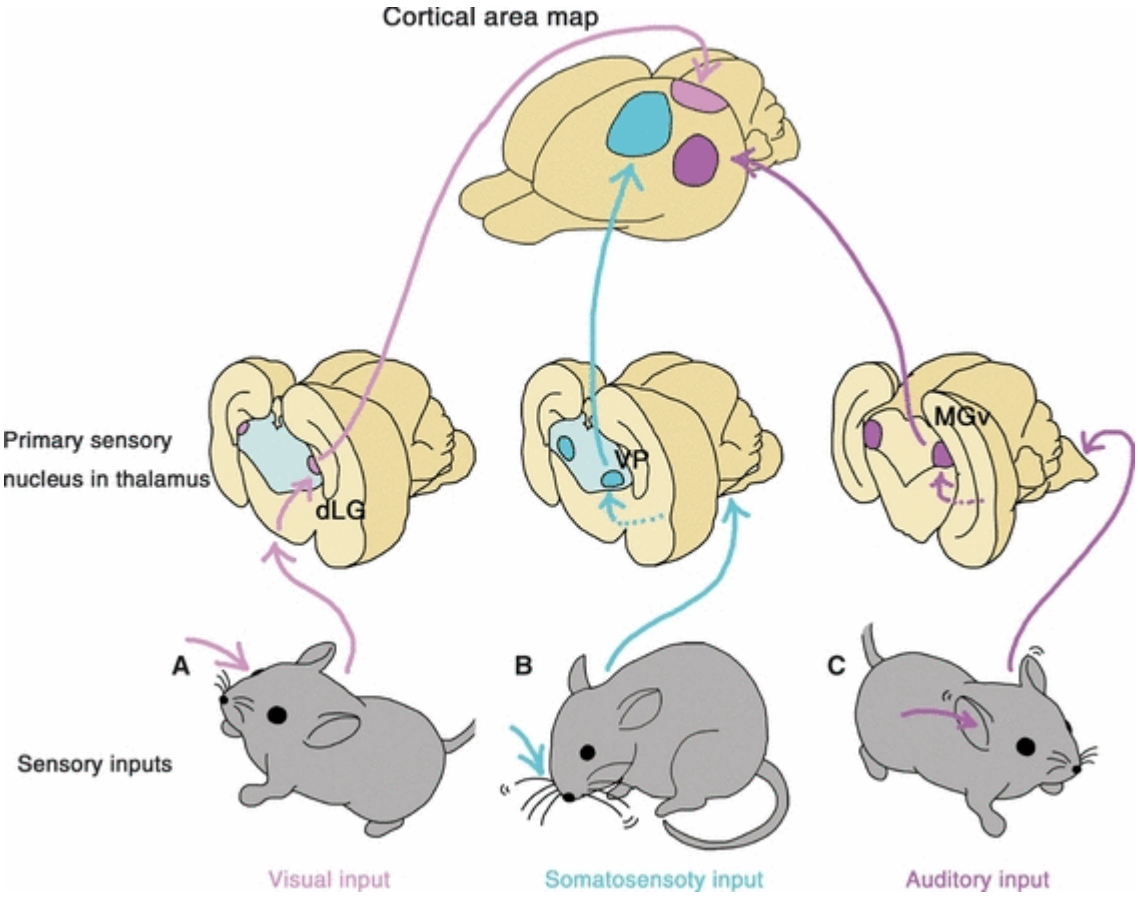

Figure 1.9. Schematic representation of the sensory input pathway in the central nervous system (CNS). (A) Visual information is transmitted to the dLG in the thalamus, which subsequently transmits it to the primary visual cortex. (B) The primary somatosensory cortex receives somatosensory information from rodent whiskers and the epidermis, which is transmitted to the VP nuclear complex via the brainstem and the spinal cord. (C) The inferior colliculus of the midbrain is reached by auditory information through the cochlear nuclei and superior olivary complex of the brainstem. This information is subsequently transmitted to the primary auditory cortex by the MGv in the thalamus. Abbreviation:ventral posterior (VP), dorsal lateral geniculate nucleus (dLGN) and medial geniculate nucleus (MGv), and terminates in the somatosensory system. The auditory impulse terminates in the auditory cortex (Source: Adapted from (Nakagawa and Shimogori, 2012) .

Thalamic nuclei are classified into two types reflecting their inputs: first order (FO), and nuclei and higher order (HO) nuclei. FO nuclei receive information from peripheral sensory organs and subcortical structures and convey it to primary sensory and motor cortical areas. The LGN: visual; the medial geniculate nucleus (MGN): auditory; the VPM/VPL: somatosensory; and the VL: motor, are among these nuclei. Sensory and motor information is transferred to layer 4 of the primary sensory and motor cortical regions, which then projects back to the same thalamic nucleus from which it received the input (Giraldo-Chica and Woodward, 2017). Unlike FO nuclei, HO nuclei, such as the mediodorsal nucleus and the pulvinar (Pul), receive most of their input directly from the cortex, cortical layer 5 of the PFC and the posterior parietal association region, respectively. Thus, the driving excitatory input to the thalamus comes from the sensory organs/subcortical areas for the FO nuclei, or cortical layer 5 in the case of the HO nuclei (Figure 1.10).

In contrast, reciprocal cortical-thalamic projections come from cortical layer 6, limiting thalamic activity by activating GABAergic neurons in the thalamic reticular nucleus, which is a small sheet of neurons derived from prosomere 3 that envelopes the thalamus. This configuration enables the cortex to modify, or block, incoming sensory/cortical data. As the principal input to these nuclei comes from the cortex, and the thalamocortical projections are more diffuse than FO relay networks, the HO nuclei play an important role in controlling cortical activity and coordinating activity amongst the cortical regions (Sherman and Guillery, 2011).

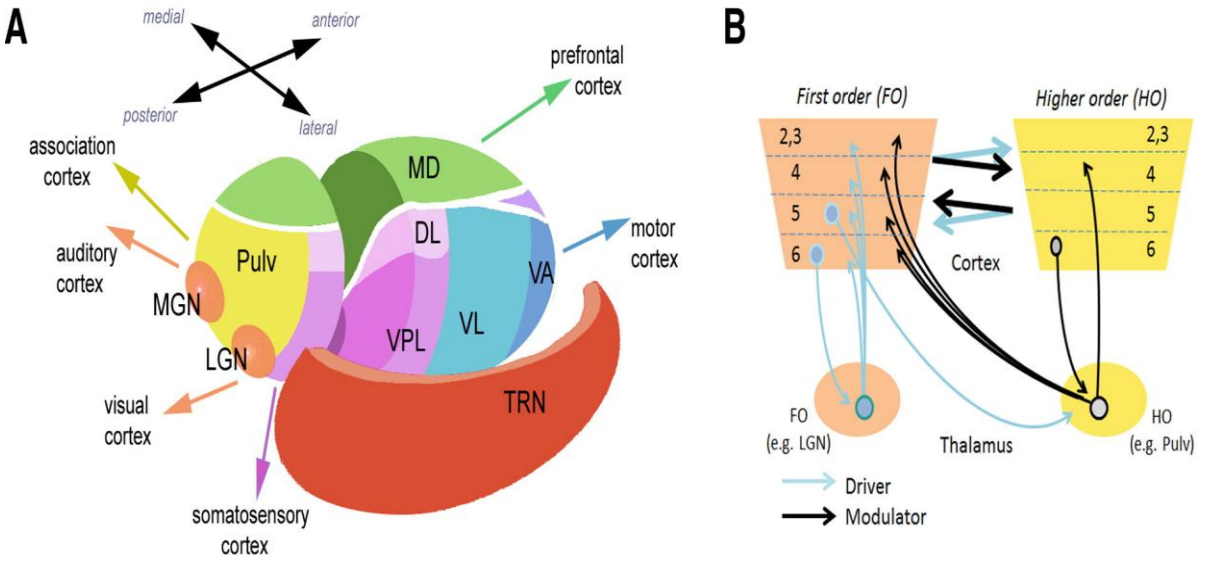

Figure 1.10. Illustrates two types of thalamic nuclei based on their cortical input in mice. (A) MGN to auditory cortex, LGN to visual cortex, VPL, DL to somatosensory cortex, VA, VL to motor cortex, MD to prefrontal cortex, Pulv to association cortex. is the ventral anterior nucleus, (B) Higher-order thalamic nuclei such as pulvinar and mediodorsal that are linked to higher cognitive processes receive input from and send output to the cortex. First-order thalamic nuclei such as the lateral geniculate nucleus receive input from the peripheral system and relay it to the cortex. Abbreviations: Pulvinar (Pulv), ventral posterior latersl (VPL), Dorsal lateral (DL), ventral lateral (VL), ventroanterior (VA), medial dorsal (MD), medial geniculate nucleus ventral (MGN), lateral geniculate nucleus dorsal (LGN) (Source (Sherman, 2012)).

1.7 Thalamocortical Afferents (TCA)

The thalamocortical (TC) and corticothalamic (CT) pathways are two of the most important pathways in the brain for transmitting sensorimotor information (Figure 1.11). The TC relays sensory information from the retina, cochlea, muscles, and skin to the neocortical sensorimotor regions via the thalamus, the major subcortical sensorimotor relay. By transmitting information from the cortex to the thalamus via the CT pathway, the feedback loop is completed. A recent study by Alzu'bi et al. (2019) indicated that at least some TC axons may innervate the cortical presubplate as early as 8 PCW. The ventrolateral thalamus extends TCA to the diencephalic/telencephalic boundary (DTB) boundary at 7.5 PCW, the presubplate (pSP) by 9.5 PCW, and they enter the intermediate zone (IZ) of the cortical wall at 11 PCW. These axons innervate the pSP and deep cortical plate (CP) between 12 and 14 PCW. Eventually, these two structures merge to form a large subplate, which is a characteristic feature of primates (Kostovic and Rakic, 1990, Wang et al., 2010, Duque et al., 2016).

The development of the CT pathway exhibits a similar pattern of instructive connectivity. Subplate neurons extend and form connections with reticular thalamic neurons prior to the establishment of connections between neurons from the deep layers of cortex (layers 5 and 6). The innervation of the subplate by TCA are thought to serve as a guide for the CT axons as they travel to their destinations in the thalamus. Once the TC and CT pathways are completed, the subplate neurons' connections are retracted and the cells die gradually (Chatterjee et al., 2012). The work by Quintana-Urzainqui et al. (2020) established the significance of the gene-expression gradients in the thalamus and their sensitivity to guidance queues in the early stages of TCA path finding (Quintana-Urzainqui et al., 2020). A study recorded thalamocortical projection anomalies resulting from the disruption of diencephalic development due to the loss of Pax6, foxg1, and Mash1 in mice. The thalamocortical tract does not develop properly in Pax6 deletion in mice; axons were noted to descend through the thalamus without infiltrating the telencephalic tissues (Pratt et al., 2002, Pratt et al., 2000). In Mash1-deficient mouse embryos, the transitory afferent tract fails to develop, and the thalamocortical tract does not invade the telencephalon (Pratt et al., 2002).

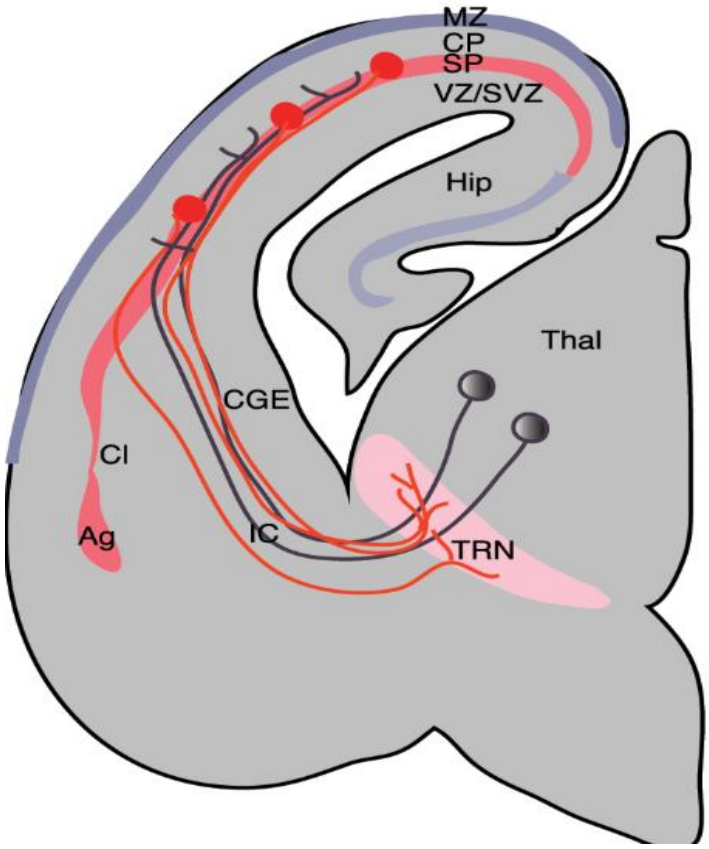

Figure 1.11. The relationships between the developing thalamocortical projections and the cortical SP zone, and the interactions between corticothalamic projections and the thalamic reticular nucleus, during mouse development at embryonic day 15. During early embryonic development, corticofugal (red) and thalamocortical (black) axons initiate extension towards each other and reach their respective targets by E15. Nevertheless, both the corticofugal projections from the supraoptic layer (SP) and layer 6 fail to reach their intended destinations, gathering instead in the thalamic reticular nucleus (TRN; pink), whereas the thalamocortical projections halt in the SP (red). Both compartments consist mostly of transitory cells that are incorporated into circuits during the initial phases. Observations of fibre decussation in the TRN and SP suggest the occurrence of rearrangements during anatomical development. Abbreviations: amygdala (Ag), claustrum (Cl), hippocampus (Hip), caudal ganglionic eminence (CGE), marginal zone (MZ), globus pallidus (GP), and internal capsule (IC), thalamic reticular nucleus (TRN). (Source: (Bandiera and Molnár, 2022))

1.8 Expression of key molecules that have been shown to guide the development of the thalamus in animal models.

This section discusses what is currently known about the genes FOXP2, GBX2, ZIC4 which are the key genes for the development of the thalamus, as shown by gene knockdown experiments. ASCL1, SP8, OLIG2, PAX6, GAD67, OTX2, NR2F2, NR2F1 were also studied. These are the genes that are important markers for a variety of cell types in the developing prosencephalon.

1.8.1 Forkhead box protein (FOXP2)

FOXP2 is a transcription factor that belongs to the forkhead family, the mutation of which is often found in patients with language disorders (Ebisu et al., 2017). Mutations of the *FOXP2* are also known to be implicated in the development of schizophrenia (SZ) in humans (Tolosa et al., 2010). The work by Tolosa et al. (2010) established the relationship between *FOXP2*, language impairment, and SZ, since SZ shares symptoms with other language related diseases (Li et al., 2013). Furthermore, the isolation of the transcriptional targets of FOXP2 revealed its capacity to regulate the genes related to the development of thalamus identity and, most importantly, the genes that are implicated in the development of SZ (Vernes et al., 2007, Tolosa et al., 2010, Li et al., 2013). The study conducted by Ebisu et al. (2017) indicated that there is an expression of FOXP2 protein in the developing thalamic cells in E14 mice. A general increase in the protein levels in the posterior region was observed, and a low level of expression was observed in the anterior thalamus. This gradient level of expression observed in E12 and E14 was lost by E16, as the expression became restricted to certain thalamic nuclei. In the mice with *Foxp2* genes that were mutated (Foxp2 (R552H) knock-in) in such a way that *Foxp2* expression was minimized, the ventral posterior nuclei were found to be smaller in size than in the non-mutated mouse sample. This indicated that *Foxp2* is important for posterior thalamic nuclei development. This mutation of Foxp2 in the thalamus highlighted the need to understand how the expression of FOXP2 with other factors guides the development of human thalamic nuclei development.

1.8.2 Gastrulation brain homeobox-2 (GBX2)

A homeobox gene is a sequence of DNA coiled around 180 base pairs, located within the genes, which functions in the morphogenesis of animals, plants, and fungi (Chen et al., 2009, Mallika et al., 2015). GBX2 is a dose dependent transcription factor that influences the regulation of the normal expression of other resultant genes (Jones and Rubenstein, 2004). The expression of GBX2 commences during gastrulation and extends to the late phases of embryogenesis (Chen et al., 2009, Chatterjee et al., 2012). The homeobox gene *Gbx2* is the main marker for defining the thalamus in the prosomere model (Bulfone et al., 1993, Puelles and Rubenstein, 1993). In the diencephalon, Gbx2 expressed in the postmitotic cells and exclude from the ventricular zone in the thalamus (Bulfone et al., 1993, Nakagawa and O'Leary, 2001). GBX2 controls signalling in the feedback systems of post mitotic cells to the dividing progenitor genes (Mallika et al., 2015). Since GBX2 expression is related to the development of the thalamus and the Ha, it is implicated significantly in the development of psychiatric disorders, such as depression and SZ (Mallika et al., 2015). One study in mice demonstrated that *Gbx2* is crucial for establishing the molecular identity of the thalamus. Notably, the elimination of thalamic identity resulting from Gbx2 ablation is linked to a partial transition toward habenular identity (Mallika et al., 2015).

1.8.3 Orthodenticle homeobox 2 (OTX2)

OTX2 is a member of the homeobox-containing transcription factor family that is associated with the Drosophila gene orthodenticle (Simeone et al., 1993). *Otx2* is expressed in the diencephalon, mesencephalon, choroid plexus, and hippocampus anlage in humans. It serves as a marker for this region in the telencephalon, as well as in the isthmus organization, VZ of ganglionic eminence, and periventricular zone of thalamus during the 7-9 week period (Larsen et al., 2010). The *Otx* genes have been demonstrated to regulate several developmental processes and specifically play a crucial role in determining the formation of the developing brain (Acampora and Simeone, 1999, Simeone et al., 2002). Previous studies conducted on rodents demonstrated that *Otx2* is expressed in the prosencephalon and mesencephalon regions of the brain, and has a distinct boundary at the mesencephalic-metencephalic border (Simeone et al., 1992, Acampora et al., 1995, Broccoli et al., 1999, Millet et al., 1999). During later stages of embryonic development, *Otx2* expression is also present in the posterior regions of the forebrain, such as the VZ of the ganglionic eminence, hippocampus, choroid plexus, and diencephalon. In addition, *Otx2* expression is present in the posterior commissure of the

mesencephalon and the cerebellum (Frantz et al., 1994, Rath et al., 2006, Rakic et al., 2009). In zebrafish, the *Otx2* gene is responsible for creating the ZLI, which separates the ventral and dorsal thalamus (Scholpp et al., 2007). In addition, *Otx2* regulates the characteristics and future development of the glutamatergic progenitors in the thalamus by suppressing the differentiation into GABAergic cells. Thus, any dysfunction of OTX2 can lead to neurological and psychiatric diseases, as GABAergic and glutamatergic neurones regulate inhibitory and excitatory networks in the brain (Puelles et al., 2006). The study by Puelles et al. (2003) found that mice with mutations in Otx2 die at birth, and identified that there was an abnormal irregular size and a cell mass in the neuroepithelium at E12. This mass is dispersed randomly in the mantle zone of the thalamus at a later stage (Puelles et al., 2003). Additionally, aberrant axonal growth in the thalamus was identified by (Larsen et al., 2010). Meanwhile, Puelles et al. (2006) presented evidence that supported an important function of OTX2 in the molecular process that determines the identity and fate of glutamatergic precursors in the thalamus by repressing the GABAergic differentiation (Puelles et al., 2006).

1.8.4 SP8

A new member of the SP zinc finger transcription factor gene family named Sp8 was identified by recent studies (Bell et al., 2003, Treichel et al., 2003). SP8 has an essential role in the early patterning of the forebrain and regulates the growth of thalamocortical afferent projections in visual and somatosensory area. In a recent study of the Sp8 knock out (KO) brain, the dLGE was retrogradely labelled via TCA projections from both the visual and the somatosensory cortex (Zembrzycki et al., 2007). In humans, SP8 is a marker for immature GABAergic neurons originating from the caudal ganglionic eminences (Alzu'bi et al., 2017). To date, no studies have explored the expression of SP8 in the thalamus.

1.8.5 Glutamate decarboxylase 1 (GAD67)

Glutamic acid decarboxylase (GAD) catalyzes the conversion of L-glutamic acid to γ-aminobutyric acid, which plays a role in inhibitory neurotransmission (Viñas-Jornet et al., 2014). Multiple previous studies suggested that the adult brain contains two isoforms of GAD, namely GAD65 and GAD67; the numbers 65 and 67 represent the molecular weights of these isoforms in kilodaltons (kDa). These isoforms are produced by two distinct genes that are controlled independently: *GAD2* and *GAD1* (Erlander et al., 1991, Bu et al., 1992). GAD67 is

a protein located in the cytoplasm that consists of 594 amino acid residues. The two isoforms have a 64% amino acid similarity, with the greatest variation observed at the N terminus. As Tavazzani et al. (2014) explained GAD67 is expressed in GABAergic neurones. Moreover, GAD67 provides first the cytoplasmic pool of GABA, which enters the tricarboxylic acid cycle to produce energy, and second is the vesicular pool of GABA (Tian et al., 1999, Lau and Murthy, 2012). The study by Tavazzani et al. (2014) demonstrated the presence of GAD67 in the ventricular, cortical, and marginal zones of the brain. GABAergic and glutamatergic neurons of the forebrain arise from different pools of progenitors. GABAergic neurons of the forebrain are generated principally in the proliferative zones of the ventral telencephalon, prethalamus, and pretectum (Luskin et al., 1993, Mione et al., 1994, Puelles and Rubenstein, 2003). GAD1 (GAD67) catalyses production of 80–90% of total brain GABA, whereas 10–20% is attributable to the activity of the analogous gene, GAD2 (GAD65) (Asada et al., 1997, Condie et al., 1997). In neurons, GAD65 is concentrated in presynaptic terminals (Kaufman et al., 1991, Gaspard, 2020) where a portion of the protein is linked to synaptic vesicles. The estimated protein, consisting of 585 amino acids, has a molecular weight of 65 kD (Pöllänen et al., 2022). The antibody for the 65-kD isoform of GAD65 serves as a biomarker for autoimmune CNS illnesses and, more frequently, for non-neurological autoimmune diseases (McKeon and Tracy, 2017). Given the expression of GAD67 in cytoplasmic pool compared to the presynaptic expression of GAD65, GAD67 is a more useful and widely used marker for GABAergic neurons.

1.8.6 Paired box 6 (PAX6)

Pax6, a gene that codes for a transcription factor with a paired domain and a homeodomain, is expressed widely in the developing forebrain of vertebrates (Walther and Gruss, 1991, Stoykova et al., 1996). *Pax6* is known to be required for normal thalamic development (Parish et al., 2016). The normal size of the pTH-C domain depends on the expression of Pax6. In mice lacking *Pax6,* the ZLI and pTH-R domains undergo expansion, thereby compromising the pTH-C domain (Caballero et al., 2014, Pratt et al., 2000). Thalamic and prethalamic progenitor cells express *Pax6* throughout the initial phases of diencephalic development. Later, it is reduced gradually in these progenitor cells and is not present in postmitotic thalamic neurons (Walther and Gruss, 1991, Mastick et al., 1997, Kiecker and Lumsden, 2004). *Pax6* expressed in the VZ in the lateral ganglionic eminence (Mo and Zecevic, 2008) and in the VZ in the cortex and dorsal thalamus (Englund et al., 2005). It is essential for the formation of thalamocortical

axons (TCAs), which establish connections between the thalamus and the cortex (Kawano et al., 1999, Pratt et al., 2000, Jones et al., 2002, Hevner et al., 2002). Mutation of *Pax6* in mice can develop defects in forebrain structure, including diencephalon and after birth (Hogan et al., 1986, Schmahl et al., 1993, Quinn et al., 1996, Stoykova et al., 1996, Carić et al., 1997, Grindley et al., 1997) and thalamocortical connections do not form (Kawano et al., 1999).

1.8.7 Nuclear receptor subfamily 2/1 group F member 2/1 (NR2F2-NR2F1)

NR2F1/2, which is also known as Chicken ovalbumin upstream promotor-transcription factor 1/2 (COUP-TF 1/2), is expressed mainly in CGE-derived GABAergic neurons in mice (Tripodi et al., 2004). The study by Reinchisi et al. (2012) found evidence that suggested NR2F1 might have a similar function in the development of the human forebrain. At later stages of development, NR2F1 expression spreads in several telencephalic regions: the cerebral cortex (archicortex, neocortex, and paleocortex primordia); the preoptic area; the thalamus; and the lateral, medial, and caudal ganglionic eminences (LGE, MGE and CGE, respectively) (Armentano et al., 2006). NR2F1 is expressed highly in the postmitotic neurons in the lateral geniculate nucleus; mutation of this gene can cause defects of the visual system, optic atrophy and intellectual disabilities (Serra, 2020). A study of mice at E12 demonstrated that *Nr2f1* is expressed strongly in the thalamus of the mouse brain (Bertacchi et al., 2019). Meanwhile, another study of mice showed strong *Nr2f1* expression in the dorsal lateral geniculate nucleus and ventroposterior in the mouse thalamus at E15 (Areas, 2013).

1.8.8 Oligodendrocyte transcription factor 2 (OLIG2)

During CNS development, Olig2 regulates the differentiation of neural precursors to neurons, oligodendrocytes, and astrocytes (Takebayashi et al., 2000). The study by Wang et al. (2021) found that Olig2 is expressed not only in oligodendrocyte precursor cells (OPCs) and oligodendrocytes, but also in some astrocytes in adult mouse CNS. $Olig2^{+}$ cells are particularly abundant in the VZ and subventricular zone (SVZ) of the LGE and MGE (Takebayashi et al., 2000, Tekki-Kessaris et al., 2001), and in the VZ of the dorsal thalamus of the forebrain (Takebayashi et al., 2002). The loss of Olig2 can cause the loss of oligodendrocytes (Szu et al., 2021, Miyoshi et al., 2007). Extant studies in the field suggested that Olig2 regulates interneuron production, a finding indicated by their unique expression patterns in the embryonic brain. Olig2 specifies GABAergic neurons in ganglionic eminences (Jakovcevski and Zecevic, 2005, Jakovcevski et al., 2009).

1.8.9 Achaete-scute family bHLH transcription factor 1(ASCL1)

ASCL1 is a class II basic-helix–loop–helix (bHLH) transcription factor that forms a heterodimer with class I bHLH E-proteins, such as E47/TCF3, to activate certain target genes. During development, *Ascl1* is expressed in distinct populations of neural progenitor domains and glial precursor cells throughout the neural tube, from the spinal cord to the brain (Vue et al., 2020). *Ascl1* is required to regulate and promote neurogenesis in the mammalian brain (Bertrand et al., 2002, Wilkinson et al., 2013). ASCL1 is a proneural transcription factor that is expressed highly in the proliferative zones throughout the rodent ventral telencephalon (Fode et al., 2000). It is expressed in the VZ of the human medial and lateral ganglionic eminence at 6.5 PCW. *Ascl1*$^{+}$ cells are mainly progenitors, as confirmed by double-labelling with cell division marker KI67 (Euiseok J. Kim, 2007). ASCL1 is a marker for all progenitor cells that engender GABAergic neurons, but is also expressed by a subset of intermediate progenitor cells in the human cerebral cortex that produce glutamatergic neurons (Alzu'bi and Clowry, 2019).

1.8.10 Zinc finger proteins *(ZIC4)*

ZIC is a gene code for a small family of zinc-finger transcription factor proteins that play a crucial role in several developmental processes, including the growth and maturation of the neural tissues and the neural crest. The *ZIC* genes are also expressed within the postmitotic cells, located within the cerebellum, and the ganglionic cells of the retina. *Zic4* is localised in the mouse embryonic diencephalon, from E9.6 (Aruga et al., 1996, Gaston-Massuet et al., 2005). Previous studies also indicated that its expression is prominent in the postnatal LGN. Research conducted in mice showed that at E11, the *Zic4* transcripts were present at higher levels in the prethalamic cells and the eminentia thalami. Meanwhile, at E12, the *Zic4* transcripts were more prominent in the thalamus, epithalamus, and prethalamus. As the thalamic nuclei developed, the cells increasingly expressed *Zic4* in the vLGN. The highest concentration of *Zic4* was observed in the vLGN, and the medial regions of the Ha in the epithalamus at birth (Li et al., 2018). However, it is noteworthy that their densities were present in intermediate levels in the dLGN, and in the zona incerta, although expression was observed to be low in the midline thalamic nuclei, for example in the middle reuniens and the rhomboid nucleus, and absent almost entirely from the VP thalamic centres, VPL and VPM. These studies demonstrated that the expression of *Zic4* contributes to the formation of thalamic nuclei when

they are close to the thalamus-prethalamus intersection, particularly the vLGN, although its expression pattern in human thalamic nuclei is yet to be understood clearly.

1.9 Developmental Comparison of the Thalamus in Primates and Rodents

Traditionally, researchers utilize mouse models to elucidate the underlying mechanisms of brain function in humans, due to the limited availability of human samples. There exist some innate differences between primate and non-primate species. For instance, the pulvinar is more complex in humans than in other primate species (Ouhaz et al., 2018). Moreover, the medial Pulvinar is not detectable, or is at best rudimentary, in rodents, and emerged first in primates (Homman-Ludiye and Bourne, 2019). This section discusses the differences and similarities of the thalamus in primates and rodents. The figure below shows morphological comparisons of mouse, non-human primate and human embryo development (Figure1.12).

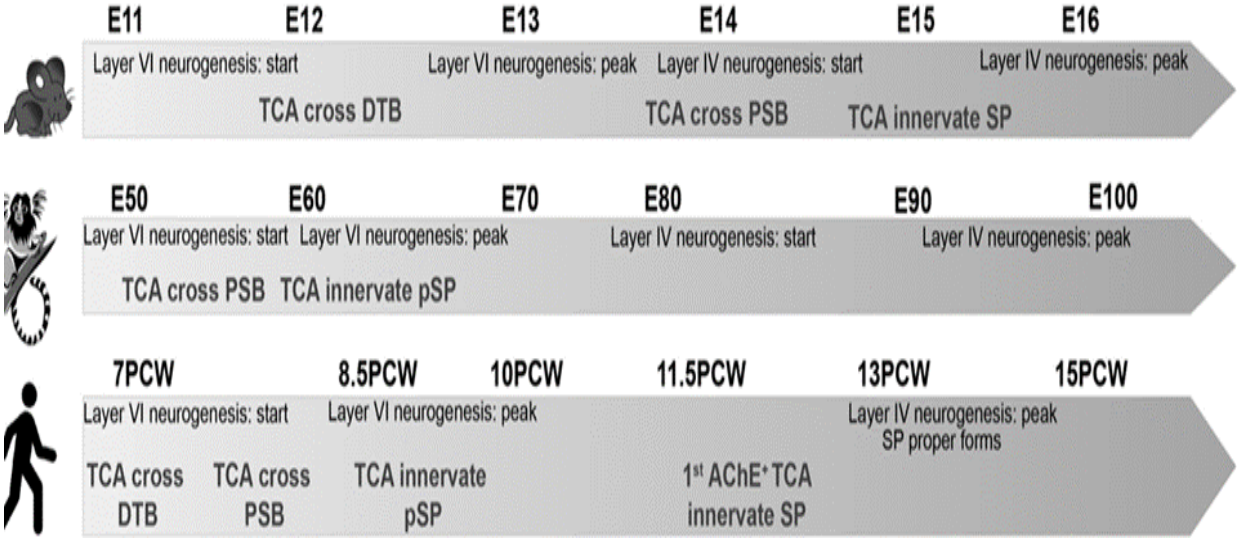

Figure 1.12. Comparison of the developmental timelines of the neocortex and TCA in the mouse, marmoset, and human. 7 PCW correspond to E11in mice and E50 in marmoset. 8.5 PCW correspond to E12 in mice and E60 in marmoset. 10 PCW correspond E13 in mice and E70 in marmoset. 11.5 PCW correspond to E14 in mice and E80 in marmoset. 13 PCW in human correspond E15 in mice and E90 in marmoset. 15 PCW in human correspond in E15 in mice and E100 in marmoset (Alzu'bi et al., 2019).

1.9.1 Size development of the thalamus

The human thalamus has expanded medial nuclei compared to rodent (Ouhaz et al., 2018). In humans, the thalamic nuclei are enlarged and there is a clear boundary between the nuclei, due to the fact that the efficient packaging of the individual cells makes it easier for the observers to delineate the nuclei. In rodents, the thalamic nuclei blend with others without clear boundaries (Jones, 2007, Puelles et al., 2012b).

1.9.2 GABAergic inhibition

The GABAergic connections that link the reticular thalamic nucleus to the rest of the thalamus act as an inhibitory pathway, and control the responsivity of the thalamic relay cells (Rodrigo-Angulo et al., 2008). In rodents and primates, the thalamus is distinct, with more GABAergic interneurons present within the individual thalamic nuclei of primates than in those of rodents (Arcelli et al., 1997, Nakagawa, 2019). Different fractions of GABAergic neurons have been identified in different thalamic regions. Previous studies demonstrated that in mice, interneurons in the FO visual thalamus, the dorsal lateral geniculate nucleus (LGNd), originate in the midbrain from an $En1^{+}Gata2^{+}Otx2^{+}Sox14^{+}$ cell lineage (Jager et al., 2016). Meanwhile, recent studies showed that while the largest proportion of thalamic interneurons in mice is generated in the $En1^{+}Sox14^{+}$ embryonic midbrain, there is an additional class that derives from the $Nkx2.1^{-}Lhx6^{-}Dlx5^{+}Foxd1^{+}$ inhibitory progenitor domains in the forebrain (Jager et al., 2021). Midbrain-born interneurons are found largely in the sensory relays, while the forebrain-generated interneurons reside in the HO thalamus, including MD, LD, and LP; Pul nuclei (Jager et al., 2021). Evidence in humans indicates that the DLX1/2-expressing ganglionic eminences (GE) in the telencephalon are the origin of interneurons for certain major HO thalamic nuclei, such as the mediodorsal nucleus and the Pul nucleus (Rakić and Sidman, 1969, Letinić and Kostović, 1997, Letinic and Rakic, 2001).

In humans, GABAergic neurons are found throughout the thalamus, originating either from extrathalamic sources or from inside the thalamus itself. Kim et al. (2023) asserted three clusters representing GABAergic inhibitory neurones (IN1-3) are contingent upon their origin in first trimester (Kim et al., 2023). IN1 and IN2 denote prethalamic neurones originating from prosomere 3, characterised by the presence of canonical markers PAX6, DLX5, SIX3, and ARX, (Mastick and Andrews, 2001, Nakagawa and O'Leary, 2001) and the absence of FOXG1, a pan-telencephalic marker. IN3 are likely GABAergic neurones originating from prosomere 2/rostral thalamus (rTh), as indicated by the expression of LHX1, NKX2.2, OTX2, and SOX14.

While OTX2 and SOX14 are expressed in GABAergic neurones originating from the midbrain and the pretectum produced from prosomere 1, NKX2.2 is not expressed in GABAergic neurones from the pretectum and midbrain. Moreover, these cells do not exhibit LMO1 and IRX3, which are markers of the caudal diencephalon also found in midbrain-derived GABAergic neurones, indicating that the migratory stream of interneurons from the midbrain has not developed during the first trimester. In the second trimester, six clusters corresponding to GABAergic neurons were identified based on the expression of GAD1 and SLC32A1. IN1 exhibited expression of OTX2 and SOX14, but predominantly lacking NKX2.2, a marker indicative of prosomere 2-derived GABAergic neurons, implying their classification as midbrain-derived GABAergic neurons (Jager et al., 2021). The GABAergic neuron subtype was absent in our first-trimester data; we hypothesise that this population likely constitutes a migratory stream that infiltrates the thalamus post-GW10. IN3 exhibited expression of EBF1, EBF3, ISLR2, and ESRRB, indicative of pretectal identity (Guo and Li, 2019, Mallika et al., 2015). IN4 exhibited markers characteristic of the thalamic reticular nucleus, namely SIX3, ISL1, and SST (Li et al., 2020). The remaining three groups (IN2, IN5, and IN6) exhibited the pan-telencephalic marker FOXG1 (Tao and Lai, 1992). Prior anatomical investigations have indicated that in humans, GABAergic neurones originating from the ganglionic eminence migrate into the thalamus (Letinic and Rakic, 2001, Rakić and Sidman, 1969). FOXG1+ clusters were identifiable by their differential enrichment of PDZRN3 in IN2; CRABP1, ANGPT2, and MAF in IN5; and PENK, RARB, and RXRG in IN6. IN5 resembles a recently identified population of primate-specific interneurons that are positive for CRABP1 and MAF1, originating from the medial ganglionic eminences (MGEs) (Schmitz et al., 2022, Krienen et al., 2020). In conclusion, it was discovered through these studies GABAergic populations originating from the diencephalon, midbrain, and telencephalon, with the latter two emerging during the second trimester of human development. However, there also exists limitations to interpreting gene expression in thalamic cells as suggestive of extrathalamic origin. For example, although SOX14 marks GABAergic cells of midbrain origin, some SOX14 cells also originate in the ventral thalamus. However, the majority of SOX14 positive cells are of midbrain origin.

1.9.3 Thalamic nuclei

Between E14.5 and E18.5 in mice, the diencephalon is progressively partitioned into discrete neuronal groups that signify their differentiation into nuclei (Jones, 2007, Chen et al., 2009). However in the study by Zoltan Molnar (2019), there was no evidence for the growth and establishment of discrete human thalamic nuclei at 8 PCW; indeed no thalamic nuclei were observed even at 12 PCW (human), the same developmental stage as mouse E14 (Molnár et al., 2019).

Recent evidence demonstrated that the mediodorsal thalamic nuclei (MD) aids with cognitive processes, such as learning integration, working memory, and adaptive decision-making in both primates and rodents. Based on the morphological features, primate MD is divided into four subdivisions: magnocellular (MDmc), parvocellular (MDpc), caudodorsal (MDcd), and lateral mediodorsal nuclei (MDl). The rodent MD shows medial, central, and lateral mediodorsal nuclei. It is important to note that all thalamic nuclei, including the MD subdivisions, receive afferents from cortical layer 6. However, the HO thalamic nuclei and the mediodorsal nuclei subdivisions also receive cortical afferents from layer 5. Furthermore, the MD receives additional inputs from the medial temporal lobes, pallidum, reticular thalamus, and MD interneurons, although only in the primate midbrain and brainstem. Pulvinar connectivity, and its functions, have been studied in depth in non-human primates, and recently in humans as well. The Pul is a higher-order thalamic nucleus that receives its cortical inputs from layers (L) 5 and 6, and sends projections back to the superficial layers of the same areas and L4 of HO areas. The Pul is the largest of the thalamic nuclei, and consists of various subnuclei, such as the anterior (PulA), medial (PulM), inferior (PulI), and lateral (PulL) Pul (Wilke and Kagan, 2024). The dorsal Pul is constituted of PulM and PulL (Figure 1.13). Meanwhile, the medial Pul nucleus connecting the prefrontal cortex with the temporal lobe is only present in a vestigial form in rodents (Ouhaz et al., 2018).

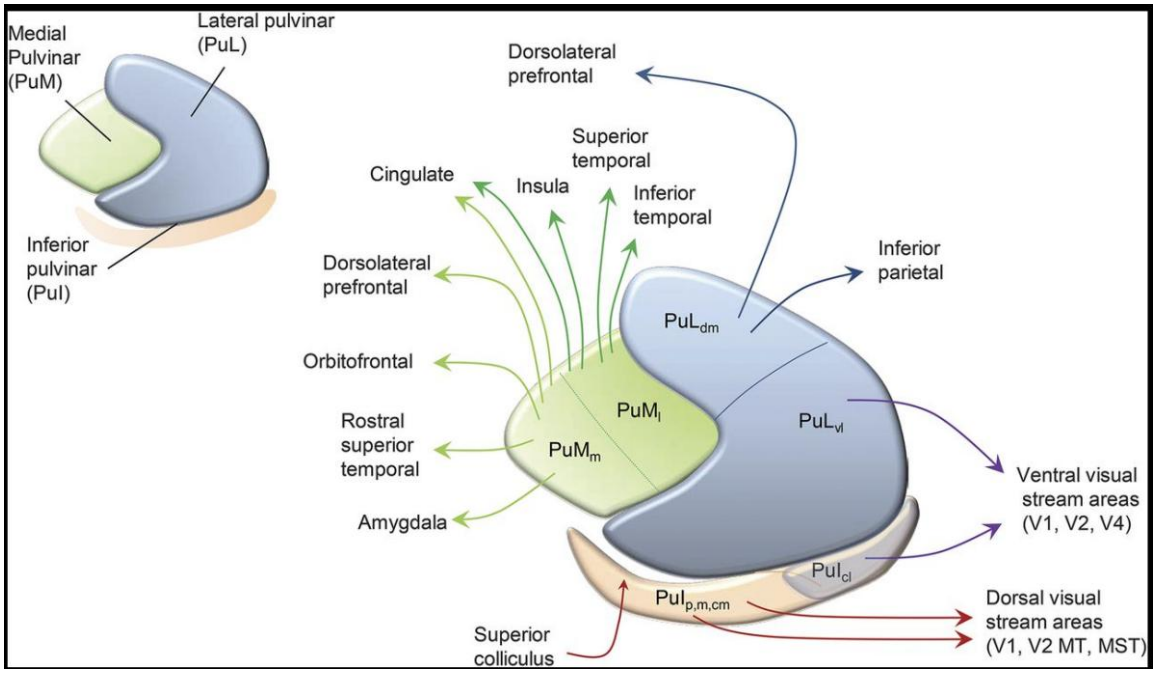

Figure 1.13. Model of the pulvinar complex, subdivided into anterior pulvinar, medial pulvinar, lateral pulvinar, and inferior pulvinar. Abbreviations: anterior pulvinar (PuA), medial pulvinar (PuM), lateral pulvinar (PuL), inferior pulvinar (PuI), pulvinar medial subnucleus (PuM_m), lateral PuM (PuM_l), centromedial (PuI_{cm}), dorsomedial nucleus of the PuL (PuL_{dm}), centrolateral nucleus of the PuI (PuI_{cl}) (Source: (Benarroch, 2015)).

1.9.4 Thalamocortical afferent (TCA)

Thalamocortical afferent (TCA) connections transmit subcortical information to the cortical areas to reconstruct a model of the external surroundings (Krsnik et al., 2017). The timeline of their development differs in different species. The study conducted by Alzu'bi et al. (2019) demonstrated that some TCA cross the diencephalic/telencephalic boundary (DTB) by 7 PCW (equivalent to E11 in mice) and reach the presubplate by 8.5 PCW in human (Alzu'bi et al., 2019). This contrasted with previous studies that used acetylcholinesterase immunochemistry (Krsnik et al., 2017), and found that the TCA innervates the presubplate by 12-14 PCW. Conversely, in mice, the TCA crosses the DTB by E12. The study conducted by Alzu'bi et al. (2019)concluded that the phenomenon of TCA innervation, guided by corticothalamic afferents, occurs at different developmental stages in different species(Alzu'bi et al., 2019).

1.10 Thalamic Dysfunction in Neurodevelopmental Disorders

The potential role of defects in thalamic function in neurodevelopmental disorders (NDDs) is not understood clearly. It has been known for a long time that SZ, for example, is a neurodevelopmental illness that arises due to defects in the prefrontal-thalamic-cerebellar circuitry (Smitha Karavallil Achuthan, 2023). Thus, it is important to study abnormalities in the thalamus, in order to determine its influence on disorders such as SZ.

1.10.1 Thalamic nuclei that may be affected by neurodevelopmental disorders

The thalamus acts as a relay centre in the brain, and controls both cognitive and motor functions. Individuals with SZ have cognitive difficulties, difficulty in tracking time with respect to space, and problems with their behaviour, displaying emotions, and maintaining interrelationships (Pergola et al., 2015). Such individuals also have difficulty with process coordination, priority determination, and retrieval, as well as with communicating (Byne et al., 2009).

The thalamus is comprised of relay and diffuse-projection nuclei that project towards motor and sensory cortical regions; it receives connections from the cortical regions, and sends them back for information processing. Defects that inhibit the relay between the cerebellum and the cortical regions through the pontine nuclei also cause cognitive disorders (Barch, 2014).

1.10.1.1 Mediodorsal nucleus

The thalamic region studied most in relation to (SZ) is the MD nucleus, which performs both executive and cognitive functions, and is impaired in SZ subjects. Studies of non-human primates revealed that the connections from the medial and lateral MD project towards the more medial and lateral regions of the prefrontal cortex (Wang et al., 2015). The ablation of the prefrontal cortex in humans causes extensive retrograde degeneration in the MD, except in its magnocellular subdivision, that sends projections to the temporal and olfactory cortex. Meanwhile, post-mortem anatomical studies observed that the volume of MD is reduced in SZ subjects, compared with control specimens (Dorph-Petersen and Lewis, 2017). A comparison by Poels et al. (2014) of the MD volume between live SZ and healthy control subjects demonstrated the presence of a smaller MD in the SZ subjects, compared with the healthy control subjects. These studies employed younger subjects, and included a large sample number, and were therefore reliable sources for understanding the volume of the MD in SZ subjects. Meanwhile, comparison between post-mortem and live MRI studies revealed

variations in the volumetric studies. In the post-mortem subjects, this may be the result of a fixation shrinkage artefact, or the inadequate handling of partial sections (Pergola et al., 2017). Previous studies also demonstrated the importance of effect size for calculating the MD volume, in both live and post-mortem subjects. In addition to the MD volume, several studies reported a significant loss of neuronal number, and a pronounced neuronal deficit in the parvocellular division (Buchmann et al., 2014). However, the differences in neuronal numbers may have been due to a small sample size, disease severity, length of time the patient had had the condition, and symptom profile (Pergola et al., 2013). Thus, it was concluded that the reduction of the MD volume in SZ is more convincing than the neuronal number decrease.

1.10.1.2 The Pulvinar

The somatosensory cortex forms connections with the anterior Pul. The ventrolateral portion of the lateral Pul has connections with the visual cortex, while the dorsomedial nucleus of the Pul is connected with the inferior parietal and prefrontal cortex. The medial Pul has connections with the sensory association areas, the cingulate cortex, and the prefrontal cortex (Benarroch, 2015). The Pul is linked to visual, attention, visuospatial working memory, and language functions. Thus, humans with Pul lesions cannot perform the dichotic listening test, even though they demonstrate a performance in the presence of auditory stimuli. According to Dorph-Petersen and Lewis (2017) the Pul is involved with cortical mechanisms performing language tasks, and damage to the Pul causes paraphasic speech, and results in the use of jargon, a pattern observed in some patients with SZ (Dorph-Petersen and Lewis, 2017). Therefore, the Pul may have a role in a variety of functions, such as perceptual and oculomotor abnormalities, directed attention, and working memory, all of which are impaired in SZ sufferers. To date, six studies conducted by three independent researchers demonstrated that the volume of the Pul in postmortem subjects, as well as in the MRI scans of SZ subjects, is reduced (Delvecchio et al., 2013). Moreover, the volume deficit in the right hemisphere of the thalamus was found to be statistically significant. The bilateral volume deficit was also observed in a postmortem study, while a deficit in the Pul, but not in the MD, was identified in schizotypal personality disorder, a syndrome within the SZ spectrum (Höflich et al., 2015). The neuronal numbers observed were found to be reduced in the right hemisphere in three postmortem studies; while one study reported the deficit only in the medial Pul, the second study revealed a neuronal deficit in both the medial and lateral Pul. The discrepancies and inconsistencies in the neuronal deficit in both the lateral and medial regions of the Pul may be

due to the differences in its parcellation (Marenco et al., 2012). In healthy subjects, the thalamus and Pul show larger volumes in the right hemisphere of thalamus, while the asymmetry is altered in SZ subjects (Pergola et al., 2015). Thus, the neuronal deficit in the lateral Pul may be due to the anomalous lateralization. The effect sizes calculated and corrected for brain size demonstrated a large effect size on the right hemisphere in males, while it was comparable in the right and left hemispheres in females (Delvecchio et al., 2013).

1.10.2 Susceptibility Genes for Schizophrenia

While several neurological diseases exhibit comparable risk factors and pathological symptoms, their pathogenic cause remains elusive (Hu et al., 2019). The genome-wide screening and the mapping of several regions of the brain has engendered the identification of distinct susceptible genes in SZ (Karoutzou et al., 2008). To begin to understand the effect of these susceptibility genes on the pathogenesis of SZ it's important to determine their location and developmental expression during normal human brain development.

Given below are the SZ susceptibility genes explored in this thesis:

1.10.2.1 Neurexin *(NXRN)*

In mammals, NXRN are coded for by three genes, namely *NRXN1, NRXN2, and NRXN3* (Reichelt et al., 2012, Kasem et al., 2018, Hu et al., 2019). Although 1,000 isoforms have been described, they can be divided into either α or β forms. The α isoform is transcribed from exon 1 onwards, while the β form is shorter, and is transcribed from areas downstream of exon 17. Neurexin- α isoforms supposedly play a role as neural receptors for toxins such as latrotoxin that is the active component of black widow venom (Ushkaryov et al., 1992), while neurexin-β isoforms are crucial for maintaining the integrity and functionality of the neural synapses (Rowen et al., 2002).

Recent genetic research indicated the link between *NRXN* mutations and numerous neuropsychiatric disorders (Kasem et al., 2018), of which *NRXN* genomic modifications were strongly linked to SZ and autism spectrum disorders (ASD) (Hu et al., 2019). Multiple studies have led to the revelation that deletions, truncations, and copy number variants in the *NRXN* genes, particularly in *NRXN1*, occur more frequently in individuals with neurodevelopmental problems than those in control groups (Reissner et al., 2013). In two separate studies, variations

in both the *NRXN1β* gene and *NRXN1α* gene have been identified in individuals with autism spectrum disorder (Feng et al., 2006, Friedman et al., 2006), respectively. In addition, the *NRXN1* gene is well known for its significant association with schizophrenia (Hu et al., 2019).

The NXRN are proteins that are expressed primarily in the pre-synaptic terminal, and have key physiological functions in synaptic development and maintenance (Matsuda and Yuzaki, 2011, Reichelt et al., 2012, Treutlein et al., 2014). Mouse models demonstrated that the removal of the first exon of neurexin-1 α enables uninterrupted access to the physiological effects of the disturbances on phenotypes related to SZ and ASD (Reichelt et al., 2012). However, the causal pathways by which *NRXN* impact the pathogenesis of the aforementioned mental and neurological conditions remains blurred, and requires further, more comprehensive, study (Kasem et al., 2018). It should also be noted that Harkin et al. (2017) demonstrated that during human cortical development, NRXNs may be expressed at locations other than the synapse, including in migrating cells and growing axons (Harkin et al., 2017).

1.10.2.2 Fasciculation and elongation protein zeta 1*(FEZ1*)

The protein fasciculation and elongation zeta-1 (FEZ1) has been shown to be involved in axon and dendrite outgrowth (Chua et al., 2021), and it potentially interacts with a range of proteins, whose roles range from intracellular transport systems to transcription regulation (Razar et al., 2022). In the human genome, the *FEZ1* gene is located on a chromosome and encodes a protein of 392 amino acids with a molecular mass of 45 kDa. FEZ1 is a mammalian ortholog of UNC-76, which is part of the family of C. elegans proteins, which were studied to elucidate the mechanisms of locomotory defects. Mice defective in Fez1 exhibit no anomalies in dopaminergic neurones; however, they demonstrate improper development of subplate neurones and thalamocortical axons, together with a loss of the fornix/fimbria system (Hirata et al., 2004). Fez1 is essential for the formation of subcerebral projection neurones in layer V of the neocortex (Chen et al., 2005a, Chen et al., 2005b, Molyneaux et al., 2005). Mice lacking in Fez exhibit atypical projections of olfactory sensory neurones and irregularities in olfactory bulb development (Hirata et al., 2006). The comparatively diminished forebrain phenotypes of Fez and Fez1-deficient mice indicate that Fez and Fez1 function redundantly in the patterning and development of the forebrain. It is also notable that FEZ1 has been demonstrated to be involved in the transport of multiple SNARE complex associated and axon growth associated proteins, e.g., syntaxin-1, SNAP25, synatoptagmin and GAP43, including other

neurodevelopmental disease susceptibility candidates, e.g., neurexins, STXBP1 and DISC1 (Toda et al., 2008, Kang et al., 2011, Chua et al., 2012, Butkevich et al., 2016, Razar et al., 2022).

Mice lacking *FEZ1* move more quickly and are more sensitive to psychostimulants (Sakae et al., 2008). Its expression has been demonstrated to be diminished in the post-mortem brains of individuals with schizophrenia, associated with mutations in DISC1 (Disrupted in Schizophrenia 1) (Lipska et al., 2006) and the peripheral blood of schizophrenia sufferers (Vachev et al., 2015). Significantly, *FEZ1*-deficient stem cell-derived human motoneurons exhibit considerable developmental impairments in axon growth and synapse formation *in vitro* (Kang et al., 2011). Recent investigations have shown that FEZ1 expression is activated early in human brain development, and that in the absence of FEZ1, neuroprogenitors exhibit ectopic localisation and cortical layer formation is disrupted (Gunaseelan et al., 2021).

1.11 Aims of this Project.

The present study was conducted using precious human samples, to acquire accurate information regarding thalamic development, due to the innate differences that exist between humans and rodents. Furthermore, the first step in understanding the potential role of susceptibility genes linked to neurodevelopmental diseases is to determine where and when these genes are normally expressed during human development. Therefore, the following were the aims of the present study:

1: To examine the cellular composition of the thalamus at 16 PCW, a pivotal stage in which thalamic nuclei begin to emerge, in order to gain critical insights into the region's developmental architecture.

2: To investigate, map and analyse gene expression patterns across the developing human thalamus from 8 to 14 PCW in order to track the development of each thalamic nucleus with a particular focus on genes previously described as important markers of thalamic development in animal experiments.

3: To understand when, where and in which cell types two schizophrenia susceptibility genes, *NRXN1* and *FEZ1* are expressed during development.

2 Chapter 2. Materials and Methods

2.1 Human Tissue

Human foetal tissue acquired from terminated pregnancies was obtained via the MRC/Wellcome Trust-funded Human Developmental Biology Resource (HDBR, http://www.hdbr.org; Gerrelli et al., 2015). The Newcastle and North Tyneside NHS Health Authority Joint Ethics Committee authorized the collection of all tissue samples obtained with the mother's informed consent. HDBR Newcastle is a tissue bank that belongs to Newcastle Biobanks (http://www.ncl.ac.uk/biobanks/) (license number 12534). The age of the foetal samples ranged from 8 to 21 PCW. The ages were determined by measuring foot length and distance from heel to the knee, as described by (HERN, 1984).

2.2 Tissue Processing and Sectioning

The staff at HDBR Newcastle were responsible for performing the processing and sectioning of the embryonic and foetal material to produce paraffin sections. The isolated brain was placed in a solution containing 4% paraformaldehyde (PFA: Sigma Aldrich) dissolved in 0.1M phosphate buffer saline (PBS) at 4°C for at least 24 hours. After fixation, smaller whole or half brains were dehydrated with graded ethanol/water mixes (70% ethanol for 15 minutes, 100% for 45 minutes, and 2 x 100% for one hour) at room temperature after being divided sagitally. The larger fixed brains were cut into approximately equal-sized blocks before being dissected, with the number of blocks dependent on the size of the brain, prior to dehydration with graded ethanol/water mixes. The blocks were then submerged in xylene for two hours before being embedded in paraffin. Sagittal, horizontal, and coronal represented the three different planes through which blocks of brain tissue were sectioned using a Leica RM 2235 microtome with a thickness of eight microns.

2.3 Haematoxylin and Eosin Staining

In order to provide reference sections, some of the paraffin sections were dewaxed with Histo-Clear for five minutes to remove the wax, and then rehydrated using a series of ethanol dilutions (100%, 95%, 70%). The sections were washed with distilled water and then immersed in Harris hematoxylin solution (Raymond A Lamb Ltd., Eastbourne, UK) for one minute. They were then rinsed with tap water. The cell nuclei staining was developed by immersion in Scott's Tap Water Substitute. The cytoplasm was then stained by treatment with eosin (1% aqueous solution, Raymond A Lamb Ltd) for 10 seconds and subsequently rinsed with tap water. The sections were re-dehydrated using a series of ethanol dilutions (70%, 95%, and 100%) and cleared in two rounds of Histo-Clear. Finally, the sections were mounted in DPX mounting media (Sigma-Aldritch, Poole, UK) according to Table 2.1.

2.4 Transcriptomic Data Analysis

In order to obtain information based on the gene expression, several databases were interrogated, including whole tissue and single-cell RNAseq. For the whole tissue RNAseq, we used the data uploaded to www.ebi.ac.uk/arrayexpress/experiments/E-MTAB-4840 from Human Developmental Biology Resource (HDBR) expression resource-RNAseq (Lindsay et al., 2016). The analysis of the tissue RNAseq in this database was performed on 138 samples of cortical tissue obtained at ages ranging from 7.5 to 17 PCW, and from diverse sites along the anterior-posterior axis of the cortex, including the temporal lobe. The normalized data is presented as RPKM (Reads per kilo base per million mapped reads) values.

$$RPKM\ of\ a\ gene = \frac{Number\ of\ reads\ mapped\ to\ a\ gene\ \times\ 10^3\ \times\ 10^6}{Total\ number\ of\ mapped\ genes\ from\ given\ library\ \times\ gene\ length\ in\ bp}$$

For single cell (sc) RNAseq, a database referred to as the Cortical Development Expression Viewer CoDEx (solo.bmap.ucla.edu/shiny/webapp/), was used in order to conduct more research into the cell type specificity of the gene expression data. This database contained information on the expression of genes from human cortical tissue samples taken at 17/18 PCW (Polioudakis et al., 2019). The output graphs from this analysis are tSNE plots of normalized gene expression.

An investigation of the cell-specific expression in the thalamus was conducted using scRNAseq data obtained a single-cell dataset from the Kriegstein laboratory, focusing on the 16 PCW

thalamus, which was available from https://nemoanalytics.org/. Briefly, single-cell transcriptomes were sequenced from microdissected regions of developing human brain tissue during the second trimester, which encompasses peak stages of neurogenesis. Cells were sampled from 10 distinct major forebrain, midbrain and hindbrain regions from 13 individuals. In addition, six neocortical areas were sampled from the same individuals: PFC, motor, somatosensory, parietal, temporal and primary visual (V1) cortex, resulting in 698,820 high-quality cells for downstream analysis. Microdissections were performed carefully to sample target regions. However, these regions are putative during development, and small numbers of cells from neighbouring regions may have been included. The processes of normalization and the scaling of the data set was undertaken using NEMO software, and the percentage of mitochondrial content was maintained below 0.05% to focus on living cells. 2000 most variable genes were chosen for further analysis. PCA calculations were also performed using the same software for dimensionality reduction to summarize, visualize, and identify patterns in high dimensional transcriptomic data, and five principal components were selected to create clusters of cells with similar expression profiles using UMAP. The UMAP analysis detected 14 discrete clusters and each cluster was allocated a separate colour for separation purposes. The software provided lists of the genes expressed most highly in each cluster, and after generating UMAPS for each gene of interest, both the marker genes and certain cell types were identified for each cluster. The Human Developmental Biology Resource (HDBR) expression resource is a new resource for studying prenatal human brain development. For the whole tissue RNAseq, we used the data uploaded to *www.ebi.ac.uk/arrayexpress/experiments/E-MTAB-4840.*

Table 2.1 Human foetal samples distributed by age and sectioning orientation. (Abbreviations: Human Developmental Biology Resource (HDBR)).

Brain no.	HDBR sample ID number	Age	Sectioning orientation	Image
1	12932	8_PCW	Sagittal	
2	13341	10_PCW	Coronal	Not available
3	N1798	12_PCW	Coronal	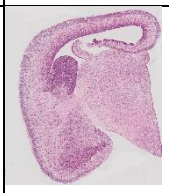
4	15208	14_PCW	Coronal	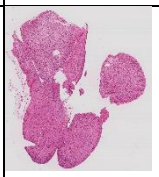
5	13411	16_PCW	Horizontal	
6	13029-14037	19_PCW	Coronal	
7	14081	21_PCW	Coronal	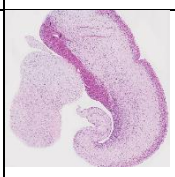

2.5 Immunohistochemistry (IHC)

2.5.1 Immunoperoxidase histochemistry

The paraffin sections were collected onto glass slides and then dewaxed in two rounds of Histo-Clear, each for five minutes. This was followed by rehydration via four changes of ethanol grades (100%, 95%, 70%, and 50%). Endogenous peroxidase activity was blocked by treatment with methanol peroxide for 10 minutes (Table 2.2). The slides were rinsed in distilled water, then placed in containers and covered with sufficient citrate buffer at pH 6. The slides were heated in a microwave at high power for 10 minutes and then cooled in the buffer for approximately 20 minutes and washed with tris-buffered saline (TBS) buffer two times for five minutes (Table 2.2). This procedure was followed by incubation with a 10% blocking serum, from the same species in which the secondary antibody was raised in Tris buffer pH 7.6 for 1 hour at room temperature (Table 2.3). The next step was incubation with a primary antibody diluted with a 10% blocking serum in TBS (Table 2.4). The sections were incubated overnight at 4°C and were washed in TBS on the second day and incubated with a secondary antibody HRP polymer kit peroxidase at room temperature for 30 minutes (Table 2.5). The sections were then washed again in TBS with two changes, each for five minutes, and diaminobenzidine (DAB) solution was added using muliple reagents from kit for 10 minutes (1 drop “Reagent 1” + 2 drops “Reagent 2” + 1 drop “Reagent 3” in 2.5ml distilled water from Kit, Vector Labs), followed by washing in running water for 10 minutes (Table 2.2). The sections were counterstained with toluidine blue for 40 seconds, and dehydrated in ethanol grades (50%, 70%, 95%, and 100%). The sections were kept in Histo-clear for one minute, and coverslipped using Histomount (Table 2.2).

Table 2.2. General materials.

Solution	Component	pH	Manufacturer	Concentration
Scott's Tap Water Substitute,	3.5g of sodium bicarbonate 20g of magnesium sulphate 1litre of distilled water	---	Sigma Aldrich	-------
10XTBS	8.75 g NaCl 6.50 g Trizma base 800 ml distilled water For preparing tris buffer saline: 100 ml from 10x TBS to 900 ml distilled water	7.5	Sigma Aldrich	--------
10XCitrate buffer	5.88 g of ($C_6H_5NA_3O_7$) H_2O_2 tris-sodium citrate 2L distilled H2O For preparing citrate buffer 100 ml from 10x citrate buffer to 900 ml distilled water	6	Sigma Aldrich	0.1M
30% hydrogen peroxide Methanol peroxide	3ml of 30% hydrogen peroxide (H_2O_2) 180 ml methanol	----	Sigma Aldrich Vector Laboratories	--------
Diaminobenzidine tetrachloride (DAB)	1 drop "Reagent 1" + 2 drops "Reagent 2" + 1 drop "Reagent 3" 2.5ml distilled water	-----	Vector Laboratories	--------
Histo-Clear	200 ml	------	Scientific Laboratory Supplies	--------
Ethanol	----------	------	Vector Laboratories	99%
Histomount	250 µL on each section	------	Scientific Laboratory Supplies	----------
Toluidine Blue	250 µL in 2.5ml distilled water	------	Sigma Aldrich	----------

Table 2.3 Manufacturer and catalogue number of each serum used for blocking.

Normal serum used for blocking	Manufacturer of normal serum	Catalogue number
Normal goat serum	Vector Laboratories, Newark, CA, 94560, USA	s-1000
Normal horse serum	Vector Laboratories, Newark, CA, 94560, USA	s-2000

Table 2.4 Primary antibodies

Primary antibody	Species	Dilution	Supplier	RRID no.
FOXP2	Mouse mAb	1/50	Santa Cruz Biotechnology, Heidelberg, Germany	AB_2721204
GBX2	Rabbit pAb	1/500	Proteintech Europe, Manchester, UK	AB_2878896
OTX2	Mouse mAb	1/200	Santa Cruz Biotechnology	AB_2921699
PAX2	Rabbit pAb	1/1000	Abcam, Cambridge, UK	AB_2750924
SP8	Rabbit pAb	1/200	Sigma-Aldrich, Sofia, Bulgaria	AB_2682340
CALB1	Rabbit pAb	1/1000	Abcam, Cambridge, UK	AB92341
CALB2	Rabbit pAb	1/500	Abcam, Cambridge, UK	AB108404
NR2F1	Mouse mAb	1/500	Abcam, Cambridge, UK	AB41858
NR2F2	Mouse mAb	1/1000	Perseus Proteomics, Tokyo, Japan	AB_2155627
OLIG2	Rabbit pAb	1/1000	MerckMilliporeKGaA, Darmstadt, Germany	AB-10141047
GAD1	Mouse mAb	1/500	Merck Millipore KGaA	AB_2278725
GFAP	Mouse mAb	1/500	Proteintech Europe, Manchester, UK	AB_10838694
ASCL1	Mouse mAb	1/1000	Santa Cruz Biotechnology	AB-10918561
NRXN1	Goat pAb	1/500	Santa Cruz Biotechnology	AB_2236323
GAP43	Mouse mAb	1/500	Santa Cruz Biotechnology	AB_627660)
FEZ1	Rabbit pAb	1/500	Proteintech Group	AB_2877825
Ki67	Mouse mAb	1/150	Santa Cruz Biotechnology	AB_627859
TBR1	Rabbit pAb	1/1000	Abcam, Cambridge, UK	AB-2200219
STXBP1	Rabbit mAb	1/500	Abcam, Cambridge, UK	AB-109023

Table 2.5 Secondary antibodies used for immunostaining.

Secondary antibody	Manufacturer	Catalogue number
HRP horse Anti-rabbit	Vector Laboratories, Burlingame, CA 94010, USA	MP-7401
HRP horse Anti-mouse	Vector Laboratories, Newark, CA 94560, USA	MP-7402
HRP horse Anti-goat	Vector Laboratories, Burlingame, CA 94010, USA	MP-7405
HRP goat Anti-rabbit	Vector Laboratories, Burlingame, CA 94010, USA	MP-7451-15

2.6 Immunofluorescence (IF)

2.6.1 Method single and double–label IF

For single IF, the Tyramide Signal Amplification (TSA) method was followed, a procedure similar to the initial steps of immunoperoxidase histochemistry described above for dewaxing, antigen-retrieval, and primary antibody incubation. The tyramide signal amplification process includes the use of horseradish peroxidase (HRP) to enzymatically convert fluorophore or chromogen tyramides to covalently bind tyrosine residues on and surrounding the protein epitope targeted by the primary antibody. After removing the excess primary antibodies from the sections with TBS washes, the sections were incubated for 30 minutes at room temperature with the appropriate horseradish peroxidase (HRP)-secondary antibodies (Table 2.5). The remainder of the procedure was conducted with minimal exposure to light. The sections were incubated for 10 minutes at room temperature with Opal 570 TSA reagent (fluoresces red; diluted in amplification buffer (1:700 dilution)), followed by TBS rinsing. The sections were then mounted with mounting medium containing DAPI (Table 2.6).

For double IF, a second round of fluorescent labelling was accomplished by repeating the citrate buffer treatment after incubation with Opal 570 in the TSA reagent. This was followed by washing in TBS, and incubation with 10% normal serum before incubating with a second primary antibody for two hours at room temperature, followed by HRP secondary antibodies for 30 minutes at room temperature. After washing, the sections were incubated with Opal 520

(fluoresces green) TSA reagent (1:700) for 10 minutes at room temperature (Table 2.6). Following TBS washing two times for five minutes each, the sections were mounted with prolong gold antifade reagent containing DAPI.

2.7 In situ Hybridization

2.7.1 Fluorescent in situ hybridization (RNAscope, multiplex v2 essay)

HDBR prepared slides were put on a hotplate at 60°C for one hour and then cooled to room temperature. The sections on the slides were dewaxed in Histo-Clear, twice for five minutes each, and were then rinsed in 100% ethanol twice, each for two minutes. The slides were allowed to air dry, then were covered with hydrogen peroxide solution (from kit RNAscope Multiplex v2 essay, Table 2.7), and incubated for 10 minutes at room temperature. They were then rinsed in distilled water, twice for five minutes each, and transferred to boiling distilled water for 10 seconds at 95°C. The slides were then transferred to the target retrieval solution (Table 2.8) at 95°C and boiled for 20 minutes. The slides were washed twice again, using distilled water, then rinsed in 100% ethanol for three minutes and allowed to dry. The sections were outlined with a hydrophobic pen. The hybridization oven was maintained at 40°C, and a moist filter paper was placed inside, upon which the slides were kept in the Hybez tray. Protease Plus (ACD Biotechne) was added to cover each section, and these were then incubated for 30 minutes at 40°C (Table 2.7).

The slides were washed twice with distilled water for five minutes. The excess water was removed, and 120 µl of the probe (*FEZ1, ZIC4, NRXN1, SOX14*) was added to the sections, which were then incubated at 40°C for two hours. The probes were designed and supplied by ACD Biotechne (see Table 2.9 for further details). The slides were then washed in wash buffer (Table 2.8), twice each for two minutes, and stored overnight in saline sodium citrate (SSC) (Table 2.8) at room temperature. The excess liquid from the slides was removed the following day, and 120 µl of multiplex v2 amplification buffer (AMP1) from the kit was added to cover the sections, which were then incubated at 40°C for 30 minutes. Next, the slides were washed twice with wash buffer, each for two minutes (20 ml wash buffer in 980 distilled water) and the excess liquid was removed. Then, 120 µl of multiplex v2 amplification buffer (AMP2) was added to cover the sections, which were incubated at 40°C for 30 minutes. The slides were washed twice with wash buffer, each for two minutes, and the excess liquid was removed. After this, 120 µl of multiplex v2 amplification buffer (AMP3) was added to cover the sections,

which were incubated at 40°C for 15 minutes (RNAscope, multiplex fluorescent detection reagent v2 essay (Table 2.7). The slides were washed twice with wash buffer, each for two minutes, and 120 µl of horseradish peroxidase (HRP-C1 RNAscope, multiplex fluorescent detection reagent v2 essay) was added to cover the sections, which were then incubated at 40°C for 15 minutes (Table 2.7). After this, the slides were washed twice with wash buffer, each for two minutes, and the excess water was removed from the slides. Fluorophore Opal 570 (Akoya Bioscience) with TSA (1:700) was added, and they were incubated for 30 minutes at 40°C in a dark place. The slides were washed twice with wash buffer for two minutes each, the excess liquid removed, and 120 µl of horseradish peroxidase (HRP) blocker RNAscope, multiplex fluorescent detection reagent v2 essay was added to cover the sections, incubated for 15 minutes at 40°C, then washed twice with wash buffer for two minutes each. Finally, the slides were mounted with Prolong gold antifade reagent with DAPI to stain the nucleus.

2.7.2 Fluorescent in situ hybridization (RNAscope, multiplex v2 essay) with IF

The protocol outlined in Section 2.7.1 was followed for one round of fluorescent RNAscope staining using only Opal 570. The sections were then rinsed in wash buffer, and the sections were placed in containers covered with sufficient citrate buffer pH 6. The slides were heated in a microwave on high power for 10 minutes and then placed in the buffer to cool for approximately 20 minutes. This was followed by an incubation period of 1 hour at room temperature in a 10% blocking serum from the same species in which the secondary antibody was raised from. Incubation with a primary antibody diluted with a 10% blocking serum in TBS followed, and the sections were incubated for two hours at room temperature. The sections were then washed in TBS and incubated with a secondary antibody polymer peroxidase kit at room temperature for 30 minutes. The sections were washed again in TBS with two changes every five minutes, and TSA (1:700) was added to the section with OPAL 520 (Akoya Bioscience). They were then washed three times with TBS for five minutes each. After washing, the sections were mounted with Prolong gold antifade reagent with DAPI to stain the nucleus.

2.7.3 RNAscope, 2.5 HD detection reagent-RED

The protocol of in situ hybridization RNAscope discussed above was followed for the first day (RNAscope, 2.5 HD detection Reagent-RED kits) and at the end of the protocol the slides were kept and allowed to dry at room temperature. The sections were drawn around with a hydrophobic pen and left overnight at room temperature. On the second day, the HybEZ oven was switched on and the water bath was set at 40°C. A piece of filter paper was placed in the HybEZ tray and dampened with water. The slides were placed in the HybEZ rack. Protease plus was added to cover each section and then incubated for 30 minutes at 40°C. The slides were washed twice with distilled water for five minutes, and then the excess water was removed from the slides and 120 µl added to the probe (*ZIC4, NRXN1, FEZ1*) to cover the section, and then incubated at 40°C for two hours. The slides were then washed in a wash buffer, twice for 2 minutes each (this was prepared from a 50x wash buffer). The excess liquid was removed from the slides and 120 µl of AMP1 from the RNAscope kit (2.5 HD detection Reagent-RED) was added to cover the sections and they were incubated at 40°C for 30 minutes; then the slides were washed in the wash buffer twice for 2 minutes each. The excess liquid was removed from the slides. This process was repeated, adding 120 µl of AMP2, followed by incubation at 40°C for 15 minutes.

Following an initial wash in the wash buffer twice for two minutes each, the slides underwent liquid removal, and 120 µl of AMP3 was applied, followed by a 40°C incubation for 30 minutes. Washes in the wash buffer 2x for 2 minutes each were then performed. After removing the excess liquid, 120 µl of AMP4 was introduced, and the slides were incubated at 40°C for 15 minutes. Additional washes in wash buffer 2x for 2 minutes each ensued. After the removal of excess liquid, 120 µl of AMP5 was added, and they were incubated at room temperature for 30 minutes. The slides were then washed in wash buffer 2x for 2 minutes each, and the excess liquid was removed before the introduction of 120 µl of AMP6, followed by a room temperature incubation for 15 minutes. Finally, the slides were washed in a wash buffer 2x for two minutes each.

The RED-B was spun briefly, and one volume of RED-B was added to 60 µl of RED-A (this must be used within three to five minutes) (Table 2.7). The excess liquid was then removed and add 2µl of RED A solution to 120 µl of RED B onto each of the tissue sections. They were then incubated at room temperature for 10 minutes. The solution was removed from the slides and washed three to five times in distilled water. The slides were dipped briefly in toluidine blue

solution to counterstain them and then rinsed in running tap water. The slides were then dried on the slide hotplate or put in the oven at 60°C for 10 minutes and then the slides were dipped in Histo-Clear, mounted with Histomount (Table 2.2) and coverslipped.

Table 2.6 Components of solutions commonly used for IF.

Reagent	**Cat. No**	**Company**	**Colour**
Opal™ 520 Reagent Pack dissolved in 70ml of dimethyl sulfoxide	FP1487001KT	Akoya Biosciences	Green dye
Opal™ 570 Reagent Pack dissolved in 70ml of dimethyl sulfoxide	FP1488001KT	Akoya Biosciences	Red dye
Plus Amplification buffer	2506493	Perkin Elmer	Buffer solution
Prolong gold antifade reagent with DAPI	P36931	Thermo Fisher Scientific	Mounting media

Table 2.7. RNAScope kits.

Kits	**Lot**	**Company**	**Ref**
RNAscope, multiplex fluorescent detection reagent v2 essay	2014108	ACD	323110
RNAscope,2.5 HD detection Reagent-RED	2012950	ACD	322360
RNAscope H2O2 and Protease reagent	2012293	ACD	322381
RNAscope protease III &IV reagent	2014291	ACD	322340

Table 2.8 Components of solutions commonly used for RNAscope.

Solution	Component	pH	Company	Lot
RNAscope wash buffer reagent	For wash buffer in 60 ml wash buffer in 3 litres of distilled water	---	ACD	2015345
RNAscope target retrieval reagent	20 ml target retrieval in 180 ml distilled water	---	ACD	2011664
20X SSC	88.23g of sodium citrate dehydrate 175.23g of NaCl 800 ml distilled water to make 1 litre	7	Sigma Aldrich	0.3MOL 3/MOL

Table 2.9. RNAscope in situ hybridization probes used.

Probe	Cat no.	Gene ID	Target region	Accession no	Gene alias	No. of base pairs
Hs-ZIC4	525661-C1	84107	2 - 1724	NM_001168378	*N/A*	*23*
Hs-NRXN1	527151-C1	9378	744 - 6787	NM_001135659	Hs.22998	20
Hs-FEZ1	468471-C1	9638	255 - 1433	NM_005103	UNC-76	*20*
Hs-SOX14	1055251-C1	8403	282 - 1657	NM_004189	Sox28	*20*

2.8 Slide Scanning

All of the images of the immunoperoxidase staining and in situ hybridization red dye presented in this investigation were captured using a Leica slide scanner (APERIO AT2) version 102.0.7.5. The images were obtained by the personnel at the Newcastle Biobank Imaging Facility at 20x image size. The exposure time was 32 ms, and image size was 95,548 x 24,705 x 1 pixels. The processing of the images, which only included adjustment of brightness and sharpness, was achieved using the Adobe Photoshop software (version 2024).

2.9 Fluorescent Microscopy

The sections marked with fluorescent molecules were observed using a ZEISS Cell-Discoverer 7 microscope and ZEN 2011 (Blue Edition) software. The double IF images were acquired with a Zeiss AXIO imager z1 and 2 equipped with a DAPI blue filter, AF488 green filter, and Cy3 red filter. Table 2.10 shows the excitation and emission values for the fluorophores utilized by this study. The images were taken using a 40x objective. The exposure time (8-180 ms) and the image size (8-16 mm) varied between images. The retouching of the images, which included adjustments to brightness, contrast, focus, colour balance, and the occasional removal of artefacts, was performed using Adobe Photoshop software (version 2024).

Table 2.10. Fluorophore information.

Filter	Excitation	Emission	Colour
AF488	493	517	green
Cy3	548	561	red
DAPI	352	455	blue

2.10 3D Mapping Model

The primary objective of this study was to identify the thalamic structures within the human foetal forebrain. This was achieved via the construction of a 3D model that depicted the neurodevelopmental gene expression patterns. Subsequently, these patterns were visualized in various planes to facilitate further analysis.

Chapter 4 presents a flowchart outlining the methodology undertaken by this study. The immunohistochemistry was performed initially on sections of the foetal brain to mark the regions of expression of transcription factors tested, which were later mapped onto virtual 3D models. Double-label IF was performed to confirm the boundaries established during the model-building process and to analyse the combinatorial gene expression.

The three-dimensional models are stored in Z:\HDBRes\data2\01_Amira. Select "Open Data" from the start screen and proceed to locate your model (foetal brain N11 13 PCW). Upon loading the file, it will shift to project view. The file is displayed as a green bar in the upper left panel. All properties will be located in the bottom left panel, while the huge panel on the right displays the 3D objects. To display an orthoslice, right-click the green bar or choose the arrow at the end, then navigate to display > orthoslice > create. Select "Display," then scroll down to "Volren" and choose "Create" to obtain a volume rendering of the model. A volume render can be integrated with a slide.

Following this stage, 3D mapping will be started using Open Amira, specifically version 2021.1 with the HDBR module installed. Upon accessing the model, navigate to File > Open Data and the gene expression images are chosen. Then select HDBR > 1-Plane Selection > generate and the selected tissue is dragged and dropped into Amira (Figure 2.1). Next, from the dropdown menu adjacent to data, the plane and angle of the models are adjusted to overlap the histological section by scrolling the mouse. The next step is to right-click on the background and to select Create Object > HDBR > Landmark Registration. Then tiepoint is added to the left images first (3model), then the corresponding place in the right image is clicked to confirm the tissue is in good position with the 3D model (Figure 2.2). After this step, the signal is filtered by right-clicking on the background and selecting Create Object > HDBR > Signal Filtration (Figure2.3). We have set the minimum and maximum threshold to exclude the brightest signals. The two photos will be displayed in the viewer windows, accompanied by blue overlays. To clean the registered filtered file, its name is chosen (it will turn green) and then the segmentation tab is clicked. The brush tool is utilised to apply paint over all elements you wish to eliminate. To visualise mapping data, select Create Object > HDBR > slice mapping, volume rendering and then voxelized rendering to integrate the slides into the 3D models (Figure 2.4).

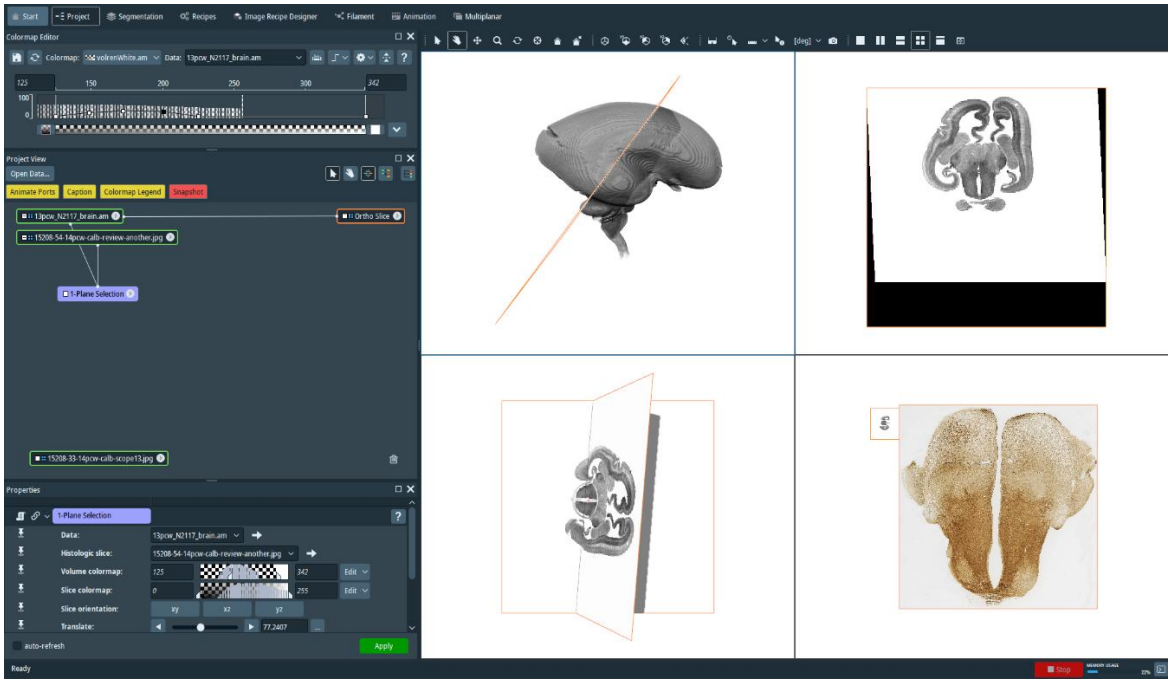

Figure 2.1. Plane selection steps in 3D models of Amira program.

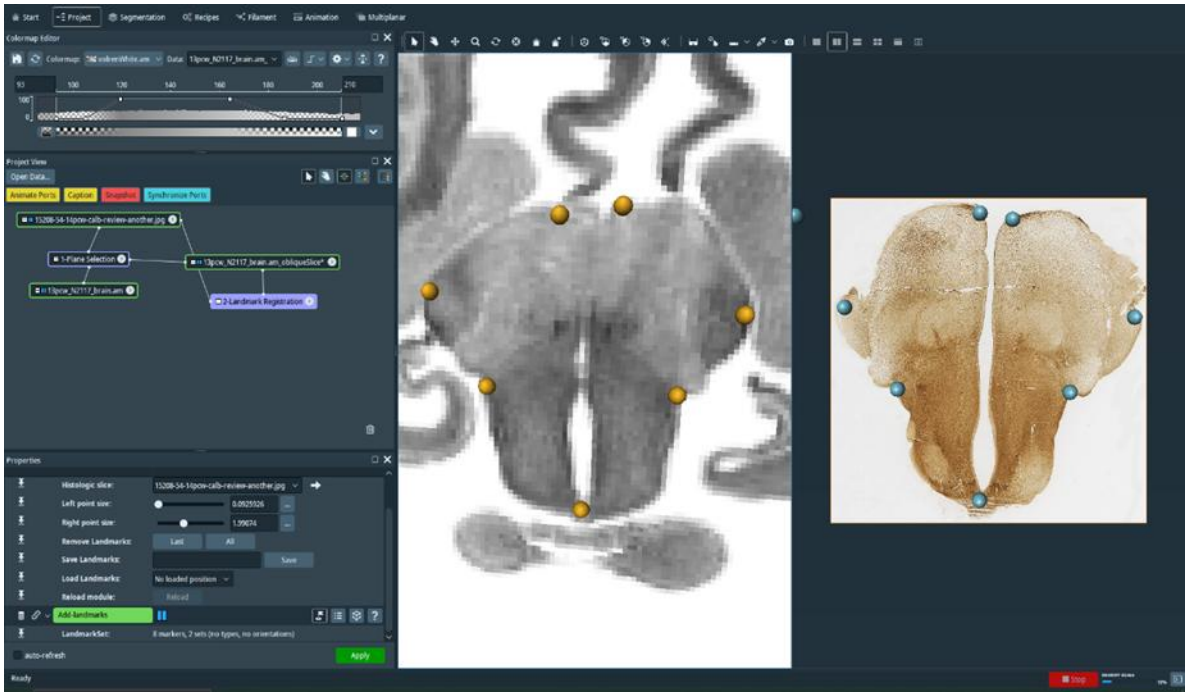

Figure 2.2. Landmark steps in 3D models of Amira program.

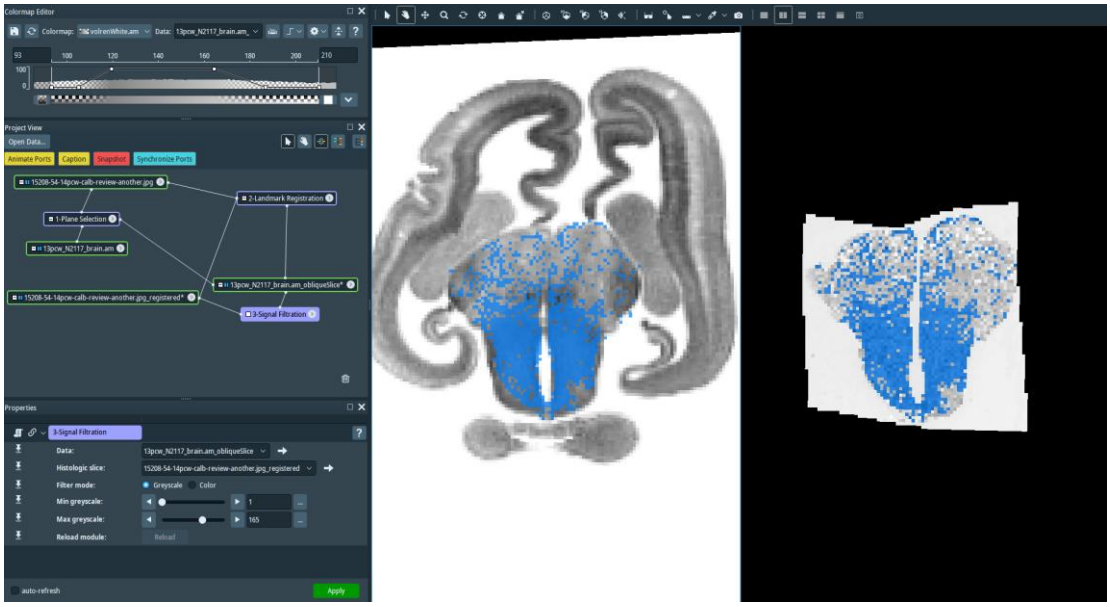

Figure 2.3. Signal filtration steps in 3D models of Amira program.

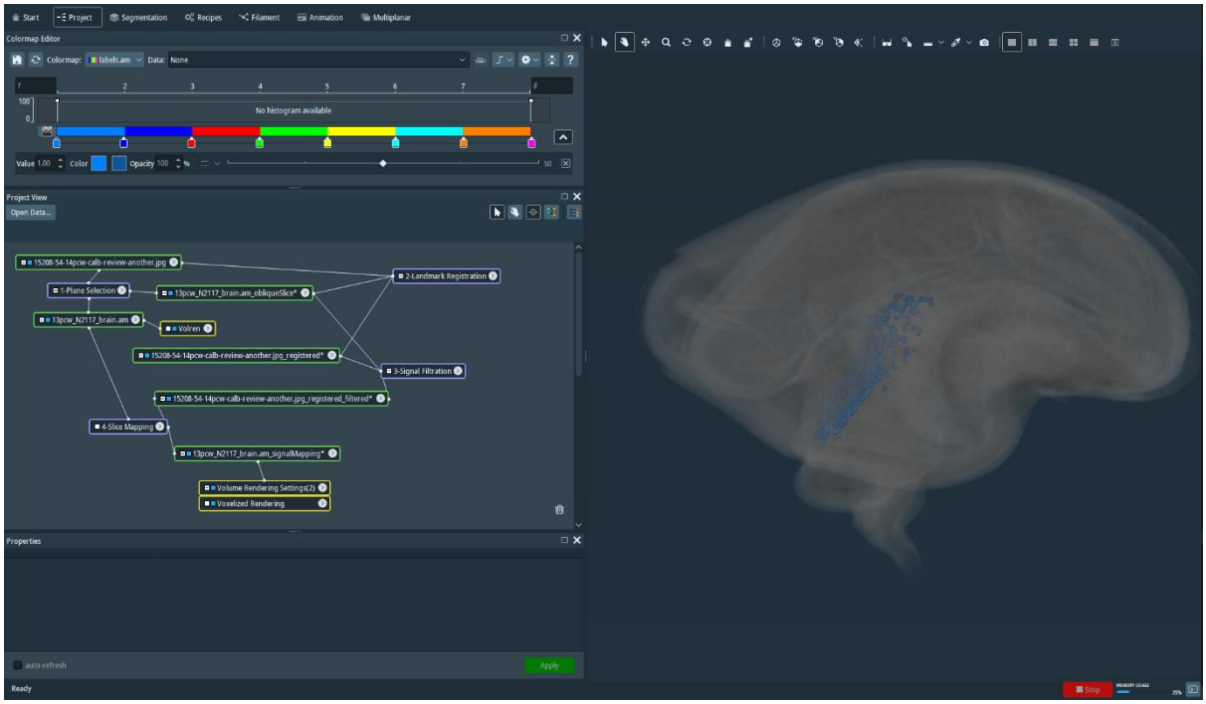

Figure 2.4 Slice mapping steps in 3D models of Amira program.

3 Chapter 3. Analysis of Single-cell RNAseq Data from the Foetal Human Thalamus at 16 PCW using Neuroscience Multi-Omic Analytics (NEMO).

3.1 Introduction

Several studies in mice have investigated gene expression patterns within the thalamus, revealing where specific genes are expressed across different thalamic nuclei. However, as previously mentioned, one of the key anatomical differences between rodents and humans is the absence of the pulvinar nucleus in the rodent thalamus. This difference is significant, as the pulvinar plays a major role in higher-order behaviours and is implicated in various neurodevelopmental disorders in humans.

To explore the complexity of the human thalamus—particularly at early stages of development—single-cell RNA sequencing (scRNA-seq) data from the foetal human thalamus at 16 PCW can be analyzed. This approach enables us to distinguish various cell types based on their unique transcriptional profiles. By identifying marker genes that are highly expressed within each cell cluster, we can classify distinct cell populations with high resolution. Following this, histological staining using these marker genes allows for spatial mapping of cell types to specific thalamic nuclei in chapter 4. This integrative approach helps us understand not only the molecular identity of thalamic cells but also their anatomical localization, offering insight into the organization and development of thalamic nuclei—particularly those unique to the human brain, such as the pulvinar. Ultimately, this can enhance our understanding of the cellular architecture of the human thalamus and its potential links to neurodevelopmental conditions

A cellular map of the 16 PCW thalamus was generated by employing basic bio-informatic methods, including PCA, followed by UMAP, for dimensionality reduction using the tools available the NEMO platform. The presence of different cell types - progenitor cells, excitatory neurons, OPC, GABAergic neurons, blood cells, and microglia in the developing thalamus was identified by confirming the expression of marker genes for each cluster, as supported by the extant literature. These findings will make a substantial contribution to the understanding of the developmental organization of the thalamus, aiding the investigation of which cell types express neurodevelopmental disease susceptibility genes, and providing crucial insights for future research into brain development and related illnesses.

For the purpose of this study, we examined the cellular composition of the thalamus during the 16 PCW, using a technique called single-cell RNA sequencing (scRNA-seq). At the 16 PCW timepoint, the thalamic nuclei start to develop**.** This method facilitated a detailed analysis of the different types of cells present in the thalamus and their specific characteristics, providing a comprehensive understanding of their diversity and developmental stage within a spatial and temporal framework. By utilizing the (NEMO) platform, we analysed a single-cell dataset from the Kriegstein laboratory, focusing on the 16 PCW thalamus, which was available from https://nemoanalytics.org/.

The Neuroscience Multi-Omic Analytics (NEMO) platform provides biologists with valuable access to single cell data, starting with the selection of a dataset for research and culminating with the use of diverse analytical techniques. One such tool is the principle component analysis (PCA), which is a statistical technique that enables dimensionality reduction while preserving as much variance as possible in the dataset. Another analysis tool, the Uniform Manifold Approximation and Projection (UMAP), facilitates the analysis of data using models to find relationships within the data. Use of UMAP after PCA enables the generation of a cluster map that facilitates the visualization of relationships in the data by, for instance, highlighting the key genes associated with specific cell type clusters in the developing human thalamus. It also highlights which genes are highly expressed (threshold mean expression > 1.5).

3.2 Aim of the Study

By using the NEMO database (https://nemoanalytics.org/) and gene mapping, we aimed to identify cell types in clusters from a single-cell dataset from the Kriegstein laboratory at 16 PCW on the developing thalamus in order to understand where/if susceptibility genes are expressed in the thalamus. The NEMO database was consulted to access gene expression data and relevant annotations, and then the list of genes associated with cell-type clusters was obtained from the datasets published previously. The experimental results were then compared with the gene mapping and cluster detection from the NEMO database analysis, in order to understand how susceptibility genes, including transcription factors, are expressed in the forebrain, and in which cell types.

3.3 Methods

We selected a single-cell data set from NEMO that covered the developmental time point and brain region 16 PCW thalamus taken from a human (Single Cell 10X RNAseq-Kriegstein) (https://nemoanalytics.org/). The processes of normalization and the scaling of the data set was undertaken using NEMO software, and the percentage of mitochondrial content was maintained below 0.05% to focus on living cells**.** For highly variable genes, PCA calculations were also performed using the same software, and five principal components were selected to create clusters of cells with similar expression profiles using UMAP. The UMAP analysis detected 15 discrete clusters and each cluster was allocated a separate colour for separation purposes (Figure 3.1 A). The software provided lists of the genes expressed most highly in each cluster, and after generating UMAPS for each gene of interest (Figure 3.1 B), both the marker genes and certain cell types were identified for each cluster. An example of a marker gene for each cluster is provided in Figure 3.1 A, however complete identification of each cluster came from an extensive investigation of several markers (see below). The marker genes were chosen using data drawn from the literature review such as genecards, human protein atlas (https://www.genecards.org/Search), Online Mendelian Inheritance in Man (OMIM) (https://www.omim.org/help/faq). In addition, a feature plot was produced to depict visually the cell markers utilised to identify each cell type. The results from the NEMO database provided a thorough delineation of the different cell types present in the thalamus at 16 PCW, offering vital knowledge concerning the developmental structure of the thalamus at 16 PCW. Each cell cluster was then examined in more detail.

3.4 Results

3.4.1 Transcriptomic cells in developing human thalamus at 16 PCW

In Figure 3.1, the single cell RNAseq data for thalamus at 16 PCW was taken from the NEMO Analytics database and is presented here. Figure 3.1 A showed how these clusters are classified as different types of cells according to the type of genes expressed in each cluster (Figure 3.1 B). UMAP plots were generated for some of the selected genes, such as GADD45B, *MKI67, OLIG1, GAD1, DOK5, TCF7L2, CLDN5, HBA1* and *CCL3*. These UMAP plots effectively highlight the differential expression of these genes across the various neuronal clusters, facilitating understanding of how specific genes are associated with their distinct neuronal

identities. For instance**,** *MKI67* is commonly identified with cellular proliferation (cluster 4, purple), while *GAD1* is a marker for inhibitory neurons (cluster 2 green). GADD45B characterizes quiescent progenitors and astrocytes (clusters 0, blue; 5, brown; 7, green) while OLIG1 expression is associated with oligodendrocyte and GABAergic neuron precursor cells (cluster 3, red); DOK5 is expressed in immature neurons and progenitor cells (9); TCF7L2 is expressed in all glutamatergic thalamic neurons (cluster 1, orange; cluster 6, pink; cluster 10, light orange; cluster 11, light green; cluster 12, rose). CLDN5 expression marks pericyte and endothelial cells (cluster 8, sky blue); HBA1 expression represents erythrocytes (cluster 13, lavender); and CCL3 expression (cluster 14, grey) is indicative of microglial cells.

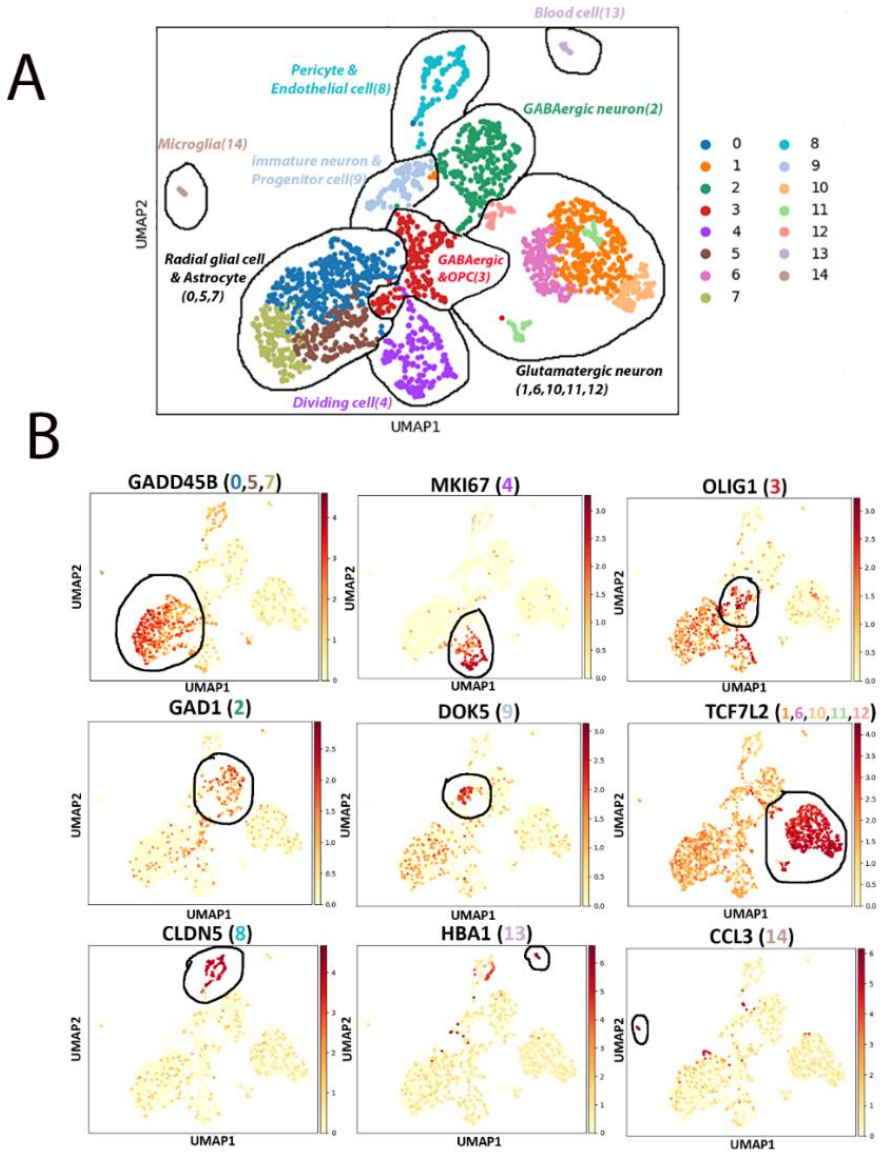

Figure 3.1. Identification of cell types found in each cluster generated from NEMO, for the time point and brain region 16 PCW (thalamus from a human). (A) The UMAP represents the 15 clusters and their corresponding cell types. (B) The UMAPs represent key marker genes used to define each cluster: Expression of *GADD45B* characterizes quiescent progenitors and astrocytes (clusters 0, blue; 5, brown; 7, green); *MKI67* (concentrated in cluster 4, purple) indicates actively proliferating cells; *OLIG1* expression is associated with oligodendrocyte and GABAergic neuron precursor cells (3, red); *DOK5* is expressed in immature neurons and progenitor cells (9); *GAD1* is expressed by GABAergic neurons (2); *TCF7L2* is expressed in all glutamatergic thalamic neurons (1, orange; 6, pink; 10, light orange; 11, light green; 12, rose). *CLDN5* expression is a marker for pericyte and endothelial cells (8, sky blue); *HBA1* expression is indicative of erythrocytes (13, lavender); and *CCL3* expression (14, grey) identifies microglial cells.

3.4.2 Clusters 0, 5, and 7. Quiescent radial glia and astrocytes

Table 3.1 and Figure 3.2 provide a detailed summary of the highly expressed genes (threshold expression > 1.5) observed in clusters 0, 5, and 7, from which we deduced that these clusters contained quiescent progenitor cells and astrocytes. The 46 genes in Table 3.1, which represent the most highly expressed genes across all three clusters, were derived from the NEMO data at 16 PCW in the human thalamus. According to the extant literature for instance, genecards, human protein atlas, Online Mendelian Inheritance in Man (OMIM), these genes are accurate indicators for determining cellular identity and state. The genes linked to radial glial (RG) cell signature profiles are highlighted in grey, while the genes associated with astrocytes are shown in green. The genes that were expressed in both the RG cells and the astrocytes are highlighted in yellow boxes, indicating their similar properties. Red indicates the expression of certain genes in all three clusters (0, 5, and 7), suggesting a possible functional or developmental overlap between the cell types. The genes that exhibited significant expression primarily in clusters 0 and 7 are indicated in blue, while those expressed mainly in clusters 0 and 5 are indicated in purple. The genes that exhibited high levels of expression in clusters 5 and 7 are indicted in brown text. In addition, there were distinct expression patterns that could be observed with the genes expressed exclusively in cluster 0, which are represented in black text. Similarly, the genes exclusive to cluster 5 are shown in orange text, while those specific to cluster 7 are displayed in green. Genes *GADD45B*, *GFAP*, *SLC6A11*, *HES1* and *HES5*, *SOX2*, *SOX9*, *PAX6*, *HOPX*, *C1orf61*, *PTPRZ1*, and *FABP7* are known to be expressed in either radial glial cells or astrocytes, or both. Their strong expression (threshold expression > 1.5) in clusters 0, 5, and 7 suggested the presence of these cell types.

Based on the gene expression patterns that were both common and distinct, it was not possible to classify any of the clusters, 0, 5, or 7, as consisting solely of astrocytes or progenitor cells. The findings presented a complicated biological continuum, in which distinct clusters contained cells that combined features from both RG and astrocyte cells. Indeed, it was observed by previous researchers that RG cells contain several glial proteins and global transcriptome analyses revealed similarities between RG cells and astrocytes (Götz et al., 2015). The next sections discuss the evidence for considering certain genes to be clear markers for certain cell types.

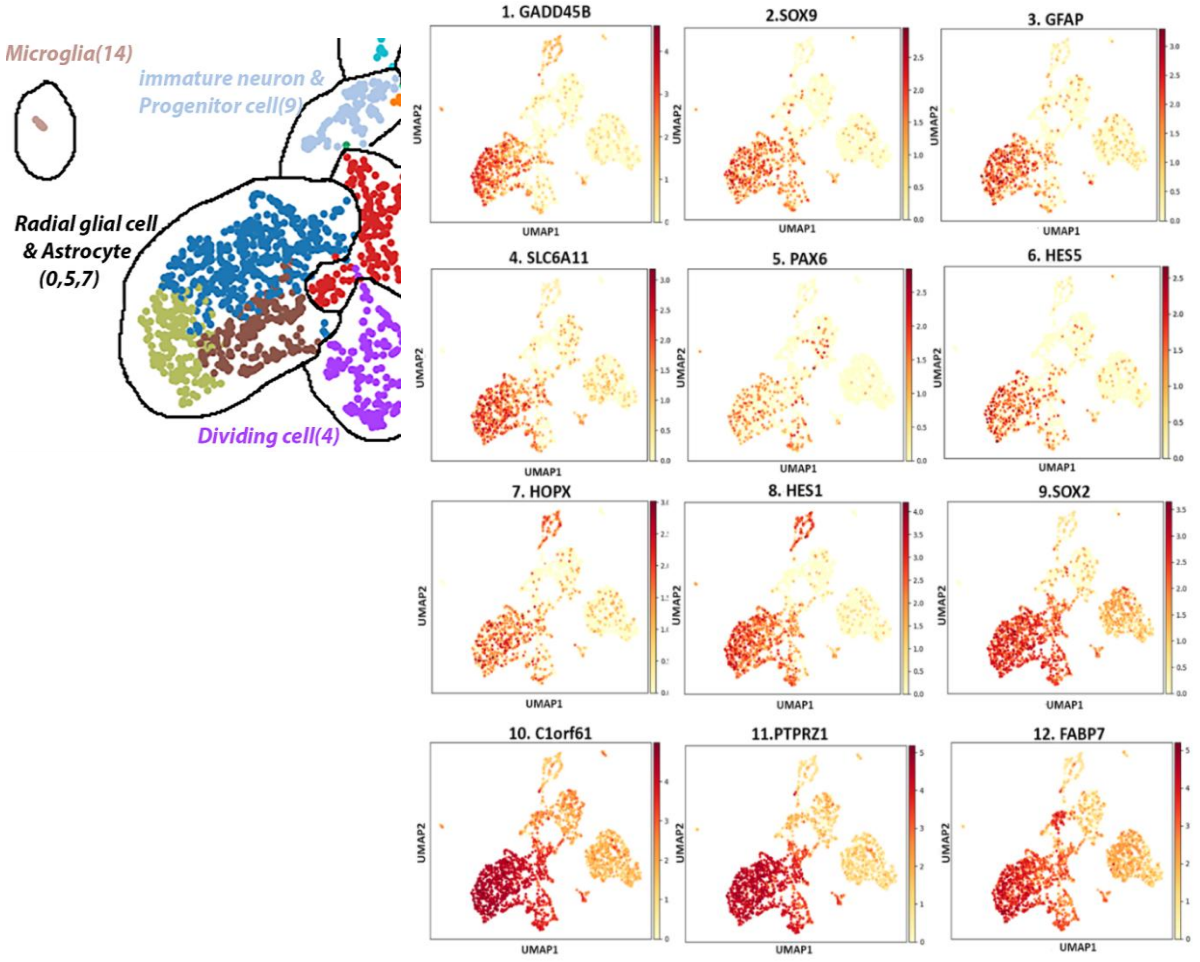

Figure 3.2. Quiescent progenitors and astrocytes. The expression of a number of marker genes within clusters 0, 5, and 7 identified as expressed by quiescent progenitors and astrocytes. SLC6A11 expression is characteristic of astrocytes, and GADD45B, GFAP, and HES5 are characteristic of progenitors and astrocytes, showing an expression pattern largely confined to these three clusters. The basal RG marker HOPX is confined to cluster 5. Other genes (SOX9, HES1, SOX2, C1orf61, PTPRZ1, and FABP7) are expressed strongly in clusters 0, 5, and 7, but also in other clusters containing actively dividing progenitors (4) or progenitor or precursor cells mixed with other cell types (3 and sometimes 9). Note that HOPX and HES1 are also expressed strongly by putative endothelial cells (8), PAX6 by some GABAergic neurons (2), and SOX2, C1orf61, and FABP7 are expressed moderately in the glutamatergic neuron cluster groups (1, 6, and 10-12).

Table 3.1. Quiescent progenitors and astrocytes (0, 5, 7). Summary of the 46 genes expressed most highly in each of clusters 0, 5, and 7. The colour of the box identifies the known cell specific markers (see legend). The colour of the text identifies the genes expressed in either single or multiple clusters. From this analysis, it was difficult to assign different cell types to a specific cluster.

0		5		7	
MFGE8	RPS15A	APOE	SLC6A11	APOE	TSC22D4
PTPRZ1	GADD45B	CST3	NTRK2	GADD45B	LUZP2
CST3	PAX6	CLU	S100A13	CST3	CXCL14
DBI	NFIA	TTYH1	PON2	C1orf61	FOS
PTN	QKI	PTN	PMP2	CLU	SOX2
FOS	RPL13A	GPM6B	ALDOC	HES5	PLPP3
MT3	NDRG2	C1orf61	CNN3	FABP7	NFIA
TTYH1	RPS27	AQP4	TSC22D4	PTPRZ1	S100A16
EGR1	RAMP1	PTPRZ1	FABP5	EDNRB	QKI
HES5	NFIB	BCAN	TFPI	TTYH1	CPE
PMP2	RPL30	EDNRB	NFIA	PTN	SLC6A11
NRXN1	VIM	DBI	NRXN1	GPM6B	HMGCS1
CNN3	SOX9	MT3	MT1E	MGST1	JUN
FABP7	S100B	CPE	PSAT1	SOX9	PMP2
SOX2	RPL41	PLPP3	NKAIN4	MT3	NCAN
HES1	H3F3B	MGST1	GJA1	AQP4	NFIB
BCAN	CXCL14	SOX2	FEZ1	ID2	SAT1
JUN	S100A13	FABP7	ID2	JUNB	ATP1A2
GPM6B	MGST1	LUZP2	NCAN	CNN3	NTRK2
TSC22D4	RPLP1	NDRG2	SERPINE2	NDRG2	H3F3B
PON2	GFAP	RAMP1	HOPX	DBI	IDI1
APOE	RPS27A	S100B	GLUD1	GFAP	PON2
FABP5	ADGRG1	CXCL14	MT2A	HES1	MFGE8

KEY:

Genes in 0, 5 and 7 clusters red

Gene in clusters 0 and 7 blue

Genes in clusters 0 and 5 in purple

Genes in clusters 5and 7 in brown

Genes in 0 cluster in black

Genes in 5 cluster in orange

Genes in 7 region in green

RG marker

ASTROCYTE marker

RG, ASTROCYTE marker

3.4.2.1 Justification for using the following marker genes to identify clusters 0, 5, and 7

GADD45B (clusters 0 and 7)

The growth arrest and DNA damage-inducible beta protein is also known as GADD45B. The study by Shen et al. (2022) noted that previous research concerning GADD45B mainly studied non-neuronal cells. GADD45B plays an essential role in the regulation of the cell cycle, controlling growth and differentiation in the mammalian central nervous system (CNS) during development. Moreover, this protein interacts with a variety of effectors to regulate DNA repair, cell cycle arrest, apoptosis, and differentiation (Shen et al., 2022). Gadd45b can also be seen in the progenitor cells of the midbrain and the hindbrain, and exhibits weak expression in the forebrain in mouse embryonic development (Sultan and Sweatt, 2013). The study by (Jun et al., 2015) demonstrated that this gene regulates the growth of quiescent radial glia-like (RGL) neural stem cells (NSCs) and non-RGL neural precursors in the hippocampus of adult mice in response to electroconvulsive shock. It was also observed in the post-mortem human prefrontal cortex that GADD45b is expressed in glial cells (Gavin et al., 2012), as observed in the co-localization of GADD45B with S100B. To our knowledge, no study to date addressed the verification of the expression of GADD45B in the developing forebrain. The mapping obtained from the NEMO database by the present study revealed a robust expression of GADD45B in the developing human thalamus at 16 PCW, particularly in the cells classified within clusters 0 and 7, which therefore likely corresponded to both RG cells and astrocytes.

SRY-box transcription factor 2 (SOX2) (clusters 0, 5, and 7)

SOX2 is expressed in different cell types within the brain; for example, progenitor cells, astrocytes, oligodendrocytes, neural precursors, GABAergic interneurons, and glutamatergic neurons (Mercurio et al., 2019, Mercurio et al., 2022). The study by (Eze et al., 2021) confirmed that SOX2 is expressed in RG cells in the early developing foetal human brain. Moreover, SOX2 is a typical apical RG protein and is also expressed in truncated RG cells (Voigt, 1989). The expression of SOX2 in astrocytes was validated by (Kim et al., 2023). In the present study, SOX2 was expressed highly across all three clusters, confirming the ubiquitous nature of this marker.

Protein Tyrosine Phosphatase Receptor Type (PTPRZ1) (Clusters 0, 5, and 7)

PTPRZ1 exhibits significant expression in glial cells, specifically OPCs, oligodendrocytes, and the astrocytes present in the CNS (Lamprianou et al., 2011; Nagai et al., 2022). Previous studies reported its presence in Purkinje cells (PCs) and in the Bergmann glia in postnatal rat cerebellar cortices and neuronal axon fibres during growth (Wang et al., 2020). In U373-MG cells, the PTN–PTPRZ complex causes PTPRZ1 tyrosine phosphatase inactivation. This signalling pathway is associated with the migration of neural cells in the brain cortex (Santana-Bejarano et al., 2023). The multiple roles potentially played by this protein were reflected in the present study by its expression in all three clusters. In conclusion, PTPRZ1 expressed in both progenitor cells and astrocytes in three clusters 0, 5 and 7.

Fatty Acid Binding Protein (FABP7) (Clusters 0, 5, and 7)

FABP7 is critical for the establishment of the RG cell fibre system, as well as the development of cortical layers (https://www.uniprot.org/uniprotkb/O15540/entry#function) in the developing brain. It is present in both the RG cells of the embryonic brain and in the astrocyte and precursor cells. Specifically, it was detected in adult brains in mammals (Gerstner et al., 2023), as well as in the astrocyte cell and oligodendrocyte progenitor cells in the developing mouse brain (Hara et al., 2020). Its expression by a broad range of cell types was reflected in the present study by its appearance as a marker for all three clusters. *Fabp7* is a downstream gene of *Pax6* and it is critical during early cortical development in rats for maintaining neuroepithelial cells (Arai et al., 2005). Therefore, FABP7 expressed in three clusters 0, 5 and 7 in both progenitor cells and astrocytes.

Chromosome 1 open reading frame 61 (C1orf61) (clusters 5 and 7)

C1orf61 is expressed in high levels in neural progenitor cells in the mouse brain (Eze et al., 2021). According to the Online Mendelian Inheritance in Man (OMIM) database, *C1orf61* is expressed in the proliferating and migrating cells of the VZ of the early-developing human brain (Entry - *618747 - CHROMOSOME 1 OPEN READING FRAME 61; C1ORF61 - OMIM). *C1orf61* is expressed in progenitor cells in the human brain by the co-expression studies of *SOX2* and *C1orf61* in the human embryonic brain at 16 PCW (Eze et al., 2021). C1orf61 expressed in cluster 5 and 7 which marks progenitor and astrocyte cells.

Solute Carrier Family 6 Member 11 (SLC6A11) (clusters 5 and 7)

SLC6A11 allows the transportation of GABA into the glial cells (Hu et al., 2020). It is important to note that GABA is a major inhibitory neurotransmitter in the CNS, and its transport is crucial for regulating GABAergic neurotransmission and for maintaining neurotransmitter homeostasis. The expression of *SLC6A11* in astrocytes was verified by the Human Protein Atlas (SLC6A11 protein expression summary the human protein atlas. Available at: https://www.proteinatlas.org/ENSG00000132164-SLC6A11), and by (Yeh et al., 2023). To my knowledge, there is no evidence in the extant literature for *SLC6A11* being expressed in progenitor cells, although the present study's analysis by the NEMO database suggested it may be present in the developing thalamus. CLC6A11 expressed in progenitor and astrocyte cells in cluster 5 and 7 which marks.

Glial fibrillary acidic protein (GFAP) (clusters 0 and 7)

GFAP, which is a type III intermediate filament, is known as a specific marker of certain classes of astrocytes (Yeh et al., 2023) and is present in the astrocytes located in the thalamus (Hol and Pekny, 2015, Torres-Platas et al., 2016, Kim et al., 2023). GFAP shows high expression in the forebrain, indicating the presence of a large population of astrocytes responsible for regulating high neuronal activity (Joppé et al., 2020). A recent study demonstrated that GFAP is expressed in the apical RG cells in the developing foetal human brain, and also identified its lack of co-expression with HOPX, which is expressed in basal RG cells (Holst et al., 2023). In contrast, (Voigt, 1989) claimed that GFAP is expressed in both the apical and basal RG cells in the developing human cortex. GFAP is present in actively dividing RG cells in the VZ at GW 13, and in the neural progenitor cells of the SVZ at later stages of gestation in the developing human cortex (Middeldorp et al., 2010, Arellano et al., 2021). Meanwhile, Arellano et al. (2021) demonstrated that GFAP is expressed in the dividing progenitor cells in macaque monkey embryos' cerebral cortex (Arellano et al., 2021). The present study confirmed that GFAP immunoreactivity is expressed in the thalamus at 19 PCW, with strong expression in the VZ (presumptive RG cell) and the astrocytes (Figure 3.3). GFAP was highly expressed in clusters 0 and 7, again suggesting that these clusters may contain both RG and astrocytes.

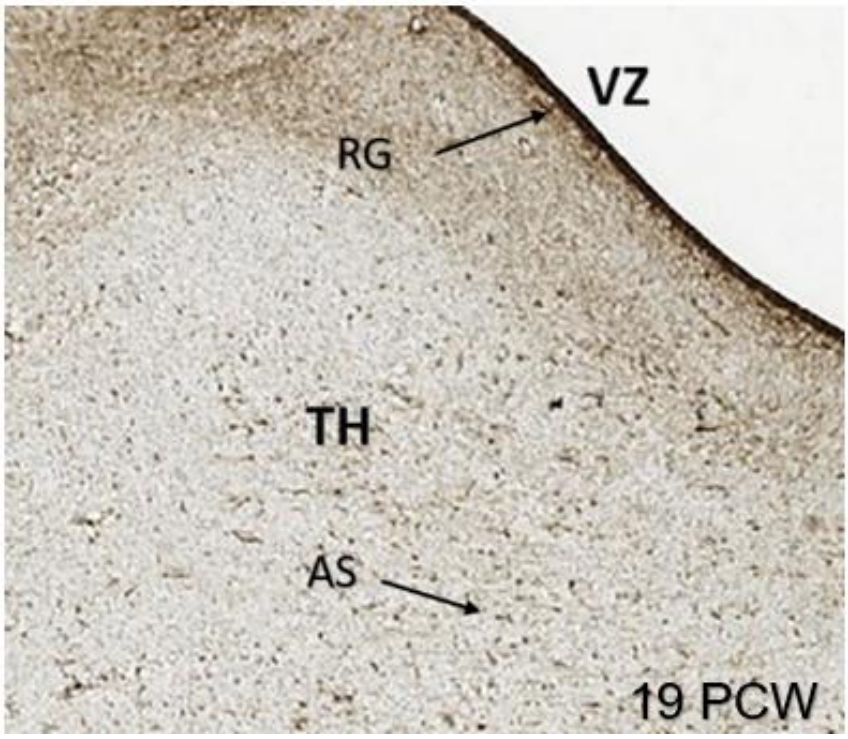

Figure 3.3. GFAP expression in the human thalamus at 19 PCW. It is highly expressed in the VZ in RG cells, and among the astrocytes in the mantle of the thalamus. Abbreviation: Thalamus (TH); ganglionic eminence (GE); ventricular zone (VZ); Cortex (CRX); hypothalamus (Hpth); astrocyte (AS); radial glial (RG).

Hairy enhancer of split homologs 1 and 5 (HES1 and HES5) (clusters 0 and 7)

HES1 and HES5 are members of the basic helix-loop-helix (bHLH) family of transcription factors. These transcription factors play a crucial role in regulating cell fate decisions, particularly in stem cells and progenitor cells, in order that progenitors are sustained in an undifferentiated state that prevents their premature differentiation to neurons (Ross et al., 2003). *HES1* is expressed in the neuronal stem cells of the developing brain (Ohtsuka et al., 2001). Moreover, it is expressed in progenitor cells in the foetal human thalamus (Kim et al., 2023). *HES5* is expressed highly in RG cells, including during the foetal embryonic human brain (Eze et al., 2021). Previous studies of the developing mouse brain suggested that hes1 and hes5 are expressed highly in the VZ, which contains RG cells (Ohtsuka et al., 2001). Moreover, Kageyama et al. (2007) observed that *hes1* and *hes5* are expressed mainly in the RG cells in the mouse brain. This suggested that clusters 0, and 7 may contain a high proportion of RG cells and/or other progenitors (Kageyama et al., 2007).

SRY-box transcription factor 9 (SOX9) (clusters 0 and 7)

SOX9 is known to be present in both astrocytes and progenitor cells in the human and mouse brain during development (Sun et al., 2017). SOX9 plays a crucial role in the process of astrogliogenesis from stem cells and progenitor cells by following a Notch-dependent pathway (Neyrinck et al., 2021). SOX9 is produced highly in the developing CNS by neural epithelial progenitor cells in the VZ of the CNS (Vogel and Wegner, 2021). Moreover, *Sox9* is upregulated by the MAPK/PI3K signalling pathway and is downregulated by miRNAs in mice (Ashrafizadeh et al., 2021). The study by Ung et al. (2021) found that the loss of SOX9 function in the astrocytes present in the olfactory bulb of an adult mouse deteriorates the neural sensory response maps, while some studies observed that *SOX9* is expressed in astrocytes in human brain development**.** In summary, SOX9 is a marker for both astrocytes and progenitor cells in two clusters 0 and 7 (Götz, 2013, Götz et al., 2015, Huttner, 2023).

Paired Box 6 (PAX6) (cluster 0)

PAX6 is expressed in the proliferative neuroepithelial of the VZ in the forebrain, hindbrain and progenitor cells during development. It also maintains mitotic cells in the SVZ in the adult mouse forebrain (Duan et al., 2013). The study by Inoue et al. (2000) found that the expression of Pax6 in the neuroepithelial cells appears during the initial stages of brain development (Inoue et al., 2000). Pax6 plays a crucial role in CNS development in processes such as brain patterning, neuronal specification, neuronal migration, and axonal projection (Osumi, 2001, Simpson and Price, 2002). Moreover, Pax6 promotes neuronal differentiation in the cerebral cortex during development (Arai et al., 2005). At the protein level, KAT2A downregulates PAX6 expression, thereby promoting neuronal differentiation (Shohayeb and Cooper, 2023). Previous studies also revealed that PAX6 is expressed strongly in RG cells during the development of the cerebral cortex in mice (Götz et al., 1998, Thakurela et al., 2016). According to Clegg et al. (2015), postmitotic neurons in the dorsal thalamus do not express this gene (Clegg et al., 2015). A recent transcriptomic study of the developing human thalamus found that *PAX6* is expressed in RG cells, other progenitor cells, and inhibitory neurons (Kim et al., 2023). *PAX6* is also expressed in RG cells in the human cortex (Bilgic et al., 2023). In the mice cortex, *pax6* is expressed in the VZ (Walther and Gruss, 1991). In the human brain, PAX6 is expressed in the proliferative zone, is weak in the SVZ, and may reach the intermediate zone at 9-11 PCW. Therefore, PAX6 is a marker for progenitor cells in cluster 0.

Homeodomain-only protein (HOPX) (cluster 5)

HOPX is a marker for the basal (outer) RG cell in the developing primate cerebral cortex, and is expressed principally in the SVZ (Nowakowski et al., 2017, Huttner, 2023). The thalamus also has an SVZ, but the existence of basal RG in the thalamus has not been explored extensively. *HOPX* also can be expressed in cortical astrocytes (Falcone et al., 2021). The present study identified a high expression of HOPX is a distinct feature of cluster 5, although it was also expressed in lower levels in clusters 0 and 7. So HOPX is marker for progenitor cells which is present in cluster 5.

Summary

In summary, the cell clusters 0, 5, and 7 identified by the database employed for the purpose of the present study represented non-dividing progenitor cells, including RG, and probably also astrocytes, that share similar gene expression profiles, which made it challenging to distinguish between the clusters. Although each cluster contained several unique highly expressed genes, each unique set contained genes that subserved a number of biological functions, which made it hard to assign a specific cell type to each.

3.4.3 Cluster 2: GABAergic Neurons

Table 3.2 and Figure 3.4 display a comprehensive compilation of the genes expressed in cluster 2. Various genes were examined to emphasise their distinct expression patterns in this cell type. The genes *GAD1, GAD2, SOX14, OTX2, FOXP2*, and *NR2F2* showed considerable expression in cluster 2 (Figure 3.4). These genes serve as crucial indicators for GABAergic neurons, confirming the identification of this specific cell type. The presence of *GAD1, GAD2, SOX14,* and *OTX2* demonstrated expression that was confined largely to cluster 2, with some expression in cluster 3, which was likely to contain immature GABAergic neuron progenitors and precursors (see below Section 3.4.4). Both *FOXP2* and *NR2F2* were also expressed strongly in cluster 2 but *FOXP2* was also expressed strongly in the glutamatergic neuron cluster grouping, and *NR2F2* was expressed strongly in the quiescent progenitor/astrocyte grouping, demonstrating that these markers are not unique to GABAergic neurons.

GAD1 and *GAD2*, *SOX14*, and *OTX2* are all important indicators for the function of inhibitory neurotransmitters in the CNS (González-Maya and González-Barrios, 2021, Pan, 2012,

Makrides et al., 2018, Golding et al., 2014). Furthermore, recent transcriptomic research performed by Kim et al. (2023) in human tissue demonstrated the expression of *SOX14* and *OTX2* in the GABAergic neurons in the thalamus, originating from the midbrain (Kim et al., 2023). At the midgestational stages of rat embryonic development, *Otx2* is expressed in some GABA-immunoreactive migrating-like neurons in the reticular thalamic migration region (Rtm) and zona limitans intrathalamica (Zli) and the dorsal thalamus (Inverardi et al., 2007). Additionally, Alzu'bi et al. (2017) investigated the expression of Nuclear Receptor Subfamily 2 Group F Member 2 (NR2F2, also known as COUPTFII), which is present in the GABAergic interneurons in the cerebral cortex, originating from the ventral caudal ganglionic eminence (Alzu'bi et al., 2017). In the diencephalon, it is expressed strongly by the GABAergic neurons of the prethalamus, which again may migrate to the thalamus (see Chapter 4, Section 4.4).

FOXP2 is expressed in the postmitotic cells between E14 and E16 in a cortical layer of the embryonic mouse brain (Kast et al., 2019). FOXP2 is also expressed in GABAergic neurons in the subpallium, posterior tuberculum, thalamus, and medulla oblongata. In the developing zebrafish brain*, foxp2* co-localizes with the GABAergic neuron marker *GAD1*, and is thereby indicative of their functional link (Lüffe et al., 2021). In conclusion, Cluster 2 highly expressed with marker genes for GABAergic neurons and can be classified as a GABAergic neuron cluster.

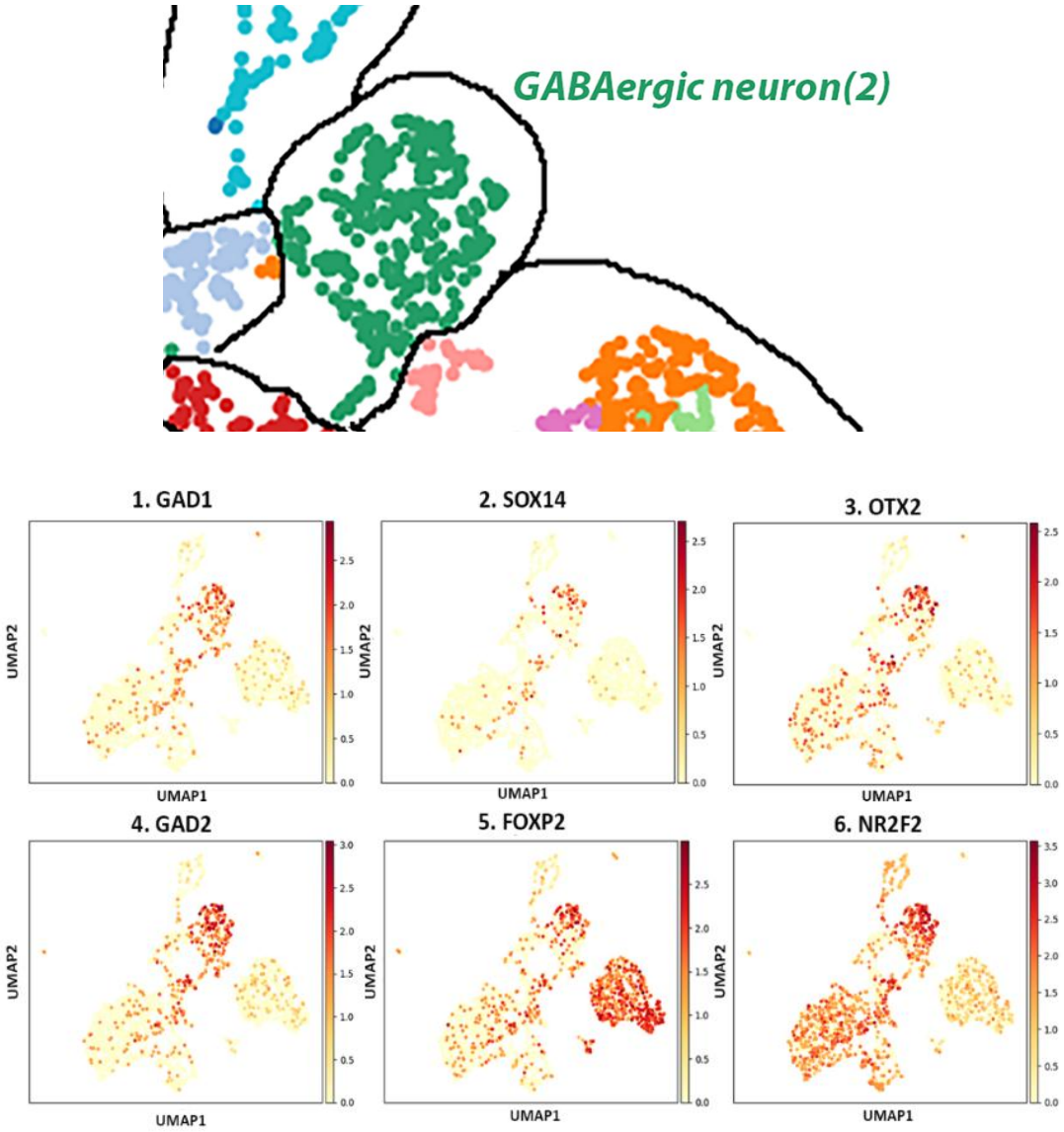

Figure 3.4. Example marker genes expressed highly in cluster 2 (GABAergic neurons). *GAD1, GAD2,* and *SOX14* expression is confined largely to cluster 2, with some expression in cluster 3 (believed to contain immature GABAergic neuron precursors). *OTX2, FOXP2,* and *NR2F2* expression is also highly characteristic of cluster 2, although O*TX2* and *NR2F2* are also expressed more widely among various clusters containing progenitor cells, and *FOXP2* shows strong expression in cells identified as glutamatergic neurons.

Table 3.2. The 28 genes expressed most highly in cluster 2 (GABAergic neurons). This list includes a number that are associated exclusively with GABAergic neurons, or their precursors, in the forebrain (green); *GAD1* and *GAD2* (coding proteins that synthesise GABA (green); *DLX1, DLX5*, and *SOX14,OTX2* (coding transcription factors that specify GABAergic neurons (blue); and other transcription factors that are associated strongly with GABAergic neurons specification and maturation, such as *LHX1, LHX5, SP8*, and *NR2F2* (red). Other highly expressed genes are characteristic of neurons in general, for example *MAP2, NRXN1*, and *CNTNAP2* (orange). The other highly expressed genes in Cluster 2 are depicted in black.

2	
GAD2	LHX5
SP8	DLX5
PTMA	GAD1
FOXP1	MAP2
SOX14	NRXN1
LHX1	BASP1
CD24	SIX3
NR2F2	AKAP9
TUBA1A	LY6H
OTX2	CNTNAP2
MARCKSL1	KIT
SOX4	CXADR
DLX1	FEZ1
ZNF804A	LMO1

3.4.4 Cluster 3: Immature GABAergic Neurons and Oligodendrocyte Precursor Cells

Table 3.3 and Figure 3.5 show that in cluster 3, like cluster 2, there was a high expression of genes such as *GAD1, NR2F2*, and *GAD2*, which is typical of GABAergic neurons. However, we also identified the expression of genes that are characteristic of OPCs, such as *OLIG1* and *OLIG2* (Oligodendrocyte Transcription Factors 1 and 2 also expressed by GABAergic neuron precursors), as well as *ADGRB1* and *PDGFRA* in this cluster (Figure 3.5). According to Szu et al. (2021), *OLIG1* and *OLIG2* are expressed in oligodendrocytes, neuronal, and glial cells in the CNS. Hence, the expression of both genes suggests the presence of OPCs, which are precursors to mature oligodendrocytes responsible for myelination. However, both genes can also be found expressed in the precursors of GABAergic neurons in the human forebrain (Alzu'bi et al., 2017). Moreover, *PDGFRA* is expressed highly in oligodendrocyte progenitor cells in the developing human thalamus (Kim et al., 2023). The transcription factor *SOX2* is expressed in different cell types within the brain, maintaining neural stem cell pluripotency, but is also expressed in post-mitotic cells, such as progenitor cells, astrocytes, oligodendrocytes, neural precursors, GABAergic interneurons, and glutamatergic neurons (Mercurio et al., 2019, Mercurio et al., 2022). Moreover, *PMP2* is expressed in oligodendrocytes in mice and in the human brain, while *PTPRZ1* is expressed among oligodendrocyte progenitor cells (Gargareta et al., 2022). Therefore, it can be concluded that cluster 3 may be a mixture of cells that include OPC and oligodendrocytes (OL), as well as immature GABAergic neurons.

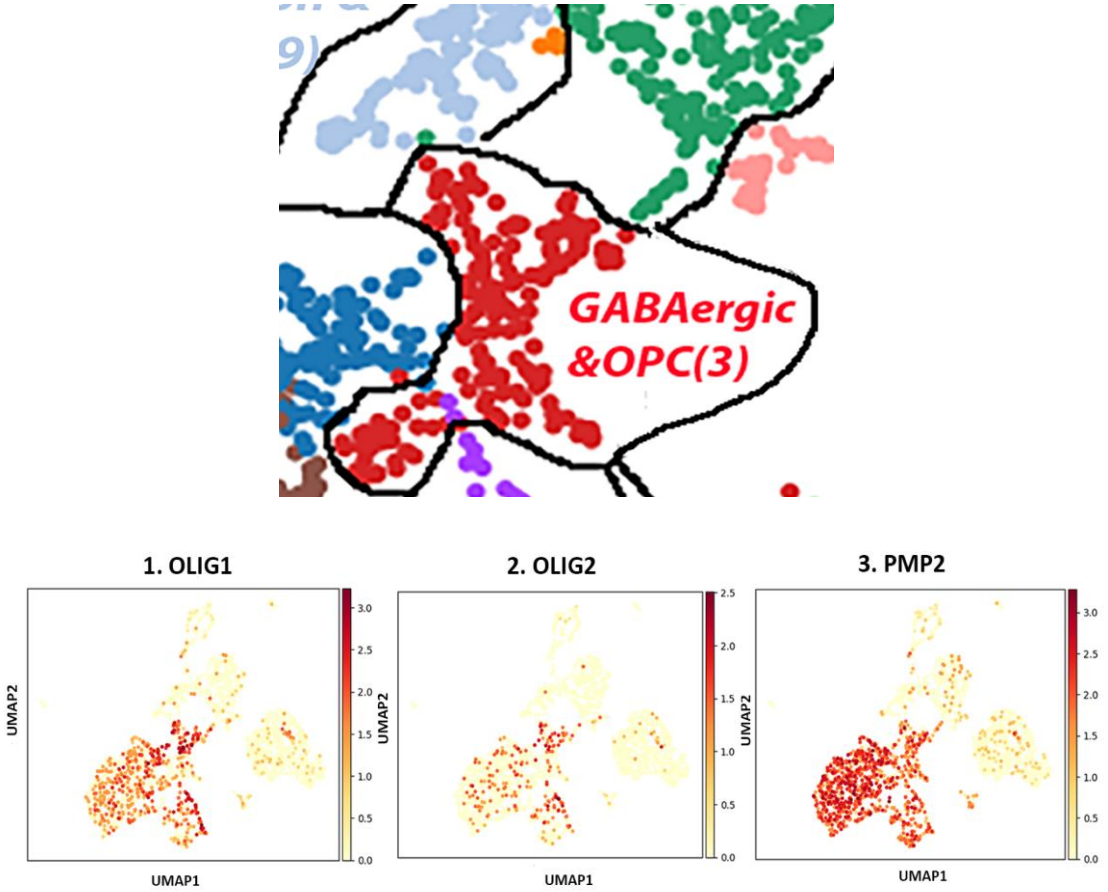

Figure 3.5. Gene expression in cluster 3. No genes were found to be expressed exclusively in cluster 3, however OLIG1, OLIG2, and PMP2 are all expressed highly in this cluster, as well as in other clusters containing dividing and quiescent progenitor cells.

Table 3.3. **Genes expressed highly in cluster3 (GABAergic neuron precursors and oligodendrocyte precursor cells).** The 30 genes expressed most highly in cluster 3 include genes associated with progenitor cells, as observed in clusters 0, 5, and 7 (green, e.g. *PTPRZ1*); markers of GABAergic neurons (orange, e.g. *GAD1, GAD2, OTX2*); genes associated with both GABAergic neuron precursors and oligodendrocyte precursors (blue, e.g. *OLIG1, OLIG2*); and markers associated exclusively with the oligodendrocyte lineage (pink, e.g. *PDGFRA, PMP2*). The other highly expressed genes in Cluster 3 are depicted in black.

3	
BCAN	SYNPR
PTPRZ1	GPM6A
SOX4	SCD5
OLIG1	DBI
APOD	TNR
PDGFRA	FABP5
C1orf61	SOX2
GAD2	IGF1
RAMP1	NR2F2
OLIG2	RPS11
SMOC1	LSAMP
OTX2	AC004158.3
NOVA1	ADGRB1
PMP2	GRIP2
GAD1	KIT

3.4.5 Cluster 4: Actively Dividing Progenitors

Table 3.4 and Figure 3.6 list genes such as *MKI67, CENPA, KIF11, TPX2, CD20*, and *KIF2C*, whose expression is a recognized indicator for actively dividing cells (Figure 3.6).

The marker of proliferation (*MKi67*), is recognized to be essential for cell proliferation in the CNS (Schonk et al., 1989, Burger et al., 1986). Previous studies found that KI67 is expressed in dividing thalamic cells (Kim et al., 2023). In our study in the embryonic human thalamus, KI67 was expressed in the ventricular zone of the thalamus at 14 PCW (Figure 3.7). Centromere protein A (CENPA) is a protein that is also involved in the formation of centromeres, which are vital for the segregation of chromosomes during the processes that comprise cell division (Smoak et al., 2016, Cao et al., 2018, Wang et al., 2022). However, the literature review conducted for this project did not provide specific data concerning the expression of CENPA in any specific class of thalamic cells. Meanwhile, KIF11 plays an essential role in cell proliferation and renewal (Jiang et al., 2017). *In vitro* studies also demonstrated that TPX2 promotes cell proliferation and cell cycle progression (Koike et al., 2022). The cell division cycle 20 (CDC20) is a protein responsible for regulating the cell cycle (Marucci et al., 2008, Malureanu et al., 2010, Bruno et al., 2022).

KIF2C, a member of the Kinesin family, is known to be crucial for cell cycle regulation. In the case of dividing cells, it is localised to the spindle poles, spindle mid zone, and kinetochores, and is also implicated in synaptic plasticity (Zhang et al., 2022, Zheng et al., 2022). In their research, McAlear and Bechstedt (2022) determined that cytoskeleton-associated protein 2 (CKAP2) is a significant proliferation marker (McAlear and Bechstedt, 2022). CKAP2 is a crucial component of cell division (Jin et al., 2004). Moreover, RAD 21 plays an important role in the cell division cycle in the CNS (Cheng et al., 2020). TUBB4B is a member of the tubulin family that forms microtubule networks, which are a component of the cell cytoskeleton. Microtubules maintain a cell's morphology, and regulate mitotic cells, cell division, and intracellular transport (Dharmapal et al., 2021).

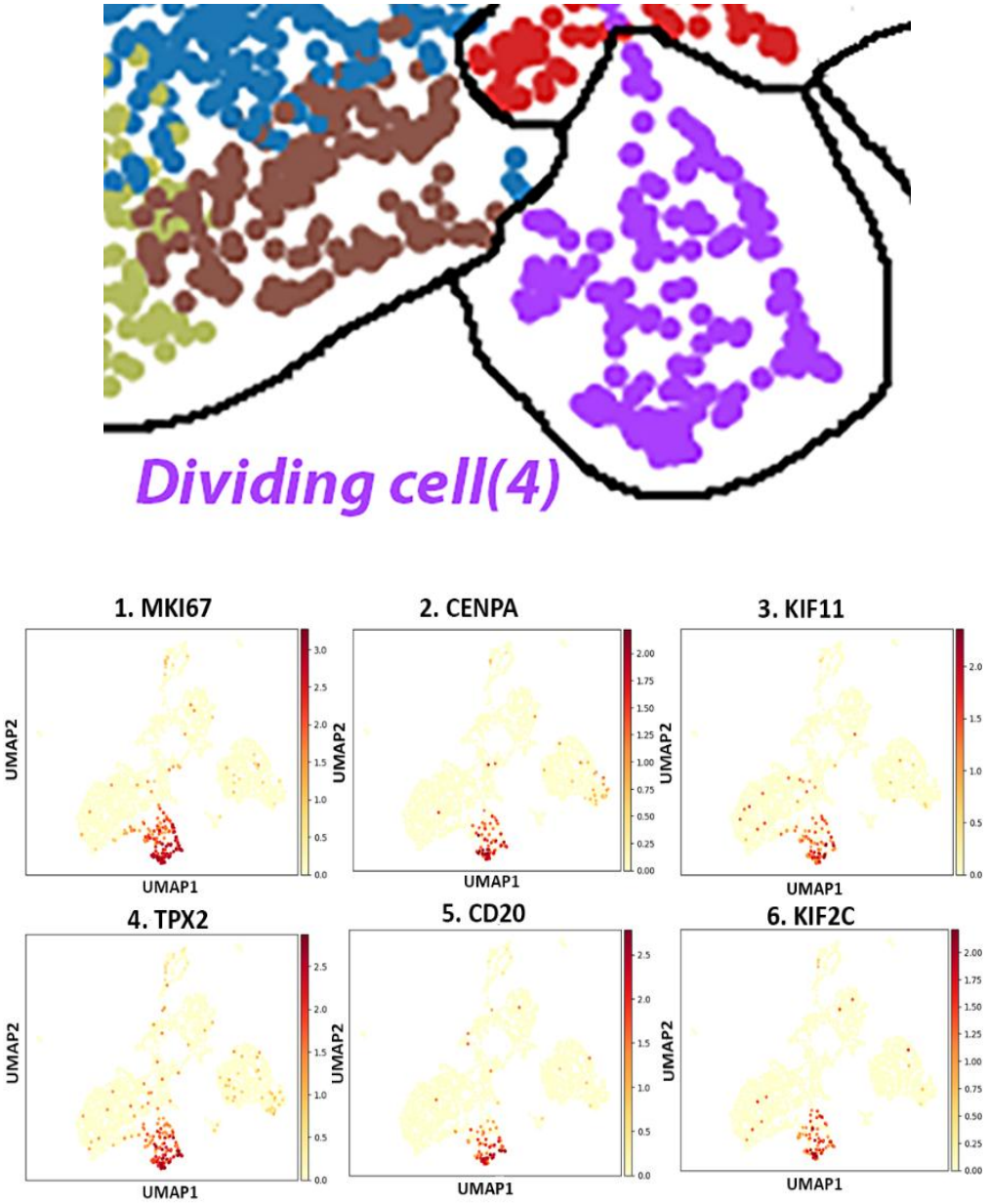

Figure 3.6. Expression maps for six genes. *MKI67, CENPA, KIF11, TPX, CD20,* and *KIF2C* highly implicated in the process of cell division, suggesting this process is highly localised to the cells in cluster 4.

Table 3.4. The 26 genes expressed most highly in cluster 4 (dividing cells). This cluster is characterized by the expression of genes implicated in the process of cell division.

4	
NUSAP1	**CCNB2**
HMGB2	**NUCKS1**
CENPF	**KPNA2**
MKI67	**TUBB4B**
TPX2	**SPC25**
CKS2	**CCNA2**
CKAP2	**SGOL1**
PRC1	**CCNB1**
CDK1	**CDC20**
H2AFV	**MIS18BP1**
ASPM	**CENPA**
H2AFX	**KIF11**
RAD21	**KIF2C**

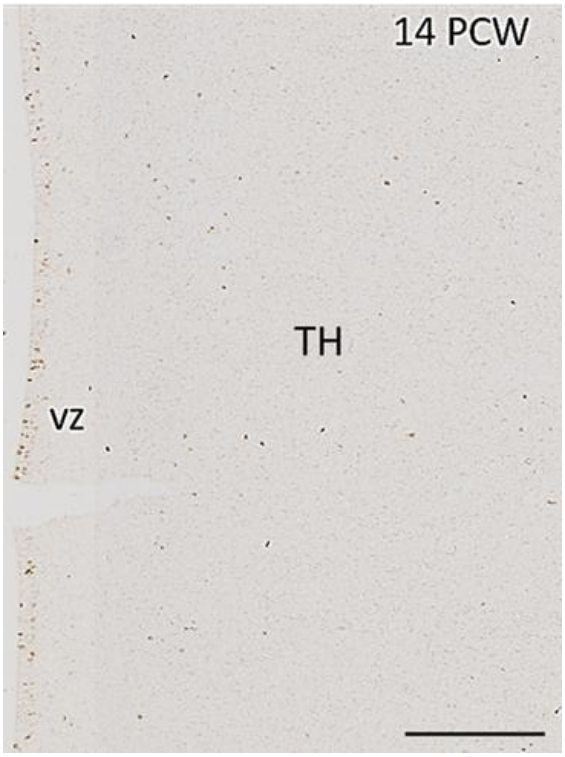

Figure 3.7. ki67 in the thalamic VZ at 14 PCW. There is expression in the VZ of the thalamus. Abbreviation: ventricular zone (VZ); Thalamus (TH); Scale bar 200 μm.

3.4.6 Cluster 9: Immature Neurons and Progenitor Cells

Table 3.5 and Figure 3.8 list the genes most highly expressed in cluster 9 and include such genes as *SLA, NPY, DOK5, FABP7, GAP43,* and *DCX*, which are known to be dependable indicators for immature neurons and progenitor cells. The genes were researched thoroughly and confirmed to be linked to the initial phases of neuronal growth.

The SLA gene is predicted to be involved in cell differentiation (Alliance of Genome Resources. https://www.alliancegenome.org/gene/MGI:104295). NPY, a peptide consisting of 36 amino acids, functions as both a neurotransmitter and neuromodulator in numerous neurones within the CNS of the mammalian brain (Tatemoto et al., 1982, Gray and Morley, 1986, Domin et al., 2006). NPY is expressed in the GABAergic neuron in the cerebral cortex (Colmers, 1990, Greber et al., 1994, Silva et al., 2005, Domin, 2021). The *DOK5* gene, which is implicated in neuronal development, is transcribed actively in neurons throughout the human brain (Grimm et al., 2001). GAP43 is expressed in excitatory neurons in the mouse brain (Nemes et al., 2017). In the developing human thalamus, excitatory neurons appear more mature with enrichment for GAP43 (Kim et al., 2023). FABP7 is expressed during the establishment of the RG fibre

system which is necessary for the migration of immature neurons, in order to develop cortical layer (De Rosa et al., 2012). Doublecortin (*DCX*) is expressed in immature and migratory neurons, as well as in GABAergic neurons in the human brain (Fung et al., 2011). FOXG1 is present specifically in the GABAergic neurons located in the thalamus, which have their origin in the ganglionic eminence (Kim et al., 2023). Furthermore, in the developing human thalamus, the *LHX2* gene is active specifically in excitatory neurons and intermediate progenitor cells (Kim et al. (2023).

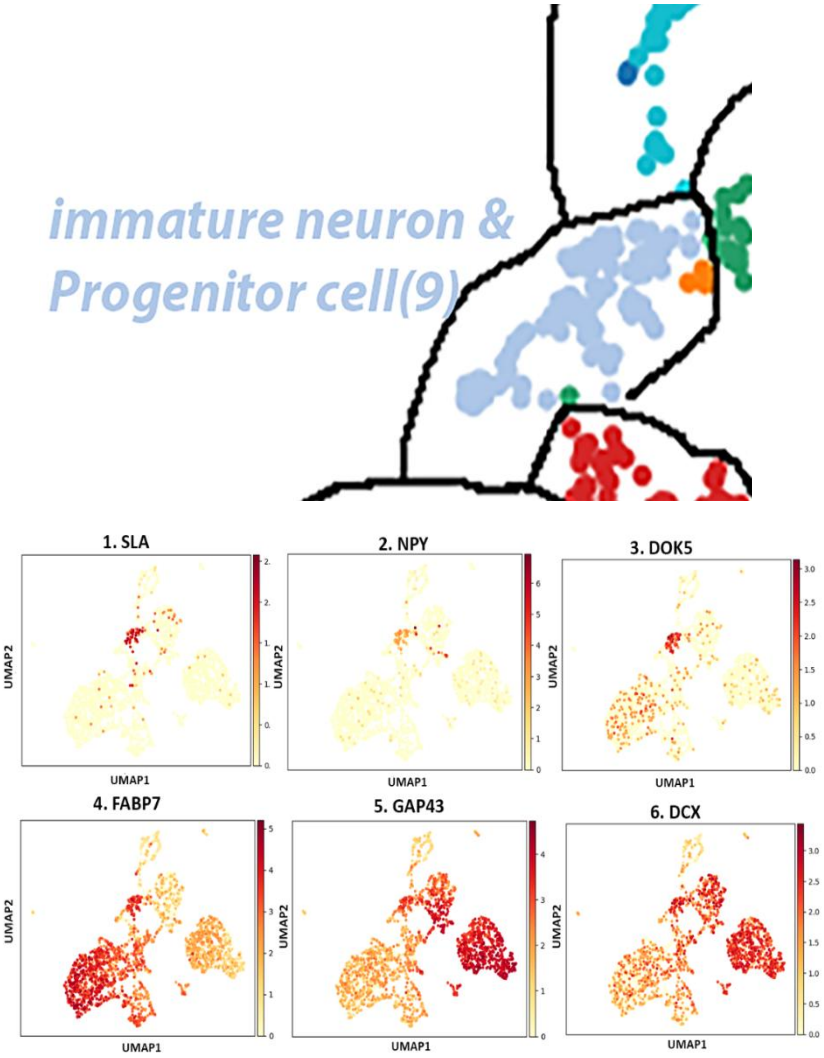

Figure 3.8. Gene expression detection in cluster 9 (immature neuron and neuronal progenitors). *SLA, NPY*, and *DOK5* expression is restricted largely to cluster 9. *GAP43* and *DCX* expression markers for immature neurons are expressed in cluster 9, but also in other clusters containing neurons. *FABP7* is a marker for cluster 9 but also for clusters containing progenitor cells, showing the dual nature of the cells in cluster 9.

Table 3.5. The 29 genes expressed most highly in cluster 9 (immature neurons and progenitor cells). This includes multiple ribosomal protein genes (e.g. RPL and RPS genes) (black). This seems to be characteristic of progenitor cells, as some were also observed to be expressed in clusters 0 and 3, but not in clusters containing post-mitotic cells. Some of the highly expressed genes are characteristic of immature neurons *(DCX, GAP43, NEUROD6, NEUROD2, DOK5, SLA*) (red) and neuronal progenitors (*LHX2, FOXG1, ASCL1, FABP7*) (orange).

9	
RPL37A	RPL19
RPL10	RPL13
RPS8	RPS15
RPS18	DOK5
NEUROD6	RPS13
NEUROD2	RPL24
Lhx2	RPS29
RPL32	RPS15A
RPSO3	RPL39
RPS19	SLA
FABP7	ASCL1
DCX	GAP43
FOXG1	NPY

3.4.7 Clusters 1, 6, 10, 11, and 12: Glutamatergic Neurons

Table 3.6 and Figure 3.9 list the genes expressed most highly in clusters 1, 6, 10, 11, and 12 and are characterized by the expression of genes characteristic of the excitatory glutamatergic neurons, such as *SLC17A6, LHX9, NRN1*, *GAP43, OLFM1, DCX*, *FOXP1, FOXP2,* and *TCF7L2*. *SLC17A6*, which codes for the vesicular glutamate transporter 2 (vGLUT2), is the definitive marker for all sub-cortical glutamatergic neurons of the CNS. *SLC17A6* codes for the transporter responsible for packaging glutamate into synaptic vesicles (*SLC17A6* solute carrier family 17 member 6 - gene - NCBI National Center for Biotechnology Information. Available at: https://www.ncbi.nlm.nih.gov/gene/84487). The study performed in mice and rat brains by Zhang et al. (2020) also demonstrated that *SLC17A6* is a glutamate transporter (Zhang et al., 2020). In the developing human thalamus, *SLC17A6* expression is a suitable marker for the identification of glutamatergic neurons (Kim et al., 2023). *SLC17A6* (vGlut2) mRNA is expressed highly in posterior regions of the thalamic nuclei, such as VP, the VL nucleus, and the posterior medial nucleus (PM) of the dorsal thalamus (Graziano et al., 2008). Recently, Kim et al. (2023) reported that *SLC17A6* exhibits significant expression in the excitatory neurons of the human thalamus (Kim et al., 2023). *SLC17A6* is expressed highly in the two major clusters of this group (1 and 6), as well as in 12, but showed moderate expression in groups 10 and 11 (Table 3.6, Figure 3.9).

As illustrated in Figure 3.9. *TCF7L2, NRN1,* and *LHX9* also showed expression that was limited tightly to this group of clusters. In mice, Transcription Factor 7 Like 2 (TCF7L2) orchestrates the overall morphological differentiation process in the thalamus by regulating stage-specific gene expression directly, or via sub-regional transcription factors, and functions as a terminal selector of postnatally induced thalamic electrophysiological characteristics (Lipiec et al., 2020). Additionally, *TCF7L2* is expressed highly in intermediate progenitor cells and excitatory neurons of the human thalamus during the development stages (Kim et al., 2023).

Additionally, the LIM Homeobox 9 (*Lhx9*) gene is known to bestow distinctive characteristics on neurons that have completed cell division in the thalamic mantle zone in zebrafish (Peukert et al., 2011). Notably, LHX9 is also expressed in intermediate progenitor cells, as well as in the new born and maturing excitatory neurons in the foetal human thalamus (Kim et al., 2023). Neuritin 1 (*NRN1*) is a gene linked to neurons that are expressed highly in postmitotic differentiation in the embryonic nervous system (Naeve et al., 1997a). This gene encodes a

member of the neuritin family and is expressed in postmitotic-differentiating neurons of the developing nervous system, and in the neuronal structures associated with plasticity in the adult. According to Naeve et al. (1997b), NRN1expression can be induced by neural activity and neurotrophins. In the developing human thalamus, NRN1 appears to be a good marker for glutamatergic neurons.

The genes that were expressed highly in this group of clusters also included general markers of neuronal identity, including *GAP43, DCX,* and *OLFM1*. Growth Associated Protein 43 (GAP43) is found at the growth cone and in extending axons, and is an essential component of the axon growth inducing machinery (Meiri et al., 1986) expressed by all developing neurons. DCX is a cytoskeletal protein that is expressed in the immature and migratory neurons in the brain of both mice and humans (Gleeson et al., 1999, Fung et al., 2011). *OLFM1* is expressed in all brain regions in adult humans (Kulkarni et al., 2000) and is implicated in various processes in neuronal development, including axon growth and guidance and synapse formation in animal models (Anholt, 2014).

Taken together, this evidence confirmed that these five clusters of cells identified by the analysis represented the maturing glutamatergic neurons of the thalamus. The differences between the clusters can however be perceived, and may indicate whether different clusters represent different functional nuclei. Parvalbumin (*PVALB*) showed high expression only in cluster 10, and in adult primate thalamus is expressed highly by the projection neurons of the ventral and lateral nuclei (Jones and Hendry, 1989). In contrast, *FOXP1* and *FOXP2* were both more highly expressed in cluster 10 than in the other clusters in this group. I studied the expression of FOXP2 at 14 PCW in the human thalamus extensively (see Chapter 4) and found it to be expressed predominantly in medial nuclei. As with the clusters identified as astrocytes/quiescent progenitor cells, it may be impossible to identify the clusters revealed by the UMAPs as specific groups of thalamic neurons within specific functional nuclei. Instead, each cluster may represent a stage of neuronal maturation.

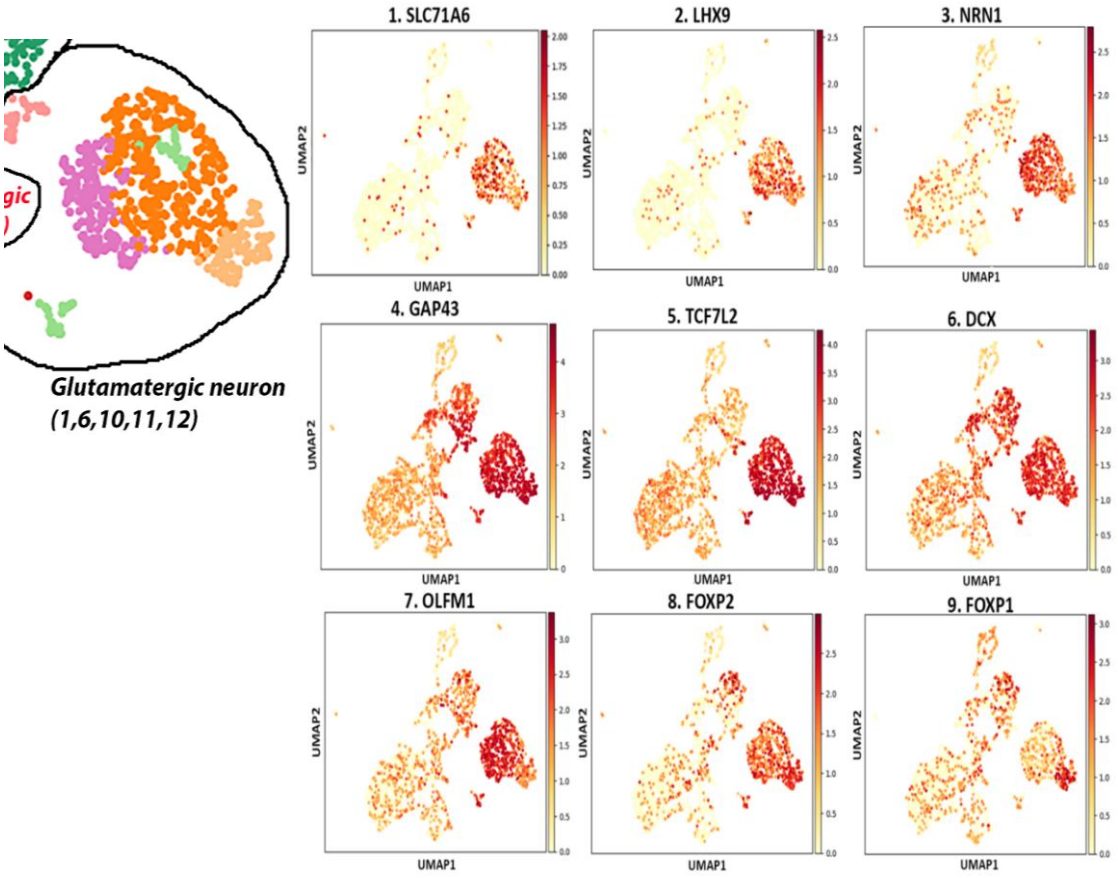

Figure 3.9. The expression of genes in clusters 1, 6, 10, 11, and 12 (glutamatergic neurons). The high expression of *SLC17A6, LHX9, NRN1*, and *TCF7L2* is largely restricted to a group of clusters (1, 6, 10, 11, and 12), identifying these clusters as containing the glutamatergic neurons of the thalamus. Other neuron specific genes, such as *GAP43*, *OLFM1*, and *DCX* are also expressed by this grouping, as well as in other clusters containing neurons. *FOXP1* and *FOXP2* show interesting patterns of expression, with both localised most strongly to cluster 10 for the glutamatergic neuron group, but also expressed in some GABAergic neurons. Conversely, *SLC17A6* is only expressed moderately in cluster 10, compared with the other clusters in the grouping.

Table 3.6. The transcription factors expressed in (glutamatergic neurons). Highly expressed genes in clusters (1, 6, 10, 11, and 12) that are characterized by the expression of genes implicated in the excitatory neurons. There are 28 highly expressed genes in cluster 1, 26 highly expressed genes in cluster 6, 19 highly expressed genes in cluster 10, 25 highly expressed genes in cluster 11, and 21 highly expressed genes in cluster 12.

1	6	10	11	12
GAP43	GAP43	GAP43	GAP43	GAP43
MAP2	MAP2	MAP2	MAP2	MAP2
DCX	DCX	DCX	DCX	DCX
TCF7L2	TCF7L2	TCF7L2	TCF7L2	TCF7L2
MAPT	MAPT	MAPT	MAPT	
ZFHX3	ZFHX3	ZFHX3	ZFHX3	
MEG3	MEG3		MEG3	MEG3
OLFM1	OLFM1		OLFM1	
NRN1	NRN1		NRN1	
NRXN1	NRXN1	NRXN1		
SLC17A6	SLC17A6			SLC17A6
PGM2L1		PGM2L1	PGM2L1	
STMN1				STMN1
STMN4				STMN4
CALM2		CALM2		CALM2
GNG3		GNG3		GNG3
RAC3	RAC3	RAC3		RAC3
HMP19		HMP19	HMP19	HMP19
RTN1		RTN1	RTN1	RTN1
PEG10	PEG10			
CDKN2D	CDKN2D			
	SCN2A		SCN2A	
	NRXN2		NRXN2	
	FEZ1		FEZ1	
MIAT	MIAT		MIAT	
MAP1B	MAP1B		MAP1B	
KLC1	ARPP21	LMO1	PROX1	TUBB2A
TMSB10	SHTN1	FOXP2	NTM	ZIC4
CNTNAP2	SPOCK1	FOXP1	FRRS1L	TUBA1A

3.4.8 Cluster 8: Pericyte and Endothelial Cells

Table 3.7 and Figure 3.10 display genes known to be expressed in pericytes, a specialized cell type located in the microvasculature. We identified pericytes in our dataset by analysing feature plots and correlating the gene expression to the cells in our database. Cluster 8 was identified as the primary cluster representing pericyte cells in our investigation. As shown in Figure 3.10, *BGN*, *CLDN5*, *CYBA*, *FN1*, *HIGDIB*, and *VAMP5* also showed expression that was limited tightly to this cluster.

BGN is a protein responsible for maintaining the endothelial structure in the cerebral cortex (Choe et al., 2022). In the study conducted by Aslam et al. (2012), expression of *CLDN5* was observed in endothelial cells in the mouse brain when examining specific genes. Moreover, Stafford et al. (2022) detected *CLDN5* in both endothelial and pericyte cells in a neurovascular environment. Furthermore, the Single-cell Omics in Low-throughput (SOLO) database indicates that *CLDN5* is expressed in endothelial and pericyte cells in the human cerebral cortex http://solo.bmap.ucla.edu/shiny/webapp/.

HIGDIB is expressed in pericyte cells in both human and mouse vascular tissue (Baek et al., 2022). Furthermore, according to the Human Protein Atlas (*Brain tissue expression of HIGD1B;* https://www.proteinatlas.org/ENSG00000131097-HIGD1B/brain.), HIGD1B is expressed in endothelial cells. Finally, Kim et al. (2023) an scRNAseq analysis and observed that *CDL4A1* and *DLC1* were expressed in the human thalamus in endothelial and pericyte cells, respectively. *IGFBP7* and *CLDN5* were also expressed specifically in endothelial cells in the human thalamus. Additionally, *FN1* is also expressed in pericytes in the brain (Li et al., 2023). *SLC2A1*, *SLC3A2*, and *SLC2A3* are expressed in brain endothelial cells, and are facilitative glucose transporters expressed highly at the blood brain barrier (Lee et al., 2017). The genes *SHE*, *KCNN3*, *VAMP5*, *SEMA3F*, *HDAC9*, *GIMAP1*, *NOS3*, and *DOCK6* show an endothelial-enriched expression pattern (Becker et al., 2023).

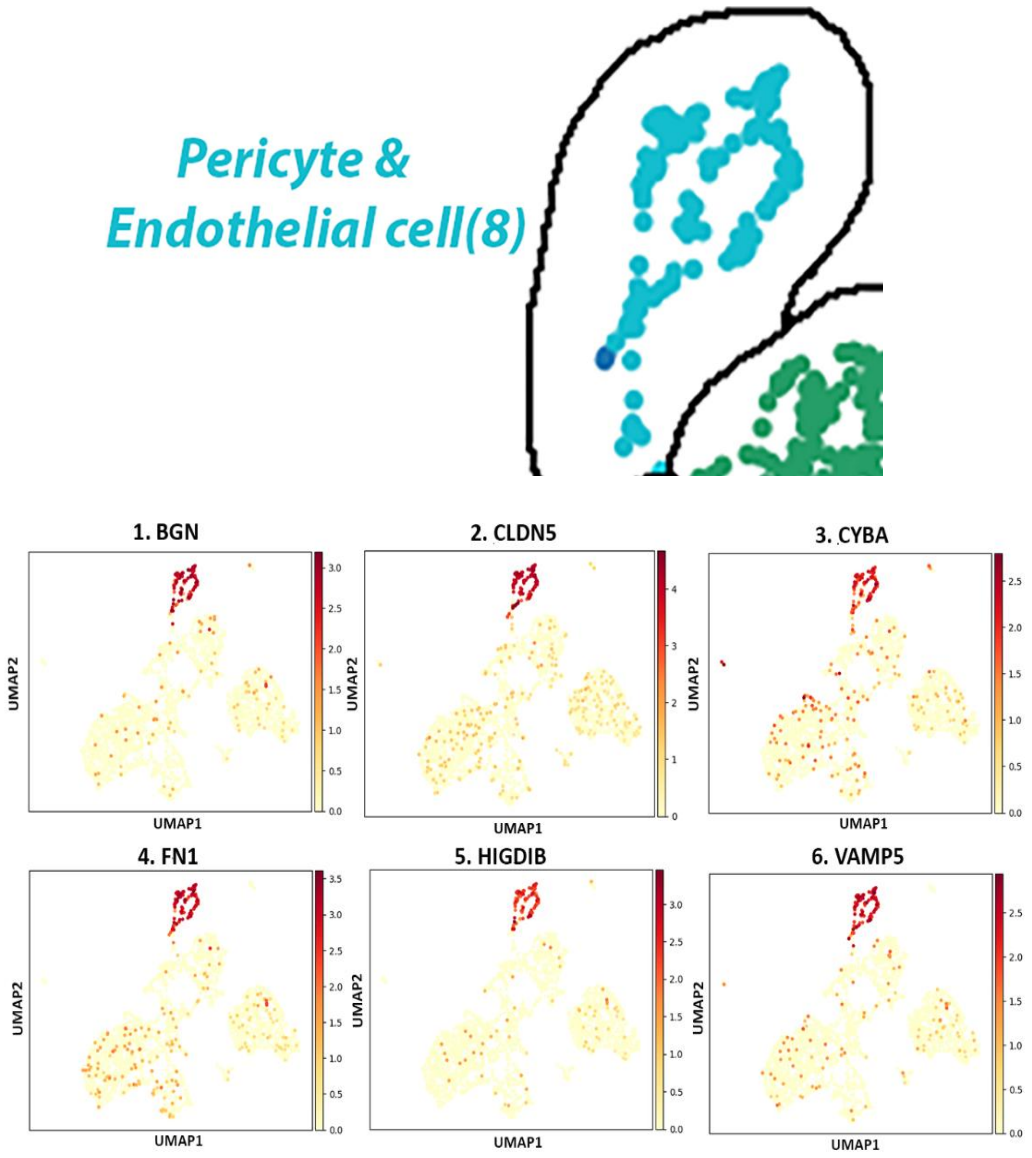

Figure 3.10. Expression of genes in cluster 8 (pericyte and endothelial cells). All six genes illustrated here (*BGN, CLDN5, CYBA, FN1, HIGDIB, and VAMP5*) have expression patterns that are highly restricted to cluster 8.

Table 3.7. The 30 genes expressed most highly in cluster 8 (pericytes and endothelial cells). High gene expression in this group shares no co-expression with other clusters, demonstrating that it stands apart from neuroectoderm derived cells. Many genes expressed by pericytes, and endothelial cells are present.

8	
IGFBP7	DLC1
FN1	ITIH5
VAMP5	C1orf54
PRKCDBP	CALD1
CYBA	MYL12A
BGN	LINC00152
CLDN5	RAMP2
A2M	SLC2A3
COL4A2	SLC2A1
COL4A1	EVA1B
NDUFA4L2	ICAM2
IFITM3	SERPINH1
SLC38A5	PFN1
SLC7A5	RHOB
HIGD1B	SLC3A2

3.4.9 Cluster 13: Red Blood Cells

Table 3.8 and Figure 3.11 show the genes that are confirmed to be expressed in red blood cells. The genes *HBA1*, *HBG1*, *HBM*, *HBG2*, *HBB*, and *HBQ1* (Figure 3.11) are responsible for the synthesis of haemoglobin, a crucial molecule that facilitates the transportation of oxygen throughout the body, which is found exclusively in red blood cells (Mussolino and Strouboulis, 2021). The alpha and beta globin chain-encoding genes *HBA1* and *HBB* strengthen the binding of oxygen to haemoglobin (Höflich et al., Filser et al., 2022). *HBQ1*, an alpha-globin gene, is known to be expressed predominantly in human foetal erythroid tissues, and recent studies identified *HBQ1* expression in alveolar epithelial cells, which are non-erythroid (Kim et al., 2023). *HBG1* and *HBG2*, which are gamma globin genes, are, under normal conditions, expressed in the foetal liver, spleen, and bone marrow, and two gamma chains, along with two alpha chains, form the foetal haemoglobin (*HbF*) that are replaced at birth by adult haemoglobin (Wulandari et al., 2020, Vathipadiekal et al., 2016).

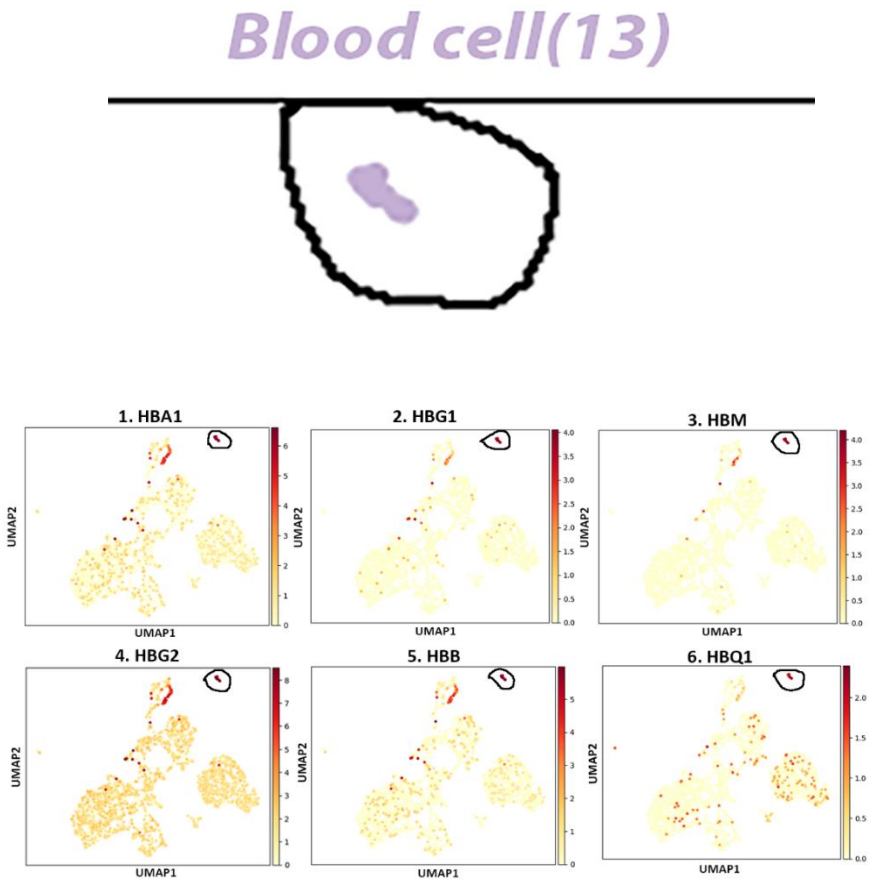

Figure 3.11. Specific gene expression in cluster 13. HBA1, HBG1, HBM, HBG2, HBB, and HBQ1 are all genes coding for haemoglobin subunits, and are all expressed highly in cluster 13.

Table 3.8. The 28 genes expressed most highly in cluster 13 (red blood cell). The genes expressed mostly highly include many components of the haemoglobin complex (yellow), identifying this cluster as containing red blood cells.

13	
HBG1	HEMGN
HBB	STRADB
HBA1	MPP1
HBA2	UBB
HBG2	FECH
HBM	KRT1
AHSP	FAM210B
ALAS2	SLC40A1
SLC25A37	PIM1
HBQ1	MKRN1
SNCA	BCL2L1
GYPC	CR1L
BLVRB	IFIT1B
GYPA	MAP2K3

3.4.10 Cluster 14: Microglia

Finally, Table 3.9 and Figure 3.12 show a compilation of genes that are known to be expressed in microglia, namely the immune cells found in the CNS. Cluster 14 shows a notable concentration of microglia-specific genes, indicating that it represented a unique group of microglial cells in our sample.

According to Chui and Dorovini-Zis (2010), astrocytes, macrophages, and microglia present in the centre of lesions and surrounding white matter express *CCL3*. A recent study conducted by Kim et al. (2023) supported this finding, illustrating that *CCL3* and *CCL4L2* are present in microglia located in the human thalamus. Additionally, chemokines *CCL4L2* and *CCL3L3* are involved in inflammatory and immune-regulatory processes (Xu et al., 2023, Bergamo et al., 2019). Based on these findings, the SOLO map database (SOLO, 2024) employed by the present study confirmed that CCL3, CCL4L2, and CCL3L3 are expressed in the microglia of the human cerebral cortex (Figure 3.12).

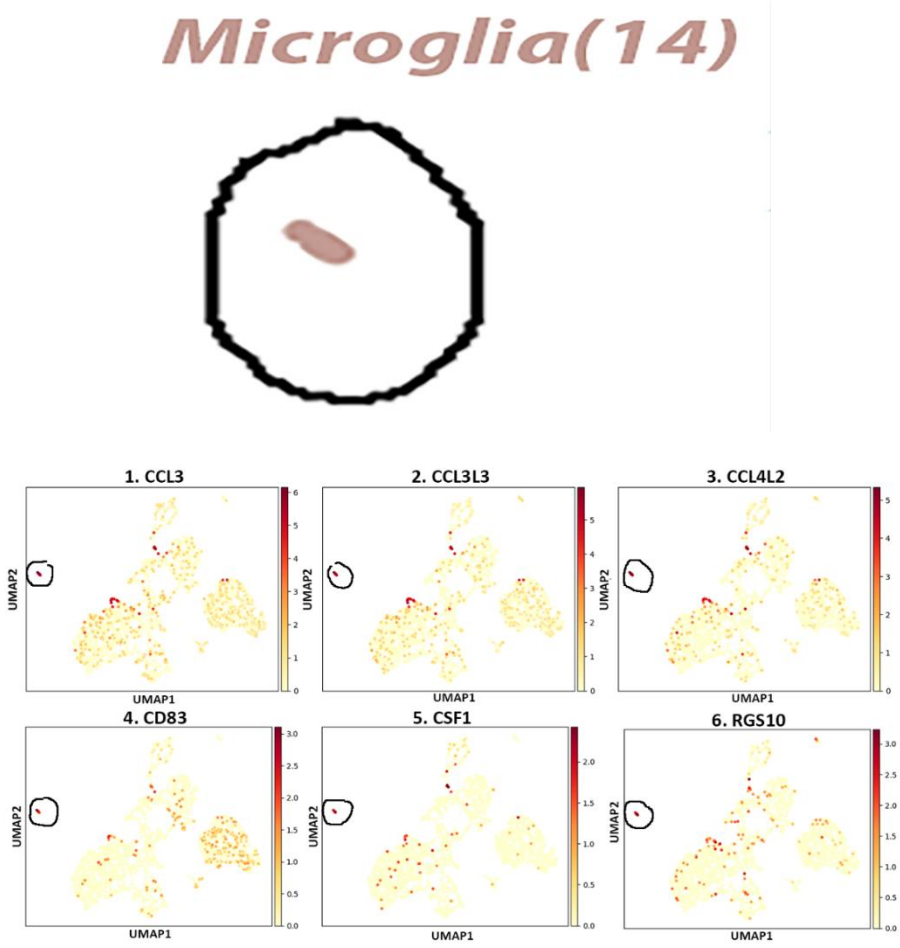

Figure 3.12. Specific gene expression in cluster 14. CCL3, CCL3L3, CCL4, CCL4L2, CD83, CSF1, and RGS10 are all genes active in microglia and are all expressed highly in cluster 14.

Table 3.9. The 26 genes expressed most highly in cluster 14 (microglial cells). Showing a compilation of genes that are known to be active in microglia, which are the immune cells found in the CNS. We identified microglia in our dataset by correlating the gene expression with the cells and analysing their distribution within the clusters. Cluster 14 shows a notable increase in microglia-specific genes, indicating that it represents a unique group of microglial cells in the sample.

14	
CCL3	NR4A2
CCL3L3	RPL21
CCL4	NEAT1
TYROBP	RPLP1
CCL4L2	ZFP36L1
AIF1	LAPTM5
FTL	RPS29
CTSB	ARPC1B
CD83	RPS27
FTH1	RPS12
CX3CR1	ITM2B
IER3	RPL23
RGS10	FCGRT

3.5 Discussion

This study demonstrated that it is possible to cluster different classes of cells in the thalamus at 16 PCW using scRNAseq data. This analysis is referred to in the rest of the study, in order to predict which type of cells express certain genes and proteins, by comparing their individual UMAPS with the schematic diagram presented in Figure 3.1 A. This can then be confirmed by IHC or in situ hybridization. This approach was adopted to explore the expression of the neurosusceptibility genes *FEZ1* and *NRXN1* (see Chapters 5 and 6).

Other insights were also provided by this study. For instance, a high proportion of dividing cells was observed, which was perhaps unexpected as cell proliferation is believed to be complete in the thalamus before 16 PCW (Kim et al., 2023). This suggested that neurogenesis, or at least gliogenesis, is still occurring at this developmental time point. A relatively high proportion of GABAergic neurons and their precursors were also present. This may reflect inclusion of the prethalamic structures in the sample, but may also reflect extensive invasion of the thalamus by GABAergic neurons of mid-brain origin (Kim et al., 2023), and possibly forebrain origin (Quinlan et al., 2009, Letinic and Rakic, 2001). This observation raised important questions regarding the developmental origins of these neurons. One possible explanation was that our samples may have included cells from the prethalamic structures, which are known to contribute GABAergic neurons to the thalamus. However, another intriguing possibility was the extensive invasion of the thalamus by GABAergic neurons originating from midbrain structures, and potentially even forebrain regions, by 16 PCW. This phenomenon may reflect a broader developmental interplay between various brain regions, whereby GABAergic neurons migrate into the thalamus to establish functional networks that are critical for sensory processing and integration.

This study not only enhanced understanding of thalamic development, but also set the stage for further investigation of the functional implications of these cellular dynamics. Future research might explore how the ongoing proliferation of specific cell types influences thalamic connectivity and the establishment of sensory pathways. Additionally, the role of neurosusceptibility genes, such as *FEZ1* and *NRXN1*, in this context may provide valuable insights into the molecular mechanisms that underlie neurodevelopmental disorders.

The clustering of cell types was analysed by their mRNA expression profiles for a scRNAseq dataset from the cells isolated from the developing human thalamus. These findings enhanced

the understanding of the cellular makeup of the human thalamus at 16 PCW, establishing a basis for future investigation of the functions and interplay of these genes in the context of neurological disease. Chapters 5 and 6 employ the knowledge gained to hypothesize which cell groups express certain neurodevelopmental disorder susceptibility genes, which were then confirmed using histological methods.

3.6 Concluding remarks

In summary, this study's findings underscored the dynamic nature of thalamic development at 16 PCW, suggesting that both neurogenesis and extensive cellular migration are pivotal processes during this crucial period. Further exploration of these phenomena is essential to determine the complexities of thalamic function, and its contribution to overall brain development.

4 Chapter 4. Mapping of the thalamus at 8- 14PCW

4.1 Introduction

Most of what is known about thalamic development comes from rodent studies, however, the increased proportion of human association cortex has co-evolved with increased thalamocortical connectivity. (Sherman, 2016). Higher order thalamic nuclei, such as the mediodorsal nucleus (MD) and the pulvinar, which relay information from one cortical region to another, are greatly expanded in primates, especially humans, relative to rodents (Baldwin et al., 2017, Pergola et al., 2018, Homman-Ludiye and Bourne, 2019). These thalamic nuclei are involved in what we understand to be uniquely human cognitive functions, such as the lexico-semantic processing of language (Assaf et al., 2006, Van Der Werf et al., 2003, Kraut et al., 2003).

According to the prosomere model of diencephalic development, caudally the first prosomeric domain (p1) gives rise to the pretectum, p2 the thalamus (or dorsal thalamus) and epithalamus and p3 the prethalamus (or ventral thalamus) anteriorly, separated from p2 by the zona limitans intrathalamica (ZLI) an organiser region secreting morphogens including sonic hedgehog (SHH) that facilitate establishment of positional identity (Kiecker and Lumsden, 2004, Nakagawa, 2019). In this study, we generally refer to the caudal part as the thalamus, whilst recognising the epithalamus as a separate, posterior and dorsal domain. Other factors such as fibroblast growth factors and SHH from basal regions are required for maintaining ZLI and for thalamic patterning (Nakagawa, 2019). The initial aim of the research undertaken for this chapter, therefore, was to examine the expression of key molecules that have been shown to guide the development of the thalamus in animal models. To this end, we studied the expression of several of the transcription factors involved in patterning, including *ZIC4*, GBX2, FOXP2, PAX6, NR2F1 and NR2F2. While these factors have been well-characterized in animal models, their expression patterns and roles in human thalamic development remain relatively poorly understood.

ZIC4 is expressed in p2 (and other dorsal and medial structures) in the early developing mouse brain (Gaston-Massuet et al., 2005), subsequently becoming more restricted to specific thalamic nuclei later in the development of the mouse and marmoset (Horng et al., 2009, Homman-Ludiye and Bourne, 2019). NR2F1 (also known as COUP-TFI) is similarly

expressed throughout p2 during mouse development (Qiu et al., 1994, Liu et al., 2000), and this is required for guidance of thalamocortical axon growth (Zhou et al., 1999).

In contrast, GBX2 in rodents is restricted to thalamic neurons from within p2, along the anterior-posterior axis projecting to the cortex, as opposed to Habenula and prethalamic regions (Chen et al., 2009). All thalamic neurons express *Gbx2* during their development and are essential for axon outgrowth and pathfinding (Chatterjee et al., 2012) as well as the suppression of Habenula identity markers (Chen et al., 2009). FOXP2 is expressed in the thalamus in the developing mouse and human (Ferland et al., 2003, Vargha-Khadem et al., 2005). A gradient of expression, higher in the posterior ventral region, was also found in the embryonic mouse thalamus, indicating that FOXP2 is essential for thalamus patterning (Ebisu et al., 2017).

NR2F2 (COUP-TFII) displays relatively reduced expression in the developing thalamus, when compared to NR2F1 in mice, but is strongly expressed in the adjacent pretectum and prethalamus (Qiu et al 1994), and its expression is also studied here. PAX6 expression is necessary for the proper development of the thalamus (Schmahl et al., 1993, Caballero et al., 2014), and thalamic progenitor cells express it throughout the initial phases of diencephalic development. It is also expressed by prethalamic progenitor cells, some of the progeny of which retain their expression as postmitotic neurons (Duan et al., 2013, Caballero et al., 2014).

The diencephalic ventricular zone (VZ) lining of the third ventricle contains apical radial glia, which divide asymmetrically generating postmitotic neurons (Nakagawa and Shimogori, 2012). These neurons then migrate to the mantle zone, where they aggregate, ultimately forming individual nuclei (Jones and Rubenstein, 2004, Nakagawa and Shimogori, 2012). Similar to the neocortex, there is a thalamic subventricular zone containing basal progenitors in both the mouse and human thalamus (Wang et al., 2011, Kim et al., 2023). The excitatory glutamatergic neurons in the thalamus all derive from the ventricular and subventricular zone of p2 (Vue et al., 2007).

GABAergic neurons within the thalamic reticular nucleus are derived from the progenitor zones of the p3 prethalamus (Puelles and Rubenstein, 2003). It is proposed that they provide the majority of the inhibitory drive to the thalamic nuclei in rodents, as very few inhibitory interneurons found within the dorsal thalamic nuclei, with the exception of some visual thalamic nuclei (Ohara et al., 1983, Warren et al., 1994, Arcelli et al., 1997). Notably, in primates, up to 30% of the neurons in all nuclei are reported to be GABAergic interneurons

(Hunt et al., 1991, Montero and Zempel, 1986), which makes this a major aspect in the evolution of the thalamus. Interneurons migrate into the thalamus during the latter stages of development (Jones, 2002). These thalamic interneurons have previously been shown to be of predominantly pretectal (p1) and midbrain origin, expressing the transcription factor SOX14 (Jager et al., 2016). More recently, studies have shown that GABAergic neurons arising from SOX14+ precursors in mouse are present in all caudal sensory relay nuclei and associated higher order nuclei. However, in the marmoset, such cells are more abundant, and also found in anterior, higher order thalamic nuclei (Jager et al., 2021). Other potential sources of thalamic interneurons include the prethalamus (as demonstrated in the mouse) (Jager et al., 2021) and ganglionic eminences, which are posited as a unique source of interneurons for human higher order thalamic nuclei (Letinic and Rakic, 2001, Bakken et al., 2021, Kim et al., 2023). The second objective of this chapter is to further illuminate the origins of GABAergic neurons in the human thalamus.

Please note that some of the data presented in this chapter has been published (Alhesain et al., 2025).

4.2 Aim of the study

To investigate, map and analyse gene expression patterns across the developing human thalamus from 8 to 14 PCW. By examining human thalamic tissues at 14 PCW, it is possible to identify the genes involved in establishing thalamic nuclei. In addition, we seek to discover which genes define and restrict specific thalamic nuclei in the late stages of foetal human development. This will elucidate how gene expression informs differentiation and organization within the thalamus. We also determine where these GABAergic neurons originate before they migrate to the thalamus. Ultimately, this information offers a basis for studying the early expression of neurodevelopmental disease susceptibility in genes (see Chapters 5 and 6).

4.3 Method:

We employed immunostaining and RNAscope in situ hybridization in 8-14 PCW tissue. Methods described in detail in Chapter 2.

4.4 Results

4.4.1 Transcriptomic cells in developing human thalamus at 16 PCW

In Figure 4.1, single cell RNAseq data for the thalamus at 16 PCW taken from the NEMO Analytics database is presented. UMAP plots were generated for genes such as (*MKI67, OLIG2, ASCL1, NR2F2, NR2F1, GAD1, SP8, OTX2, SOX14 GBX2, FOXP2, ZIC4, PAX6*) and classified different neuronal clusters (see Chapter 3). This chapter details the findings when thalamus sections were stained for these transcription factors to identify and distinguish thalamic nuclei and determine which type(s) of cells can be expressed in thalamic nuclei. The UMAP plots show different types of cells in the thalamus at 16 PCW and we have tried to identify the essential marker gene for each type of cell to classify the clusters. For instance, MKI67, the essential marker for dividing cells is highly expressed in cluster 4, and GADD45B is highly expressed in cluster (0, 5, 7) which is classified to be progenitor cells. OLIG2 is highly expressed in cluster 3 which is GABAergic and oligoprogenitor cells. FOXP2 is highly expressed in glutamatergic neurons and belong to cluster (6,10,1,11,12). SOX14, OTX2 and GAD1 are marker genes for GABAergic neurons which is in cluster (2). In summary, we have identified the respective cell type in the thalamus by essential marker genes for each type of cells. We have chosen 16 PCW for the scRNAseq data as it is the closest age group found to 14 PCW that we have used for the histological experiments.

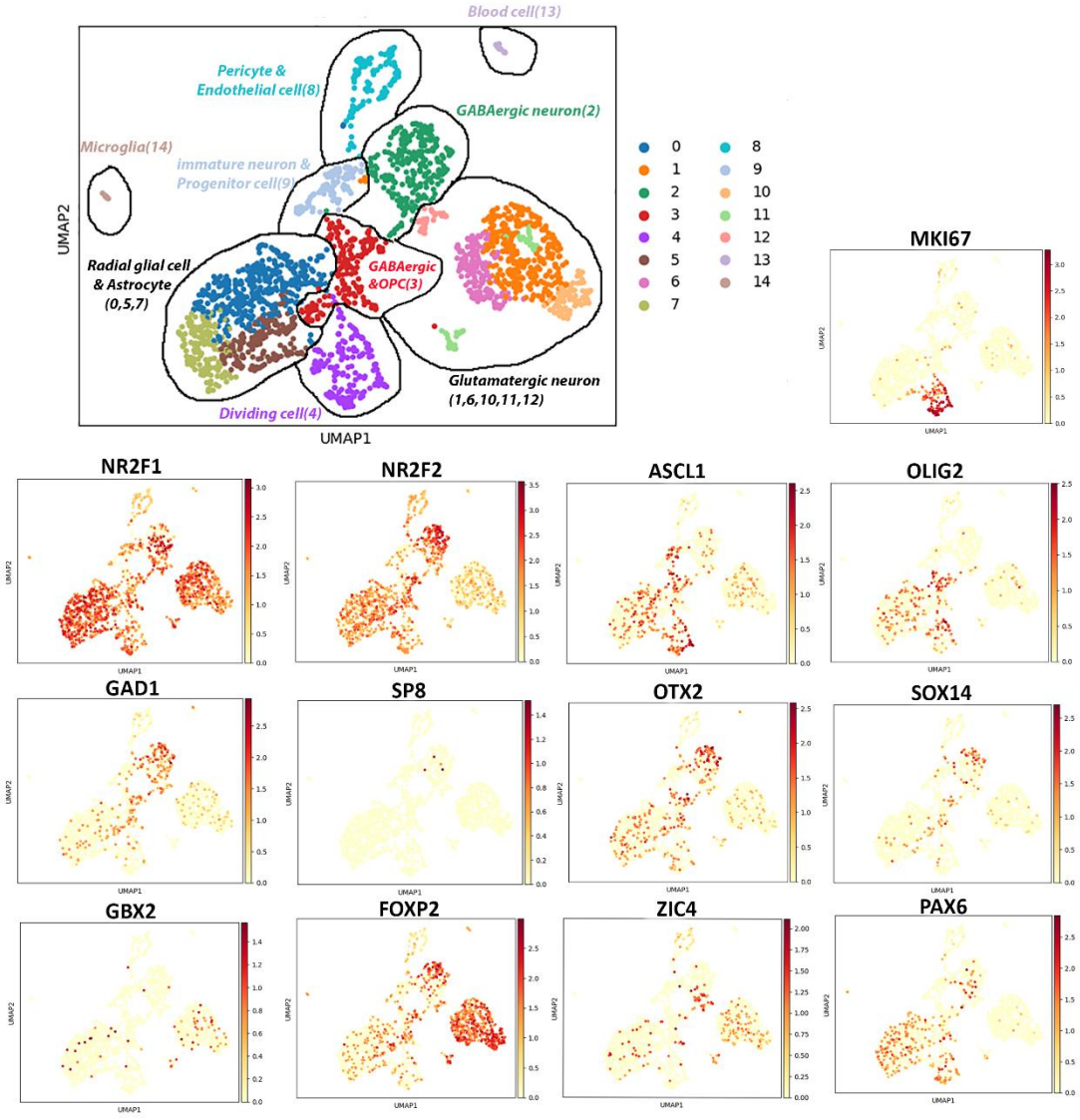

Figure 4.1. Identification of cell types found in each cluster generated from NEMO, for time point and brain region 16 PCW -thalamus. UMAPs represent the key marker genes used to define each cluster: *FOXP2* is expressed in the GABAergic and glutamatergic neurons. *MKI67* is expressed in dividing cells. *ZIC4* is expressed in GABAergic, progenitor cells and glutamatergic neurons. *PAX6*, showed expression in the GABAergic neuron, progenitor cell and dividing cells. *NR2F1* is expressed in GABAergic neuron, the dividing cells and the immature neurons and excitatory neurons. *NR2F2* is expressed in GABAergic, progenitor cells, and immature neurons. *GBX2* expressed in the excitatory neurons. *ASCL1* is expressed in dividing cells, progenitor cells and immature GABAergic and immature neurons. *SOX14*, *SP8* and *GAD1* is expressed in the GABAergic neurons. *OTX2* is expressed in the immature and mature GABAergic neurons and in progenitor cells. *OLIG2* is expressed in the immature neurons and oligo progenitor cells, dividing and progenitor cells.

4.4.2 Histological studies of transcription factor expression at 8 PCW in human thalamus

8 weeks post- conception, the thalamus was clearly recognizable in haematoxylin and eosin (H&E) stained sagittal sections as an ovoid structure, dorso-anterior to the mesencephalic flexure (Figure 4.2 A). The precise delineation of the thalamus could be ascertained by examining the expression of *SHH*, alongside that of three transcription factors, *ZIC4*, GBX2 and FOXP2. *SHH* expression marks the zona limitans (the embryonic boundary between p2 (containing the thalamus) and p3 (containing the prethalamus) (Kiecker and Lumsden, 2004). It was strongly expressed in cells located within the ventricular zone (VZ) at the boundary, and in a smaller number of cells along the ZLI (Figure 4.2 B). The alar portion of p2 was characterised by strong expression of *ZIC4* throughout, including the dorsal most prethalamus and up to and including the ZLI (Figure 4.2 C). GBX2 and FOXP2 were confined to the thalamus and excluded from the prethalamus showing largely uniform expression throughout (Figure 4.2 D, E). FOXP2+ cells were more prevalent in the VZ of the thalamus than GBX2+ cells, confirming prior evidence (Alzu'bi et al., 2019). OTX2 was also expressed in the thalamus, but showed a different pattern of expression, being strongly expressed in both the VZ and post-mitotic zones. It was expressed uniformly throughout the thalamus in the medial sections, but in the lateral sections it was confined to regions close to the ventricles (Figure 4.2 F, G). This suggests OTX2 is expressed by thalamic progenitor cells and more immature, possibly migratory thalamic neurons, with expression becoming downregulated as the neurons mature. SP8, a transcription factor associated with GABAergic neurons derived from the ventral telencephalon (Waclaw et al., 2006, Ma et al., 2013, Alzu'bi et al., 2017) was confined in its expression to the GABAergic prethalamus rather than being observed in the thalamus (Figure 4.2 H). NR2F1 was expressed by thalamic progenitors in the ventricular zone (Figure, 4.2 I), while NR2F2 was expressed both in the VZ and postmitotic zones in the thalamus and the prethalamus (Figure 4.2 J). OLIG2 is expressed in the progenitor cells of the ventricular zone of the prethalamus but not in the thalamus (Figure 4.2 K).

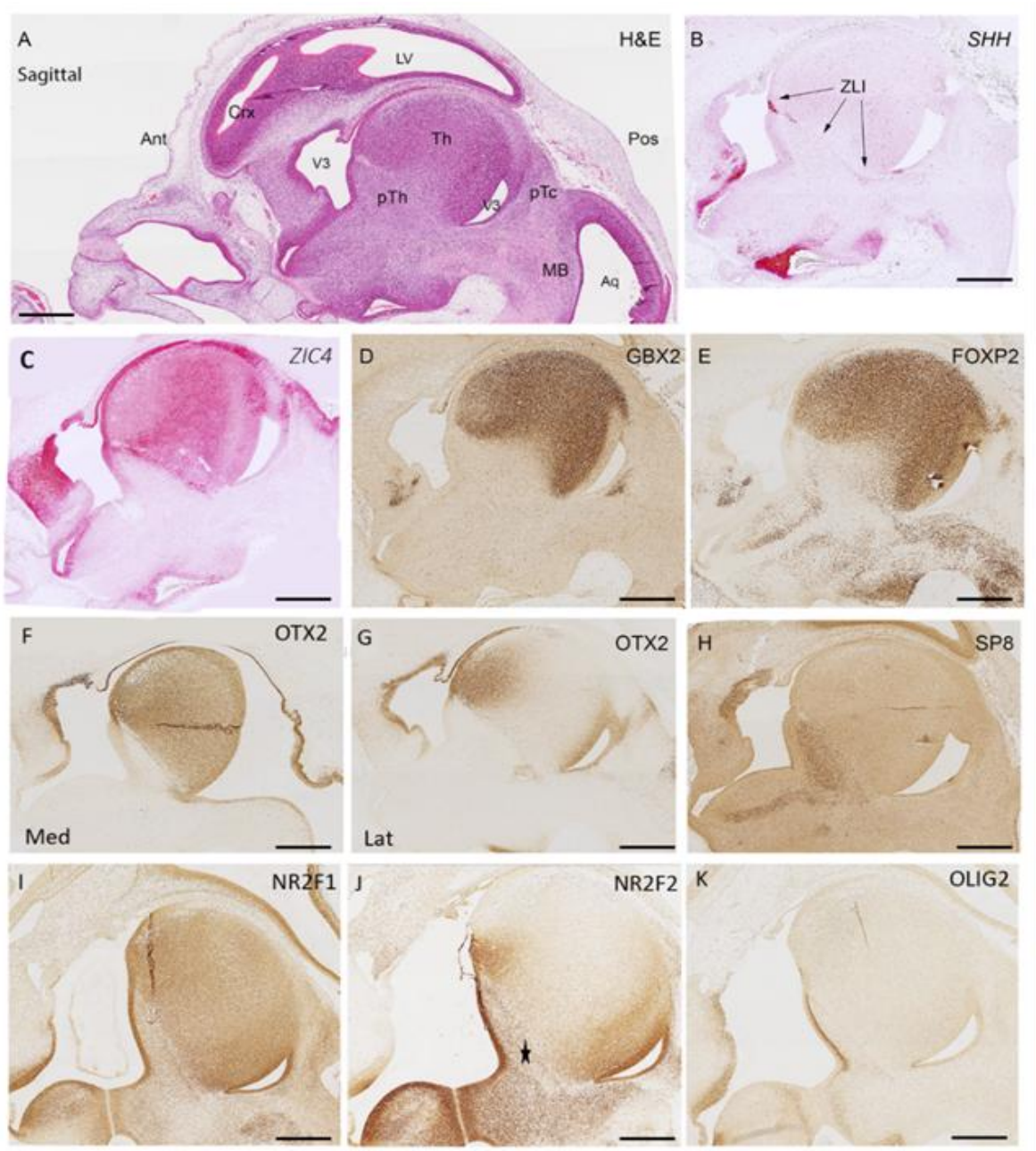

Figure 4.2. Immunoperoxidase histochemistry of *SHH*, *ZIC4*, GBX2, FOXP2, OTX2, SP8, NR2F1, NR2F2, OLIG2 at the 8 PCW sagittal section. H&E staining in the sagittal section at 8 PCW (A). SHH is expressed in zona limitans (ZLI) (B). ZIC4 is expressed in the thalamic neurons and the progenitor cells (C). GBX2 exhibited strong expression in the postmitotic neurons (D), and FOXP2 is expressed in the postmitotic thalamus as well (E). OTX2 is expressed in the entire thalamus at the medial side (F), whereas on the lateral side it is more restricted to ventricle (G). SP8 is expressed in the prethalamus but not in the thalamus (H). NR2F1 is expressed in the thalamus in the ventricular zone, and in the postmitotic neurons (I). NR2F2 was strongly expressed in the ventricular zone and restricted more to ventricle, as well as in the prethalamus (star) (J). OLIG2 is only expressed in the progenitor cells in the prethalamus (K). Abbreviations: Anterior (Ant); Aqueduct (Aq); posterior (Pos); cortex (Crx); Thalamus (Th); prethalamus (pTh); pretectum (pTc); Zona limitans intrathalamic (ZLI); Lateral ventricle (LV); Third ventricle (V3); Midbrain (MB). Scale bar 1mm. (Images A, B prepared by Dr Alzu'bi; F, G, H by Ms Sankar; D, E. I, J, K, L by myself; and C by Ms Sankar and myself. Interpretation of the staining patterns is my own work).

In the coronal sections of the thalamus at 8 PCW, *SHH* expression was clearly apparent in a small group of cells in the thalamic ventricular zone (VZ) immediately dorsal to the hypothalamic sulcus (Figure 4.3 B, Figure 4.4 B). In the posterior region, *SHH* was expressed in the ventricular zone (VZ) of the pretectum (Figure 4.5 B). OTX2 immunoreactivity extended throughout the VZ of thalamus, the epithalamus, thalamic eminence, and the choroid plexus (Figure 4.3 C, Figure 4.4 G). OTX2 immunoreactivity also marked the postmitotic cells within the medial thalamus (Figure 4.4 G). *ZIC4* was expressed throughout prosomere 2, including the VZ and the epithalamus (Figure 4.4 C). FOXP2 and GBX2 were both expressed medially in the anterior thalamus, while FOXP2 was also expressed in the lateral ganglionic eminence (LGE) (Figure 4.3 D, E). Expression of FOXP2 and GBX2 in the middle thalamus was also relatively weak in the more lateral regions of the thalamus, compared to *ZIC4* (Figure 4.4 C, D, E). In the posterior thalamus, *ZIC4* was found to be weakly expressed, compared to the anterior region, but strongly expressed in the epithalamus (Figure 4.5 C). FOXP2 and GBX2 immunoreactivity was highly expressed in the thalamus compared to *ZIC4* but was not present in the epithalamus (Figure 4.5 D, E). NR2F2 in the middle section was expressed in the prethalamus and the ventricular zone of the thalamus, which contains progenitor cells, as well as in the ganglionic eminence, which produces GABAergic neurons (Figure 4.4 H). PAX6 was expressed in the ventricular zone of the thalamus and the cortex and the prethalamus (Figure 4.4 I). As predicted from the animal experiments (Puelles et al., 2013), the expression patterns of the transcription factors and other molecules clearly delineate p2 from p1 and p3, with p2 and p3 being separated by *SHH* positive ZLI. At this stage, the thalamus can also be distinguished from the epithalamus. *ZIC4*, GBX2, FOXP2 were expressed throughout the entirety of the thalamus, while OTX2 expression was confined to more medial locations only.

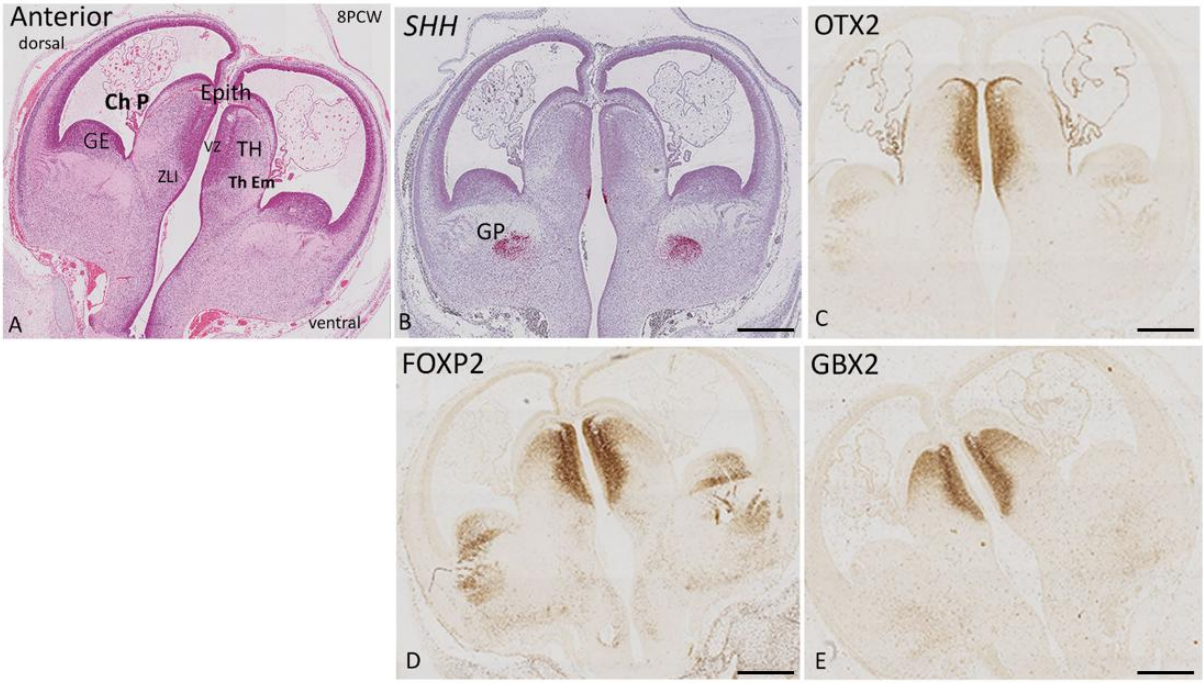

Figure 4.3. Immunostaining GBX2, FOXP2, OTX2 and in situ hybridization of *SHH* in the coronal sections of the anterior thalamus at 8 PCW. H&E staining in the sagittal section at 8 PCW anterior (A). *SHH* was expressed in the zona limitans intrathalamic (ZLI) (B). OTX2 was expressed in the thalamus near to the ventricular zone and the epithalamus (C). FOXP2 was expressed in the thalamus medially in the anterior (D). GBX2 was expressed in the postmitotic cells in the medial thalamus (E). Abbreviations: Ganglionic eminence (GE); Globus pallidum (GP); epithalamus (Epith); Thalamus (TH); Zona limitans (ZLI); Ventricular zone (VZ); Choroid plexus (ch P); Thalamic eminence (Th Em). Scale bar 1mm. (Images prepared by Dr Alzu'bi. Interpretation of the staining patterns is my own work).

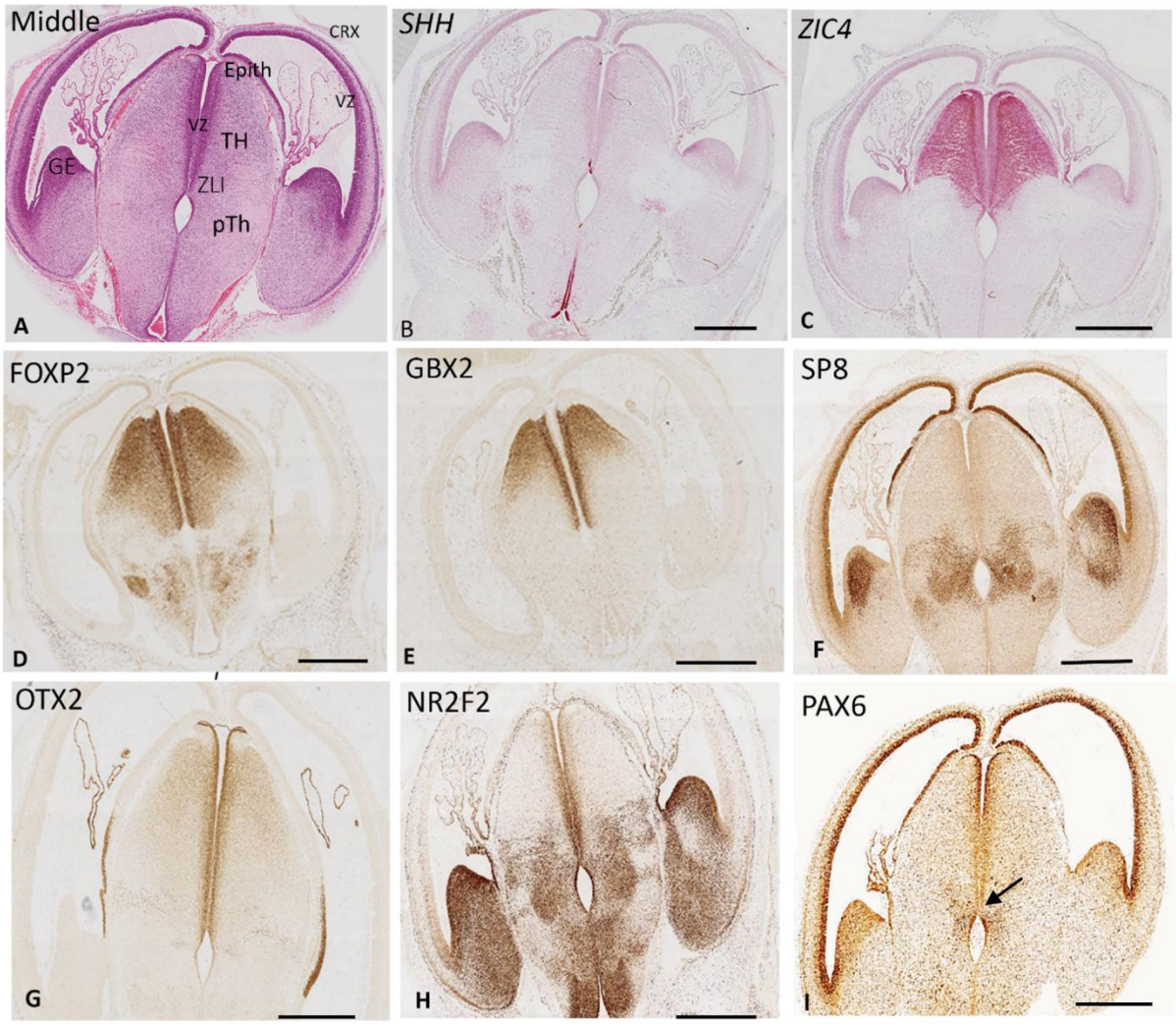

Figure 4.4. Immunostaining GBX2, FOXP2, OTX2, SP8, NR2F2, PAX6 and in situ-hybridization of *SHH* and *ZIC4* in coronal sections of the mid-thalamus at 8 PCW. H&E staining in the sagittal section at 8 PCW middle (A). *SHH* was expressed in the zona limitans intrathalamic (ZLI) (B). *ZIC4* was expressed in the progenitor and thalamic neurons and in the epithalamus (C). FOXP2 was expressed throughout the thalamus (D). GBX2 was expressed more in the dorsal region of the thalamus and excluded from the ventricular zone (E). SP8 was expressed in the prethalamus, ganglionic eminence and the ventricular zone of the cortex (F). OTX2 was expressed in the ventricular zone of the thalamus and the epithalamus (G). NR2F2 was expressed in the prethalamus, in the ventricular zone of the thalamus and in the ganglionic eminence (H). PAX6 was expressed in the ventricular zone of the thalamus, as well as in the ganglionic eminence and the ventricular zone of the cortex and excluded from zona limitans (black arrow) (I). Abbreviations: Ganglionic eminence (GE); Epithalamus (Epith); Thalamus (TH); Zona limitans intrathalamic (ZLI); Prethalamus (pTh); ventricular zone (vz). Scale bar 1mm. (Images A-H prepared by Dr Alzu'bi. Interpretation of the staining patterns is my own work).

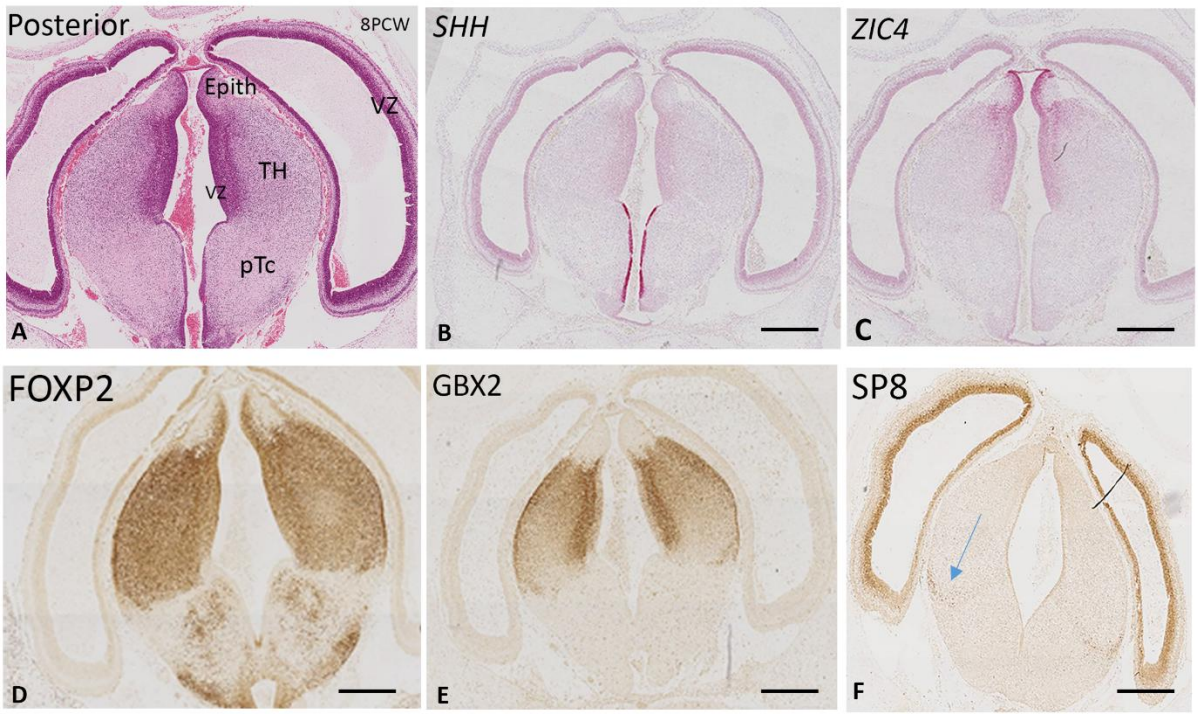

Figure 4.5. Immunostaining GBX2, FOXP2, SP8 and in situ-hybridization of *SHH* and *ZIC4* anterior coronal sections at 8 PCW. H&E staining in the sagittal section at 8 PCW posterior (A). *SHH* was expressed in the ventricular zone of the pretectum (B). *ZIC4* showed strong expression in the epithalamus and the ventricular zone of the thalamus (C). FOXP2 also was expressed in the thalamus (D). GBX2 was expressed in the thalamus, excluded from ventricular zone (E). SP8 was expressed in the most ventral and lateral part of the thalamus (blue arrow) (F). Abbreviations: epithalamus (Epith); thalamus (TH); pretectum (pTc); ventricular zone (vz). Scale bar 1mm. (Images (B,C) prepared by Dr Alzu'bi, (D, E, F) prepared by me. Interpretation of the staining patterns is my own work).

4.4.3 Immunostaining in the coronal section at 10 PCW

At the 10 PCW coronal section, PAX6 was expressed in the progenitor cells in the ventricular zones of the thalamus, cortex and habenula, as well as in the boundary between the prethalamus and the thalamus and ganglionic eminence (Figure 4.6 A). GBX2 and FOXP2 show immunoreactivity throughout the extent of the thalamus, but are excluded from the ventricular zone, and FOXP2 is expressed in the ganglionic eminence (Figure 4.6 B, C). NR2F2 is strongly expressed in the prethalamus, but also in both the VZ of the thalamus and the ganglionic eminence, as well as in the hypothalamus; there is also no co-expression between FOXP2 and NR2F2 (Figure 4.6 D, E, F). *ZIC4* was expressed in the whole thalamus, habenula and the ganglionic eminence (Figure 4.6 G). Co-staining with FOXP2 revealed *ZIC4* shows relatively homogenous expression throughout p2, whereas FOXP2 showed relatively stronger expression in the mediodorsal regions (Figure 4.6 H). Staining for the presynaptic protein syntaxin binding protein 1 (STXBP1) revealed synapse formation in the thalamus is absent in these early stages, although immunoreactivity for STXBP1was observed in the prethalamus, hypothalamus and habenula, as well as in the intermediate zone and the presubplate of the cerebral cortex (Figure 4.6 I). This agrees with observations made in other species, suggesting corticothalamic innervation is preceded by a waiting period during which cortical axons first synapse with cells in the prethalamus (the future reticular nucleus) (Grant et al., 2012).

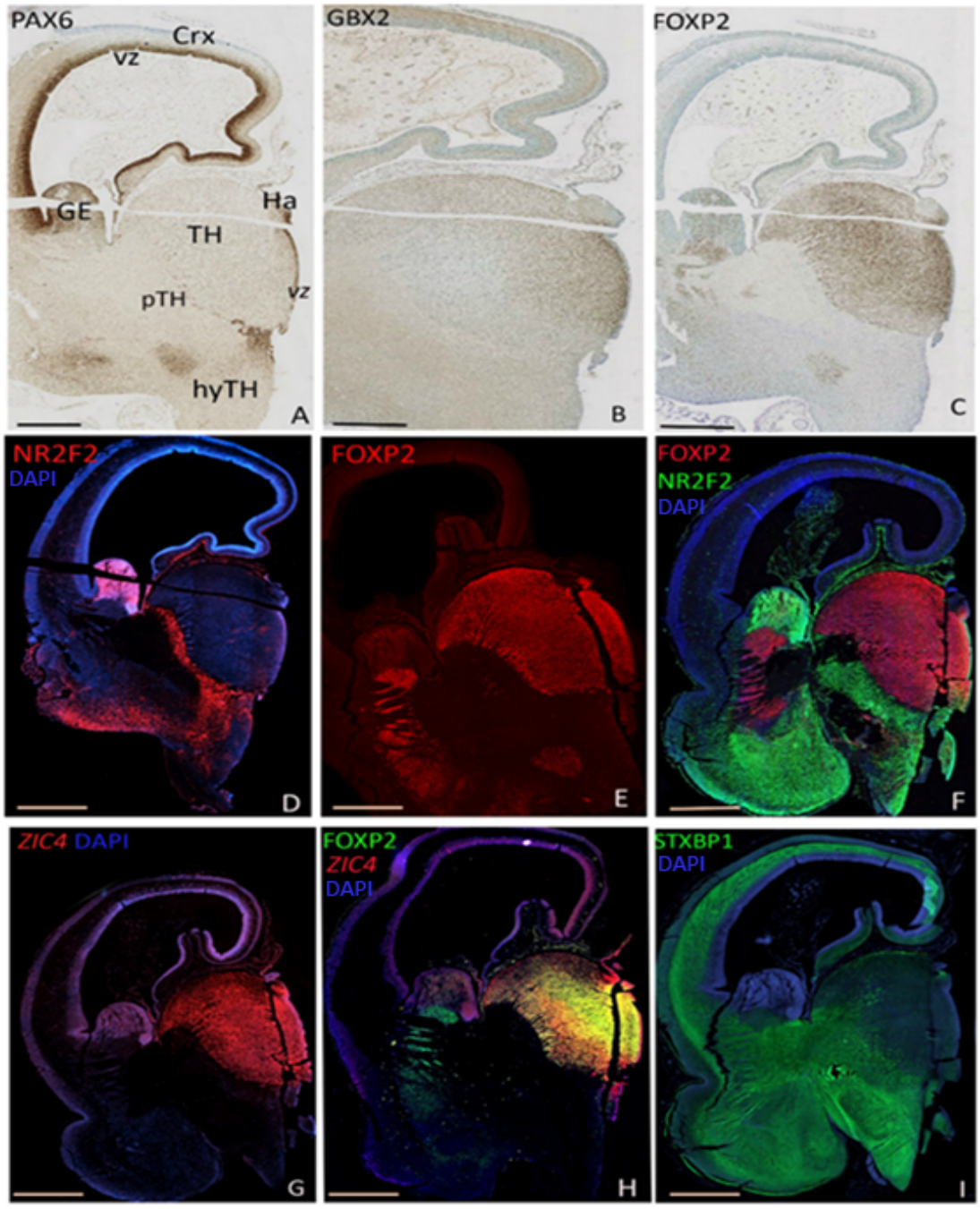

Figure 4.6. Immunostaining of coronal section at 10 PCW. Immunoperoxidase histochemistry - PAX6 was expressed in the ventricular zone of the thalamus and the cortex; it was also expressed in the prethalamus and in the ganglionic eminence (A). GBX2 and FOXP2 were expressed in the postmitotic zone in the thalamus (B, C). Immunofluorescence - NR2F2 showed strong expression in the prethalamus, ganglionic eminence and in the ventricular zone of the thalamus (D), while FOXP2 was expressed in the entire thalamic neuron and in the ganglionic eminence (E), and no co-expression was observed between FOXP2 and NR2F2 (F). RNAscope double immunofluorescence - *ZIC4* was expressed in the entire thalamus and in the ventricular zone of the thalamus (G). There was also co-expression of *ZIC4* with FOXP2 in the thalamic neurons (H). Immunofluorescence - STXBP1 was observed in the prethalamus and habenula, and in the intermediate zone and presubplate of the cerebral cortex (I). Abbreviations: Habenula (Ha); cortex (Crx); ventricular zone (vz); Thalamus (TH); prethalamus (pTH); hypothalamus (hyTH); ganglionic eminence (GE). Scale bar 1 mm.

4.4.4 Emergence of thalamic nuclei at 14 PCW

We considered several sections through the thalamus, an extensive set taken from a 14 PCW specimen stained for multiple mRNAs and proteins and cut along the coronal plane. The precise plane could be deduced by comparing the histological sections with virtual sections from a 3-D MRI image of the foetal brain supplied by the Human Developmental Biology resource (https://hdbratlas.org/fetal-stages/13pcw.html). By 14 PCW, it was apparent that the thalamus was dividing into discrete regions, identifiable by patterns of gene expression and containing relatively cell dense and cell poor regions.

In Figure 4.7 A-L, the most anterior and dorsal sections, the pulvinar is distinguished by the expression of various markers. CALB2 was restricted in the lateral pulvinar, habenula and the midbrain (Figure 4.7 D), whereas CALB1 was expressed in the medial pulvinar and in the midbrain (Figure 4.7 E). PAX6 was expressed in the midbrain's ventricular zone (Figure 4.7 F). NR2F1 is present throughout the pulvinar (Figure 4.7 G). GAD67, an essential marker for GABAergic neurones, exhibited robust expression in the midbrain and the inferior and medial regions of the pulvinar (Figure 4.7 H). OTX2 was expressed in the putative GABAergic neurons in the pulvinar inferior and in the midbrain regions (Figure 4.7 I). NR2F2 is expressed in the pulvinar inferior and in the midbrain, where it is linked to GABAergic neurons that have migrated from the telencephalon to the thalamus (Figure 4.7 J). FOXP2 and GBX2, which serve as critical indicators of thalamic identity, were expressed across the pulvinar, while FOXP2 was also expressed in the midbrain (Figure 4.7 K-L).

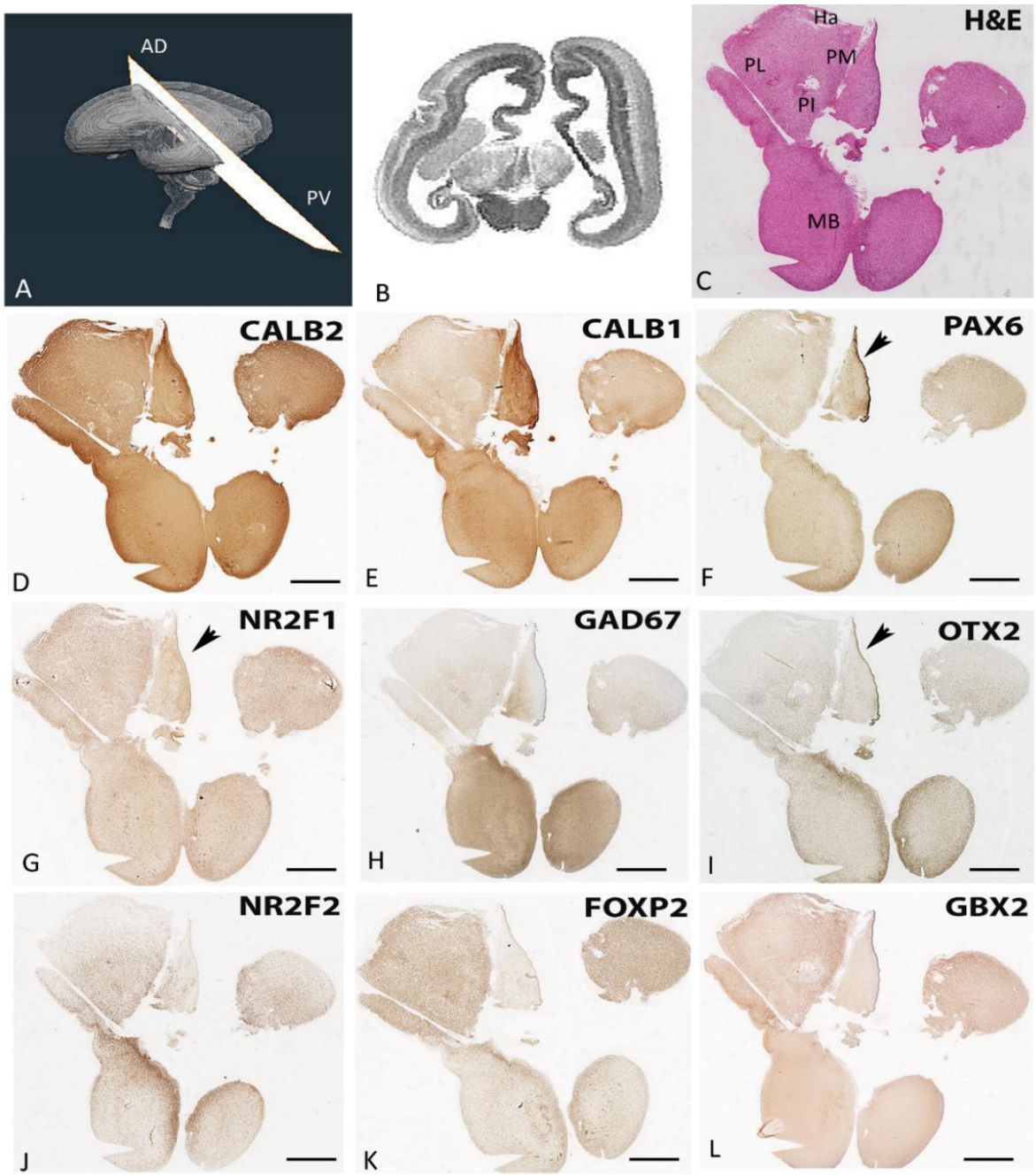

Figure 4.7. Immunostaining of CALB2, CALB1, PAX6, NR2F1, GAD67, OTX2, NR2F2, FOXP2 and GBX2 in the human thalamus at 14 PCW. (A, B) Plane section of 3D model in CT scan to show the place of sectioning in the thalamus. H&E staining shows the thalamus and midbrain (C). CALB2 was present in the pulvinar lateral, Habenula and midbrain (D). CALB1 was found in the midbrain and the Pulvinar medial (E). PAX6 exhibited low expression in the pulvinar but was expressed in the ventricular zone of the midbrain (F). NR2F1 demonstrated robust expression across the whole pulvinar (G), whereas NR2F2 was confined to the pulvinar inferior with midbrain (J). GAD67 showed strong expression in the midbrain and in the pulvinar medial and inferior (H). OTX2 was also expressed in pulvinar inferior and in the ventricular zone of the midbrain (black arrow) (I). FOXP2 and GBX2 were present in the whole pulvinar, but GBX2 was absent from the midbrain (K, L). Abbreviations: medial pulvinar (PM); lateral pulvinar (PL); inferior pulvinar (PI); habenula (Ha); anterodorsal (AD); posteroventral (PV), midbrain (MB). Scale bar 1mm.

Moving on, sections that were slightly anterior dorsal (Figure 4.8 A-O) in the H&E staining were examined, and it can be distinguished here as the lateral geniculate nucleus, medial geniculate nucleus, ventroposteriolateral, pulvinar lateral, pulvinar medial, pretectum and habenula (Figure 4.8 C). CALB2 was expressed everywhere in the thalamus (Figure 4.8 D). CALB1 exhibited strong expression in the medial geniculate nucleus, pretectum and Habenula (Figure 4.8 E). OTX2 was regionalized in the ventroposteriolateral and the medial geniculate nucleus and pretectum. Additionally, concentrated expression in the progenitor cell in the ventricular zone of the thalamus was observed (Figure 4.8 F). GAD67 showed the same pattern as OTX2; that is, strong expression in the ventroposteriolateral and strong expression in the medial geniculate nucleus, in the pretectum and habenula and the midbrain (Figure 4.8 G). ASCL1 and OLIG2 were both expressed in the proliferative zone of the thalamus (Figure 4.8 H, I). NR2F1 also showed high expression, which was largely exclusive to the thalamus, but displayed relatively higher expression in the lateral geniculate nucleus (Figure 4.8 J). NR2F2, followed a partly complimentary pattern, with strong immunoreactivity in the pretectum, also being expressed in the ventroposteriolateral nucleus (Figure 4.8 K) that can be seen in the 8 PCW (Figure 4.2 J). GBX2 showed strong expression in the posteromedial, compared to the posterolateral thalamic nuclei, as well as in the medial geniculate nucleus (MGN) (Figure 4.8 L). FOXP2 localization provided the most striking visualization of putative thalamic nuclei. The extent of the pulvinar complex was further delineated by moderate to strong FOXP2 expression, with expression being stronger in the lateral and inferior pulvinar regions than the medial pulvinar and the lateral geniculate nucleus, which we were able to observe as a discrete nucleus by the developmental stage. The lateral geniculate nucleus occupied a more dorsal location lateral to the main body of thalamus than where it was found in the adult thalamus. As has been previously described, the later developing pulvinar gradually displaces the lateral geniculate nucleus in a latero-ventral direction (Hitchcock and Hickey, 1980). The lateral geniculate nucleus had not adopted a laminar structure by 14 PCW, also confirming prior findings (Hitchcock and Hickey, 1980) (Figure 4.8 M). SP8 could be detected in the pretectum, habenula, lateral and medial geniculate nucleus in the section (Figure 4.8 N). PAX6 exhibited strong expression in the ventricular zone of the pretectum and thalamus, and also in the putative cell in medial and lateral geniculate nucleus (Figure 4.8 O).

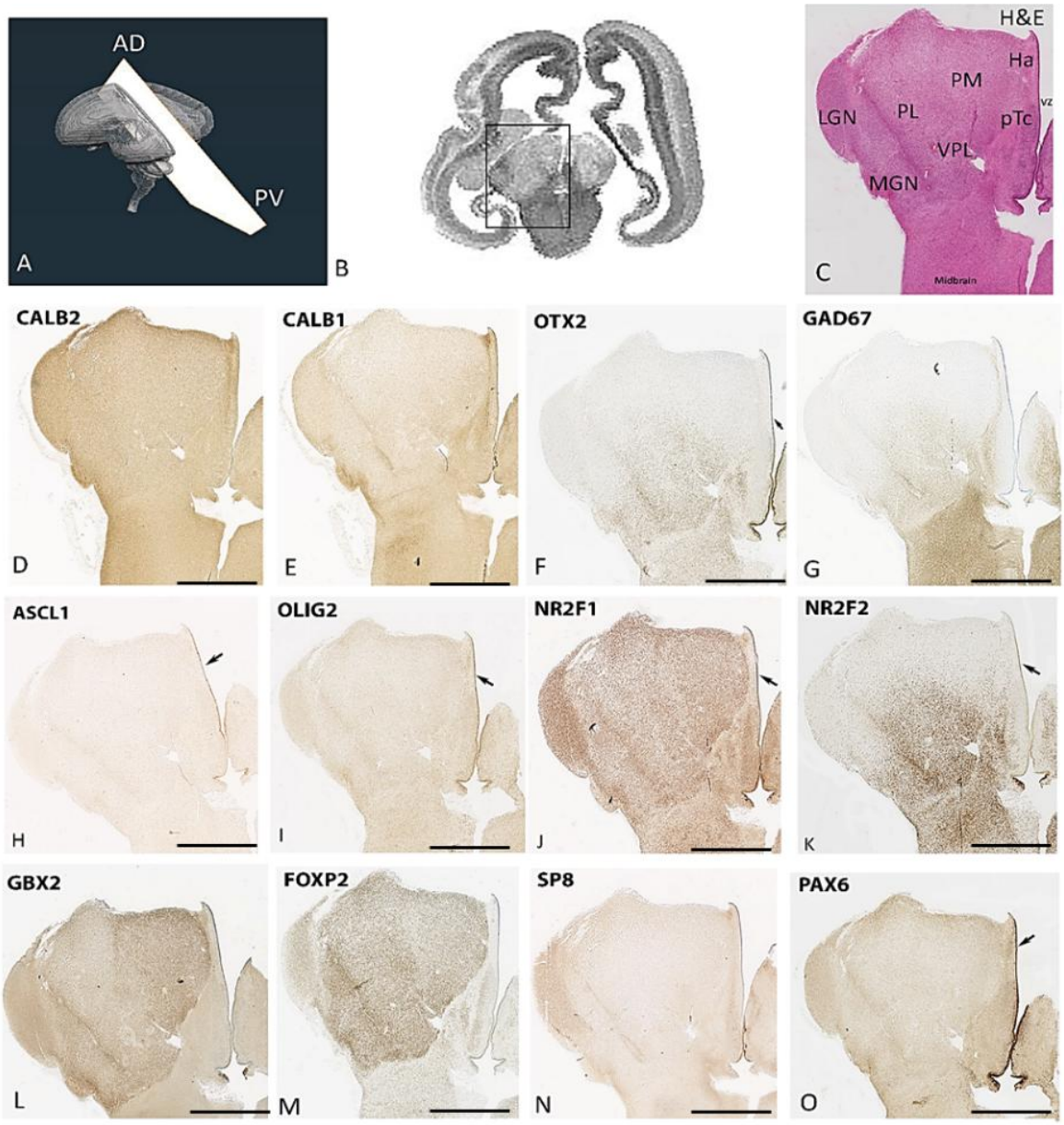

Figure 4.8. Immunostaining of CALB2, CALB1, OTX2, GAD67, ASCL1, OLIG2, NR2F1, NR2F2, GBX2, FOXP2, SP8 and PAX6 in the human thalamus at 14 PCW anterior dorsal. (A, B) Plane section of 3D model in CT scan to show the place of sectioning in the thalamus. H&E staining shows the thalamic nuclei and midbrain (C). CALB2 was present everywhere in the thalamus (D). CALB1 was expressed in the medial geniculate nucleus, pretectum and habenula (E). OTX2 displayed strong expression in the ventricular zone of the thalamus, as well as expressed in the medial geniculate nucleus and posterioventrolateral (F). GAD67 was strongly expressed in medial geniculate nucleus and posterioventrolateral, and also in pretectum, habenula and the midbrain (G). OLIG2, PAX6, ASCL1 were all strongly expressed in the progenitor cells of the thalamus (H, I, O). NR2F1 showed strong expression throughout the entire thalamus and in the lateral and medial geniculate nucleus (J). NR2F2 exhibited strong expression in medial geniculate nucleus and in ventroposteriolateral (K). GBX2 showed stronger expression in the medial portion of the thalamus compared to the lateral part (L). FOXP2 was strongly expressed in the whole thalamus (M). SP8 was expressed in the medial and lateral geniculate nucleus, as well as in pretectum and habenula (N). Abbreviations: later pulvinar (PL); medial pulvinar (PM); medial geniculate nucleus (MGN); lateral geniculate nucleus (LGN); pretectum (pTc); habenula (Ha); ventroposteriolateral (PVL). Scale bar 1mm.

In sections located through the middle region of the thalamus located posteriorly and ventrally (Figure 4.9 A- M), distinct boundaries were observed between the thalamic nuclei, and between the thalamus and pretectum. CALB2 expression was noted in the medial geniculate nucleus and the lateral geniculate nucleus (Figure 4.9 D). CALB1 was expressed in the lateral geniculate nucleus, the lateral dorsal area of the thalamus and pretectum (Figure 4.9 E). CALB1 and CALB2 showed no expression in the centromedian nucleus, which has very strong expression for FOXP2, GAD67, NR2F1, NR2F2. OTX2 displayed weak expression in the ventroposteriomedial and the centromedian (Figure 4.9 F). In terms of NR2F1 expression, this was homogenous throughout the thalamus, strong in the thalamus and weak in the pretectum. Expression was especially marked in the LGN and an anterior region, as well as in the centromedian nucleus (Figure 4.9 G). NR2F2 expression was strong in the pretectum extending to the ventroposterior half of the thalamus, covering the centromedian nucleus/parafascicular complex and the areas lateral to it, and excluding LGN. NR2F2 expression was observed in the reticular formation (Figure 4.9 H). PAX6 expression was observed in the progenitor cells in the ventricular zone of the thalamus. In addition, PAX6 was noted to be more highly expressed ventrally (V) with low expression dorsally (D) in the ventricular zone and close to the boundary with p3 (Figure 4.9 I, black arrow). GAD67 displayed strong expression in the parafascicular nucleus and the centromedian, as well as in pretectum (Figure 4.9 J). FOXP2 expression was very strong in the putative centromedian nucleus and the parafascicular complex. It was also moderately expressed close to the midline and in the medial geniculate nucleus, although immunoreactivity was lower in the lateral portions of the thalamus. FOXP2 showed no expression in the anterior part, which was very strong in terms of NR2F1 expression (Figure 4.9 K). GBX2 in this section was expressed in the medial geniculate nucleus and in the medial part of the thalamus (Figure 4.9 L). SP8 showed strong expression in the lateral geniculate nucleus, in the reticular formation and in the anteromedial part of the thalamus and at the boundary between p2 and p3 (Figure 4.9 M). To the best of our knowledge, this is the first time that SP8 expression has been described in the thalamus.

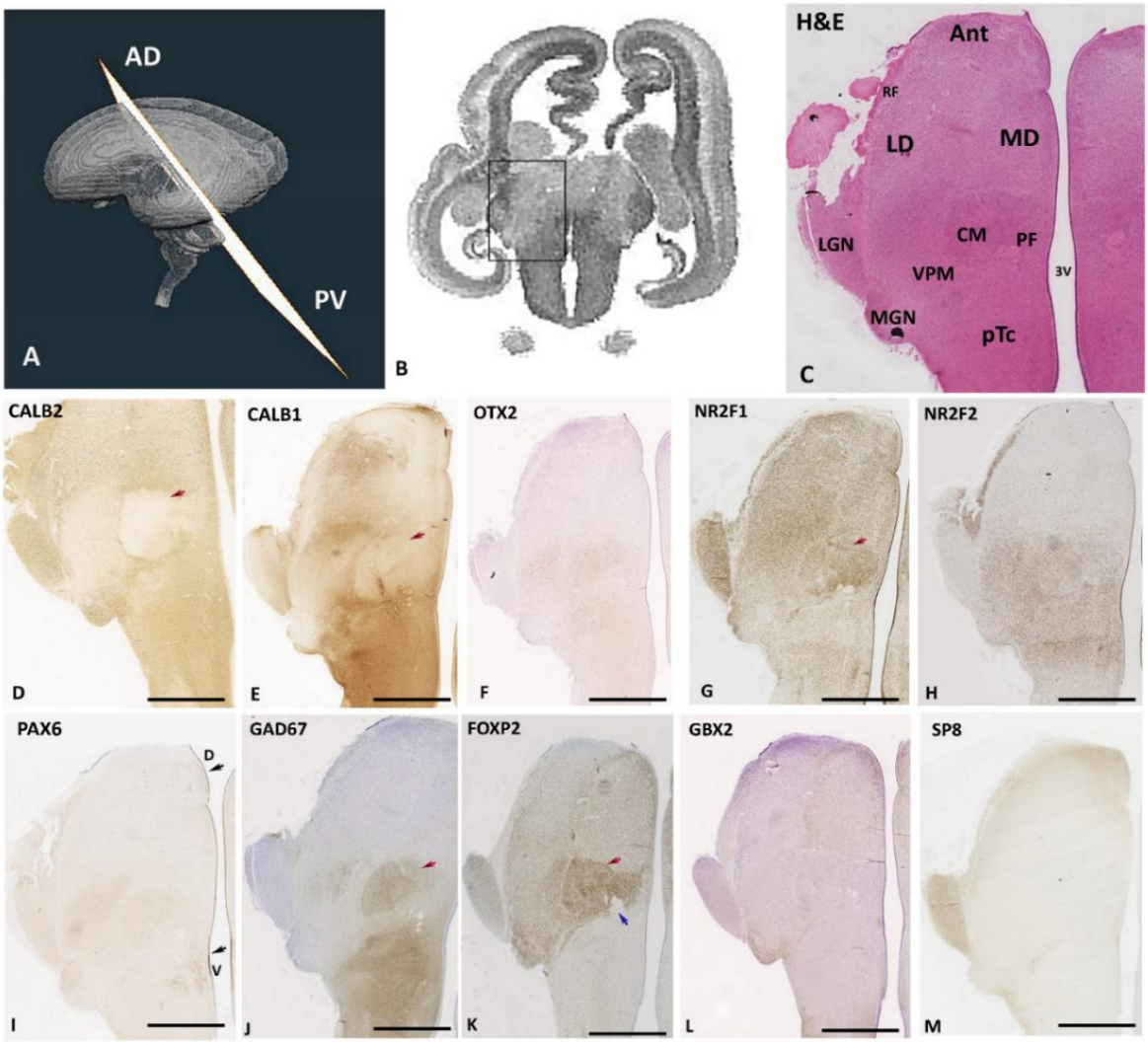

Figure 4.9. Immunostaining of CALB2, CALB1, OTX2, NR2F1, NR2F2, PAX6, GAD67, FOXP2, GBX2 and SP8 in the human thalamus more posterior ventral at 14 PCW. (A, B) Plane section of 3D model in CT scan to show the place of sectioning in the thalamus. H&E staining shows the thalamic nuclei (C). CALB2 showed strong expression in the lateral and medial geniculate nucleus, but no expression in centromedian (red arrow) (D). CALB1 was strongly expressed in lateral dorsal, but not expressed in centromedian (see red arrow) (E). OTX2 displayed weak expression in both centromedian and ventroposteriomedial (F). NR2F1 immunoreactivity was high across the thalamus, but strongest anteriorly and in the lateral geniculate nucleus, centromedian (red arrow) (G). NR2F2 showed expression in the ventroposteriomedial, centromedian, medial geniculate nucleus and reticular formation, except for the lateral geniculate nucleus (H). PAX6 was strongly expressed in the dorsal ventricular zone of the thalamus, contrasting with the dorsal ventricular zone of the thalamus (black arrow) (I). GAD67 displayed strong expression in the centromedian, parafascicular nucleus and in pretectum (J). FOXP2 expression was highest in the centromedian (red arrow), lateral and medial geniculate nucleus and parafascicular nucleus was close to the habenulo peduncular tract (blue arrow) and weakest in the anterior thalamus (K). GBX2 displayed strong expression in medial geniculate nucleus and in mediodorsal (L). SP8 was strongly expressed in the lateral geniculate nucleus, anteromedial part of the thalamus (M). Abbreviations: mediodorsal (MD); lateral dorsal (LD); centromedian (CM); parafascicular nucleus (PF); pretectum (pTc); medial geniculate nucleus (MGN) lateral geniculate nucleus (LGN); Anterior (Ant); ventroposteriomedial (VPM); Reticular formation (RF). Scale bar 1mm.

Figure 4.10 A-L shows the more posterior and ventral set of sections in the thalamus. CALB2 was found to be strongly expressed in the whole thalamus and in the ventral part of lateral geniculate nucleus (red arrow), but not at all in the dorsal part (blue arrow) and was absent from the centromedian nucleus (green arrow). CALB1 was expressed in the lateral dorsal nucleus and the lateral geniculate nucleus (Figure 4.10 E). Meanwhile, NR2F1 was also detected in the thalamic reticular formation (black arrow) (predominantly originating from p3 (Puelles et al., 2013; Puelles & Rubenstein, 2003)), and formed a lateral boundary to the thalamus (Figure 4.10 F), as well also appearing in the lateral geniculate nucleus (Figure 4.10 F). The reticular formation was likewise strongly immunoreactive for NR2F2 (Figure 4.10 G black arrow). It was also expressed in the pretectum and midbrain, with expression also extending into the dorsomedial and ventrolateral regions of the thalamus (Figure 4.10 G). GAD67 was expressed in the centromedian, dorsal part of the lateral geniculate nucleus, which is absent from FOXP2, SP8 and CALB2 (Figure. 4.10 H, blue arrow). GBX2 was expressed in the medial dorsal nucleus of the thalamus, and in the medial geniculate nucleus and at the boundary between p2 and p3 (Figure 4.10 I). FOXP2 was expressed in the centromedian and parafascicular (Figure. 4.10 J). PAX6 was highly expressed in the ventricular zone of the thalamus (Figure. 4.10 K). High expression of GAD67 was also observed anterodorsal to the lateral geniculate nucleus (Figure. 4.10H). SP8 but not GAD67 was detected to be expressed in ventral lateral geniculate nucleus, suggesting the SP8+/GAD67- neurons could be postmitotic cells and not interneurons**.** FOXP2 and SP8 were not detected in the dorsal area of the lateral geniculate nucleus (Figure. 4.10 J, L). NR2F2 and SP8 both showed expression in the reticular formation (Figure. 4.10 G, L), suggesting that SP8 derived from GABAergic neurons of prethalamic origin and NR2F2 derived from pretectum, midbrain and prethalamus.

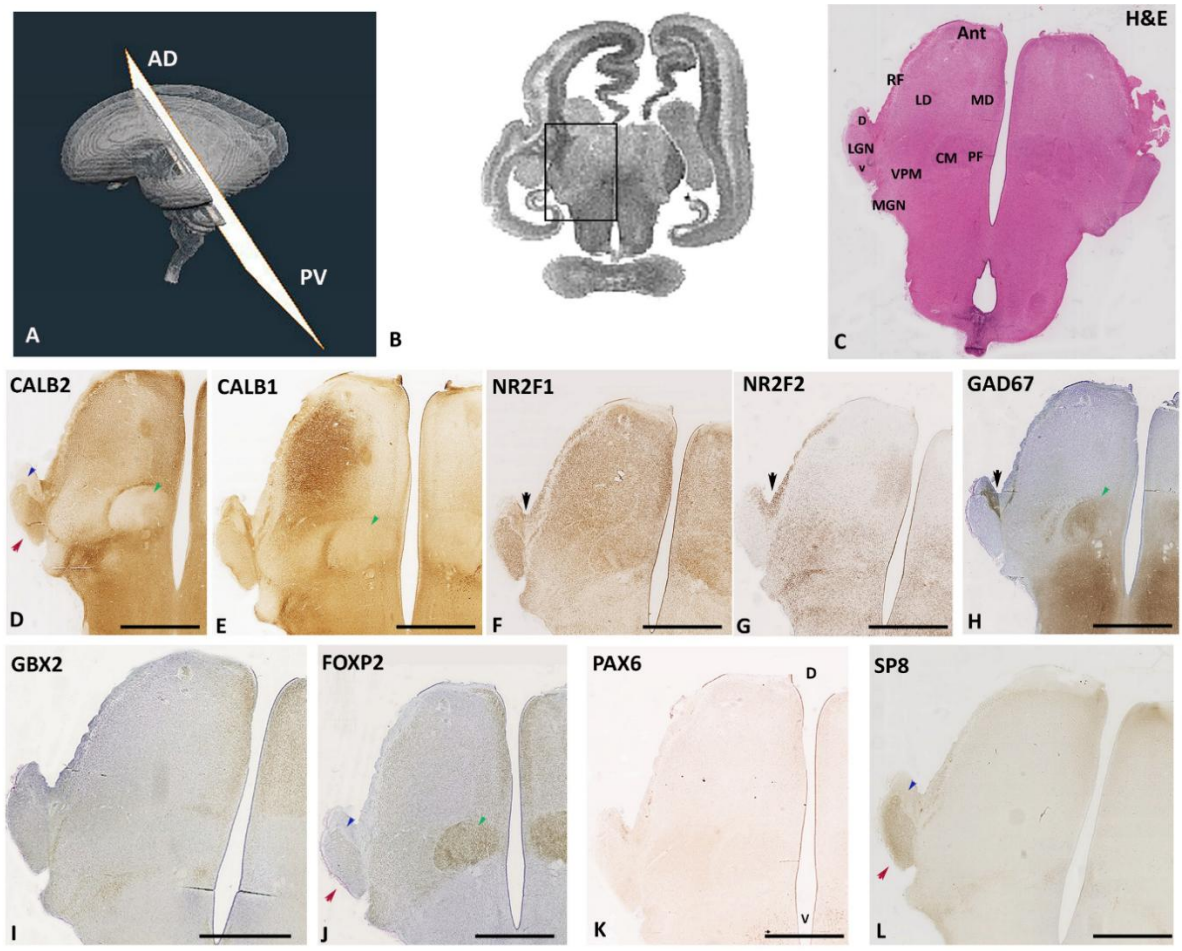

Figure 4.10. Immunostaining of CALB2, CALB1, NR2F1, NR2F2, GAD67, GBX2, FOXP2, PAX6, and SP8 in the human thalamus, most posterior ventral at 14 PCW. (A, B) Plane section of 3D model in CT scan to show the place of sectioning in the thalamus. H&E staining shows the thalamic nuclei (C). CALB2 was found to be strongly expressed in the whole thalamus and in the ventral part of lateral geniculate nucleus (red arrow), but not at all in the dorsal part (blue arrow) as well as absent from the centromedian nucleus (green arrow) (D). CALB1 displayed strong expression in the lateral dorsal, but no expression in the centromedian (green arrow) (E). NR2F1 immunoreactivity was high across the thalamus as well as in the lateral geniculate nucleus, but no expression was present in the anterior, also expressed in the reticular formation (black arrow) (F). NR2F2 expression was confined to the posterior half of the thalamus, except for the lateral geniculate nucleus, and was expressed in the reticular formation (G). GAD67 displayed strong expression in the dorsal part of lateral geniculate nucleus and in the centromedian nucleus (H). GBX2 expression was observed in the mediodorsal and the medial geniculate nucleus (I). FOXP2 was most highly expressed in the centromedian and parafascicular nucleus, having weak expression in the anterior and the lateral geniculate nucleus (J). PAX6 was expressed in the proliferative zone of the thalamus (K). SP8 exhibited expression in the anteriomedial part of the thalamus, but strong expression in the ventral lateral geniculate nucleus (red arrow), although not in the dorsal (blue arrow) (L). Abbreviations: mediodorsal (MD); lateral dorsal (LD); lateral geniculate nucleus (LGN); medial geniculate nucleus (MGN); Anterior (Ant), Parafascicular nucleus (PF), Ventroposteriomedial nucleus (VPM); centromedian (CM); reticular formation (RF). Scale bar 1mm.

When compared to the other segments, the most posterior and ventral set of sections (Figure 4.11A- L) offered a different perspective. CALB1 was expressed in the ventrolateral nucleus and lateral geniculate nucleus, but not expressed in the medial geniculate nucleus (Figure 4.11 D). CALB2 was expressed in the ventromedial nucleus, ventral of the lateral geniculate nucleus, while NR2F2 and GAD67 were absent from the ventral part of the lateral geniculate nucleus (Figure 4.11 E). NR2F2 was strongly expressed in the reticular formation, also being expressed in the pretectum, with expression also extended into the dorsomedial and ventrolateral regions of the thalamus, whereas there was relatively weak expression in the anterodorsomedial domains (Figure 4.11 F). In addition, NR2F2 was expressed in the dorsal part of the lateral geniculate nucleus. NR2F1 was strongly expressed in the whole thalamus, but also detectable in the thalamic reticular formation (Figure 4.11 G), as well as in the dorsal and ventral part of lateral geniculate nucleus. SP8+ positive neurons were present in the anterior thalamus, in the LGN, as well as at the boundary between the thalamus and pretectum as well as in the reticular formation (Figure 4.11 H). FOXP2 was present in the ventroposteriomedial and in the ventral lateral geniculate nucleus (Figure. 4.11 I). GBX2 expression was weak in the thalamus at this stage, but could be detected in the medial geniculate nucleus at the boundary between the pretectum and the thalamus (Figure. 4.11 J). GAD67 exhibited strong expression in the dorsal lateral geniculate nucleus which is absent from FOXP2 immunoreactivity (Figure 4.11 K). PAX6 was expressed in the ventral and dorsal part of the lateral geniculate nucleus, and in the ventricular zone of the thalamus (Figure 4.11 L). In summary, we identified marker genes for specific thalamic nuclei as listed in the a forementioned paragraphs. Some GABAergic neurons come from extra thalamic regions which expressed the reticular formation markers such as NR2F2, NR2F1, SP8.

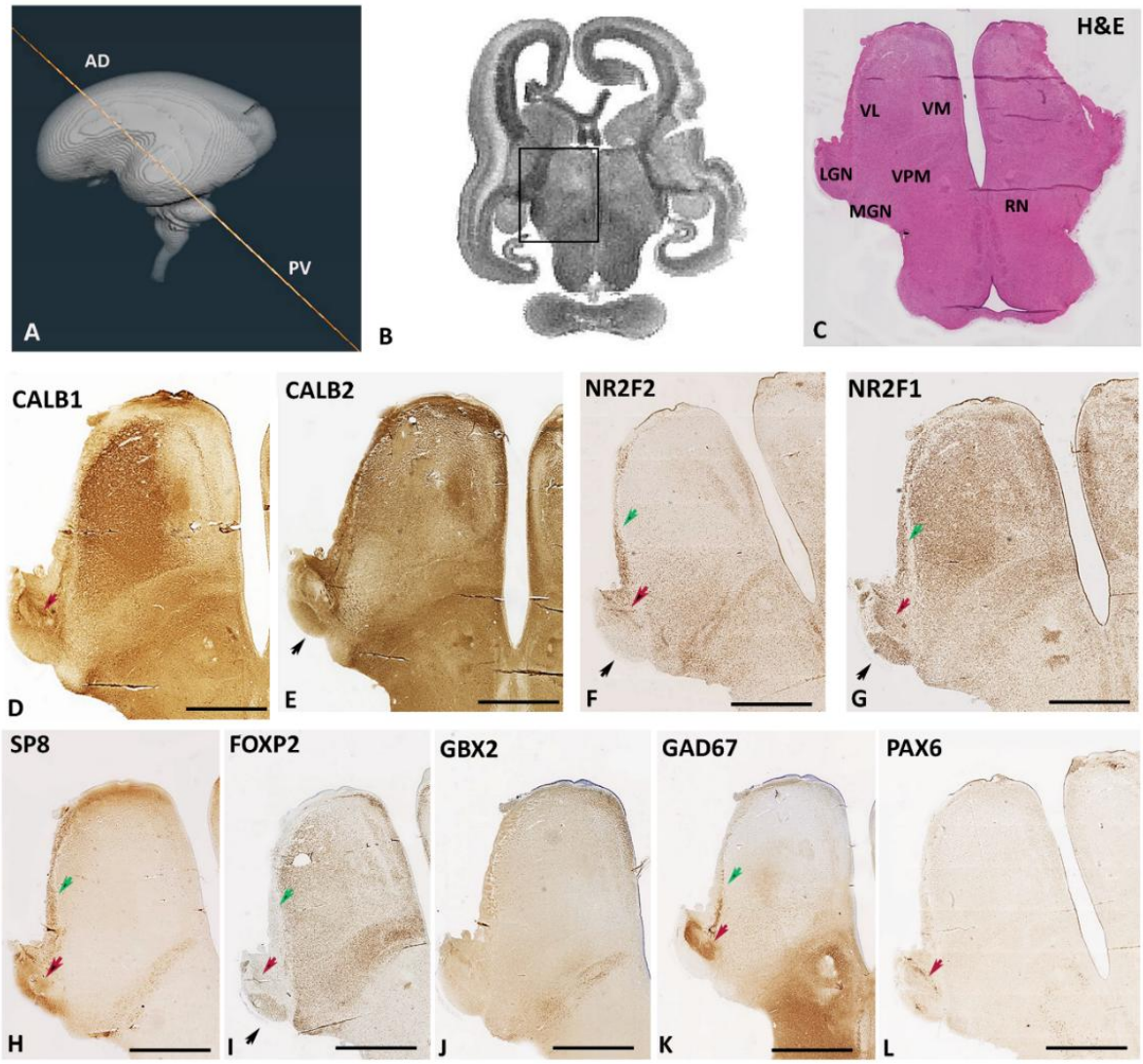

Figure 4.11. Immunostaining of CALB1, CALB2, NR2F2, NR2F1, SP8, FOXP2, GBX2, GAD67 and PAX6 in the human thalamus more posterior ventral at 14 PCW. (A, B) Plane section of 3D model in CT scan to show the place of sectioning in the thalamus. H&E staining shows the thalamic nuclei (C). CALB1 can be seen in ventral lateral and in lateral geniculate nucleus (red arrow) (D). CALB2 was expressed in the reticular formation, ventral medial and the ventral lateral geniculate nucleus (black arrow) (E). NR2F2 was expressed in the reticular formation (green arrow), as well as in the dorsal lateral geniculate nucleus (red arrow), and in the anteromediodorsal part of thalamus, and it was absent from the ventral part of lateral geniculate nucleus (black arrow) (F). NR2F1 expression was evident in the whole thalamus and in the ventral and dorsal lateral geniculate nucleus (G). SP8 appeared in the boundary between the pretectum and the thalamus, as well as in the reticular formation (green arrow), and in the lateral geniculate nucleus (H). FOXP2 was expressed in the ventral lateral geniculate nucleus (black arrow), and in the whole thalamus, with weak expression was seen in the ventromedial (I). GBX2 showed strong expression in the boundary between the thalamus and the pretectum as well as in the medial geniculate nucleus (J). GAD67 was strongly expressed in the dorsal lateral geniculate nucleus (red arrow), and in the reticular formation (green arrow) (K). PAX6 can be seen in the lateral geniculate nucleus (red arrow) (L). Abbreviations: ventrolateral (VL); ventromedial (VM); lateral geniculate nucleus (LGN); medial geniculate nucleus (MGN); ventroposteriomedial (VPM); reticular nucleus (RN). Scale bar 1mm.

4.4.5 Mapping of *ZIC4* and *SOX14* expression during the emergence of thalamic nuclei

As found in a previous mouse study (Li et al., 2018), *ZIC4* is essential for the development of the thalamus. *ZIC4* was expressed in all pulvinar nuclei, medial, lateral and inferior parts and in the habenula (Figure 4.12 A). *ZIC4* was no longer expressed throughout p2, but was strongly expressed in the putative habenula and the antero-dorsal edge of the thalamus at this level, as well as in some medial parts of the pretectum. It was also strongly expressed in the LGN (Figure 4.12 B). It was highly expressed in the anterior thalamic nuclei, anteromediodorsal part of the thalamus as well as in the lateral geniculate nucleus (Figure 4.12 C, D). *ZIC4* was further seen to be expressed in the lateral geniculate nucleus and in ventromedial thalamic nuclei (Figure 4.12 E). We therefore identified *ZIC4* as a marker gene for postmitotic cells and observed its expression in specific thalamic nuclei.

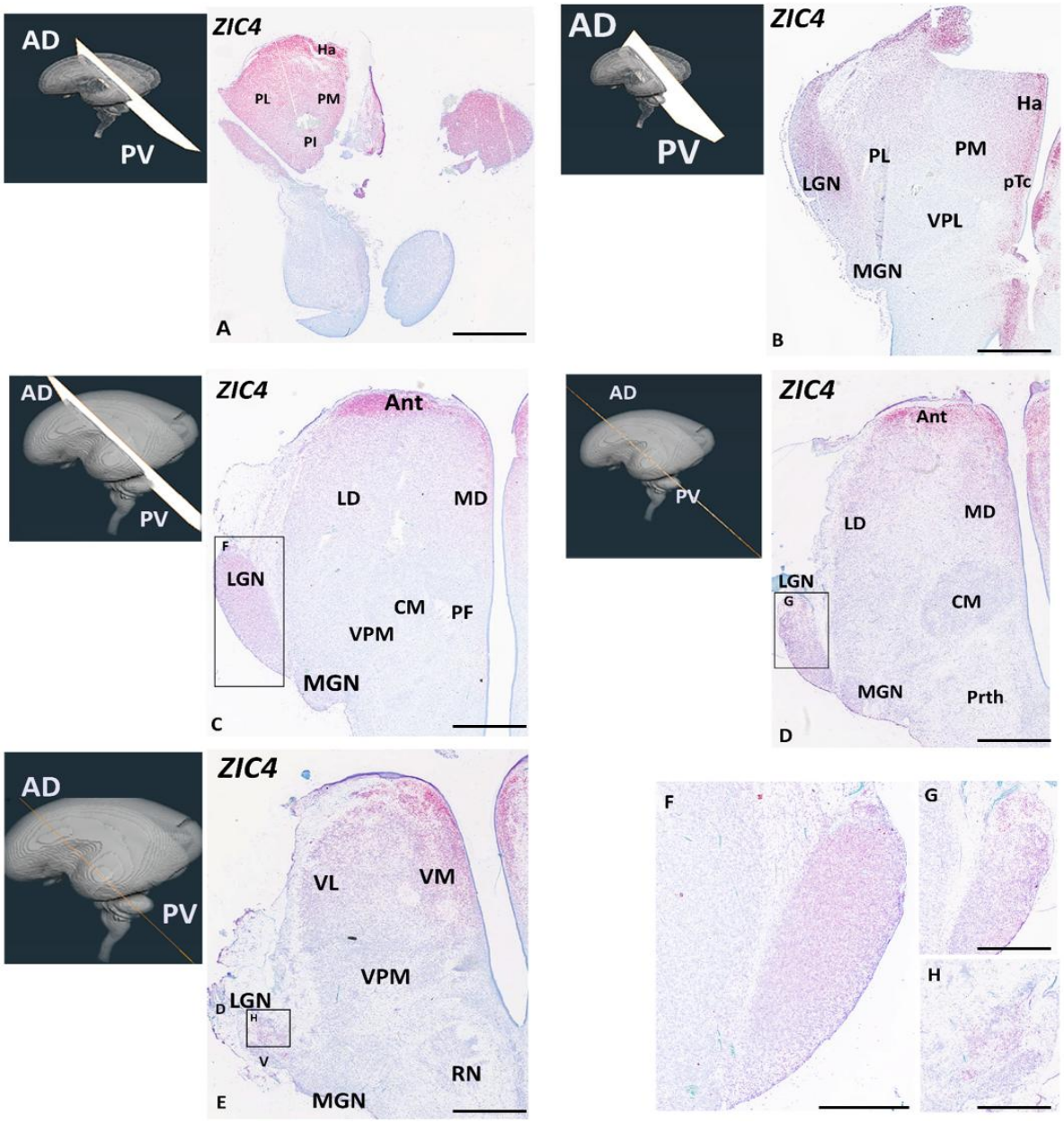

Figure 4.12. In situ hybridization for ZIC4 at 14 PCW. In the anterior and dorsal set of sections (A, B). Posterior and ventral set of sections (C, D, E), ZIC4 showing strong expression in (PL, PI, PM) and in (Ha). ZIC4 was expressed in the whole pulvinar and habenula in the anterior dorsal part (A). ZIC4 was strongly expressed in the putative habenula and at the antero-dorsal edge of the thalamus and in some medial parts of the pretectum and lateral geniculate nucleus in the more anterior dorsal part of the thalamus (B). ZIC4 was expressed in the anterior nuclei, lateral geniculate nucleus and the anteromediodorsal part of the thalamus, as well as in the anterior dorsal lateral geniculate nucleus in the ventral posterior part of the thalamus (C, D). ZIC4 was expressed in the ventromedial nucleus and in the lateral geniculate nucleus in the anterodorsal part in the most ventral and posterior part of the thalamus (E). Abbreviations: ventral lateral (VL); ventral medial (VM); lateral geniculate nucleus (LGN); ventroposteriomedial (VPM); lateral dorsal (LD); medial geniculate nucleus (MGN); Anterior (Ant); Parafascicular nucleus (PF), centromedian (CM); Medial dorsal (MD); lateral dorsal (LD); pretectum (pTc); Anterior (Ant); later pulvinar (PL); medial pulvinar (PM); inferior pulvinar (PI); habenula (Ha); ventroposteriolateral (PVL); Anterodorsal (AD); red nucleus (RN). Scale bar 1mm; 300 µm.

4.4.6 Mapping of *SOX14* expression during the emergence of thalamic nuclei

SOX14 is expressed in GABAergic neurons of midbrain origin (Jager et al., 2021). As detected in the dorsal and anterior sections, *SOX14* was strongly expressed in the midbrain (Figure 4.13 A, B). *SOX14* expression was confined to the same medial and ventroposterior areas of the thalamus, corresponding to the lateral and medial pulvinar, as well as in the midbrain, pretectum and the more posterior parts of the thalamus at the mid-thalamic level (Figure 4.13 B). *SOX14* expression was almost entirely absent from the anterior portions of this section (Figure 4.13 C). Expression was found to be stronger in the lateral posterior thalamus, but relatively weak in the adjacent lateral geniculate nucleus but showed expression in the medial geniculate nucleus (Figure 4.13 C, F). In the more ventral and posterior sections, *SOX14* expression was comparatively weak, and largely confined to the lateral margins in the lateral geniculate nucleus (Figure 4.13 D, E, F). We thus identified *SOX14* as a marker gene for GABAergic neurons and observed its expression in specific thalamic nuclei.

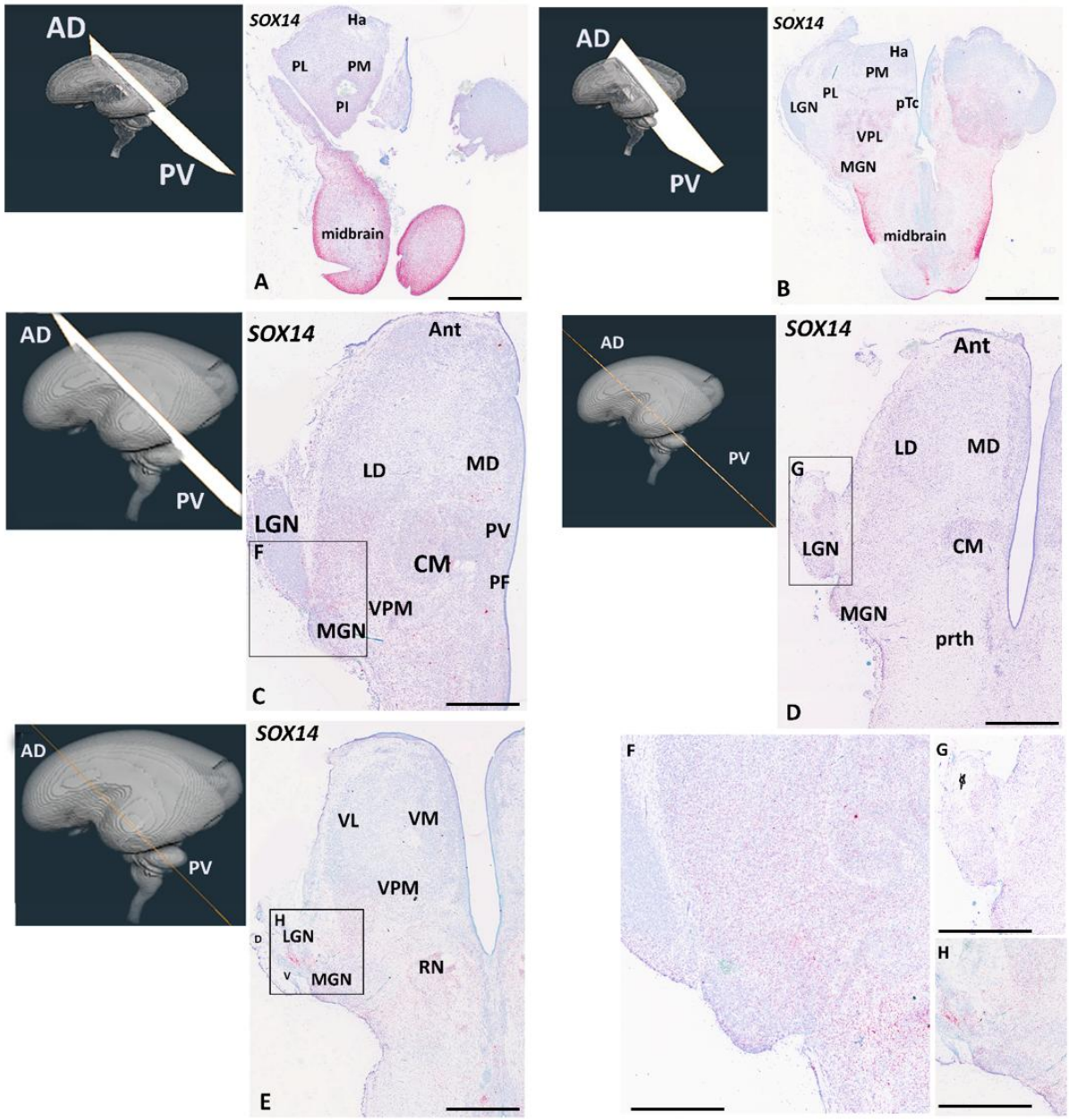

Figure 4.13. In situ hybridization for *SOX14* at 14 PCW. In the anterior and dorsal set of sections (A, B). Posterior and ventral set of sections (C, D, E). In the anterior and dorsal section (A), SOX14 showed strong expression in the midbrain. In the more anterior dorsal set of sections (B), SOX14 was strongly expressed in the midbrain, pretectum, ventroposteriolateral and medial area of thalamus. In the ventral and posterior section (C, F), expression was also stronger in the lateral posterior thalamus and in the lateral part of the lateral geniculate nucleus. In the more posterior and ventral set of sections (D), SOX14 displayed no expression in the anterior nuclei, lateral geniculate nucleus (D, G) and weak expression in the medial geniculate nucleus. SOX14 was observed in lateral geniculate nucleus and reticular nucleus in the most posterioventral part (E, H). Abbreviations: ventral lateral (VL); ventral medial (VM); ventroposteromedial (VPM); lateral geniculate nucleus (LGN); medial geniculate nucleus (MGN); Anterior (Ant); Parafascicular nucleus (PF), centromedian (CM); Medial dorsal (MD); lateral dorsal (LD); prethalamus (prth); pretectum (pTc); Anterior (Ant); later pulvinar (PL); medial pulvinar (PM); inferior pulvinar (PI); habenula (Ha); ventroposteriolateral (PVL). Anterodorsal (AD); red nucleus (RN). Scale bar 1mm; 300 µm.

At 14 PCW, the three potential markers for the GABAergic neurons and their precursors, GAD67, *SOX14* and NR2F2 were all generally expressed in the more posterior parts of the thalamus. Expression in the pretectum and midbrain appeared in a gradient across the thalamus, high at the thalamo-pretectal border, and declining towards the dorsal and anterior thalamus (Figure 4.8 G, Figure 4.9 J, Figure 4.10 H, Figure 4.13). These patterns of expression generally overlapped, suggesting a migration of the cells from the pretectum and the midbrain into posterior regions of the thalamus. GAD67 exhibited particularly striking expression in the centromedian nucleus and parafascicular nucleus, as previously shown at 16 PCW (Alhesain et al., 2023) (Figure 4.9 J, Figure 4.10 H) where there was clear co-expression of *SOX14* in the individual cells (Figure 4.14 B, D). However, GAD67 was not expressed just lateral to these nuclei, where SOX14 expression was witnessed (Figure 4.14 C). At one particular level of sectioning, in a region just anterodorsal to the lateral geniculate nucleus, high expression of GAD67 was observed (Figure 4.10 H, Figure 4.11 K). This area also expressed *ZIC4*, suggesting it was thalamic in origin, but not FOXP2 or SP8, unlike the nearby putative lateral geniculate nucleus (Figure 4.10 J, L). Lack of expression of SP8 suggested it was not part of the thalamic reticular formation, and nor did it contain cells originating from the ventral caudate ganglionic eminence. This region also expressed ASCL1+ cells as a marker for immature GABAergic neurons in the forebrain (Poitras et al., 2007, Castro et al., 2011), as well as *SOX14* and NR2F2, suggesting these may be GABAergic neurons of pretectal or midbrain origin (Figure 4.11 F, Figure 4.13 D). However, it is unclear why they accumulate to such a high degree in this unidentified nucleus. We conclude that, between 10 and 14 PCW, the thalamus is partially invaded by *SOX14*+, NR2F2+ cells of pretectum/midbrain and prethalamic origin, respectively. However, certain nuclei, for instance the medial dorsal nucleus and medial pulvinar, remained devoid of these cells even by 16 PCW, suggesting migration had stopped. However, in some locations, the maturation of these cells was quicker than in others. For example, the SOX14+ cells of the centromedian nucleus expressed GAD67 at this stage, whereas those of the lateral geniculate nucleus did not.

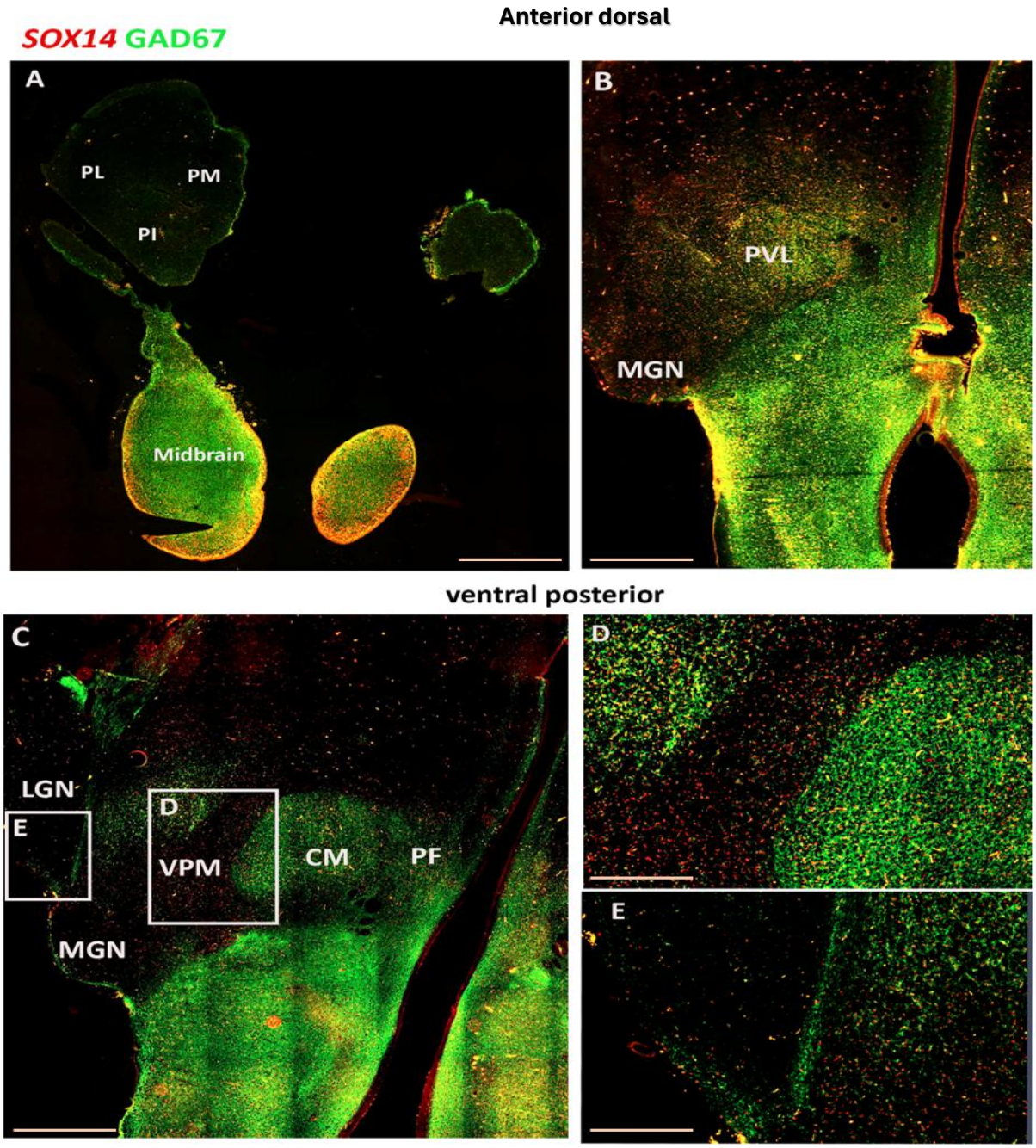

Figure 4.14. Double labelling between GAD67 (green) and *SOX14* (red) at 14 PCW. (A) GAD67 and *SOX14* displayed strong expression in the midbrain and co-localisation between these markers. (B) In the more anterior dorsal region, there was also co-expression of GAD67 and *SOX14* in the midbrain and the pretectum. (C) In the more posterior and ventral section, GAD67 exhibited particularly striking expression in the centromedian nucleus and the parafascicular nucleus, along with co-expression with *SOX14* in the individual cells. However, GAD67 was not expressed lateral to these nuclei where *SOX14* expression was observed. SOX14 does not exist in the lateral geniculate nucleus(D). Abbreviations: lateral geniculate nucleus (LGN); medial geniculate nucleus (MGN); ventroposteriomedial (VPM); centromedian (CM); parafascicular (PF); ventroposteriolateral (VPL). Scale bar 1mm; 300 µm.

The immunofluorescence analysis at 14 PCW revealed prominent expression of PAX6 in the ventral ventricular zone of the thalamus when contrasted with the dorsal area of the thalamus (Figure 4.15 A, B). Notably, PAX6 showed colocalization with NR2F2 within these areas, suggesting a potential interplay between these two transcription factors during the process of development and differentiation of these thalamic structures. The presence of both these proteins in the lateral and medial geniculate nucleus (Figure 4.15 A, C). This highlights their possible collaborative roles in the maturation of sensory processing pathways, whereas their expression in the ventricular zone indicates their involvement in progenitor cell dynamics during thalamic development.

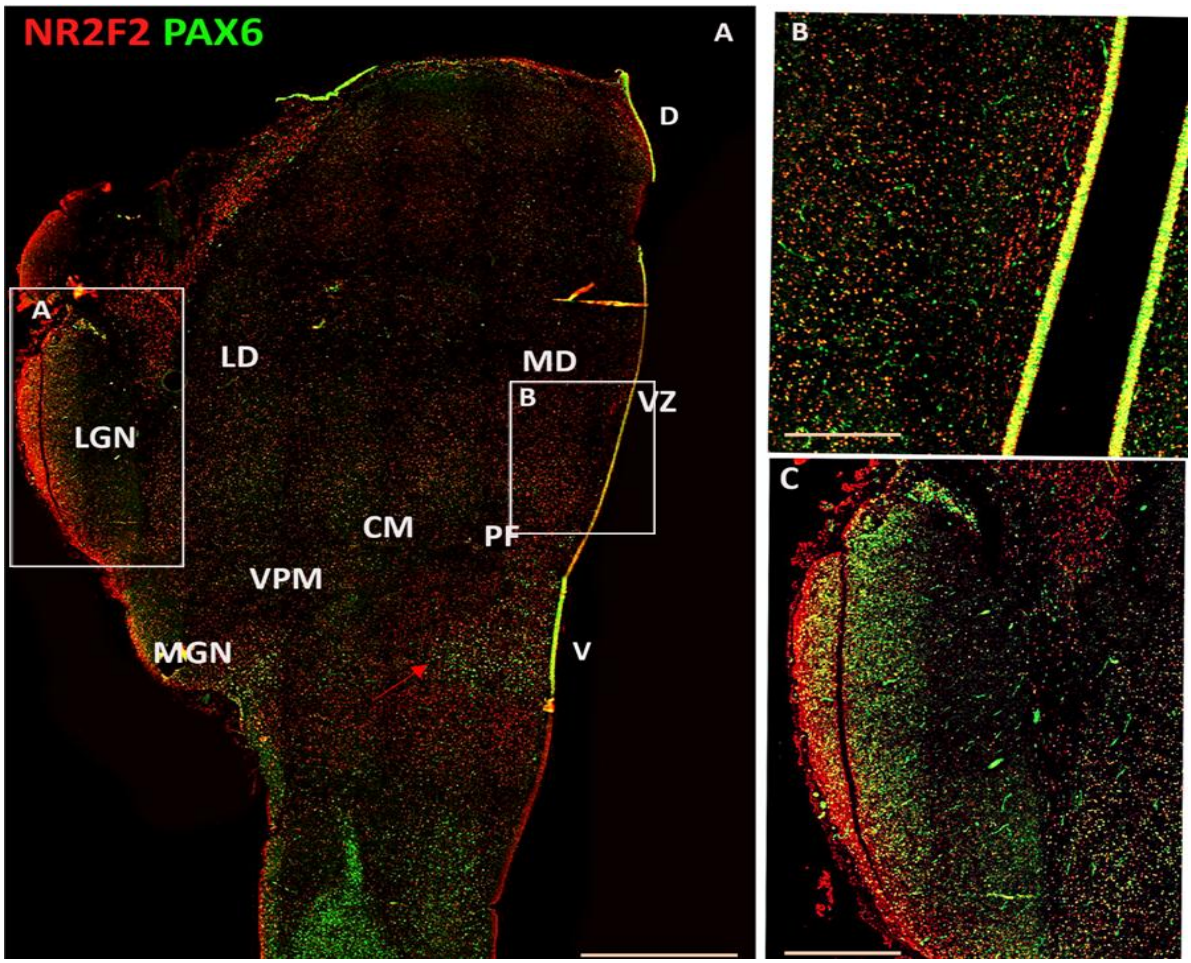

Figure 4.15. Double labelling of PAX6 (green) and NR2F2 (red) at 14 PCW. PAX6 shows strong expression in the ventricular zone of the thalamus and the prethalamus (red arrow) (A). NR2F2 was also strongly expressed in the lateral geniculate nucleus and in the reticular formation. Moreover, there was co-expression between these markers in the ventricular zone of the thalamus dorsal and ventral regions (B) and in the lateral geniculate nucleus (C). Abbreviations: lateral geniculate nucleus (LGN); medial geniculate nucleus (MGN); lateral dorsal (LD); medial dorsal (MD); centromedian (CM); parafascicular (PF); ventricular zone (VZ); Dorsal (D); ventral (V); ventroposteriomedial (VPM). Scale bar 1mm; 300 µm.

Figure 4.16 demonstrates the expression patterns of GBX2 and SP8 in the most posterior ventral thalamus section at 14 PCW, which exhibited a notable resemblance, with both being expressed in the postmitotic cells more medially than laterally. Their expression was prominently noted at the boundary of the thalamus and the pretectum (Figure 4.16 B). SP8 was expressed in the reticular formation and in the ventrolateral part of the thalamus (Figure 4.16 A). The co-localisation of GBX2 and SP8 was shown in the anteromedial region of the thalamus (Figure 4.16 B, C).

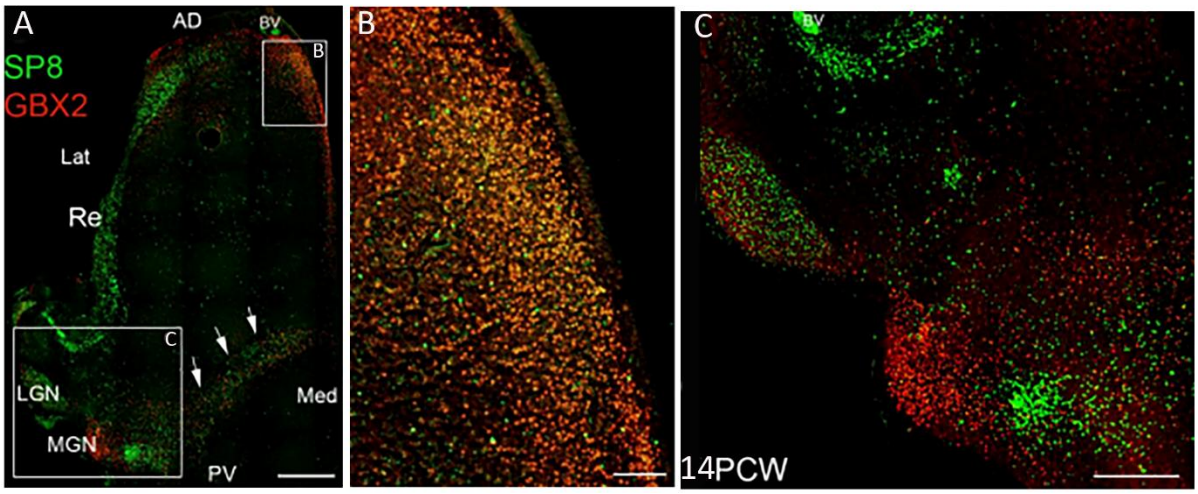

Figure 4.16. Double labelling of GBX2 (red) and SP8 (green) at 14 PCW in the most posterior ventral section. (A)SP8 showed strong expression in the reticular formation and the dorsal and ventral lateral geniculate nucleus as well as at the boundary between the thalamus and pretectum. (B) GBX2 was expressed in the medial part of the thalamus except for in the ventricular zone. There was co-localisation at the boundary between the thalamus and the pretectum (A, white arrow), as well as the anteromedial part of the thalamus (B). Abbreviations: lateral geniculate nucleus (LGN); medial geniculate nucleus (MGN); lateral (Lat); Medial (Medial), reticular formation (Re); Antrodorsal (AD) (VZ); Posterioventral (PV). Scale bar 1mm (A); 300 μm (B, C).

It was found that SP8 exhibited expression within the reticular formation and lateral geniculate nucleus. Moreover, GBX2 showed expression specifically in the medial dorsal nucleus, the ventrolateral part of the thalamus and medial geniculate nucleus. Interestingly, co-expression was observed in the medial nucleus among postmitotic cells. This indicated a unique pattern of gene expression within those regions, suggesting potential roles in the development and function of the neural structures. Further research may be warranted to elucidate the significance of co-expression in postmitotic cells within the medial geniculate nucleus (Figure 4.17).

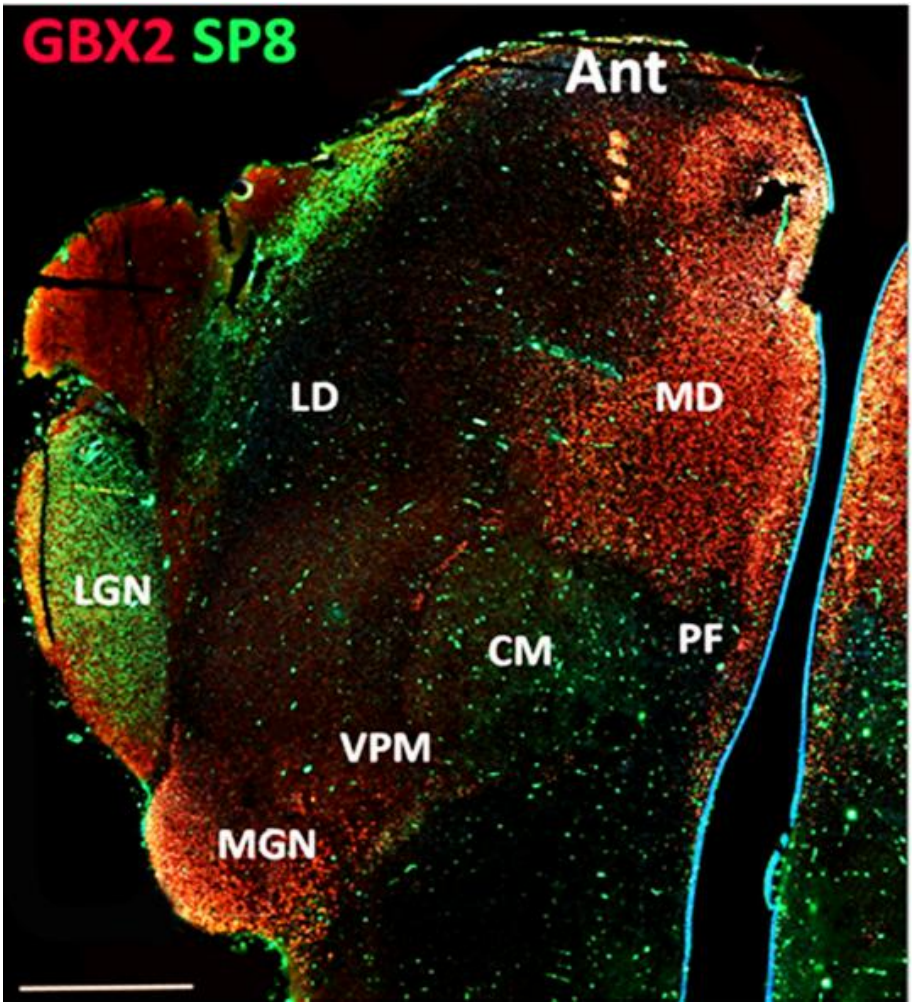

Figure 4.17. Double labelling GBX2 (red) and SP8 (green) at 14 PCW in the posterior ventral section. GBX2 showed strong expression in the medial nucleus and in ventrolateral part but not in lateral dorsal part of the thalamus, as well as expression in the medial geniculate nucleus (A). SP8 was also strongly expressed in the lateral geniculate nucleus and in the reticular formation. There was co-localisation between these markers in the medial part of the thalamus in the medial nucleus (B). Abbreviations: lateral geniculate nucleus (LGN); medial geniculate nucleus (MGN); lateral dorsal (LD); medial dorsal (MD); centromedian (CM); parafascicular (PF); ventroposteriomedial (VPM); anterior (Ant). Scale bar 1mm.

4.5 Discussion

In this study we observed a relatively rapid transition from the largely homogenous gene expression patterns in the thalamic mantle at 8 PCW to some evidence of differentiated patterns of expression by 10 PCW and recognizable thalamic nuclei by 14 PCW. A summary of transcription factor expression in both proliferative and post-mitotic compartments is provided in Figure 4.18. In mice, the equivalent time points would be E12.5, E14.5-15.5 and E18.5 (Suzuki-Hirano et al., 2011, Gezelius et al., 2017, Nakagawa, 2019) and equivalent to 9 PCW, 13PCW and 19 PCW in humans (Workman et al., 2013). Thus, additional evidence had been provided to show that human thalamic development follows a relatively accelerated time course compared to that of the mouse. It has further been demonstrated in mice that nucleus specific gene expression may be maintained by thalamocortical connectivity (Gezelius et al., 2017), and our observations suggest earlier thalamocortical connectivity in human coincides with earlier thalamic nucleus formation.

4.5.1 Protomap of the thalamic ventricular zone

There was an anterior ventral to posterior dorsal gradient of *SHH* concentration across the developing thalamus, and this morphogen was secreted from the anteriorly located zona limitans intrathalamic and ventrally located basal plate (Nakagawa, 2019, Kiecker and Lumsden, 2004). *SHH* is known to sometimes suppress PAX6 expression (Ericson et al., 1997), consequently it was expected that there would be higher PAX6 expression in the ventricular zone posteriorly and dorsally, and not in the zona limitans intrathalamic (Figure 4.4 I). However, PAX6 was expressed strongly in the prethalamus of p3 (Figure 4.2 L) which would be expected if we are to receive a relatively high concentration of *SHH*, indicating the co-expression and regulation of specific receptors and regulators of *SHH* signalling pathways in target cells is also important (Carballo et al., 2018). PAX6 expression was stronger and more persistent than that observed in the mouse, where weak expression dorsally was only observed up to E10.5 (Parish et al., 2016) at the age of onset of neurogenesis in the mouse thalamus (Angevine Jr, 1970). It is unclear why PAX6 expression extends throughout human thalamic neurogenesis, and ranges from as early as 6 PCW to at least 15 PCW (Rakic and Sidman, 1968, Workman et al., 2013, Alzu'bi et al., 2019).

We observed a different gradient of expression of NR2F2 in the thalamic ventricular zone (Figure 4.2 J, Figure 4.10 G). In this case, expression was highest posteriorly and ventrally.

Thus, we had identified four zones to the human thalamic progenitor zone; the anterior/ventral which is NR2F2+/PAX6-; the anterior dorsal which is NR2F2-/PAX6-; the posterior/ventral which is NR2F2+/PAX6- and the posterior/dorsal which is NR2F2+/PAX6+. A more extensive future study of the expression patterns in humans might be informative. We also observed very weak expression of OLIG2 immunoreactivity in or near the ventricular zone, although unfortunately we only looked at 8 PCW and 14 PCW.

Cell lineage tracing studies in the mouse have demonstrated that the neuroprogenitors located in specific regions of the thalamic ventricular zone give birth to neurons that are destined to populate discrete thalamic nuclei (Shi et al., 2017). Thus, anterior and dorsal thalamic ventricular zone promotes glutamatergic neurons that will populate anterior and medial higher order cognitive nuclei, whereas the middle and ventral thalamic ventricular zone populate higher order dorsolateral sensorimotor nuclei, and first order sensory nuclei located ventrally, posteriorly and laterally, respectively. It appears likely that a combinatorial protomap of transcription factor expression guides the specification of thalamic neurons.

4.5.2 The emergence of thalamic nuclei

Previous studies have shown that a variety of transcription factors can display universal expression in thalamic post-mitotic neurons, revealing restricted expression to specific nuclei as development proceeds. For instance, mouse *Gbx2* is expressed by all thalamic neurons after leaving the cell cycle (Chen et al., 2009), but then becomes restricted in expression to mostly medial and anterior nuclei, with certain lateral and ventral nuclei also posteriorly excluded from the paraventricular nucleus and from the lateral geniculate nucleus (this occurs in both mice and monkeys) (Jones and Rubenstein, 2004). We have demonstrated that this also the case in humans. In another study in mice, *Gbx2* is expressed in the centrolateral and the mediodorsal nucleus (Ebisu et al., 2017). GBX2 immunoreactivity is expressed in the thalamus medially and excluded from ventricular zone at 8 PCW (Figure 4.4 E). It became restricted to the medial and posterior regions of the thalamus as early as 10 PCW (Figure 4.6 B), and by 14 PCW was confined to medial locations and the medial geniculate nucleus (Figure 4.8 L, Figure 4.9 L, Figure 4.10 I). *Gbx2* is crucial for the establishment of the molecular identity of the thalamus in a mouse study. The ablation of Gbx2 results in loss of thalamic identity, which is correlated with a partial change to Habenula identity. Furthermore, *Gbx2* regulates a feedback mechanism from the postmitotic cells in the mantle zone, to modulate the growth of thalamic progenitor

cells. Additionally, *Gbx2* deletion altered gene expression, not only in the mantle zone, but also in the intermediate and the ventricular zone of the thalamus. Thus *Gbx2* deletion causes abnormal cell proliferation in the thalamus (Mallika et al., 2015).

We have also observed FOXP2 expression shift from being homogenous across the thalamus at 8 PCW (Figure 4.2 E), to becoming widespread but stronger medially and posteriorly at 10 PCW (Figure 4.6 C), to being strongly expressed in specific nuclei only (e.g. centromedian, medial geniculate nucleus) and absent from the anterior nuclei by 14 PCW (Figure 4.9 K). Increasing expression from anterior to posterior was previously reported in the mouse brain (Ebisu et al., 2017), but no medial to lateral gradient was reported. Using transgenic mice expressing mutant *Foxp2*, (Ebisu et al., 2017) demonstrated that FOXP2 directs the development of posterior nuclei, and interacts with GBX2 in the counter gradients of expression. The posterior nuclei were smaller, whereas the intermediate nuclei expanded along with the thalamic territories, expressing *Gbx2* and *Cadh6*. The anterior nuclei were unaffected. Our evidence suggests something similar occurs in humans, although it is interesting that this interaction to form a protomap would arise in postmitotic cells, as these transcription factors are not expressed in ventricular zone progenitors, even at 8-10 PCW (Figure 4.2 D E, Figure 4.3 E, D, Figure 4.4 D E, Figure 4.5 D E).

Conversely, *ZIC4* expression was widespread in the human thalamus at 8 PCW (Figure 4.2 C), as well as being expressed in the epithalamus and thalamus in the middle part of the thalamus at 8 PCW (Figure 4.4 C), maintaining expression laterally where FOXP2 expression was weaker in the middle part of the thalamus compared to *ZIC4* .In the posterior region *ZIC4* was expressed only in the epithalamus (Figure 4.5 C) while FOXP2 strong expression in the thalamus in this section. *ZIC4* then showing expression confined to the anterior and medial structures, and the lateral geniculate nucleus, by 14 PCW (Figure 4.12 C D E). In the mouse, it is known that *Zic4* is preferentially expressed in LGN, and *Foxp2* in medial geniculate nucleus during post-natal development, and plays a role in guiding the development of visual and auditory pathways respectively (Horng et al., 2009). Interestingly, it has been shown in the mouse that the expression of *Zic4* in cells with reduced *Pax6* expression prompts lateral geniculate nucleus neurons that maintain *Zic4* expression (Li et al., 2018). As we have shown that the human thalamus also has a ventral and posterior *ZIC4*+ PAX6- domain early in development, we can also surmise this might be the location for the production of lateral geniculate nucleus neurons, as demonstrated in mouse in cell lineage tracing studies (Shi et al.,

2017). However, humans seem to differ significantly from mice in not expressing *ZIC4* as strongly in the prethalamus (Li et al., 2018).

Detection of so much SP8 immunoreactivity in the thalamus was a surprising finding. We employed it as a marker of GABAergic neurons, originating either from the prethalamus or the caudal ganglionic eminence. We observed SP8 expression in the prethalamus at 8 PCW (Figure 4.4 F), and found that by 14 PCW, it was a strong marker for the reticular formation (Figure 4.11 H). In addition, it emerged to be a reliable marker for lateral and medial geniculate nucleus. It showed strong co-expression with GBX2 at the cellular level in the anterior medial thalamus, but in the posterior regions it was co-expressed in the same nuclei, but less than at the cellular level. We have provided evidence for a potential novel role for SP8 in thalamic development, which may be human specific, as it has not previously been reported in other studies in other species.

4.5.3 Invasion of the thalamus by GABAergic interneurons

GABA (γ-aminobutyric acid) is the principal inhibitory neurotransmitter in the mammalian central nervous system (CNS). Its fundamental inhibitory role has been shown to be to regulate, attenuate, and synchronize the excitability of the primary excitatory neurones, which constitute the basic conduits of neural communication within and between the brain's neuronal networks (Freund and Buzsáki, 1996, Whittington and Traub, 2003, Jonas et al., 2004).

Evidence shows that in the primate thalamus there is a far higher proportion of GABAergic interneurons within the nuclei, than thalamic reticular neurons providing inhibition to thalamic neurons from a location outside the thalamus (Arcelli et al., 1997). The dorsal thalamic nuclei also include local interneurons, another type of neuron. The ratio of interneurons fluctuates based on the nuclei and the species. They may constitute as much as 30% of cell bodies, as indicated by the glutamic acid decarboxylase (GAD) staining. This enzyme converts glutamate into GABA. The primate thalamus contains a greater proportion of interneurons than the rodent thalamus. In the mouse somatosensory thalamus, interneurons are absent (Arcelli et al., 1997), whereas in the dorsal lateral geniculate nucleus, interneurons comprise 20% of the neuronal population (Gabbott et al., 1988). In primates, local GABAergic neurones constitute around 35-40% of the neuronal population in the dorsal lateral geniculate nucleus (Arcelli et al., 1997).

Comparative histological analyses suggest that interneurons constitute roughly 15–20% of cortical neurones in rodents, but represent a greater percentage in primates (Džaja et al., 2014).

In both rodents and primates, the source of these interneurons is either the rostral midbrain, for those expressing SOX14 and OTX2 (80% in rodents, 90% in marmoset), or from the forebrain, using cell tracing studies (Jager et al., 2021), but is not from the dorsal thalamic ventricular zone in either rodents or primates.

In rodents, the forebrain origin of GABAergic interneurons is the prethalamic (p3) progenitor zone (Jager et al., 2021) although the rostral most thalamic ventricular zone may give rise to GABAergic projection neurons of the intergeniculate leaflet and ventral LGN (Vue et al., 2007). This is also the case in marmosets but in human, it has long been argued that late born thalamic neurons can derive from the medial CGE (Letinic and Rakic, 2001, Krienen et al., 2020, Kepecs and Fishell, 2014) and this has been recently confirmed by transcriptomic studies of cell lineage which found thalamic neurons expressing the telencephalic marker FOXG1(Bakken et al., 2020, Kim et al., 2023). However, *in situ* hybridisation studies have demonstrated a complete absence of expression of FOXG1, in the thalamus at 15 PCW (Ding et al., 2022) suggesting these neurons arrive later in development.

The current study confirmed *SOX14*, OTX2 and GAD67 expressing cells appear in the posterior two thirds of the thalamus by 14 PCW. Elsewhere, it has previously been observed that there is a posterior to anterior appearance of interneurons across the thalamus in non-human primates and carnivores (Jones, 2002), and that interneurons arrive late in the thalamus, mid-gestation in monkeys, and at birth in ferrets (Jones, 2002). Our observations therefore concur that the appearance of interneurons in the thalamus proceeds posterior to anterior, and are co-incident with the emergence of thalamic nuclei, but again stresses that the process of human thalamic development begins relatively earlier than predicted.

We found no evidence that interneurons progress significantly further anteriorly between 14 and 16 PCW, leaving open the question of whether anterior nuclei are populated by midbrain origin GABAergic neurons much later in the developmental process, or whether they are populated by cells of prethalamic or telencephalic origin. The anterior nuclei have the highest proportion of interneurons in humans and macaques (Hunt et al., 1991, Dixon and Harper, 2001, Popken et al., 2002) possibly due to supplementation from the caudal ganglionic eminences. Meanwhile, whereas in rodents midbrain origin interneurons preferentially cluster in the posterior and lateral nuclei and forebrain origin neurons in the anterior and medial (Jager

et al., 2021), recent analysis of non-human primates and human data suggests a more homogenous distribution of the two interneuron classes across the thalamic nuclei (Bakken et al., 2020, Jager et al., 2021), possibly indicating a pause in migration.

Although *SOX14+* presumed that GABAergic interneurons were distributed throughout the posterior two thirds of the thalamus at 14 PCW, a large proportion did not co-express GAD67, suggesting a lack of functionally maturity. However, certain nuclei did show precocious expression of GAD67, namely the centromedian nucleus and associated parafascicular complex. Consequently, it is thought these nuclei may mature more quickly than other nuclei. In the adult brain, the centromedian receives both multimodal sensory input and the ascending reticular activating system; while projecting primarily into sensorimotor areas, it connects indirectly via other thalamic nuclei with a large proportion of the forebrain, and is thus understood to play a role in arousal and attention (Kinomura et al., 1996, Van der Werf et al., 2002, Jang et al., 2014, Ilyas et al., 2019). In development, thalamo-cortical innervation occurs first in the subplate sensorimotor cortex (Krsnik et al., 2017, Alzu'bi et al., 2019) and projections from the centromedian/ parafascicular may initiate early coordinated spontaneous activity in the thalamus and the cortical subplate that drives development (Molnár et al., 2020b, Molnár et al., 2023).

To summarize, we studied the emergence of the thalamic nuclei in human foetal brain development. Our results suggest a combinatorial protomap of transcription factor expression that guides specification of thalamic neurons. Our observations further concur that the appearance of interneurons in the thalamus proceeds posterior to anterior, and is co-incident with the emergence of thalamic nuclei, but again then stresses the point that human thalamic development arises relatively earlier than might have been anticipated.

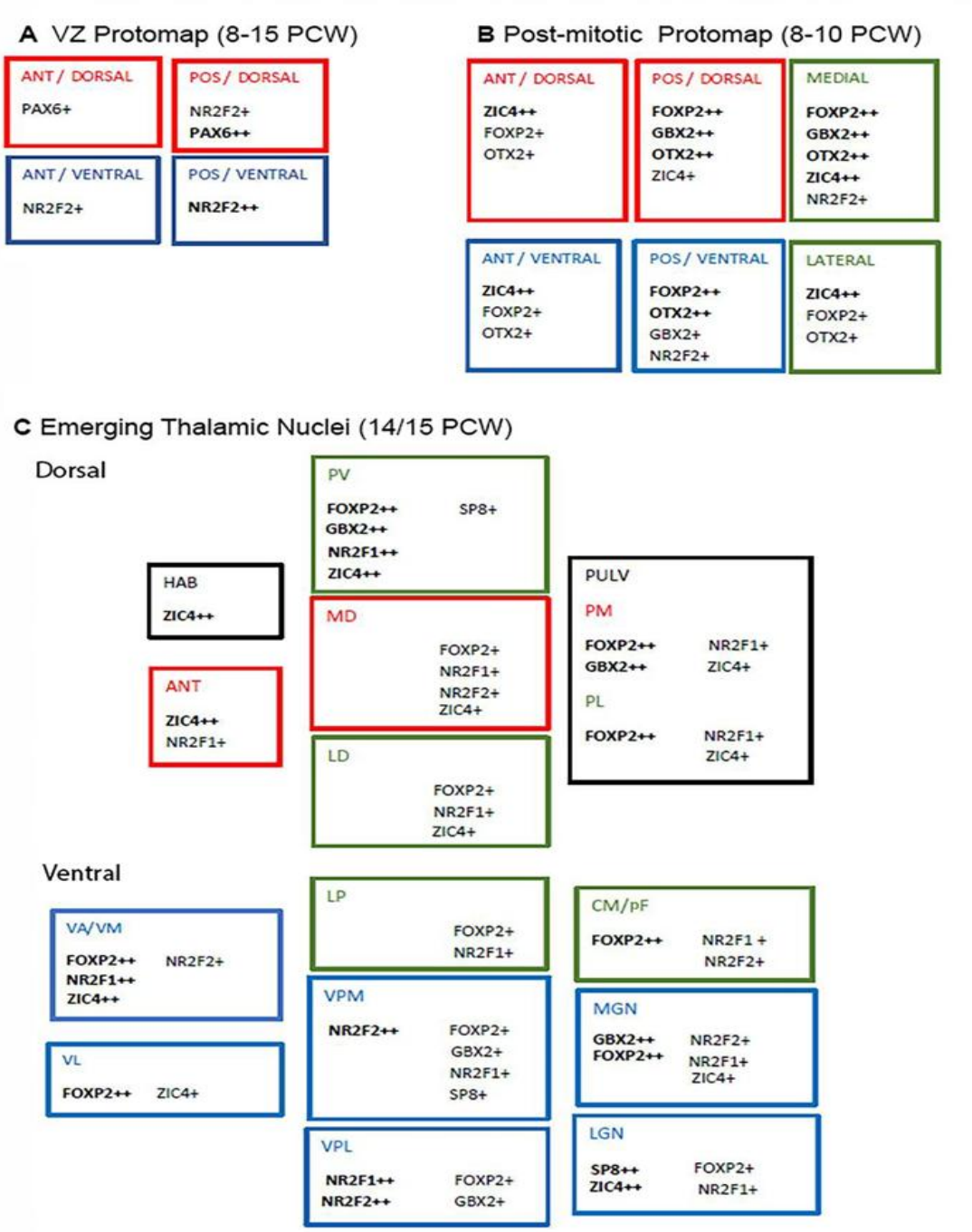

Figure 4.18. A summary of transcription factor expression in emerging thalamic nuclei within proliferative and post-mitotic compartments. (A) Protomap of the ventricular zone from 8–15 post-conception weeks (PCW): Regional domains include anterio/dorsal and posterior/dorsal regions (shown in red), anterio/ventral and posterio/ventral regions (blue). (B) Protomap of post-mitotic cells from 8–10 PCW: Similar regional organization is observed, with anterio/dorsal and posterio/dorsal regions marked in red, and anterio/ventral and posterio/ventral regions in blue, and medial and lateral regions (green). (C) Transcription factor expression in emerging thalamic nuclei at 14–15 PCW: Ventral nuclei (blue): ventroanterior/ventromedial (VA/VM), ventral lateral (VL), ventroposterior medial (VPM), ventroposterior lateral (VPL), medial geniculate nucleus (MGN), and lateral geniculate nucleus (LGN); lateral posterior (LP), centromedian/parafascicular (CM/Pf) in green. Dorsal nuclei: habenula (HAB) and pulvinar (PULV) in black; anterior and mediodorsal (MD) nuclei in red; laterodorsal (LD), and posterioventral (PV) in green.

5 Chapter 5 *NRXN1* expression in the human fetal forebrain

5.1 Introduction:

Neurexins are presynaptic cell adhesion molecules that play an essential role in the synaptic connectivity of neurons. In mammals they are coded for by three genes, *NRXN1, NRXN2,* and *NRXN3*. The majority of neurexins are situated on the presynaptic membrane and possess a solitary transmembrane domain (Chen et al., 2011). *NRXN* genes are the biggest in the human genome, and are more than one megabase pair (Mbp) long with 23 exons, and can be spliced differently producing thousands of isoforms (Missler and Südhof, 1998, Rowen et al., 2002). Neurexins are proteins that play important roles in the synapses including exocytosis of the vesicles, synapse formation, and cell-cell recognition via binding with other synaptic proteins, such as neuroligins (Reichelt et al., 2012).

5.1.1 NRXN isoforms and interactions with neuroligins

Neurexin 1, as encoded by the *NRXN1* gene, is typically expressed as a protein translated from the longer *NRXN1-α* and shorter *NRXN1-β* mRNA isoforms (Ullrich et al., 1995). The NRXN1-α protein isoform comprises three epidermal growth factor like domains (Höflich et al., 2015) and six laminin/NRXN/sex-hormone binding globulin (LNS) domains. Additionally, the NRXN1-α isoform includes PDZ-binding sequences in its cytoplasmic tail. However, NRXN1-β has just a single extracellular LNS domain, with the same transmembrane and cytoplasmic domain as NRXN1-α. Six differential splicing sites have been identified in *NRXN1-α* (splice sites SS1–6), whereas two, of which 4 and 5 are also present in *NRXNβ* (Schreiner et al., 2014). A shorter variant of NRXN1, known as NRXN1-γ, does not possess the EGF-like and LNS domains, and only contains the transmembrane region and cytoplasmic tail (Yan et al., 2015) (Figure 5.1).

Presynaptic neurexins form trans-synaptic adhesion complexes with postsynaptic neuroligins (NLGNs) and other transmembrane proteins (Jenkins et al., 2016) (Figure 5.2). The extracellular LNS domain plays a crucial role in the attachment of ligands, which is vital for pre and postsynaptic development (e.g., neuroligin) (Zhang et al., 2018). NLGN/NRXN adhesion complexes are fundamental for the development of glutamatergic and GABAergic synapses, and dictate the balance of excitatory and inhibitory synapse formation and function (Zhang et al., 2010). NRXN1-α is involved in the development of inhibitory GABAergic

synapses (Graf et al., 2004, Boucard et al., 2005, Kang et al., 2008), whereas NRXN1-β predominantly binds to glutamatergic postsynaptic partners (Graf et al., 2004, Boucard et al., 2005, Chih et al., 2006, Siddiqui et al., 2010). αNRXN*s* are involved in Ca2+-dependent neurotransmitter release that arises when their intracellular PDZ domain binds to proteins such as calcium/calmodulin-dependent serine protein kinase (CASK), which couple NRXN-mediated cell adhesion to synaptic vesicle exocytosis machinery (Hata et al., 1996). They also play a role in ensuring the proper assembly of synapses into a fully functional unit, although they are not required during the initial formation of synapses (Missler et al., 2003). This also suggests NRXNs may be required for synapse formation in the later developmental stages. While βNRXNs also attract other PDZ domain proteins to the presynaptic membrane, their chief interaction is with neuroligin (NLGN) proteins on the other side of the synaptic gap through their extracellular domain (Ullrich et al., 1995, Koehnke et al., 2010). Certain αNRXN splice variants similarly bind to neuroligin proteins (Boucard et al., 2005, Reissner et al., 2013). Different roles in synaptogenesis and synaptic transmission have been attributed to αNRXNs and βNRXNs, due to separate ligand interactions (Reissner et al., 2013, Petrenko et al., 1996). Interestingly, and in contrast with the absence of a role for αNRXN in synapse formation, it has been reported that expression of *NRXN1* is sufficient to stimulate the creation of synapses in cultured non-neuronal cells, indicating that NRXN1 may be a crucial mediator of synapse development (Jenkins et al., 2016).

The binding affinities between different pairs of NRXNs and NLGNs vary. This variation is regulated by alternate splicing of both binding partners (Comoletti et al., 2006). NRXNs and NLGNs are also produced in all the excitatory and inhibitory neurons located throughout the brain in vertebrates (Ichtchenko et al., 1995, Ichtchenko et al., 1996, Ullrich et al., 1995). The variants α*NRXNs* and β*NRXNs* are expressed together in the same group of neurons (Ullrich et al., 1995). However, each *NRXN* type 1, 2, or 3 (Ullrich et al., 1995) has different α splice variants, mRNA, and proteins (Schreiner et al., 2014), distributed in varying quantities among distinct neuronal types. Moreover, a link has been observed between certain members of the neuroligin family and genetic susceptibility for neurodevelopmental and/or neuropsychiatric conditions, such as schizophrenia and autism spectrum disorder (Sun et al., 2011).

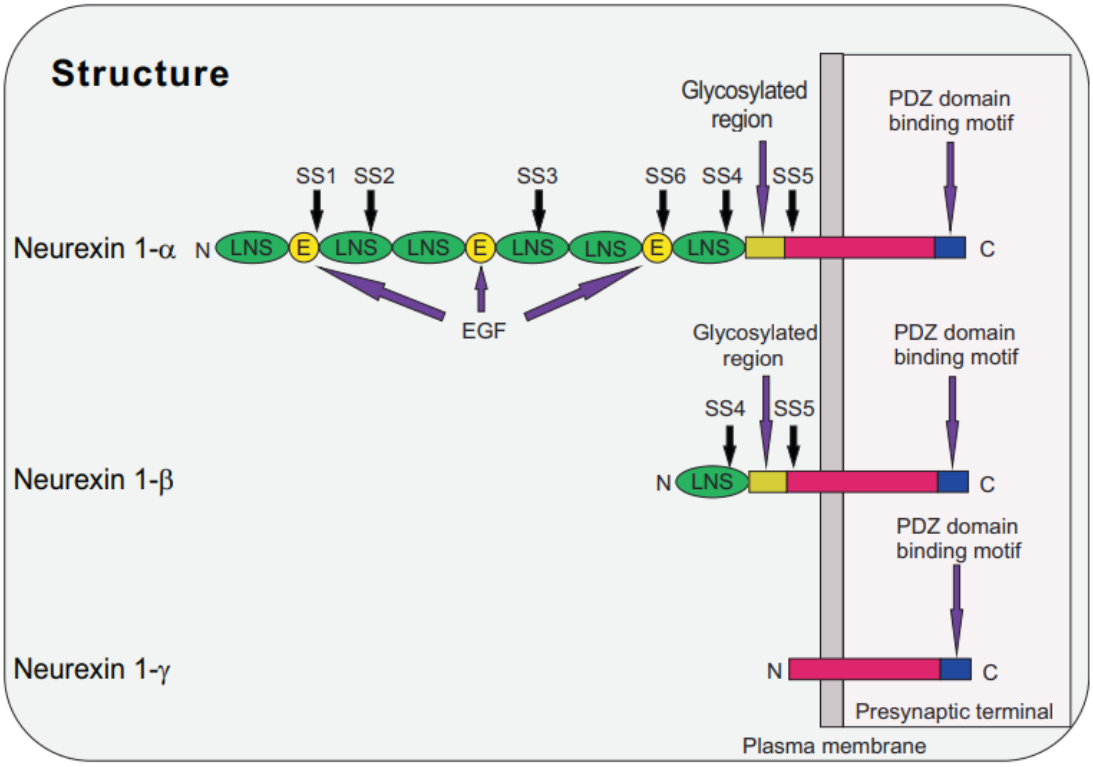

Figure 5.1 Thestructure and function of neurexin 1. NRXN1- α and NRXN1-β isoforms are generated from NRXN1 gene. The neurexin 1-α isoform comprises three EGF (epidermal growth factor)-like domains, six LNS (protein-binding domains for laminin, neurexins, and sex hormones) domains, a highly glycosylated region, and a PDZ domain binding motif. Neurexin 1-β has a single LNS domain and identical sequences to neurexin 1-α at their carboxy-terminus. Neurexin 1-γ lacks all EGF-like and LNS domains. Alternative splicing sites (SS1–SS6) are indicated (Hu et al., 2019).

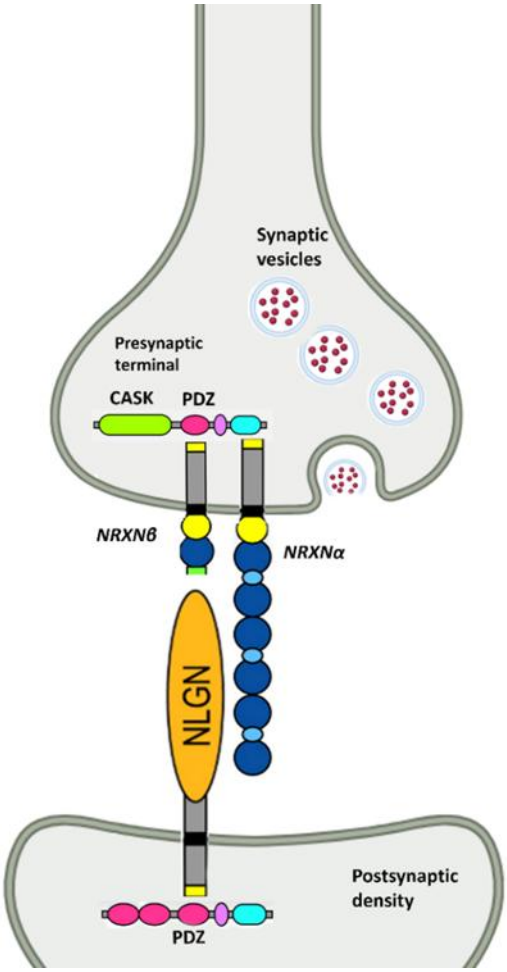

Figure 5.2 Interaction between Neurexin (NRXN) and Neuroligin (NLGN) at a synapse. Presynaptic neurexins form trans-synaptic adhesion complexes with postsynaptic neuroligins (NLGNs). The extracellular LNS domain plays a crucial role in the attachment of ligands. αNRXNs are involved in Ca2+-dependent neurotransmitter released from their intracellular PDZ domain, binding to proteins such as calcium/calmodulin-dependent serine protein kinase (CASK) and coupling with NRXN-mediated cell adhesion to synaptic vesicle exocytosis machinery. Meanwhile β NRXNs also attracted by other PDZ domain proteins to the presynaptic membrane, and their main interaction is with neuroligin (NLGN) proteins on the other side of the synaptic gap through their extracellular domain by M.Alhesain in (Biorender software) (Südhof, 2008).

5.1.2 Expression and role of NRXN1 in the developing nervous system

Additional research has further indicated that NRXN1 is highly concentrated in the pre-synaptic compartment and associated structures, for example growth cones (Dean et al., 2003). *NRXN1*-β is especially abundant in brain regions that are associated with cognition, such as the cortical plate, thalamus, and some areas of the hippocampus (Puschel and Betz, 1995). Furthermore, it is believed that the NRXN1β primarily exerts an excitation impact, while the NRXN1α is involved in both excitation and inhibition. Continued discussion is taking place on the function of NRXN1 in the maturation of neurones. The role played by *NRXN1* in neuronal maturation continues to be debated (Wu et al., 2023). One study has found that morphological properties, including total neurite length, number of primary processes, and neurite branch points remained unchanged in *NRXN1* mutant human neurons (Pak et al., 2015), while another showed reduced neurite numbers and total length in $NRXN1^{+/-}$ hiPSC-neurons (Flaherty et al., 2019). Meanwhile, triple *NRXN*α knockout mice died soon after birth, suggesting that having at least two intact *NRXN*α is critical to survival (Missler et al., 2003).

5.1.3 Role of NRXN1 in neurodevelopmental and neuropsychiatric disorders

The promoter region of the *NRXN1*α isoform has been affected in patients with schizophrenia (Kirov et al., 2008, Ikeda et al., 2010). Multiple subsequent research provided data supporting *NRXN1* as a potential gene, which, when mutated, increases vulnerability to autism spectrum disorder, schizophrenia, and intellectual disability (Kirov et al., 2008, Kim et al., 2008, Glessner et al., 2009, Rujescu et al., 2009, Ching et al., 2010, Gauthier et al., 2011, Viñas-Jornet et al., 2014, Marshall et al., 2017, C Yuen et al., 2017). Furthermore, deletion of *NRXN1* is also believed to cause attention deficit hyperactivity disorder (ADHD) (Schaaf et al., 2012). *NRXN1β* coding sequences are left intact in most *NRXN1* deletions seen in autism spectrum disorder and schizophrenia, which are localised to the promoter and initial exons of *NRXN1α* (Reichelt et al., 2012).

The prefrontal cortex (PFC) is crucial for social cognition and emotional regulation (Sakamoto and Yashima, 2022), playing important roles in cognitive flexibility and attention. In mice with heterozygous *NRXN1α* deletion, the efficiency of functional brain networks is diminished with effects such as reduced thalamic-prefrontal cortex (PFC) interconnectivity (B Hughes et al., 2020). In patch-clamp electrophysiological experiments, it emerged that patient-derived stem cells with deletion in *NRXN1*α exhibit hyperexcitability, with the potential to lead to epilepsy

at the network level (Avazzadeh et al., 2021). Research indicates that *NRXN1* is most highly expressed in the human prefrontal cortex during crucial periods of development (Jenkins et al., 2016). Further, abundant detection of the *NRXN1* mRNA has been reported in the early postconceptional week (12 PCW) in the human embryonic neocortex, and is found to peak at birth before slowly decreasing with age. *NRXN1* expression levels in the prefrontal cortex are found to be altered in individuals with schizophrenia and bipolar disorder comparative to control groups (Skiba et al., 2021).

Synaptic deficits in rodent models associated with deletion of *NRXN1* include decreased excitatory postsynaptic currents in the CA1 pyramidal neurons (Etherton et al., 2009), lowered inhibition in a subpopulation of hippocampal interneurons (Uchigashima et al., 2020), reduced thalamic and cortical excitatory drive to striatal neurons (Davatolhagh and Fuccillo, 2021), disrupted synaptic transmission from the prefrontal cortex to the amygdala, and impaired amygdala feedforward inhibition (Asede et al., 2020). Behaviourally, *NRXN1* knockout (KO) mice and rats displayed learning deficits, increased grooming behaviour, deficits in sensorimotor gating and altered social behaviour which can be likened to autistic traits in humans (Esclassan et al., 2015, Forsingdal et al., 2019). *NRXN1*α KO rats have also previously showed auditory processing deficits, hyperactivity, and major oscillatory abnormalities as also seen in schizophrenia and ASD (Janz et al., 2022). Moreover, *NRXN1α* KO mice exhibit high anxiety levels and altered social behaviour, however with intact working memory (Grayton et al., 2013).

Given its role in shaping synaptogenesis and possible neurogenesis, among other functional roles, and its genetic susceptibility in neurodevelopmental and neuropsychiatric disorders, it is crucial to map the expression of *NRXN1* in the developing human foetal forebrain, which the present study sought to investigate. This has not been fully established in the developing human cortex.

It had been previously shown in the laboratory setting, based on tissue RNAseq, qPCR and immunohistochemistry, that NRXN1 is highly expressed in the developing human cerebral cortex from 8-12 PCW, and that this protein is not confined to the synaptic zones of the subplate and marginal zone, but is also present in the cell bodies of both post-mitotic neurons and neuroprogenitor cells (Harkin et al., 2017). As this was a surprising finding, we decided to search for confirmatory evidence for cell types expressing NRXN1 by conducting RNAscope in situ hybridization combined with immunohistochemistry targeting different cell markers.

5.2 Aim of the study

By understanding when, where and in which cell types NRXN1 is expressed during development, it may be possible to understand how mutations in this gene lead to neurodevelopmental diseases. Our research aimed looked at the thalamus, and ventral telencephalon between the ages 8-12 PCW. Tissue and Single-cell RNAseq databases were also consulted.

5.3 Methods:

All the methods employed, including single and double labelling immunofluorescence as well as RNA scope in-situ hybridization with immunofluorescence, are described in detail in Chapter 2. The *Hs-NRXN1* RNAscope probe and NRXN1 primary antibody detect both isoforms of NRXN1.

5.4 Results

5.4.1 Transcriptomic analysis of *NRXN1* expression in human forebrain

Multiple databases were searched for data pertaining to the expression of *NRXN1*. Whole tissue RNA sequencing data stored at the website (www.ebi.ac.uk/arrayexpress/experiments/E-MTAB-4840) was utilised (Lindsay et al., 2016). This comprises 138 samples of cortical tissue taken at ages ranging from 7.5 to 17 PCW from different sites along the anterior-posterior axis of the brain, including the temporal lobe (Figure 5.3 A). A significant increase in *NRXN1* expression was revealed correlating with age (Figure 5.3 B). The expression of *NRXN1* was shown to be high from the first phase of cortical plate formation (7.5 PCW) to the later developmental stage, and expression level rose considerably with age. A similarly significant relationship between *NRXN1* expression with age up to 12 PCW has previously been reported by (Harkin et al., 2017). We found the samples at 7.5, 9, 10, 13 PCW showed expression in the top 25% of protein coding genes (more than 40 normalized RPKM) and the remaining samples that had expression in the top 5% had normalized RPKM values greater than 160, at 11, 12, 14, 15, 16 and 17 PCW (Figure 5.3 B). This suggests that *NRXN1* is instrumental in the development of the cortical region. Its expression increases with age and may primarily be expressed in postmitotic cells. Furthermore, there is a correlation between the age of the

cortical region and the proportion of postmitotic cells present (Figure 5.3 B) (Miller et al., 2014).

The cerebral development expression viewer (CoDEx) database, which is a scRNAseq database, was interrogated to investigate the cell type specificity of *NRXN1* expression further. According to (Polioudakis et al., 2019), this provides information regarding the expression of human cortical tissue samples taken at 17/18 PCW (solo.bmap.ucla.edu/shiny/webapp). *NRXN1* was found to be ubiquitously expressed in a high proportion of cells, including the glutamatergic and GABAergic neurons, as well as subtypes of progenitor cells. Expression was consistently highest in the more mature glutamatergic neurons (presumably from the subplate and lower cortical plate) and lower in dividing progenitor cells when compared to quiescent progenitors. *NRXN1* showed the lowest expression in cells of non-neuroectodermal origin, such as microglia, pericytes and endothelial cells. Expression levels were highly variable in many of the cell types (Figure 5.4 A). Likewise, single-cell RNAseq data for the thalamus at 16 PCW revealed distinct expression patterns for *NRXN1* among the various cell types, with differential expression observed between progenitor cells, GABAergic neurons, and glutamatergic neurons. *NRXN1* was also widely expressed in the thalamus, co-localizing with both glutamatergic (*SLC17A6*/vGLUT2 expressing) and GABAergic (*GAD1*/GAD67 expressing) neurons, as well as potential progenitor cells and astrocytes (GADD45B expressing) (Chapter 3; Figure 5.4 B). These findings underscore the multifaceted expression patterns of *NRXN1* in neuronal subtypes in both the cerebral cortex and the thalamus, shedding light on its potential functional significance in the development of the early human brain.

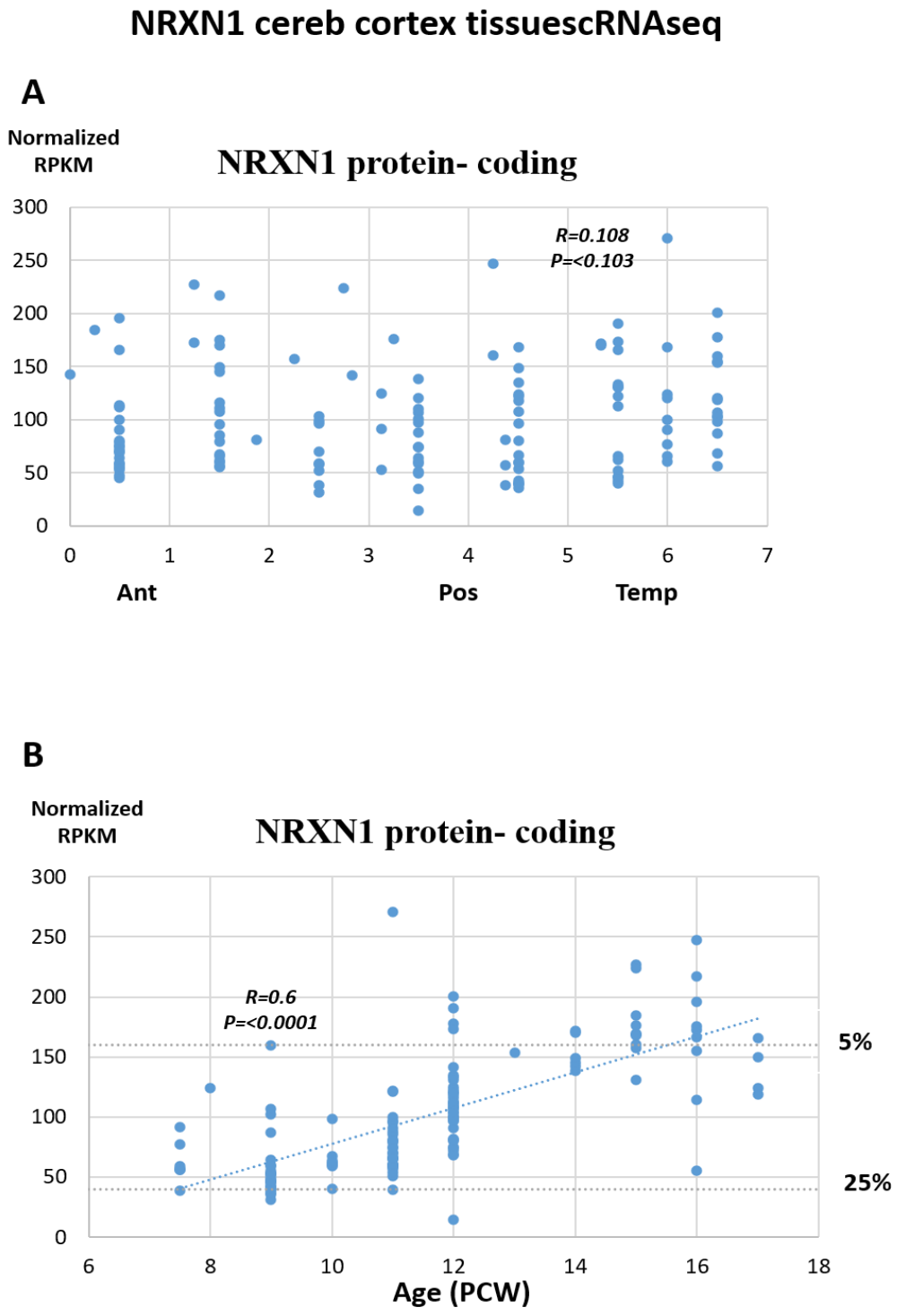

Figure 5.3. *NRXN1* gene expression in the cortex across development. (A) Normalized RPKM for 138 cortical samples of varying ages, plotted against their location on the anterior to temporal axis, where 0 corresponds to the anterior pole of the cortex, 5 to the posterior pole and 7 to the temporal pole (Miller et al., 2014). (B) Normalized RPKM values for 138 cortical samples taken from various cortical locations plotted against age (PCW), show a linear relationship in terms of increasing expression of NRXN1 with age (Lindsay et al., 2016). The expression of *NRXN1* some ages expressed in the top 5% (more than 160 RPKM) and some of them in the top of 25% (more than 40 RPKM).

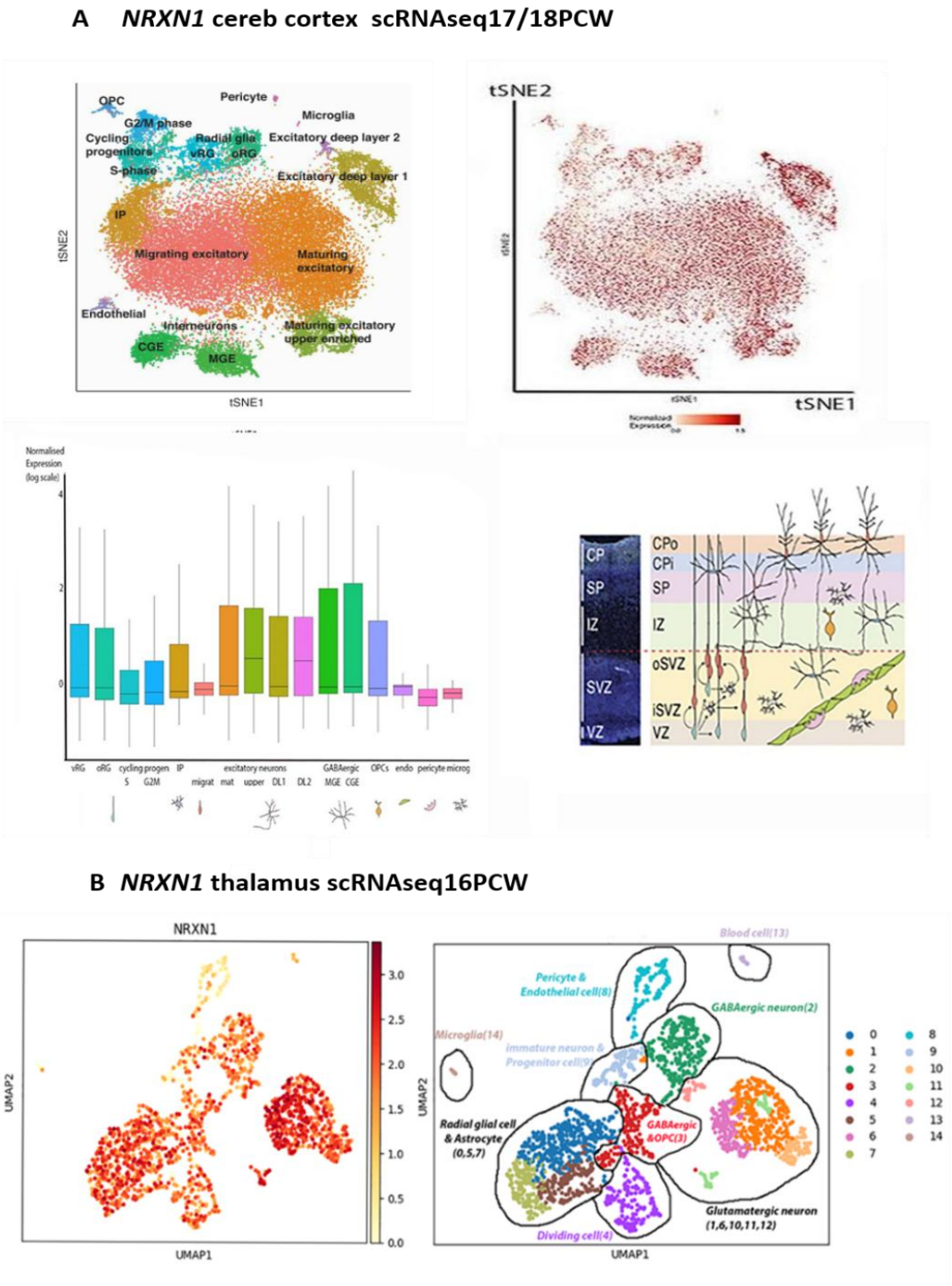

Figure 5.4. (A) Single-cell NRXN1 RNAseq data for the cerebral cortex at 17/18 PCW taken from solo.bmap.ucla.edu/shiny/webapp/. t-distributed stochastic neighbour embedding (tSNE) map and accompanying bar charts revealed NRXN1 is ubiquitously expressed in neuroectoderm-derived cell types, but especially so in more mature excitatory (glutamatergic) neurons, mature GABAergic neurons (both CGE and MGE derived) and non-dividing radial glia. Expression was lower in the dividing progenitor cells. **(B)** Single-cell RNAseq data for the thalamus at 16 PCW was taken from NEMO Analytics UMAP plots generated for NRXN1. For data concerning the classification of cell clusters see Chapter 3.

5.4.2 RNA in situ hybridization and immunohistochemical studies of *NRXN1* expression at 8PCW

The highest level of *NRXN1* expression was observed in the cortical plate followed by the subplate (SP) at 8 PCW (Figure 5.5 B). This predominantly contains immature excitatory neurons, and stronger expression was seen in the anterior region compared to the posterior region of the cortex, although this may reflect the greater cellular density in the anterior cortex at this stage (Figure 5.5 A). There was also intermediate expression of the gene in the cells of the subventricular zone (SVZ), which contain a combination of progenitor cells and newborn neurons, and low expression in the progenitor cells of the ventricular zone (VZ). In a further region of the forebrain (which principally produces glutamatergic neurons), there was high expression of *NRXN1* in the post-mitotic mantle of the thalamus at 8 PCW, and in the subventricular zone. However, the ventricular layer, which largely contains neuroprogenitors, exhibited low levels of expression (Figure 5.5 C). Interestingly, in the ganglionic eminences, which principally produce GABAergic neurons, strong expression of *NRXN1* was observed in parts of the ventricular zone (GE); being highly expressed in the ventral lateral ganglionic eminence (vLGE) and LGE-like caudal ganglionic eminence (lCGE), but not in the dorsal LGE (dLGE) or medial ganglionic eminence-like CGE (mCGE). There were also lower levels of expression in the subventricular and mantle regions of the ganglionic eminences (Figure 5.5 D).

There was strong expression in the ventral pallium in both the cortical plate and the proliferative layers (Figure 5.5 and 5.6). To confirm *NRXN1* was highly expressed in the ventral pallium, we co-stained a section at 8 PCW for NR2F1 by immunofluorescence, and for *NRXN1* by RNA scope in situ hybridization (Figure 5.6). NR2F1 was strongly expressed throughout the layers of the ventral pallium (VP), as previously described (Alzu'bi et al., 2017), as well as in the same location as *NRXN1* staining, confirming its expression in the VP. However, in all the other cortical regions, NR2F1 and *NRXN1* was differentially localised to VZ and CP, respectively. There was also no co-expression in the posterior region of the cortex (Figure 5.6).

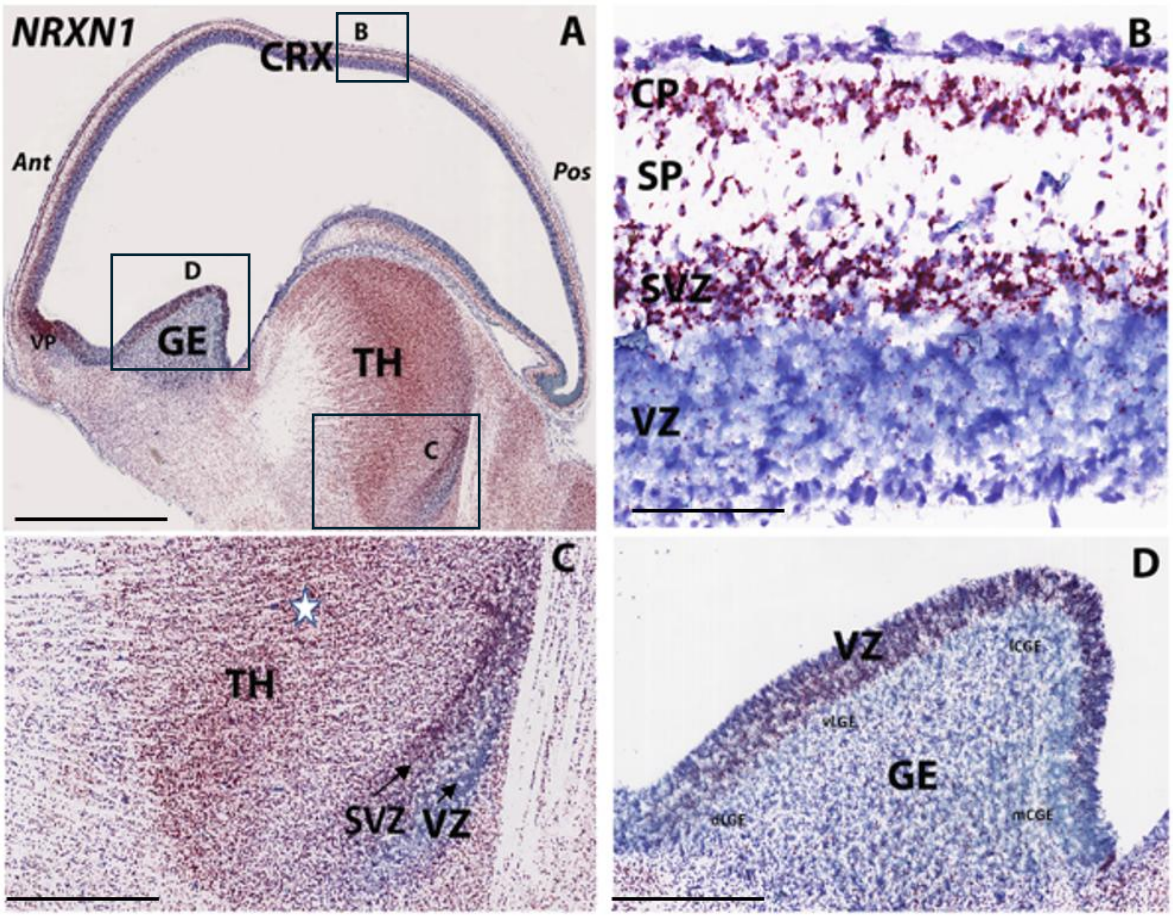

Figure 5.5. In situ hybridization for *NRXN1* mRNA expression in the medial sagittal section at 8PCW. (A) The sagittal section at 8 PCW shows *NRXN1* mRNA expression throughout the forebrain, but this is strongest in the ventral pallium and the proliferative zones of the ganglionic eminence (counterstained with toluidine blue TB). (B) Shows the dorsal neocortex at a higher magnification. *NRXN1* expression was also highest on the cortical plate, and there was moderate expression in the subventricular zones and weak expression in the ventricular zone. The was also high expression in the mantle zone (white star) and in the subventricular zone but not in the ventricular zone of the thalamus (black arrow) (C). *NRXN1* was highly expressed in the proliferative zones of the ventral lateral ganglionic eminence and the lateral caudate ganglionic eminence and there was weak expression in the dorsal lateral ganglionic eminence and medial caudate ganglionic eminence (dLGE, mLGE) (D). Abbreviation: ventral pallium (VP); subventricular zone (SVZ); ventricular zone (VZ); ventral lateral ganglionic eminence (vLGE); lateral caudate ganglionic eminence (lCGE); dorsal lateral ganglionic eminence (dLGE); medial caudate ganglionic eminence (mLGE); Thalamus (TH); cortex (CRX). Cortical plate (CP); subplate (SP); Anterior (Ant); Posterior (Pos). Scale bars; A, 1 mm; B–D, 200 µm.

Figure 5.6 depicts that in the ganglionic eminences, *NRXN1* expression was largely confined to parts of the ventricular zone, whereas NR2F1 was found in both progenitors and postmitotic cells. NR2F1 was also expressed throughout the ventricular zone of the ganglionic eminences, whereas co-expression with *NRXN1* was only evident in the vLGE and lCGE. In addition, in the thalamus, the VZ exclusively expressed NR2F1, and the SVZ showed a high degree of co-localisation of NR2F1 with NRXN1, although in the postmitotic region *NRXN1* showed greater expression (Figure 5.6).

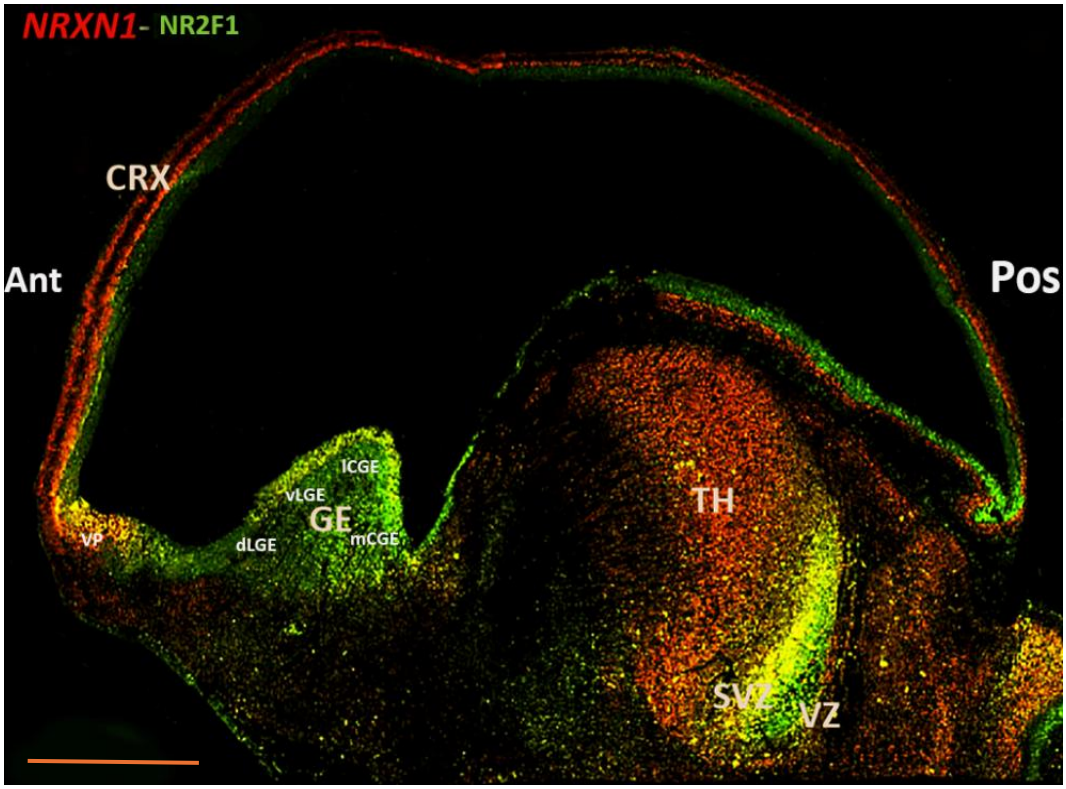

Figure 5.6. In situ hybridization for *NRXN1* mRNA expression and NR2F1 immunostaining in the medial sagittal section at 8PCW. NR2F1 was highly expressed in the progenitor cells of the ventricular zone of the cortex. Co-expression of NRXN1 and NR2F1 occurred in the intermediate progenitor cells in the subventricular zone in the anterior cortex, but there was no co-expression in the posterior region. However, NR2F1 was co-expressed with NRXN1 throughout the ventral pallium. There was also co-expression in the post-mitotic neurons and intermediate progenitor cells in the subventricular zone of the thalamus. NR2F1 exhibited strong expression in the cells of the ventricular zone of the thalamus. NR2F1 expression extended throughout the ganglionic eminence, but co-expression was restricted to the ventricular zone of the ventral lateral ganglionic eminence (vLGE) and LGE-like caudal ganglionic eminence (lCGE), while being absent from the dorsal LGE (dLGE) and MGE-like CGE (mCGE). Abbreviation: subventricular zone (SVZ); ventricular zone (VZ); thalamus (TH); ventral lateral ganglionic eminence (vLGE); lateral caudate ganglionic eminence (lCGE); dorsal lateral ganglionic eminence (dLGE); medial caudate ganglionic eminence (mLGE); ventral pallium (VP). Scale bars; 3mm.

5.4.3 RNA in situ hybridization and immunohistochemical studies of *NRXN1* expression at 10PCW

At 10 PCW the posterior region, the pattern of *NRXN1* expression observed at 8 PCW was maintained. It showed stronger expression in the cortical plate of the cortex and lower expression in the dorsal and lateral cortical progenitor zones, when compared to the compartment of the medial pallium corresponding to the cortical hem (Figure 5.7). Similar to the ventral pallium, the cortical hem forms a boundary between the pallium and subcortical structures, and consequently, it is intriguing to note high *NRXN1* expression in both these locations.

In the thalamus, *NRXN1* expression proved to be strongest in the postmitotic regions containing glutamatergic neurons, although it was also high in the progenitor cells of the epithalamus. In the ganglionic eminences, expression was high in the ventricular zone, but not in the sub-ventricular and post-mitotic regions. *NRXN1* mRNA expression was also high in the ventricular zone but showed weak expression in the post-mitotic cells in the hypothalamus (Figure 5.7).

Analysis of immunoreactivity for NRXN1 and KI67 (a marker for actively dividing cells) in a coronal section of the 10 post-conception week (PCW) posterior region human brain revealed intriguing patterns, indicative of their roles in early neurodevelopment. KI67 exhibited only isolated co-expression with NRXN1 in the SVZ and VZ in the cortex (Figure 5.8 A), indicating that NRXN1 expression was sparse in the dividing cells of the cortex and thalamus, while there was relatively strong co-expression of NRXN1 with KI67 in the ganglionic eminences**.** NRXN1 also showed strong expression in the postmitotic neurons as well as in the VZ of the cortex and ganglionic eminences (Figure 5.8 B, C).

NRXN1 and PAX6 immunostaining at the same coronal level showed strong co-expression in the cells on the apical (ventricular) surface where cell division was taking place (Taverna and Huttner, 2010) (Figure 5.9 A, B). Additionally, co-expression was observed in the proliferative ganglionic eminences, as was strong expression in the medial ganglionic eminence (MGE), when compared with that in the lateral ganglionic eminence (Figure 5.9 C). In addition, there was co-expression with NRXN1 in the ventricular zone cells of the thalamus, and in the VZ of epithalamus (Epith), emphasizing the potential roles played by cell division and the maintenance of progenitor status (Figure 5.9 D). These findings provide valuable insights into the coordinated regulation of NRXN1 and PAX6 during neural progenitor proliferation and

differentiation, also highlighting their significance in terms of shaping the developing human brain.

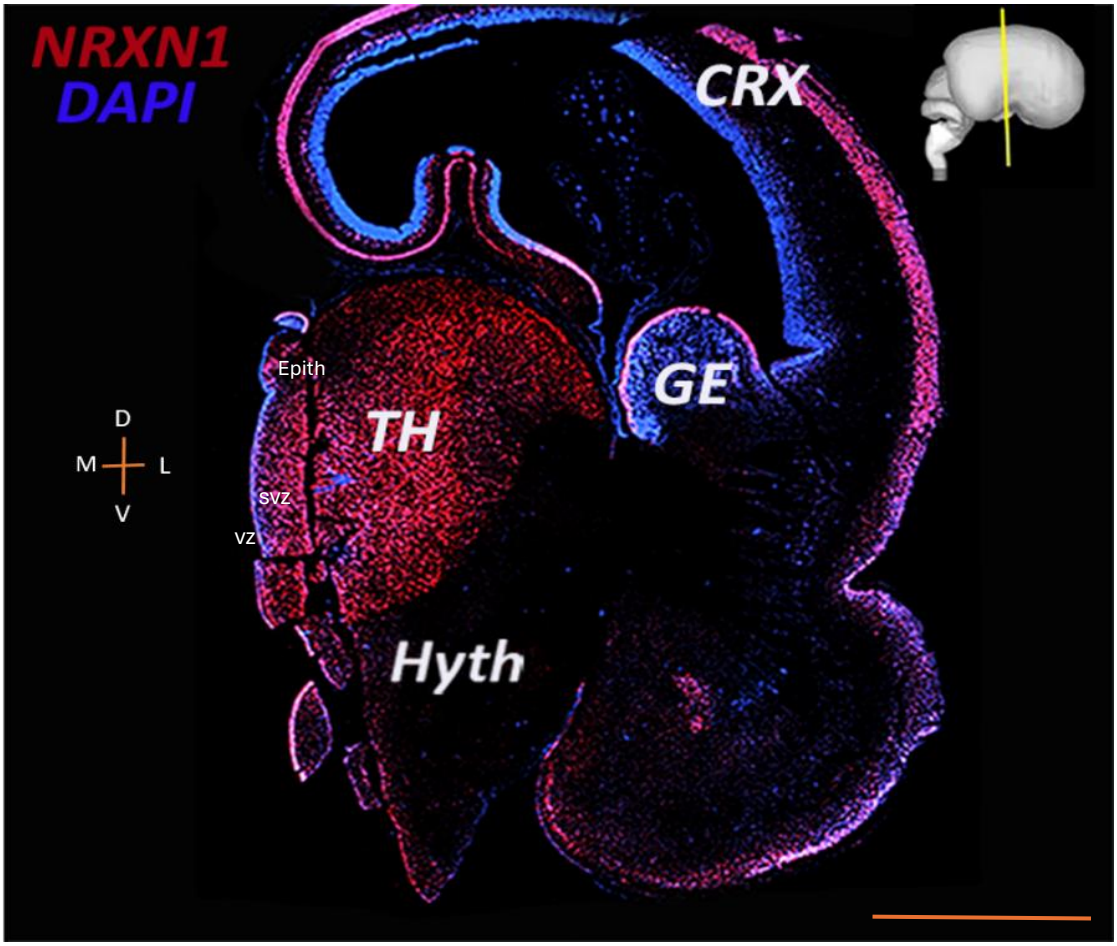

Figure 5.7. In situ hybridization for *NRXN1* mRNA expression in a coronal section at 10 PCW posterior region. There was high expression of *NRXN1* in the post-mitotic glutamatergic neurons in the cortical plate and the VZ in the medial region of cortical hemisphere, and no expression in VZ containing progenitor cells. High expression was also noted in the ganglionic eminences in the VZ. High expression was present in the postmitotic cells in the mantle zone, but not in the VZ of the thalamus, although there was high expression in the dorsal VZ of Prosomere 2 containing the epithalamus. It was also highly expressed in the VZ of the hypothalamus but there was weak expression in the post-mitotic cells of the Hypothalamus. Abbreviation: cortex (CRX); thalamus (TH); epithalamus (Epith); Hypothalamus (hyth); ventricular zone (VZ); subventricular zone (SVZ); dorsal (D); ventral (V); medial(M); lateral (L). Scale bars; 3 mm.

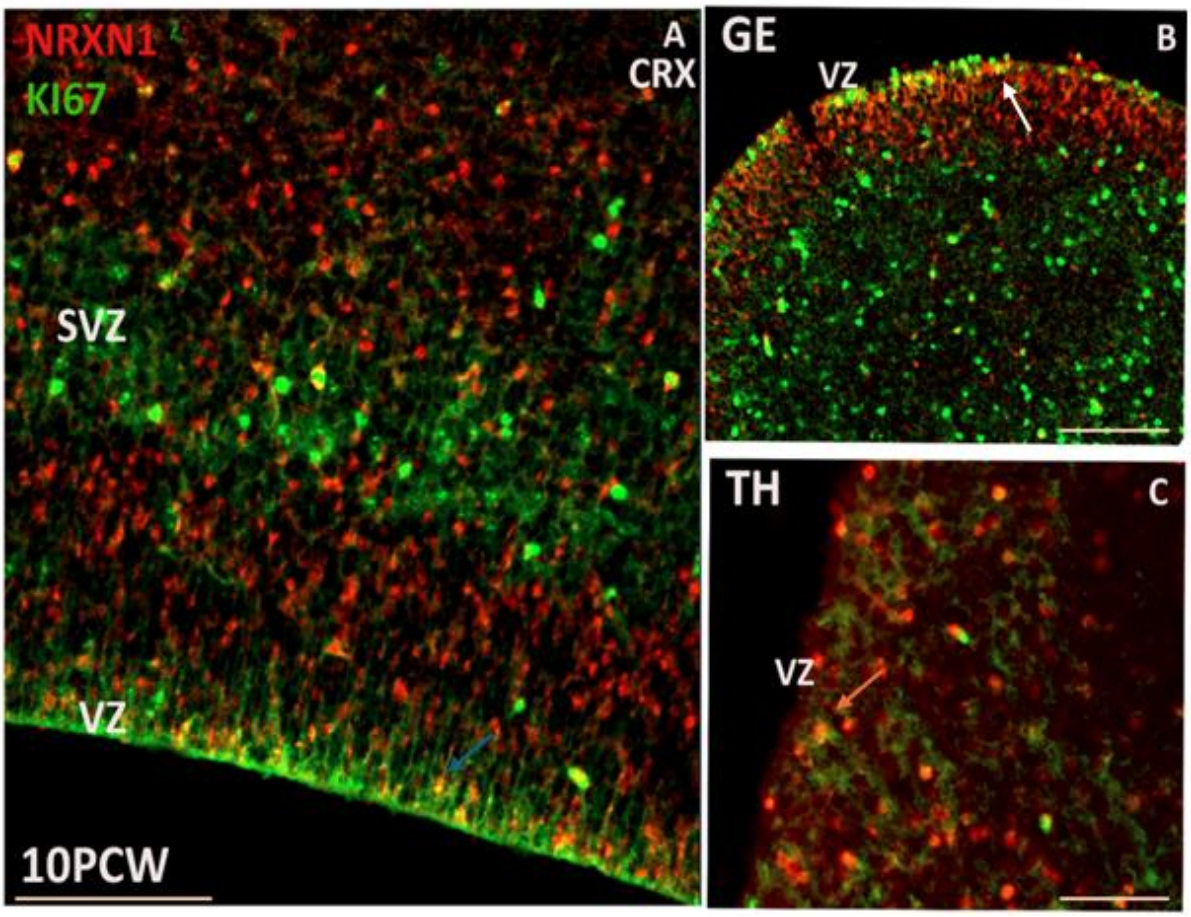

Figure 5.8. Double immunofluorescence staining for NRXN1 and the dividing cell marker KI67 in a coronal section of 10PCW human foetal brain. KI67 showed co-expression with NRXN1 in the subventricular zone as well as in ventricular zone of the cortex (A, blue arrow). KI67 showed co-expression in the proliferative zones of the ganglionic eminences (B, white arrow), and the ventricular zone of the thalamus, but only to a very limited extent (C, orange arrow). Abbreviations: Subventricular zone (SVZ) ; cortex (CRX); ventricular zone (VZ) ; thalamus (TH) ; ganglionic eminence (GE). Scale bars : A, 1 mm ; B–C, 300 µm.

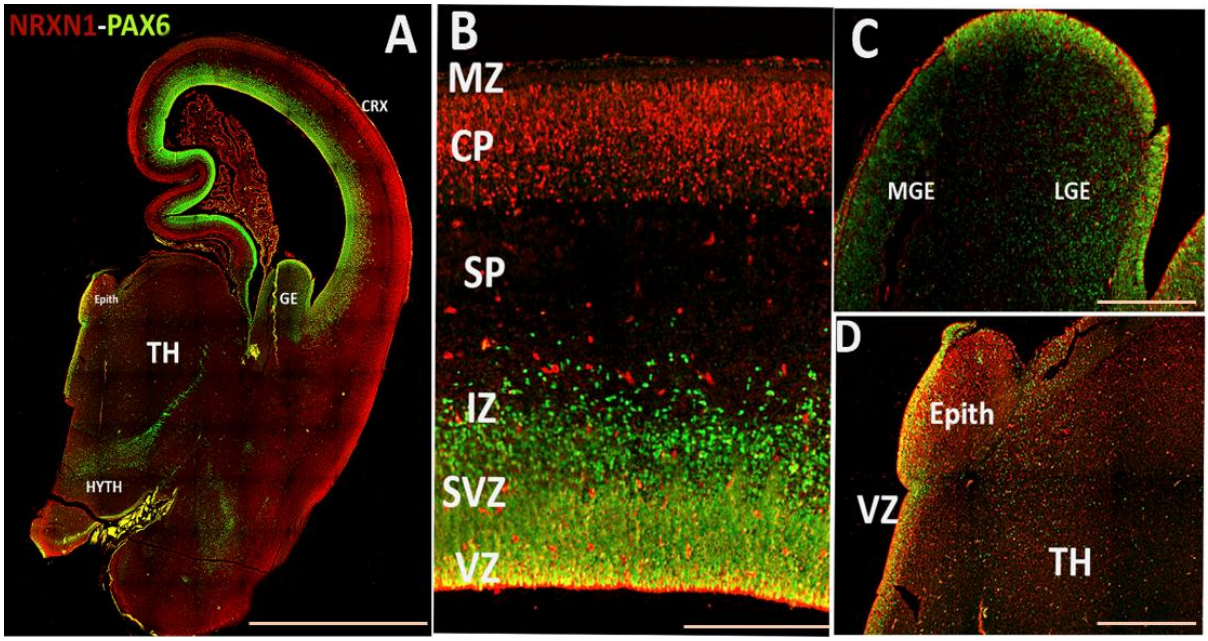

Figure 5.9. Immunofluorescence double labelling for NRXN1 and PAX6 in a coronal section of 10 PCW human brain. NRXN1 was highly expressed in the postmitotic glutamatergic cells in the cortical plate, but showed low expression in the ventricular zone containing progenitor cells. High co-expression with PAX6 in the proliferative zones of the lateral ganglionic eminences compared with the medial ganglionic eminences, and there was co-expression in the ventricular zone of the thalamus and the epithalamus. Abbreviations: hypothalamus (HYTH); marginal zone (MZ); subplate (SP); intermediate zone (IZ); subventricular zone (SVZ); lateral ganglionic eminences (LGE); medial ganglionic eminences (MGE); thalamus (TH); epithalamus (Epith). Scale bars : A, 1 mm ; B–D, 300 µm.

5.4.4 NRXN1 immunostaining at 12 PCW

NRXN1 immunoreactivity was evident at 12 PCW in the cortex, in the glutamatergic neurons, and also in the progenitor cells in the ventricular zone of the cortex (Figure 5.10 A, B). NRXN1 was also expressed in the postmitotic cells in the thalamus, with strong expression in the dorsal thalamus, which is the putative dorsal lateral geniculate nucleus (Figure 5.10 E). Additionally, strong expression was seen in the proliferative zones of the ganglionic eminences (Figure 5.10 C). High expression was also observed in the cells in the ventricular zone of the thalamus and the epithalamus (Figure 5.10 D). Therefore, from these findings we can infer the NRXN1 protein is expressed in the postmitotic neurons and progenitor cells of the cortex and ganglionic eminences, as well as in the thalamus and epithalamus.

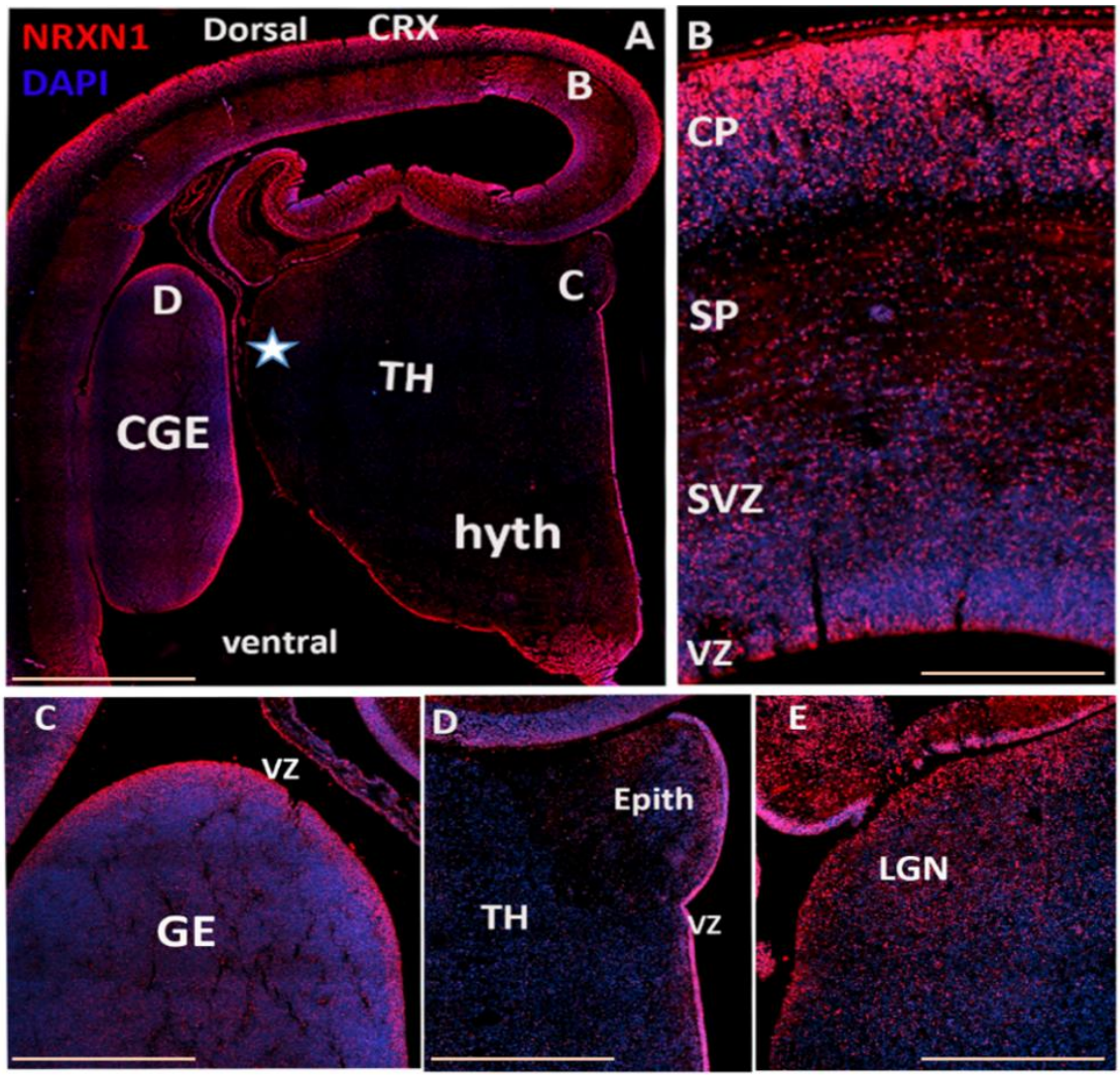

Figure 5.10. NRXN1 immunostaining in a coronal section of the 12 PCW human brain. NRXN1 was highly expressed in the glutamatergic neurons in the cortical plate (A, B). It was also expressed in the progenitor cells in the ventricular zone of the cortex. Additionally, high expression within the progenitor cells in the ganglionic eminences (C), as well as in the ventricular zone cells of the thalamus and the epithalamus (D). There was also strong expression in the dorsal thalamus, which is the putative lateral geniculate nucleus (E, white star). Abbreviations: epithalamus (Epith); ganglionic eminences (GE); cortex (CRX); hypothalamus (hyth); caudate ganglionic eminence (CGE); cortical plate (CP); subplate (SP); subventricular zone (SVZ); ventricular zone (vz); lateral geniculate nucleus (LGN). Scale bars: A, 1 mm; B-D, 300 μm

5.4.5 *NRXN1* expression at 14 PCW

When examining sections cut in a ventral posterior to anterior dorsal plane at 14 PCW, expression of *NRXN1* mRNA was strong throughout the thalamus, but also appeared very strong in certain thalamic nuclei, including the lateral geniculate, medial geniculate and the pulvinar nuclei. The insitu hybridization and immunofluorescence assays revealed distinct expression patterns of *NRXN1* mRNA and protein in the human thalamus at 14 PCW (Figure 5.11 and 5.14). *NRXN1* exhibited strong expression in the cells of the ventricular zone, some of which were still dividing at this stage, also expressing the radial glia marker GFAP (chapter 3). Additionally, intense expression was observed in the dorsolateral geniculate nucleus, when compared with the ventrolateral geniculate nucleus, as well as in the medial geniculate nucleus (Figure 5.11, sections 70-90). Strong expression of *NRXN1* mRNA was observed in the postmitotic cells in the pulvinar, and also in isolated groups of cells in the midbrain (Figure 5.11, sections 14-30). In addition, high expression was observed in the post-mitotic neurons in the medial and lateral geniculate nuclei (MGN, LGN), the ventroposterolateral nucleus (VPL) and the lateral pulvinar, and medial pulvinar (PL, PM) (Figure 5.11 D, section 30). There was strong expression in the post-mitotic cells in some thalamic nuclei, which included the putative centromedian nucleus, and the anterior nuclei (Figure 5.11 sections 50-70) which are more posterior and ventral (C-H). There was also strong expression observed in the lateral geniculate nucleus (section 50) and the radial glial cells in the ventricular zone of the thalamus. Furthermore, the double labelling of the thalamic tissues revealed a higher co-expression of *NRXN1* mRNA with GAD67 (Figure 5.12) in the ventroposterior region of the thalamus.

Further, co-expression of *NRXN1* mRNA with FOXP2 highlighted the potential interactions regulating gene expression and neuronal differentiation within specific thalamic nuclei (Figure 5.13 A). Co-expression was also identified in the medial part of the thalamus, as well as *NRXN1* highly expressed in the ventricular zone of the thalamus (Figure 5.13 B). We also observed co-expression centromedian nuclei, as well as in the medial geniculate nucleus (Figure 5.13 C, D). Furthermore, NRXN1 immunostaining showed co-expression with FOXP2 in the ventral and dorsal lateral geniculate nucleus, in the medial geniculate and in the centromedian nucleus (Figure 5.14 A, C section 70). Additionally, limited co-localisation with GAD67 was observed, suggesting *NRXN1* expression is primarily found in the glutamatergic neurons rather than GABAergic neurons in the cortex and thalamus at 16 PCW (Figure 5.15). Additionally,

mutations in NRXN1 genes were found to be more likely to have a direct effect upon glutamatergic neurons and their synapses than on GABAergic neurons.

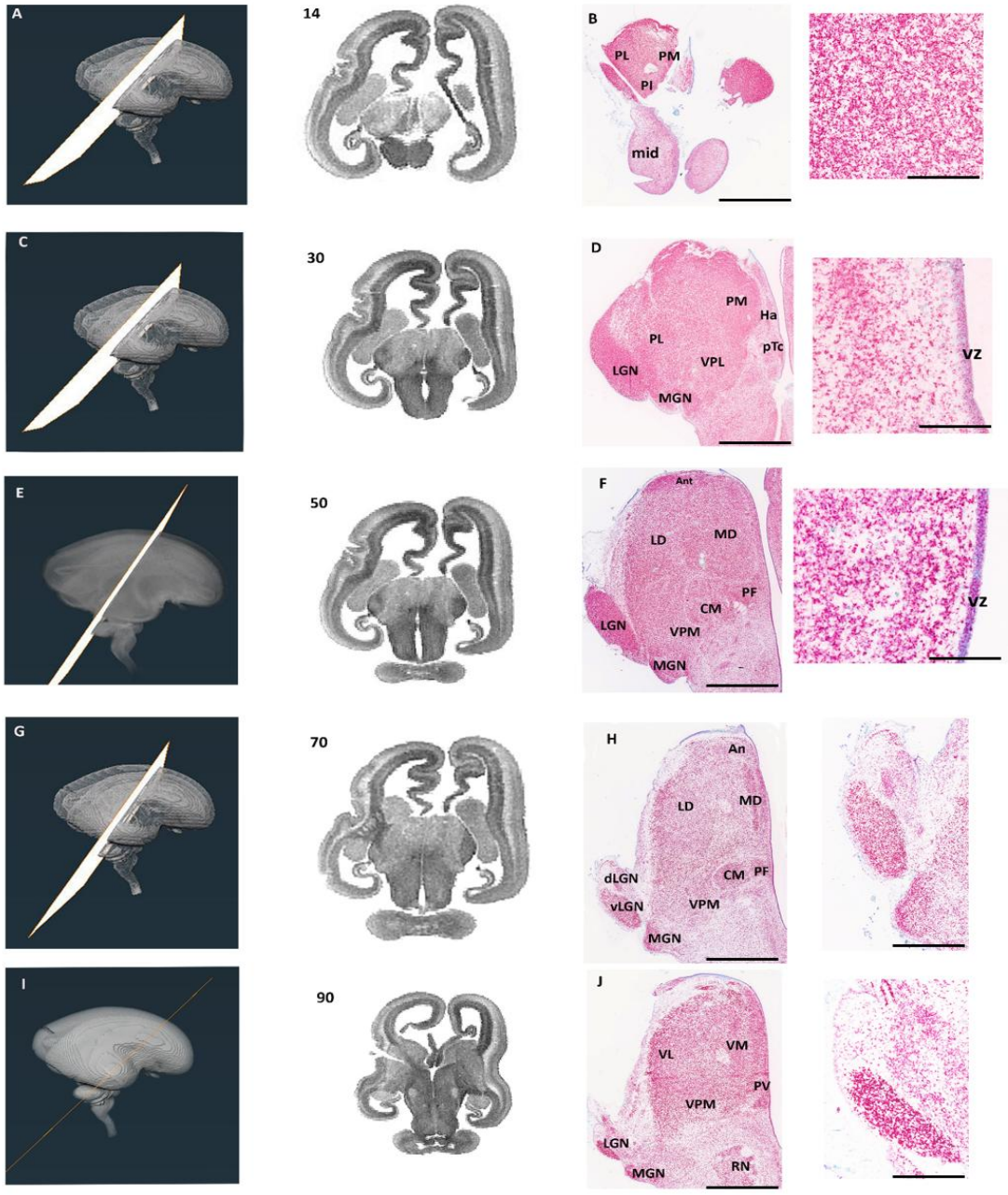

Figure 5.11. ***NRXN1*** **mRNA expression in a coronal section at 14 PCW.** In sections (A-C, 14, 30). Anteriodorsal and ventroposterior (D-J, 50-7-90). NRXN1 exhibited strong expression in the pulvinar nucleus, and isolated cells can be seen in the midbrain (A, B). There was also strong expression in medial and lateral geniculate nucleus (MGN, LGN) (C-D, 30), ventroposterolateral (VPL) and lateral and medial pulvinar (PL, PM). In section (50,70,90) ventroposterior (C-J) strong expression in centromedian, and in the anterior nucleus. There was strong expression in lateral geniculate nucleus (50), strong expression in the dorsal lateral geniculate nucleus (dLGN) when compared with ventral lateral geniculate nucleus (vLGN) (70, 90), as well as in the medial geniculate nucleus (MGN). Scale bars: 2 mm.

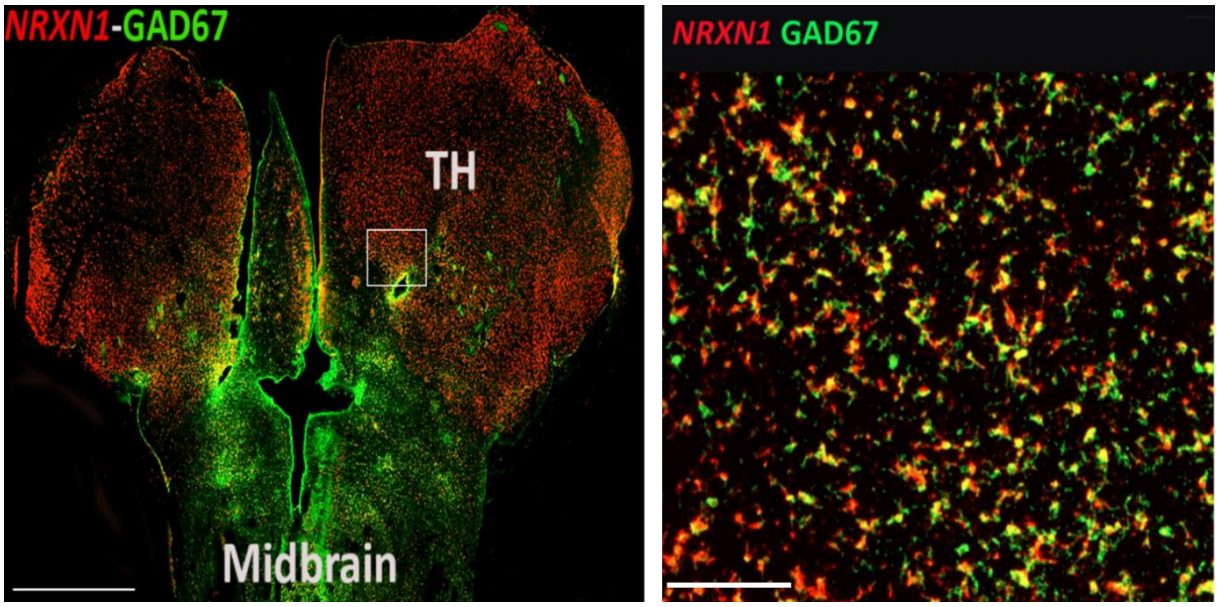

Figure 5.12. ***NRXN1*** **mRNA (red) expression combined with GAD67 (green) immunofluorescence in the coronal section 14 PCW foetal human thalamus.** *NRXN1* mRNA was more strongly expressed in the thalamus (TH), and GAD67 in the pretectum and midbrain. However, the high power image shows co-expression in some neurons in the more medial parts of the thalamus. Abbreviations: thalamus (TH); Scale bars 1 mm; 300 µm.

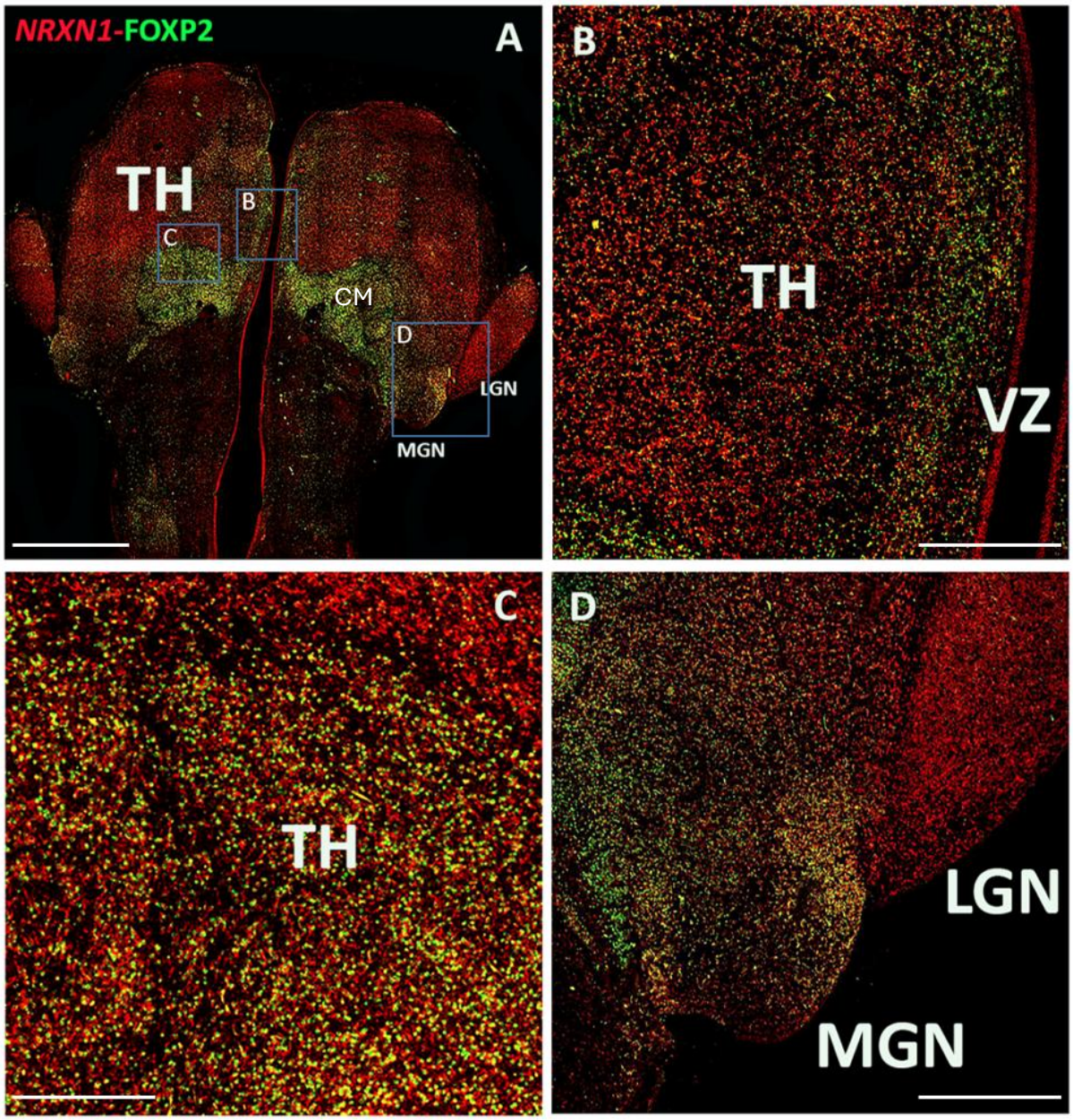

Figure 5.13. In situ hybridization of *NRXN1* mRNA expression (red) combined with FOXP2 immunofluorescence on the human thalamus ventral posterior sections at 14 PCW (A). Co-expression of *NRXN1* and FOXP2 was detected in the medial thalamus (B), and in the centromedian thalamus (C), and in specific nuclei, including the medial geniculate nucleus (D), and the isolated cells of the lateral geniculate nucleus (D). NRXN1 also exhibited strong expression in the postmitotic neurons of the thalamus, and the cells in the ventricular zone. Furthermore, it was found to be strongly expressed in certain nuclei located in the midbrain . Abbreviations: thalamus (TH); centromedian (CM); lateral geniculate nucleus (LGN); medial geniculate nucleus (MGN); ventricular zone (VZ). Scale bars: A, 1 mm; B–D, 200 μm.

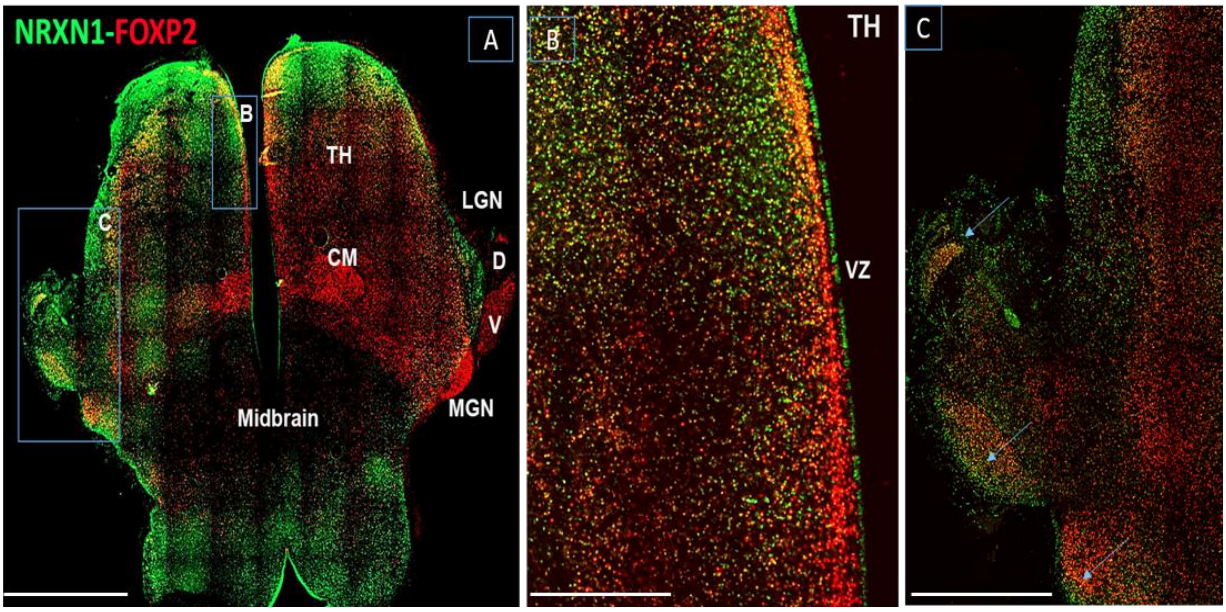

Figure 5.14. Double labelling immunofluorescence FOXP2 (red) combined with NRXN1 (green) in the human thalamus posterior dorsal sections at 14 PCW. (A) FOXP2 was detected in some thalamic nuclei, and there was also co-expression of FOXP2 and NRXN1 in the medial part of the thalamus (B), as well as in the medial geniculate nucleus and ventral and dorsal lateral geniculate nucleus (blue arrow, C), as well as the post-mitotic cells of the thalamus Abbreviations: thalamus (TH); centromedian (CM); lateral geniculate nucleus (LGN); medial geniculate nucleus (MGN); ventricular zone (VZ); dorsal (D); ventral (V). Scale bars; A, 1 mm; B–C, 200 μm.

5.4.6 NRXN1 expression at 16 PCW

In the human cortex sections at 16 PCW, the combined immunostaining of the NRXN1 protein with GAD67 immunofluorescence revealed a distinct expression pattern. Notably, the NRXN1 protein did not co-localize strongly with GAD67, which is a marker of GABAergic neurons, within the cortex. This suggests NRXN1 expression is primarily limited to the glutamatergic neurons in this region. (Figure 5.15).

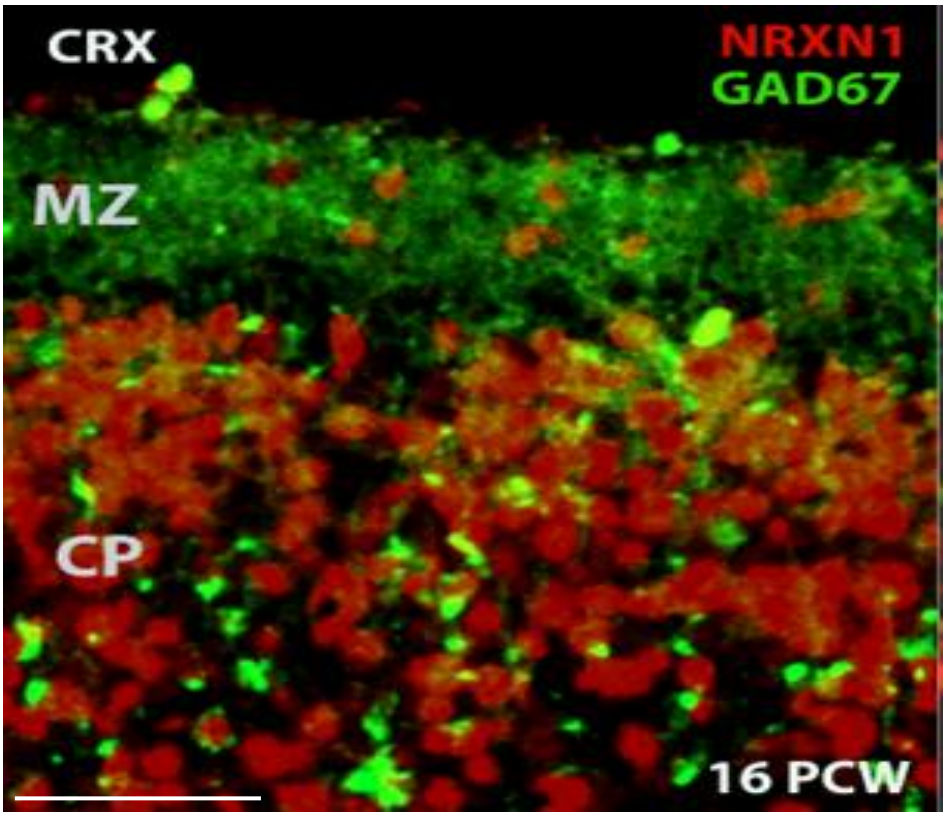

Figure 5.15. Double Immunofluorescence for NRXN1 and GAD67 in human cortex coronal sections at 16 PCW. In the cortex (CRX), NRXN1 protein was not strongly co-expressed with GAD67, which is a marker of GABAergic neurons and their processes; thereby suggesting NRXN1 expression was largely confined to glutamatergic neurons. Abbreviations: marginal zone (MZ); cortical plate (CP); cortex (CRX). Scale bars: 300 μm.

5.4.7 *NRXN1* expression at 19 PCW

At 19 PCW, *NRXN1* exhibited a variable expression pattern in various regions of the developing human forebrain, according to the in situ hybridization assay (Figure 5.16). There was also expression in the hippocampus, cortex, thalamus and ganglionic eminences (Figure 5.16 A). In the cortex, *NRXN1* was expressed in both the cortical plate and the ventricular zone (VZ), indicating its involvement in the later stages of cortical neurogenesis, or possibly in gliogenesis (Figure 5.16 B). Weak expression was observed in the thalamic ventricular zone, while strong expression was detected in postmitotic cells of the thalamus (Th), which points to a role in thalamic neuron maturation (Figure 5.16 C). The caudal ganglionic eminence (CGE) also showed *NRXN1* expression, particularly in the ventricular zone, which is indicative of its involvement in the later stages of GABAergic neurogenesis, as well as in the earlier stages of development (Figure 5.16 D). These findings highlight the spatial and temporal specificity of

NRXN1 expression during mid-foetal brain development, affording insights into its potential roles in neurogenesis.

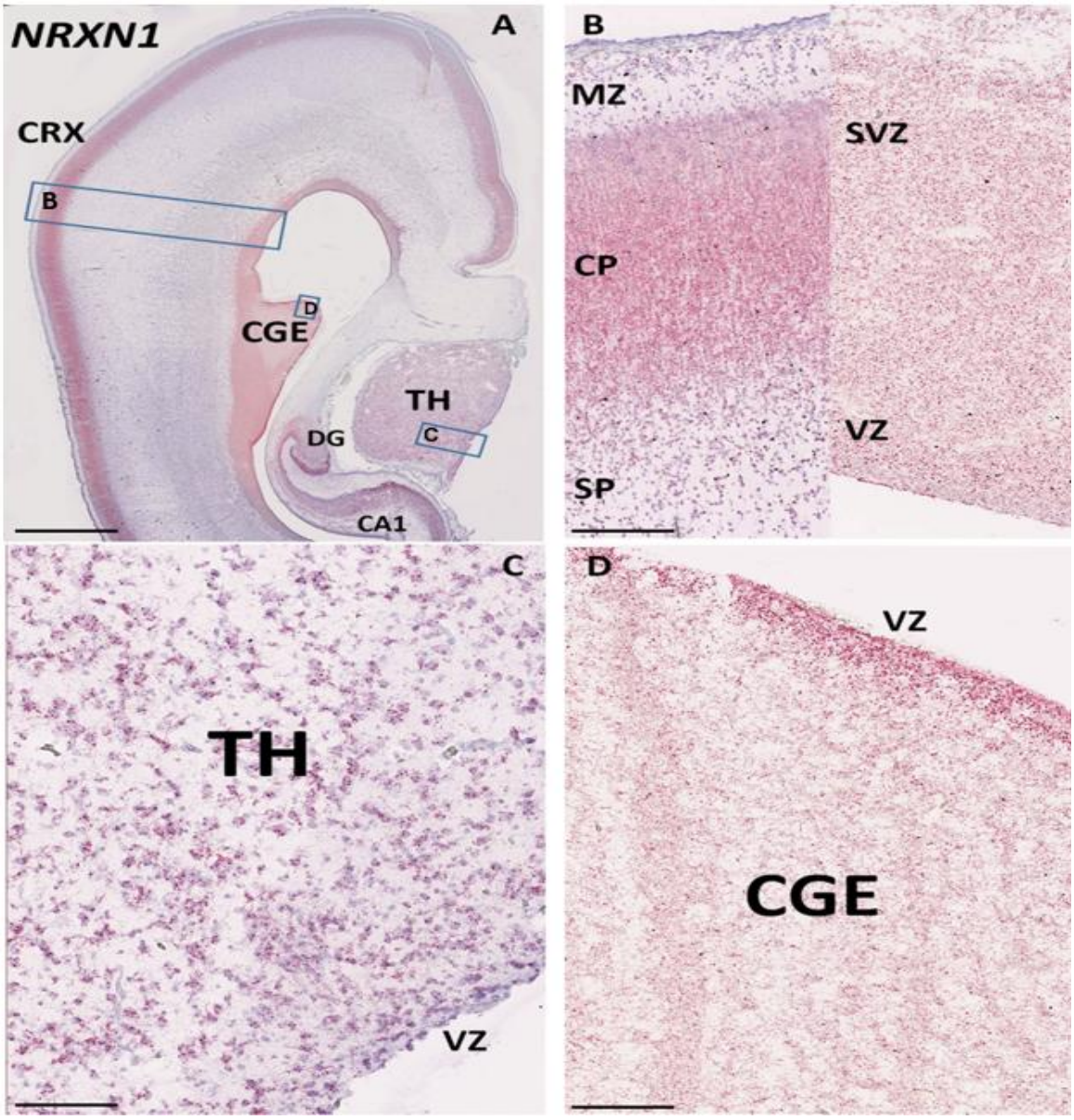

Figure 5.16 In situ hybridization of NRXN1 mRNA expression in the posterior coronal section at 19 PCW. (A) RNAscope in situ hybridization for NRXN1 at 19 PCW shows expression in the medial cortex (CRX), thalamus (TH), and caudal ganglionic eminences (CGE) as well as in the hippocampus. (B) NRXN1 RNAscope in the lateral cortical wall exhibits strong expression in the outer cortical plate and the ventricular zone (VZ); moreover, moderate expression is detected in the subventricular zone (SVZ) and expression is weak in the subplate (SP). (C) Strong NRXN1 expression is detected in the post-mitotic cells of the thalamus (TH), and weak expression in ventricular zone (VZ). (D) NRXN1 expression is especially strong in the ventricular zone of the CGE, which contains GABAergic neuroprogenitor cells; NRXN1 expression is weak in the post-mitotic cells of the CGE. Abbreviation: marginal zone (MZ); cortical plate (CP); cortex (CRX); subplate (SP); ventricular zone (VZ); subventricular zone (SVZ); thalamus (TH); caudate ganglionic eminence (CGE). Scale bars: 1mm; 300 μm.

5.4.8 *NRXN1* expression at 21 PCW

The RNAscope analysis at 21 PCW displayed a distinct regional expression pattern for *NRXN1* within the developing human forebrain (Figure 5.17). In the thalamus, *NRXN1* expression was notably richer in specific thalamic nuclei, such as the pulvinar nucleus (PUL), the lateral geniculate nucleus (LGN) and the medial geniculate nucleus (MGN). This implies it has a potential role in thalamic circuitry and sensory processing (Figure 5.17 A, C, D). Additionally, *NRXN1* was expressed in the hippocampus, notably in the pyramidal cell layer, highlighting its probable involvement in both hippocampal neuron development and synaptic connectivity (Figure 5.17 E). In the hippocampal stratum pyramidale (SP), which contains predominantly glutamatergic neurons, there was very high expression per cell compared to the stratum oriens (SO), which contains predominantly GABAergic neurons (Figure 5.17 E). In the neocortex, *NRXN1* expression was highest in the outer layers of the cortical plate (Figure 5.17 B). These findings are indicative of its importance in cortical development and neuronal differentiation; hence, elucidating the spatial distribution of *NRXN1* expression and its potential functional implications in the period of late-foetal brain development.

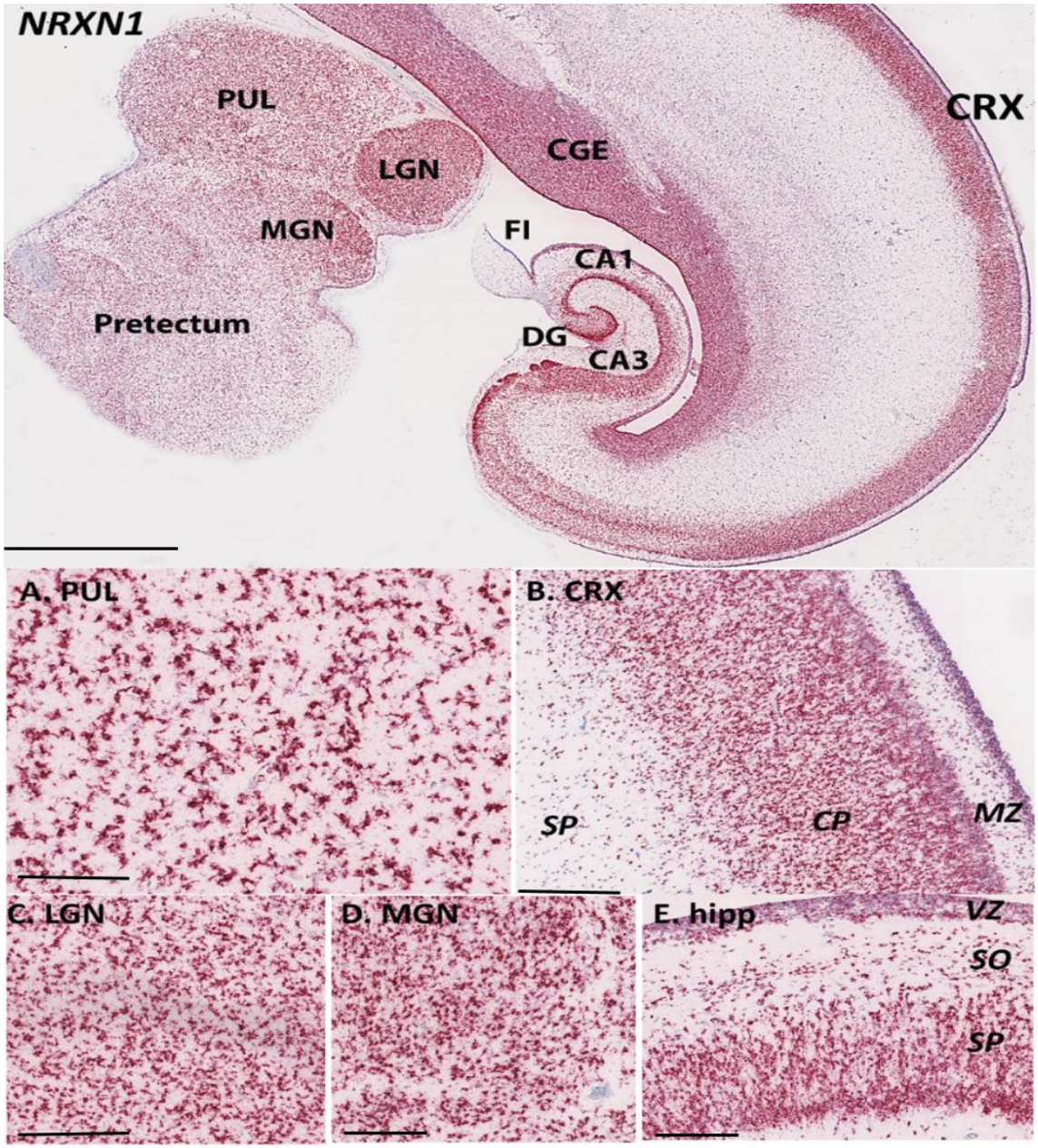

Figure 5.17. In situ hybridization of *NRXN1* mRNA expression at 21 PCW. (A) coronal section showing temporal cortex (Temp CRX), caudal ganglionic eminences (CGE) and certain posterior thalamic nuclei (PUL, MGN and LGN). At low magnification, expression was present in both the progenitor and postmitotic cell zones and was positively correlated with cell density. However, expression appeared especially dense in the hippocampus in the pyramidal cell layer. Higher magnification images of the thalamus showed that pulvinar region exhibit strong expression (PUL; B). In the neocortex, (B) expression was highest in the outer layers of the cortical plate. A higher cell density, with a similar density of staining was observed in the Lateral Geniculate Nucleus (LGN; C) and Medial Geniculate Nucleus (MGN; D). However, in the cortical areas the hippocampal stratum pyramidale (SP) contained predominantly glutamatergic neurons, and there was very high expression per cell compared to the stratum oriens (SO), which contains predominantly GABAergic neurons (E). Ca, caudate nucleus; MGN, medial geniculate nucleus; MZ, marginal zone; Ptc, pretectum; SPL, subplate. VZ, ventricular zone. Scale bars: A, 1 mm; B–E, 200 µm.

5.5 Discussion

Overall, in situ hybridisation for *NRXN1* expression has largely confirmed and advanced observations made following immunoperoxidase staining for NRXN1 in a previous study by Harkin et al. (2017). Transcriptomic data analysis demonstrated that *NRXN1* was highly expressed in the developing human forebrain in diverse cell types including progenitor cells and post-mitotic neurons. Histological experiments also confirmed this, revealing that while NRXN1 (mRNA and protein) were strongly expressed by cortical glutamatergic neurons and weakly expressed by their progenitors, the opposite was true for the GABAergic cells of the ganglionic eminences in the early stages of development, when expression is significantly stronger in progenitor cells than in post-mitotic cells. In the diencephalon, NRXN1 was determined to be highly prominent in glutamatergic neurons and intermediate progenitor cells, and weakly expressed by progenitor cells in the ventricular zone in the early developmental stages (8, 10 PCW). At 12-14 PCW, *NRXN1* mRNA in the thalamus and epithalamus was expressed in quiescent progenitor cells in the ventricular zone and postmitotic neurons. At later stages 21 PCW *NRXN1* was expressed in the hippocampus predominantly GABAergic neurons, predominantly glutamatergic neuron and pyramidal cell layer. Additionally, *NRXN1* expression was notably richer in specific thalamic nuclei

5.5.1 In situ hybridisation versus immunofluorescence

Existing transcriptomic databases suggest NRXN1 is expressed in progenitor cells, glutamatergic cells, dividing cells and GABAergic neurons. However, an interesting yet confounding result was that NRXN1 mRNA appeared not to be highly expressed in the cortical ventricular zone in the cell body, although the NRXN1 protein did appear to be highly expressed in the cell body, echoing work by (Harkin et al., 2017). This suggests the possible non-specificity of the anti-NRXN1 antibody, the identification of which was one of the initial motivations for carrying out the study. However, Sebastian et al. (2023) formerly proposed potential roles for NRXN1 in neurogenesis, based on transcriptomic studies of human brain organoids derived from iPSCs carrying SCZ-associated NRXN1 deletions. Possibly, *NRXN1* mRNA experiences a high turnover, while the NRXN1 protein has a greater half-life (Greenbaum et al., 2003) resulting in higher detection of NRXN1 in immunostaining experiments as opposed to in the in situ hybridisation. A further suggestion is that the NRXN1 protein is expressed in the ventricular zone, but not at the mRNA level initially, due to possible

post-transcriptional modifications of the mRNA interfering with probe binding during in situ hybridisation (Zhao et al., 2017). At 16PCW, the NRXN1 protein is not co-expressed with GABAergic cells in the cortical plate, while in transcriptomic data and in situ hybridization studies, *NRXN1* mRNA shows co-expression with GAD67 (a marker of GABAergic neurons). Thus, the insitu hybridisation results for *NRXN1* agree more closely with transcriptomic studies than with immunohistochemistry. NRXN1 also appeared to be strongly expressed in the cell bodies of some cell groups, but at this stage did not appear in the subplate or marginal zone, where synapses are forming. The first possibility is that NRXN1 is subject to post-transcriptional control, which means that although mRNA is present, translation is delayed until later stages of development. It is also possible that the protein is expressed at levels that are lower than the detection threshold of the antibodies that are being utilised, or that the antibodies themselves do not possess the sensitivity or specificity that is necessary to detect NRXN1 in a reliable manner. NRXN1 is a membrane-bound synaptic protein that has the potential to be moved away from the cell bodies where mRNA is identified, which results in a limited overlap in spatial localisation where the protein is located. Additionally, the protein may be subjected to quick degradation, or translation may be strictly regulated in order to coincide with the creation of synapses, which has not yet taken place in the subplate or peripheral zone. It is quite likely that these circumstances are responsible for the lack of a distinct immunohistochemistry signal, despite the fact that robust transcript detection was used. In the later stages of development (14, 19, 21 PCW) *NRXN1* mRNA was expressed in the postmitotic cells in all the nuclei of the thalamus. This suggests NRXN1 is important for thalamic development and that potentially mutations in NRXN1 could alter thalamic development resulting in neurodevelopmental disorders.

5.5.2 Telencephalic expression

An increase in *NRXN1* expression with age was previously reported between 14 PCW and birth in the human prefrontal cortex, when measured by qPCR (Jenkins et al., 2016). In addition, Harkin et al. (2017) demonstrated, by both tissue RNAseq and qPCR, that *NRXN1* was expressed, and increased in expression, throughout the cortex from 8-12 PCW. When examined at 8-10 PCW, *NRXN1* showed a strong expression pattern in the cortical plate (similar to (Harkin et al., 2017), where the cortical plate was shown to have the highest expression), as well as also in the apical ventricular zone of the cortex. The expression pattern of the *NRXN1* gene was indicated to be high in the post-mitotic cells of the cortical region in the human foetal

forebrain, corresponding to (Konopka et al., 2012), and in the apical surface of the ventricular zone, as per (Harkin et al., 2017). Therefore, it appears that mutations in *NRXN1*α in early cortical development could trigger subtle alterations in the rates and quantity of neuroblast production from the radial glia (Harkin et al., 2017). PAX6 identifies radial glial cells in the proliferative ventricular (VZ) and subventricular (SVZ) zones. At 10 PCW, NRXN1 showed co-localisation with PAX6 in the proliferative zones, confirming NRXN1 is expressed in the radial glial cells as reported by (Harkin et al., 2017). However, expression of NRXN1 in the apical ventricular cells was higher in the ganglionic eminences than the cortex. Moreover, it was observed in ventral but not dorsal LGE, LGE-like CGE, and MGE (Figure 5.5). This is known to be the major site of GABAergic neuron production in the forebrain. Potentially, NRXN1 mutations expressed in the progenitor cells of the ganglionic eminences have the greatest capacity to cause alterations to the production of cortical interneurons, and neurons of the basal ganglia. Alterations to excitatory inhibitory balance have been posited as a major cause of neurodevelopmental diseases (Liu et al., 2021).

5.5.3 Thalamic expression

NRXN1 expression at 8 PCW was in the thalamic postmitotic cells in the mantle zone, as well as in the subventricular zone, but not in the progenitor cells. NRXN1 expression at 10 PCW showed the same pattern as that observed at 8 PCW but was not observed to be expressed in the progenitor cells of the ventricular zone (Figure 5.5-5.7). However, in immunofluorescence experiments at 10 PCW, NRXN1 showed strong expression in the progenitor cells of the ventricular zone (Figure 5.9). At 14 PCW, *NRXN1* expression was high, compared to in the midbrain and subthalamic structures, in all the thalamic nuclei including pulvinar, lateral geniculate, and medial geniculate nuclei, which suggests an important role for *NRXN1* in the thalamic circuitry establishment, also indicating its universal role in thalamic development. High expression was not restricted to specific thalamic nuclei, contrary to our hypothesis that NRXN1 might be expressed differentially in higher order thalamic nuclei. There was also strong expression in the glutamatergic neurons, certain GABAergic neurons and radial glial cells as reported previously (Sebastian et al., 2023). A similar pattern of expression was clear at 19 PCW, with stronger expression in the ventricular zone of the thalamus and weaker expression in the caudate ganglionic eminences. Indeed, *NRXN1* haploinsufficiency in the developing forebrain affects glutamatergic and GABAergic neurons, as well as forebrain progenitor cells and astroglia (Sebastian et al., 2023). By 21 PCW, the expression of *NRXN1*

was regionalized more distinctly in the thalamic nuclei and was thus also expressed at this stage in the pyramidal cell layer of the hippocampus and the cortical plate. Aside from individual expression of the *NRXN1* gene, the study also unveiled the co-expression of *NRXN1* with suitable markers, elucidating its association with MKI67 (cell division), PAX6 (progenitor cells) in the ventricular zone of the thalamus and the cortex, *FOXP2* (postmitotic cells) at 14 PCW in post-mitotic cells of the thalamus, and at 14 and 16 PCW with GAD67 (GABAergic neurons), respectively, emphasizing its multifaceted role in neurodevelopment throughout gestation.

5.5.4 Difference in NRXN1 expression between GABAergic and Glutamatergic neurons

The expression pattern confirmed the stronger presence of the *NRXN1* gene in the proliferative zones in ganglionic eminences harbouring GABAergic neurons. This may also mean that *NRXN1* has cell-type specific functions in GABAergic neurons and their progenitors, where *NRXN1* is expressed in more immature states, differing from glutamatergic neurons, where *NRXN1* is expressed in more mature states. However, according to Sebastian et al. (2023) at 14 PCW, glutamatergic neurons showed the highest expression of NRXN1, although at 16 PCW, both glutamatergic and GABAergic neurons showed the highest quantity of NRXN1-expressing cells. Based on these results, we can infer that NRXN1 expression affects the developmental trajectories of both glutamatergic and GABAergic neurons.

5.5.5 NRXN1 expression in the ventral and medial pallium

The pallium is the dorsal portion of the telencephalon, and is responsible for the development of the cerebral cortex in mammals. The pallium is divided into medial, dorsal, lateral and ventral segments. The medial pallium corresponds to the early form of the hippocampus, while the dorsal pallium gives rise to the neocortex. The lateral pallium is responsible for producing the dorsal section of the olfactory cortex, the primary portion of the claustrum, and certain nuclei in the amygdala, whereas the ventral pallium gives rise to the ventral olfactory cortex, a smaller portion of the claustrum, and a larger portion of the amygdaloid complex (Puelles et al., 2000, Puelles, 2001, Medina et al., 2004).

We observed that NRXN1 was highly expressed in the ventral pallium at 8 PCW. This was confirmed by demonstrating co-expression with NR2F1, which is present in the ventral pallium (Alzu'bi et al., 2017). The ventral pallium is a developmental structure, located at the lateral edge of the dorsal telencephalon. It transforms into the ventral olfactory cortex, a smaller portion of the claustrum, and a larger portion of the amygdaloid complex (Puelles et al., 2000, Puelles, 2001, Medina et al., 2004). It produces glutamatergic neurons for these structures, becoming a gateway for interneuron precursors migrating laterally from either the medial ganglionic eminence or the caudal ganglionic eminence into the cortex (Clowry et al., 2018, Alzu'bi et al., 2017). These results suggest that, given its strong expression, *NRXN1* is also a marker gene for the ventral pallium. We further observed strong *NRXN1* expression in the cortical hem, which forms the medial boundary between the dorsal and ventral telencephalon.

5.5.6 Regulation of alternative splicing and synapse formation

The interaction between presynaptic NRXNs on developing axons and NLGNs expressed on developing dendrites is widely recognized as a method by which to stabilize the postsynaptic location and facilitate accumulation of vesicles at the presynaptic site (Graf et al., 2004, Chen et al., 2010). Based on research conducted by Bayatti et al. in 2008, it is probable that GABAergic synapses exist in the human pSP during this stage of development at 16 PCW (Bayatti et al., 2008, McLeod et al., 2023). These findings also indicate that both NRXNα AS4– and NRXNβ AS4+ isoforms, and NLGN2, play a role in their formation. According to (Chih et al., 2006, Vuong et al., 2016), they may be expressed in the pSP during this developmental stage. NRXNα plays a crucial role in the formation of GABAergic synapses, as demonstrated in a study using triple Nrxnα knock-out mice, which showed a 50% decrease in the density of their cortical GABAergic synapses (Missler et al., 2003).

Our findings, aligning with Harkin et al. (2017) indicate that NRXN1 is not localised to the subplate, although they did observe immunoreactivity for NRXN2 in the subplate. Additionally, NRXN1 showed low expression in the postmitotic GABAergic neurons in the cortex, contrasting with its strong expression in certain areas of the thalamus.

5.5.7 NRXN1 in cell migration

The VZ, SVZ, and IZ cells' expression of the NRXN protein may signify the protein is essential for cell migration from the proliferative zones (Harkin et al., 2017). NRXN expression was also higher in the outer region of the CP, which younger neurons migrate to, which contrasts with the inner region, in which older cells arise having completed their migration (Bystron et al., 2008). Cell adhesion molecules are instrumental in the movement of neurons (Maness and Schachner, 2007) and molecules; for instance, cadherins, which are also present at the synapses within the developed nervous system, being considered essential for the migration process (Redies et al., 2012). Undoubtedly, the mutation of *cntnap2*, a gene associated with autism, which is similar in structure to NRXNs causes the atypical migration of neurons in transgenic mice. This affects both cortical projection neurons and interneurons, resulting in epilepsy and behavioural deficits that resemble autism (Peñagarikano et al., 2011). NRXNs may also potentially play as yet undiscovered roles in cell migration and neurite outgrowth.

5.5.8 NRXN Mutations and Neurodevelopmental Disorders

Genetic studies of neurodevelopmental conditions have shown the majority of mutations affect NRXN1α expression and not NRXN1β (Reichelt et al. 2012). NRXN1 was expressed in substantial amounts in the developing cortex, with a higher proportion likely to be expressed in the α form; especially at 9 PCW, where protein expression arises in the VZ (Harkin et al., 2017). Consequently, mutations in NRXN1α during the early stages of cortical development can bring about minor changes in the rates and quantities of neuroblast formation from radial glia.

The significance of NRXN1 in neurodevelopment is emphasized by its elevated expression throughout the process of foetal cortical development, and is controlled by genetic risk single nucleotide polymorphisms (SNPs) (Jaffe et al., 2018, Hu et al., 2019). The co-expression of NRXN1 with synaptic and cell signalling genes, including established schizophrenia candidates, suggests it may have a potential impact on risk of schizophrenia (Mozhui et al., 2011). The combined results emphasise the importance of NRXN1 in schizophrenia, highlighting its potential as a therapy target. It has also been considered important relative to ASD, since (Feng et al., 2006) reported a correlation between NRXN1 and ASD through candidate gene investigations, by examining the three β-neurexin genes in both ASD patients

and controls. Through this analysis, they identified two missense mutations connecting NRXN1 with ASD. These mutations were identified relative to the established neuronal role played by β-neurexins (Feng et al., 2006). Following initial reports, subsequent investigations revealed additional genetic abnormalities present in *NRXN1*, suggesting it increases the probability of ASD (Williams et al., 2019).

5.6 Concluding remarks

Our findings suggest NRXN1 is involved in the development of the human forebrain, and we have detailed the expression patterns at different stages of the development of the human foetal forebrain. *NRXN1* is also expressed in the earliest stages of human cortical development, showing distinct expression patterns. These findings could potentially pave the way for future diagnostic and therapeutic approaches to targeting neurodevelopmental disorders involving *NRXN1*. Future functional experiments should therefore be designed to probe the potential roles of NRXN1 in cell migration and axon guidance, axon outgrowth, regulation of neuronal proliferation, and early development of subplate circuitry.

6 Chapter 6: FEZ1 expression in the developing human forebrain

6.1 Introduction

FEZ1 has been directly linked to schizophrenia susceptibility by gene association studies (Yamada et al., 2004, Tang et al., 2017), however this finding has also been unsuccessfully replicated (Hodgkinson et al., 2007, Koga et al., 2007, Nicodemus et al., 2010). It is mainly expressed in the brain, and it is thought that suppression of *FEZ1* expression in cultured embryonic neurons causes deficiency of neuronal differentiation (Maturana et al., 2010). Mice lacking *FEZ1* move more quickly and are more sensitive to psychostimulants (Sakae et al., 2008). FEZ2 may partially compensate for FEZ1 deficit, which could explain why there didn't seem to be any discernible impact on brain morphology or performance on a battery of cognitive tests (Maturana et al., 2010). Nonetheless, its expression has been demonstrated to be diminished in the post-mortem brains of individuals with schizophrenia, associated with mutations in DISC1 (Disrupted in Schizophrenia 1) (Lipska et al., 2006) and the peripheral blood of schizophrenia sufferers (Vachev et al., 2015). In addition, *HDAC11* is a schizophrenia susceptibility gene (Kebir et al., 2014) the knock down of which downregulates expression of FEZ1, as shown by (Bryant et al., 2017). Kang et al. (2011) demonstrated there was no significant direct correlation identified between variations in the FEZ1 gene and schizophrenia risk; however, an epistatic interaction was observed, indicating that individuals with a FEZ1 mutation exhibit approximately a 2.5-fold increased risk for schizophrenia, but only when in conjunction with a mutant DISC1 background. Significantly, *FEZ1*-deficient stem cell-derived human motoneurons exhibit considerable developmental impairments in axon growth and synapse formation *in vitro* (Kang et al., 2011). Gunaseelan et al. (2021) indicated that human neurones may exhibit distinct responses compared to rat neurones in cases of FEZ1 deficiencies. Recent investigations have shown that FEZ1 expression is activated early in human brain development, and that in the absence of FEZ1, neuroprogenitors exhibit ectopic localisation and cortical layer formation is disrupted(Gunaseelan et al., 2021).

FEZ1's primary function is as a Kinesin-1 adapter protein. Kinesin-1 is a motor protein that attaches to microtubules and facilitates the transport of protein complexes or organelles along cellular extensions (Figure 6.1) (Hirokawa and Noda, 2008). Adaptor proteins, including FEZ1, control these transport mechanisms by modifying and guiding the transport of particular payloads (Hirokawa et al., 2009). FEZ1 has been shown to participate in the transport of various SNARE complexes related to axon growth and associated proteins, such as syntaxin-1,

SNAP25, synaptotagmin, and GAP43, as well as others recognised as candidates for neurodevelopmental disease susceptibility, including neurexins, STXBP1, and DISC1 (Figure 6.2) (Toda et al., 2008, Kang et al., 2011, Chua et al., 2012, Butkevich et al., 2016, Razar et al., 2022). FEZ1 initiates distinct interactions with the Netrin-1 receptor, which is absent in Colorectal Cancer, and the Semaphorin-3A receptor complex within the growth cone. Consequently, it may function downstream of guidance cues to modulate axon and dendrite outgrowth by directing the transport of cargoes, facilitating process expansion through exocytosis involving SNARE proteins (Cotrufo et al., 2011, Chua et al., 2021). It is evident that changes in FEZ1 function may interfere with the development and maintenance of axons and dendrites as well as synaptic networks. Nonetheless, FEZ1 is also localised in the nucleus and engages with several transcriptional regulators. (Teixeira et al., 2019). For instance, FEZ1 interacts with short coiled proteins (SCOC), associated with axon development and autophagy (Toda et al., 2008, McKnight et al., 2012, Qinlin et al., 2022), and appears to play a role in induction of expression of the neural transcription factor SOX2 (Figure 6.2 A). (Papanayotou et al., 2008). FEZ1 has been shown to interact with the retinoic acid receptor, and in the presence of retinoic acid, it induces a significant upregulation of the transcription factor HOXB4 (Bertini Teixeira et al., 2018). FEZ1 may significantly influence the transcriptional regulation of neurones and their progenitors (Figure 6.2 B).

Therefore, it is hypothesized that mutations in FEZ1 or its interacting partners may contribute to the manifestation of neurodevelopmental diseases by disturbing the early trajectory of forebrain development through the disruption of axon/dendrite outgrowth and early synapse formation, also possibly altering the gene expression programs that control cell phenotype specification. To test these hypotheses, it is first necessary to establish the expression of FEZ1 in development; identifying key regions, cell types and developmental time points. In the present study, we have combined data mined from gene expression databases with histological investigations using human tissue samples to describe FEZ1 mRNA and protein expression in the developing forebrain.

Please note that some of the data presented in this chapter has been published (Alhesain et al., 2023).

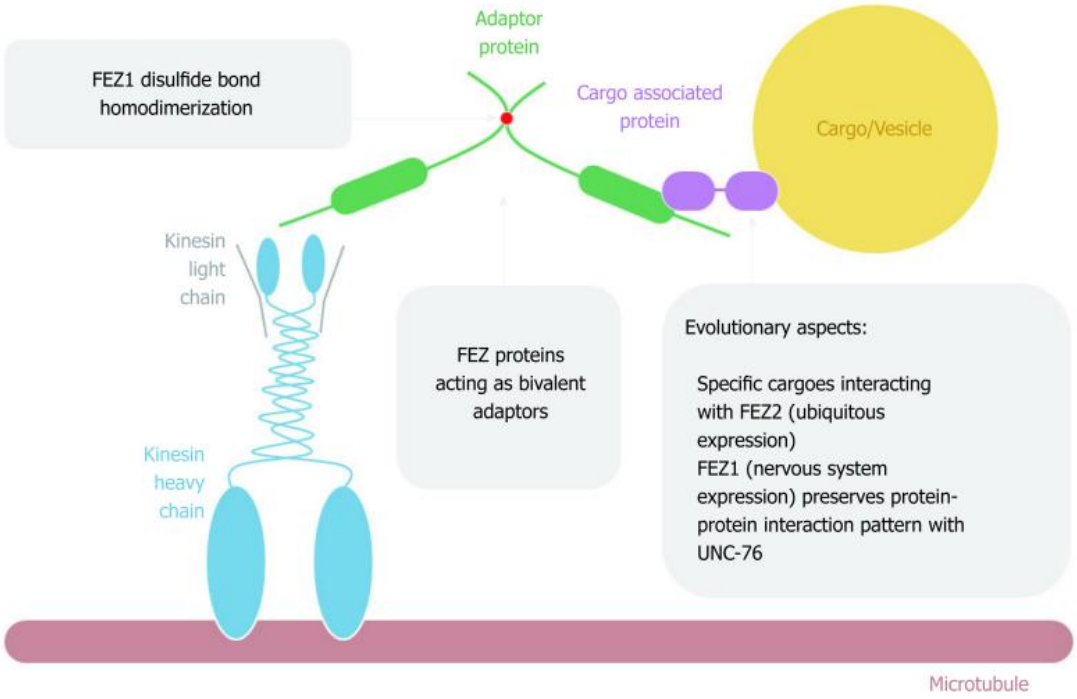

Figure 6.1 FEZ proteins cytoplasmic function as transport bivalent adaptors. Interacts with various proteins whose roles range from intracellular transport systems to transcription regulation. Work as adaptor protein by binding the kinase and cargo, involved in the transport process of SNARE components, MUNC18 or syntaxin (Teixeira et al., 2019).

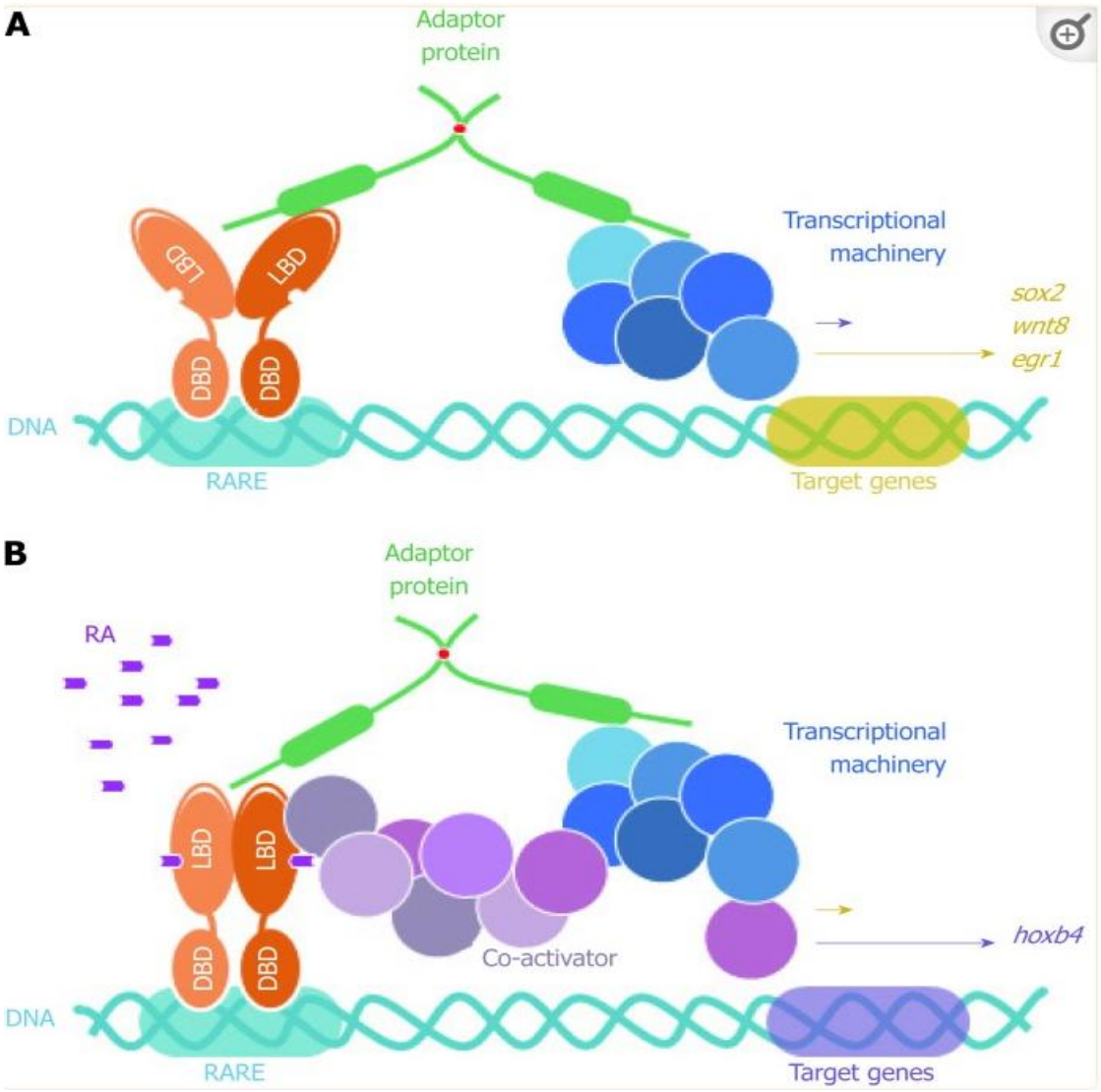

Figure 6.2 FEZ proteins serve a nuclear function as a scaffold between nuclear receptors (retinoic acid receptor) and transcriptional machinery. (A) work as transcription machinery factor of the neural transcription factor (SOX2, wnt8, egr1). (B) FEZ proteins serve a nuclear function as scaffold to binds transcriptional machinery and retinoic acid receptors in transcriptional regulation. DBD: DNA binding domain; LBD: Ligand binding domain; RARE: Retinoic acid response element; RA: Retinoic acid (Teixeira et al., 2019).

6.2 Aim of study

Our primary aim in this study was to examine the expression of *FEZ1* in the developing human ventral telencephalon and thalamus. To collect confirmatory evidence for cell types expressing *FEZ1* we performed an RNAscope in situ hybridization combined with immunohistochemistry to identify different cell markers. Additionally, we examined how FEZ1 protein is expressed in fasciculating thalamocortical axons. The range of brain areas and stages of development were also expanded to take in the ventral telencephalon and thalamus from 8 PCW up to 21 PCW. Tissue and Single-cell RNAseq databases were also consulted. By understanding when, where and in which cell types FEZ1 is expressed during development, it may be possible to clarify the mechanisms by which mutations in this gene lead to neurodevelopmental disorders.

6.3 Methods:

All the methods employed, including single and double-labelling immunofluorescence and RNAscope in situ hybridization with immunofluorescence, are described in detail in Chapter2.

6.4 Results

6.4.1 FEZ1 transcriptomics in the human forebrain

A number of databases were consulted to provide information on FEZ1 expression, including whole tissue and single cell RNA sequencing (scRNAseq).

Using data deposited at www.ebi.ac.uk/arrayexpress/experiments/E-MTAB-4840 (Lindsay et al., 2016), 138 samples of cortical tissue taken at ages ranging from 7.5 to 17 PCW, and from various positions along the anterior posterior axis of the cortex including the temporal lobe were analysed for tissue RNAseq; no statistically significant difference in expression was observed between the cortical regions. (Figure 6.3A). As shown in (Figure 6.3 B), *FEZ1* was highly expressed from the beginning of cortical plate formation (7.5 PCW) until the latest developmental stage studied, and expression increased significantly with age. We found all samples expression levels were in the top quartile for protein coding genes (> 40 normalized RPKM), and samples expression levels were in the top 5% of protein coding genes (> 160 normalized RPKM) (Figure 6.3 B). This suggests a crucial role is played by *FEZ1* in cortical development, and this might be predominantly expressed in post-mitotic cells, which increase with age as a proportion of the cell population in the cortical wall. This suggests FEZ1 does not play a role in cortical arealisation, or not along the anterior to posterior axis at least.

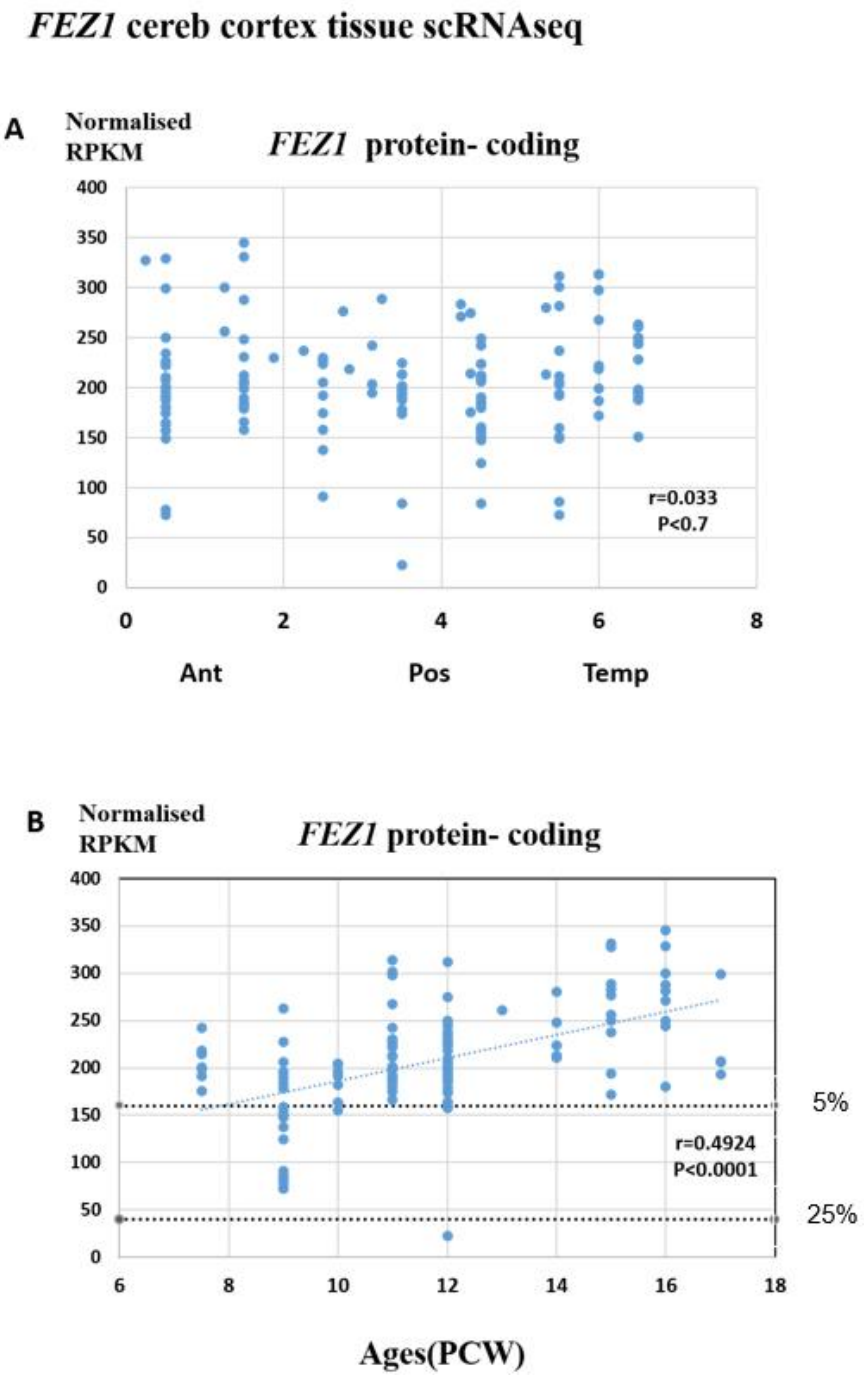

Figure 6.3. FEZ1 gene expression in the cortex across development. (A) Normalized RPKM for 138 cortical samples of varying ages plotted against their location on the anterior to temporal axis with 0 corresponding to the anterior pole of the cortex, 5 to the posterior pole and 7 to the Temporal pole (Miller et al., 2014). (B) Normalized RPKM values for 138 cortical samples taken from various cortical locations, plotted against age (PCW), showing a linear relationship between increasing expression of FEZ1 and age. The expression of FEZ1 some ages expressed in the top 5% (more than 160 RPKM) and some of them in the top of 25% (more than 40 RPKM).

The cortical development expression viewer (CoDEx)2, a scRNAseq database, was searched to explore the cell type specificity of *FEZ1* expression further. This dataset provided information on expression from human cortical tissue samples at 17/18 PCW (Polioudakis et al., 2019). As shown in (Figure 6.4 A), *FEZ1* was ubiquitously expressed in a high proportion of cells, including glutamatergic and GABAergic neurons, and subtypes of progenitor cells. Expression was consistently highest in more mature glutamatergic neurons (subplate and lower cortical plate), lower in the dividing progenitor cells compared to quiescent progenitors, and lowest in cells of non-neuroectodermal origin (such as microglia, pericytes and endothelial cells). Expression levels were highly variable in many of the cell types examined.

Altered development of thalamocortical circuits has previously been strongly implicated in schizophrenia (Jiang et al., 2021). Thus, cell specific expression in the thalamus was explored using data from an 16 PCW human thalamus sample deposited at NEMO Analytics (Orvis et al., 2021). UMAP plots were constructed for *FEZ1* and markers of various cell phenotypes (Chapter 3), revealing that *FEZ1* is also widely expressed in the thalamus, co-localizing with both glutamatergic and GABAergic neurons, as well as progenitor cells and astrocytes (Figure 6.4 B).

Taken together, it appears that FEZ1 is expressed by neurons maturing in distinct locations in the cortex and the thalamus, where it may play a role in axon, dendrite and synapse formation, but is also widely expressed in progenitor cells, where it may regulate transcriptional programs, but possibly also play a role in the extension of radial glial fibres.

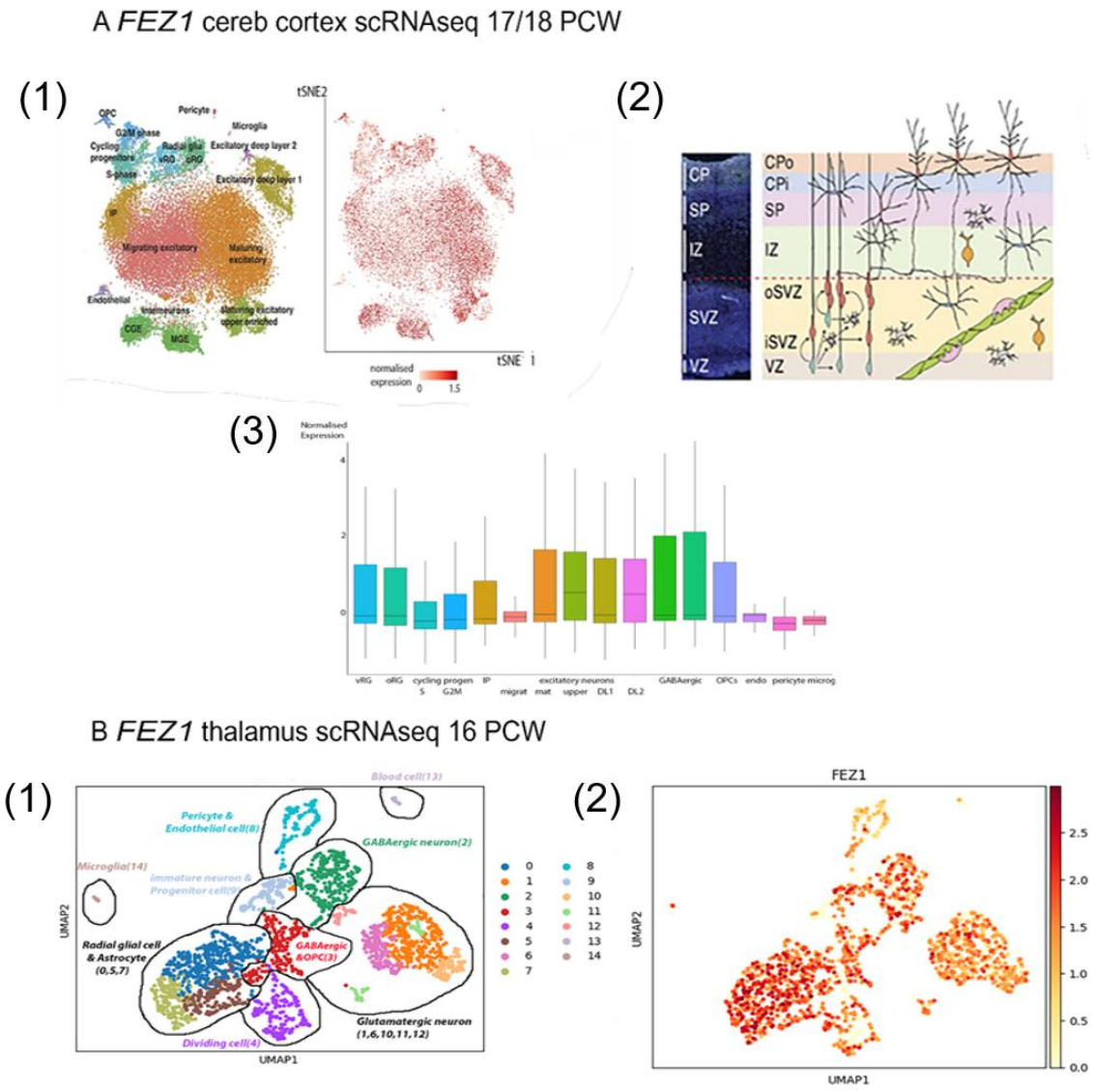

Figure 6.4. FEZ1 expression: transcriptomic analysis. (A) Single cell RNAseq data for cerebral cortex at 17/18 PCW taken from solo.bmap.ucla.edu/shiny/webapp/. (1) t-distributed stochastic neighbour embedding (t-SNE) map and accompanying bar charts revealed FEZ1 is ubiquitously expressed in neuroectoderm derived cell types, but especially in more mature excitatory (glutamatergic) neurons, less mature GABAergic neurons (CGE and MGE) and non-dividing radial glia. Expression was lower in dividing progenitor cells and the more mature GABAergic neurons (interneurons). (2) shows the type of cell in each layer of the cortex. (3) shows levels of *FEZ1* expression in each cell type in the cortex. (B) Single cell RNA data for the thalamus at 16 PCW was taken from NEMO Analytics. (1) shows cell clustering in the thalamus. (2) UMAP maps generated for FEZ1, and a marker for progenitor cells, GABAergic neurons and glutamatergic neurons revealed FEZ1 was also ubiquitously expressed in the thalamus at this stage of development.

6.4.2 RNAscope in situ hybridization and immunohistochemical studies of *FEZ1*/FEZ1 expression at 8-10 PCW

In the cerebral cortex at 8 PCW, just after the onset of cortical plate formation, the expression of both the *FEZ1* mRNA and FEZ1 protein was highest in the postmitotic neurons of the subplate (SP) and cortical plate, but expression was detectable in progenitor cells containing ventricular and subventricular zones VZ and SVZ (Figure 6.5 A, B). However, in the progenitor zones of the diencephalon and in the proliferative ganglionic eminences (GE) and (Figure 6.5 C, D), expression is higher than in sub-cortical postmitotic neurons. This dichotomy is maintained at 10 PCW (Figure 6.6 A, D). Interestingly *FEZ1* mRNA expression in dorsal and lateral cortical progenitor zones appeared to have decreased compared to medial zones, although this was not supported by the immunohistochemical detection of FEZ1 protein expression (not shown). *FEZ1* at 10 PCW was not expressed in the proliferative zone in the lateral ganglionic eminence (Figure 6.6 B). Protein expression was also higher in neurons (identified by doublecortin immunoreactivity) and was settled in the cortical plate compared to those migrating through the subplate and intermediate zone, suggesting there is no FEZ1 expression in DCX+ migrating neurons and the neurites found in these locations (Figure 6.7A). *FEZ1 mRNA* was strongly co-localised with TBR1, which is a marker for postmitotic glutamatergic neurons, but was also expressed in non-TBR1 positive cells in the VZ and SVZ, presumably progenitor cells (Figure 6.7 B). The transcriptomics studies (Figure 6.4) suggested actively dividing cortical cells show low levels of FEZ1 expression. Immunohistological evidence suggested that while putative dividing of KI67+ progenitors in the SVZ reveals little evidence of FEZ1 co-expression, ventricular zone radial glial cells with cell bodies located at the apical surface where they undergo mitosis (Taverna and Huttner, 2010) strongly co-express these proteins (Figure 6.7 C, Figure 6.8).

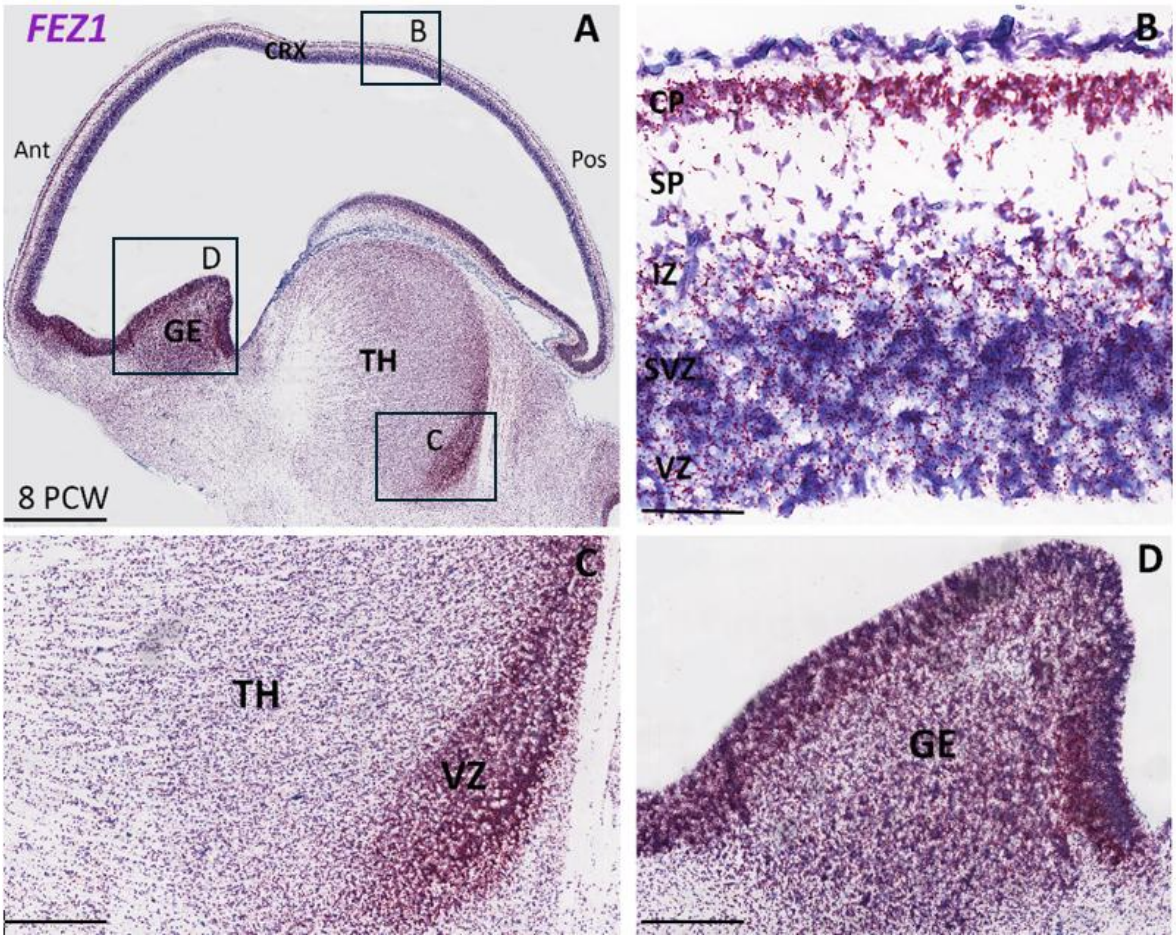

Figure 6.5. In situ hybridization of *FEZ1* expression at 8 PCW. (A) Sagittal section (8 PCW) shows *FEZ1* mRNA expression throughout the forebrain, and this is strongest in the ganglionic eminences and proliferative zones of the thalamus (counterstained with toluidine blue TB). (B) shows the dorsal neocortex at higher magnification. *FEZ1* expression was highest on the cortical plate, and there was moderate expression in the intermediate zone (IZ), ventricular and subventricular zones (VZ and SVZ). (C) shows *FEZ1* mRNA expression in the thalamus, strong expression in the proliferative zone and in postmitotic cells. (D) illustrates *FEZ1* expression in the ganglionic eminence, highly expressed in proliferative zone and in post mitotic cells. Abbreviations: anterior (Ant); posterior (Pos); thalamus (TH); ganglionic eminence (GE); cortex (CRX). Scale bars: A, 1 mm; B-D, 200 μm.

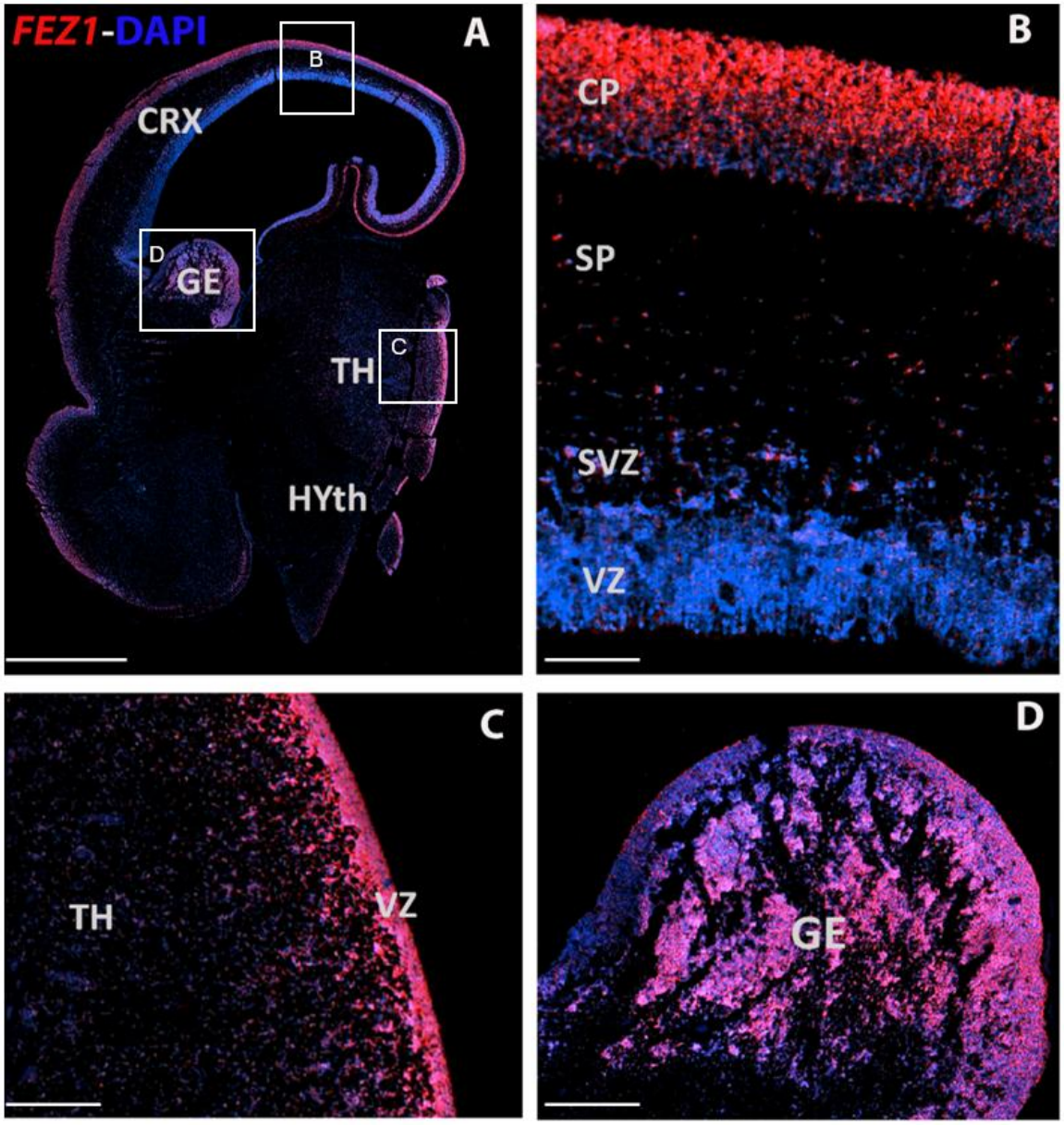

Figure 6.6. In situ hybridization of *FEZ1* expression at 8 PCW. (A) Coronal section (10 PCW) confirms the continued expression of *FEZ1* at this developmental stage, and the alternate pattern of stronger post-mitotic neuron expression in the cortex, and stronger progenitor zone expression in the ganglionic eminences and thalamus. (B) *FEZ1* was strongly expressed in the cortical plate, but weak expression was observed in the subventricular zone and in the ventricular zone of the cortex. (C) thalamus marks the location of higher magnification panels, showing strong expression in the ventricular zone and weak expression in the mantle zone. (D) Highly expressed in the postmitotic and ventricular zone of the ganglionic eminence but weak expression in the ventricular zone of the medial side of the ganglionic eminence. Abbreviations: cortex (CRX); subventricular zone (SVZ); ventricular zone (VZ); ganglionic eminences (GE); thalamus (TH); cortical plate (CP); subplate (SP); hypothalamus (HYth). Scale bars A,1 mm; B-D, 200 µm.

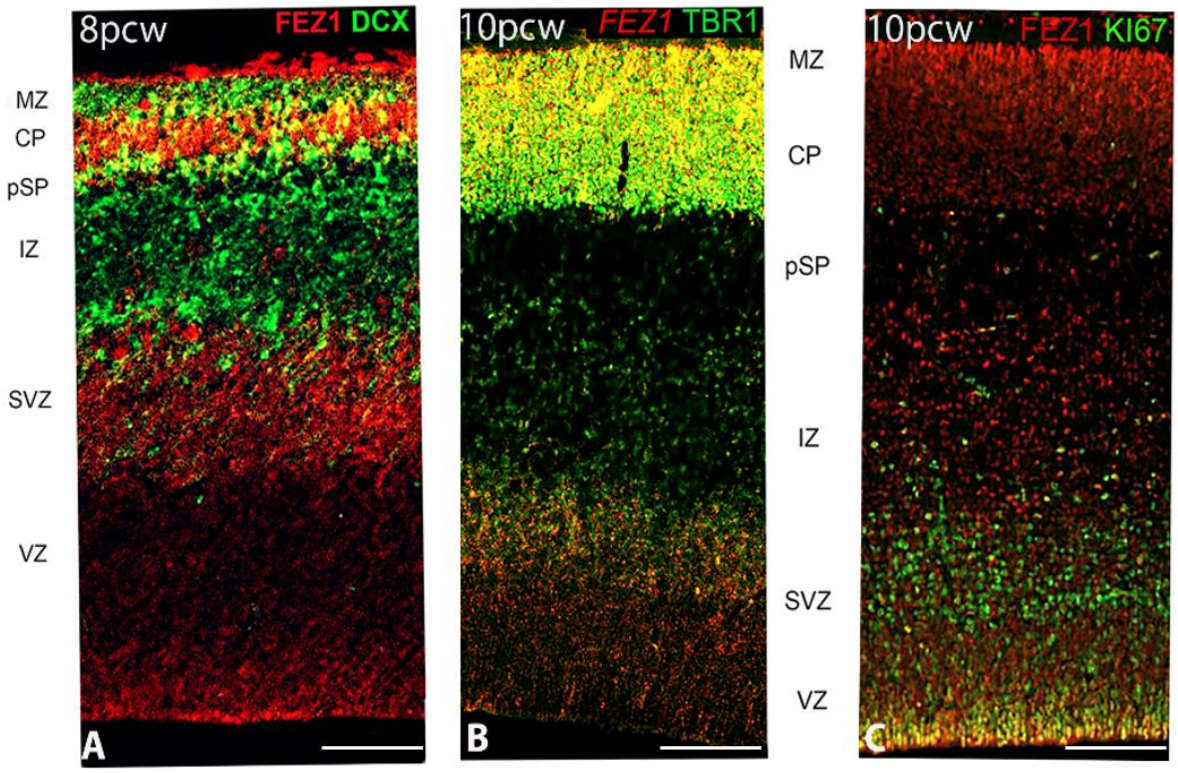

Figure 6.7. FEZ1 expression; protein and RNAscope 8-10 PCW. (A) Double immunofluorescence staining for the FEZ1 protein and the immature neuron marker doublecortin (DCX). FEZ1 was strongly expressed in the CP and also in the VZ and SVZ. There was also co-expression (yellow) with DCX in the CP, but not in the marginal zone, presubplate or the intermediate zone. (B) Fluorescent RNAscope/immunofluorescence staining for FEZ1 and the postmitotic neuron marker TBR1 shows strongest co-expression. (C) Double immunofluorescence staining for FEZ1 and cell division marker KI67. Strong co-expression (yellow) was seen in the cells on the apical (ventricular) surface, but there was minimal co-expression in the subventricular zone. Abbreviations: marginal zone (MZ); cortical plate (CP); presubplate (pSP); intermediate zone (IZ); subventricular zone (SVZ); ventricular zone (VZ). Scale bars A, B, C 300 μm.

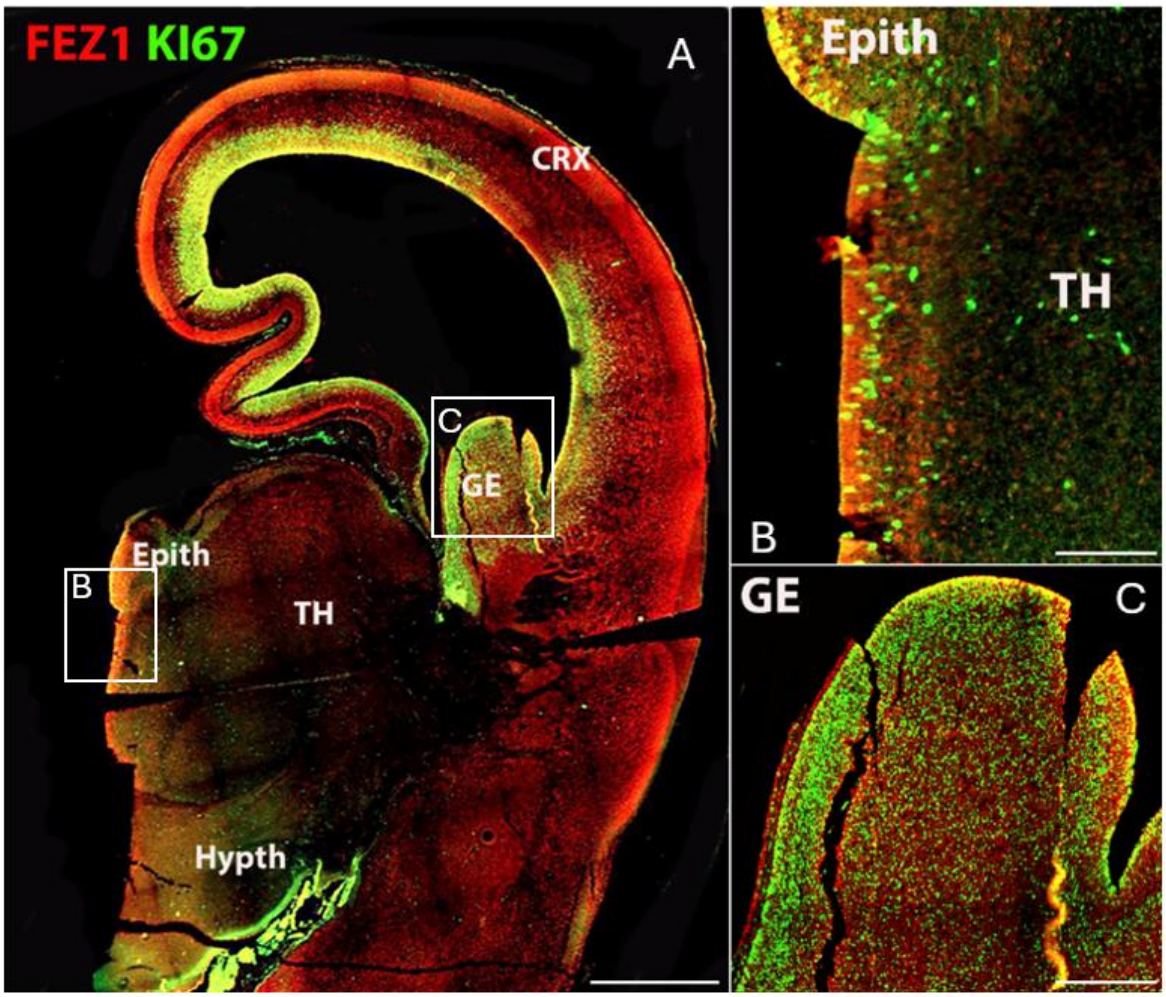

Figure 6.8. Immunofluorescence double labelling for FEZ1 and KI67 in a coronal section of 10 PCW human brain. FEZ1 was highly co-expressed in the ventricular zone in the cortex. High co-expression with KI67 in the proliferative zones of the ganglionic eminences (GE), co-expression in the ventricular zone of the thalamus and epithalamus. Abbreviations: epithalamus (Epith); cortex (CRX); ganglionic eminences (GE); thalamus (TH); hypothalamus (Hypth). Scale bars: (A) 1 mm, (B,C) 300 μm.

6.4.3 FEZ1 immunostaining at 12PCW

FEZ1 immunoreactivity was shown at 12 PCW in the cortex and the glutamatergic neurons, as well as in the progenitor cells in the ventricular zone of the cortex (Figure 6.9). FEZ1 was also expressed in the postmitotic cells present in the thalamus. Additionally, strong expression was evident in the proliferative zones of the ganglionic eminences and the postmitotic cells. High expression was evident in the cells in the ventricular zone of the thalamus, as well as in the epithalamus. Therefore, based on these findings, we can infer the FEZ1 protein is expressed in the post-mitotic neurons and progenitor cells in the cortex and ganglionic eminences, as well as in the thalamus and epithalamus.

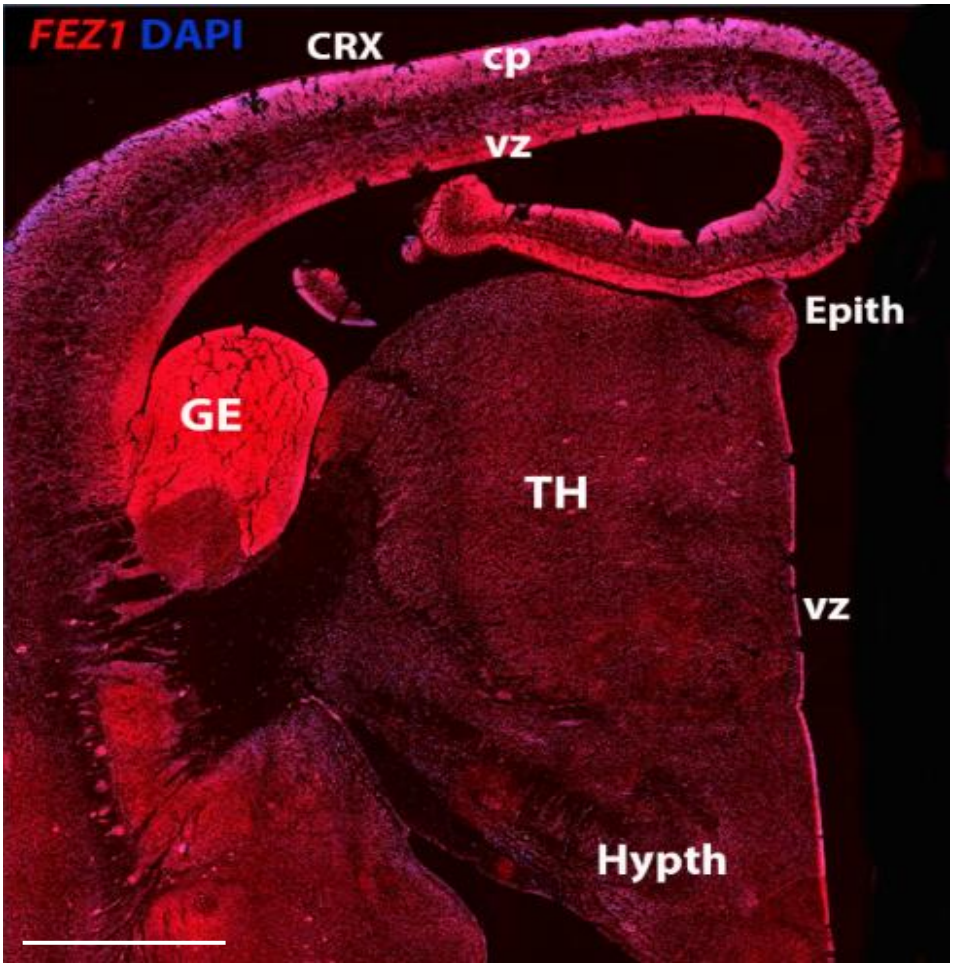

Figure 6.9. FEZ1 immunostaining in a coronal section of the 12 PCW human brain. FEZ1 was highly expressed in the glutamatergic neurons in the cortical plate (A, B). It was also expressed in the progenitor cells in the ventricular zone of the cortex (CRX). Additionally, there was high expression within the progenitor cells in the ganglionic eminences (GE), as well as in the VZ cells of the thalamus and of epithalamus. Abbreviations: epithalamus (Epith); cortex (CRX); ganglionic eminences (GE); thalamus (TH); hypothalamus (Hypth); cortical plate (cp); ventricular zone (vz). Scale bars; 1 mm.

6.4.4 *FEZ1* mRNA expression in a coronal section at 14PCW.

In Figure 6.10, the double labelling of the thalamic tissues revealed higher co-expression of *FEZ1* mRNA with GAD67 in the dorsoposterior region of the thalamus. Meanwhile, *FEZ1* showed strong expression in the LGN, MGN, VPL, PL and PM. Also, in the Ha and pretectum (pTC).

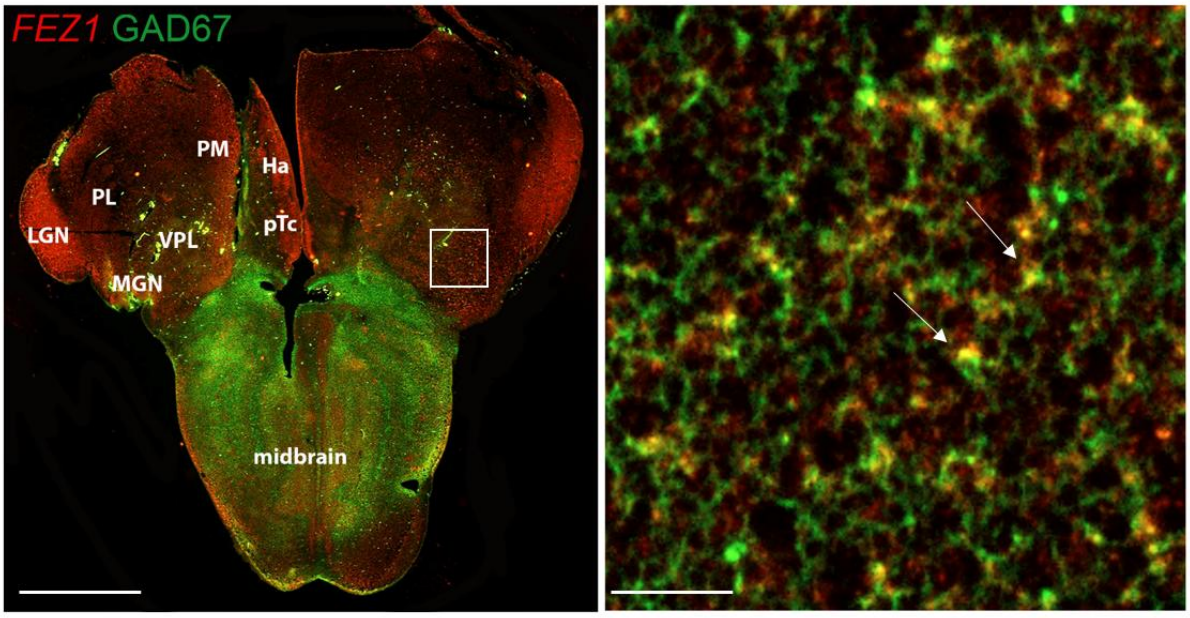

Figure 6.10. *FEZ1* mRNA expression combined with GAD67 immunofluorescence in the coronal section of the foetal human thalamus at 14 PCW. *FEZ1* was more strongly expressed in the thalamus, and GAD67 in the midbrain. However, the high power image shows co-expression in some neurons in the more lateral parts of the thalamus (white arrow). Abbreviations: lateral geniculate nucleus (LGN), medial geniculate nucleus (MGN), ventroposterolateral (VPL) and lateral and medial pulvinar (PL, PM); pretectum (pTc); habenula (Ha) Scale bars 1 mm; 300 μm.

6.4.5 FEZ1 protein expression with double labelling at 16 PCW

We explored the apparent reduced expression of FEZ1 by the GABAergic neurons by examining co-expression of GAD67 and FEZ1 by immunohistochemistry at 16 PCW. The reticular nucleus of the thalamus, which upon maturation comprises a sheet of GABAergic neurons surrounding the dorsal and lateral portions of the thalamus, showed high expression of GAD67, as expected, but little expression of FEZ1 (Figure 6.11). As demonstrated, there was a gradient of expression of GAD67 from the ventral and lateral to dorsal portions of the thalamus (Figure 6.11 A, B). Many FEZ1+ cell bodies were intermingled with GAD67+ cells in the more ventral parts of the thalamus, but there was little evidence of co-expression. This suggests thalamic post-mitotic thalamic glutamatergic neurons express FEZ1 at this stage of development. It also reveals potential pathways for the migration of GABAergic neurons into the thalamus from the prethalamus (precursor of the reticular nucleus) and the subthalamic midbrain regions at this stage of development. In other areas of high GABAergic cell density, such as the nascent basal ganglia, GAD67 immunoreactivity was high, although FEZ1 expression was relatively low. FEZ1 expression remained high in the adjacent subpallial GABAergic neuroprogenitor zones (Figure 6.11 C).

By 16 PCW, GABAergic neurons had increased in the cortex, having largely migrated there from the ganglionic eminences (Ma et al., 2013, Alzu'bi and Clowry, 2019). The majority of cortical GAD67+ neurons showed no double labelling for FEZ1 at 16 PCW, whether in or near the marginal zone, which is a major pathway for migrating GABAergic neurons at this stage of development (Zecevic and Rakic, 2001, Meyer and González-Gómez, 2018). Some small double-labelled cells were observed predominantly near or close to the MZ (Figure 6.11 D). These may be the small calretinin positive GABAergic interneurons previously described elsewhere (Meyer and González-Gómez, 2018, Alzu’bi and Clowry, 2020).

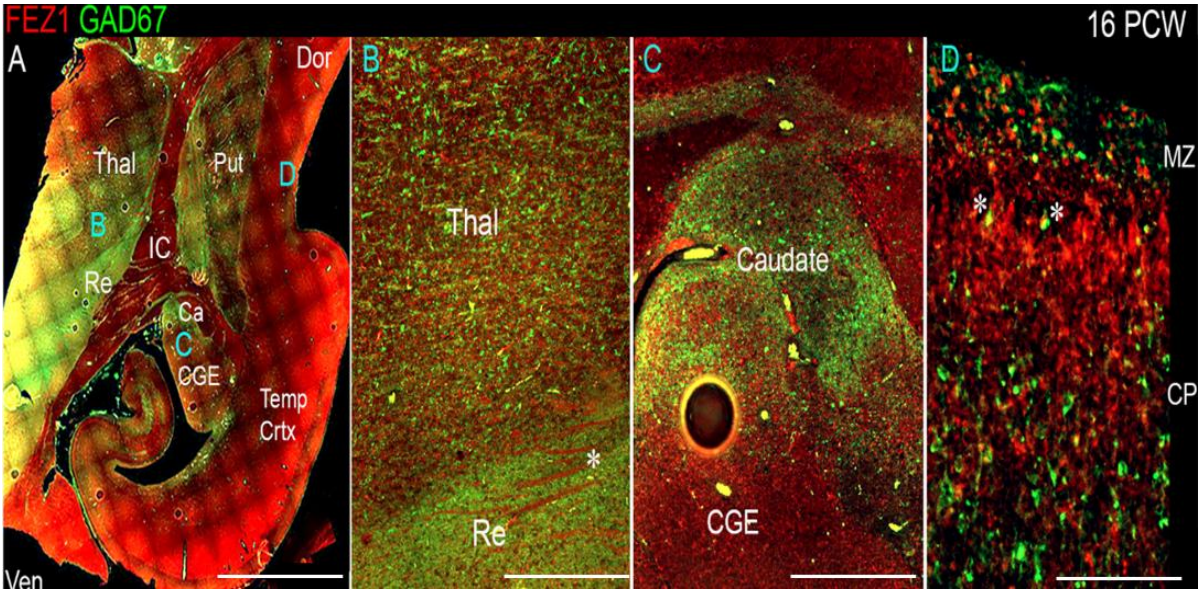

Figure 6.11. FEZ1/GAD67 immunofluorescence at 16 PCW. Coronal section showing temporal cortex, basal ganglia and thalamus (A). FEZ1 protein expression was seen throughout the section, GAD67 expression was strongest in the thalamic reticular nucleus and the subthalamic regions. FEZ1 was also moderately expressed in the putamen, caudate, ventral regions of the thalamus and cortical ventricular zone extending away from the caudal ganglionic eminence towards the hippocampal formation. (B) Close up of the boundary between the thalamic reticular nucleus and the latero-ventral part of the thalamus. In both locations there was little evidence of the co-expression of both markers in the same cell, although a higher proportion of red FEZ1+ cells can be seen in the thalamus. Also evident were bundles of FEZ1 positive axons (*), which are putative thalamocortical fibres. (C) A higher magnification image of the caudal ganglionic eminence (progenitor zone for basal ganglia and GABAergic cortical neurons) and the caudate nucleus (containing predominantly GABAergic neurons), illustrating how GABAergic neuron progenitors strongly expressed FEZ1 (red); whereas post-mitotic GAD67+ neurons (green) did not express FEZ1. Likewise, in the cortex (D) in the cortical plate GAD67+/FEZ1+ neurons were rare, although isolated examples of double labelled cells were seen close to the border with the marginal zone (asterisks). Abbreviations: dorsal (Dor); internal capsule (IC); ventral (Ven); caudal ganglionic eminence (CGE); thalamic reticular nucleus (Re); putamen (Put); caudate (Ca); thalamus (Thal); temporal cortex (Temp Crtx); marginal zone (MZ); cortical plate (CP). Scale bars A, 1 mm; B, C, 200 µm; D, 100 µm.

Relatively low FEZ1 expression in the subplate contrasted with stronger expression of both the growing axon marker GAP43 and FEZ1 in the cells of the cortical plate, and immunoreactivity in the inner fibre layer was less than in the ventricular zone (Figure 6.12). Double labelling for GAP43 and FEZ1 demonstrated a concentration of FEZ1 in selected axon pathways at 14 and 16 PCW. In the internal capsule at 16 PCW, FEZ1 was expressed by what appeared to be thalamocortical axons, whereas the adjacent corticofugal axons were GAP43+ only. We interpret this as showing that FEZ1 is selectively expressed by thalamocortical axons; although, more strongly in fasciculated axons proximal to the thalamus, than in the distal terminal branches in the subplate. FEZ1 expression is stronger in the cell bodies of glutamatergic neurons of the cortical plate than in the growing corticofugal axons in the internal capsule.

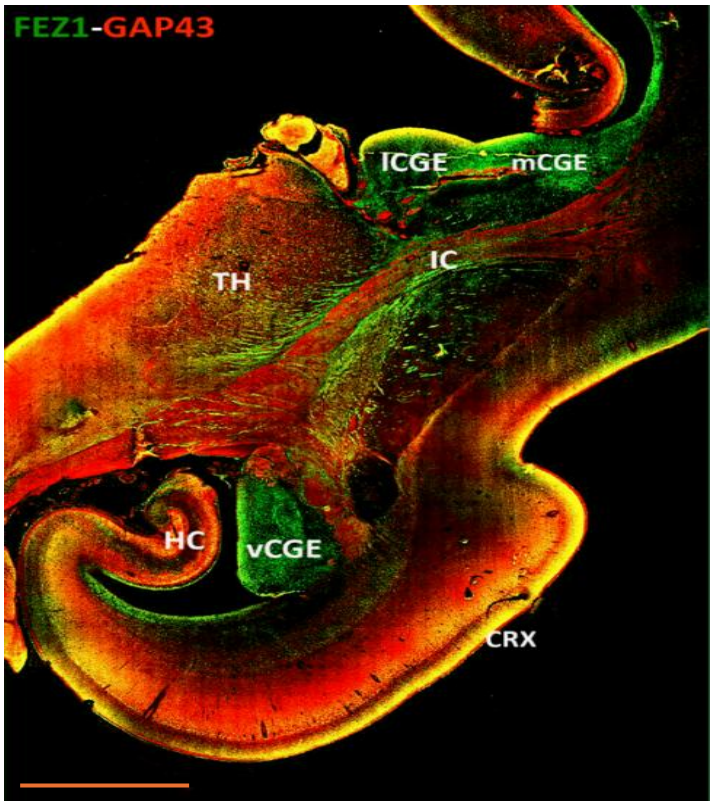

Figure 6.12. Double immunofluorescence for FEZ1 and GAP43; coronal section 16 PCW. GAP43 principally marks growing axons (Benowitz and Routtenberg, 1997) in the internal capsule (IC) FEZ1 and GAP43 marked different bundles of axons, suggesting FEZ1 may be expressed in fasciculating thalamocortical axons and GAP43 in growing corticofugal axons. FEZ1 was also strongly expressed in the proliferative medial and ventral caudal ganglionic eminences. Abbreviations: medial caudal ganglionic eminences (mCGE); ventral caudal ganglionic eminences (vCGE); lateral caudal ganglionic eminences (lCGE); Thalamus (TH); Cortex (CRX); Hippocampus (HC); Internal capsule (IC). Scale bar 1mm.

6.4.6 FEZ1 expression at 19 PCW

FEZ1 protein expression in the later developmental stages was not confined to neuronal cell bodies, but showed selective enrichment in certain axon pathways. For instance, strong expression was observed in the fornix and certain callosal axons at 19 PCW (Figure 6.13) but in the lateral cortical cortex, expression in the cortical intermediate zone, where large numbers of growing axons are found, was weak.

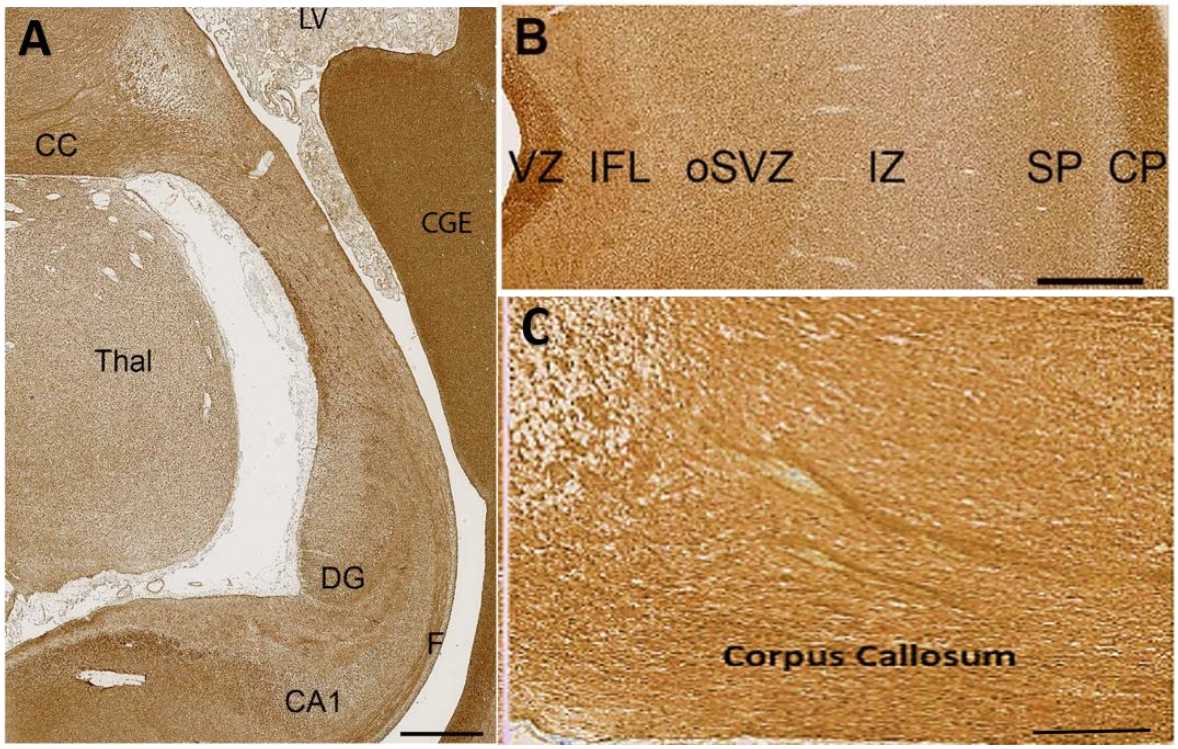

Figure 6.13. **FEZ1 expression in axons At 19 PCW.** (A) Posterior coronal section immunoperoxidase stained for FEZ1 at 19 PCW, containing medial cortex, thalamus (Thal) and caudal ganglionic eminence (CGE). The hippocampal cortex is evident and axons in the fornix (F) are strongly immunoreactive. Axons in the corpus callosum (C; CC) are also strongly positive, as is the CGE, which contains GABAergic neuroprogenitor cells. (B) FEZ1 immunoreactivity in the lateral cortical wall; strong in the outer cortical plate and ventricular zone (VZ) moderate in the inner fibre layer (IFL) outer subventricular zone (oSVZ) and subplate (SP) and weak in the axon rich intermediate zone (IZ). Abbreviations: Thalmus (Thal); Caudate ganglionic eminence (CGE); lateral ventricle (LV); corpus callosum (CC); dentate gyrus (DG); ventricular zone (VZ); inner fiber layer (IFL); outer subventricular zone (oSVZ); subplate (SP); intermediate zone (IZ); cortical plate (CP). Scale bar:1mm; 300µm.

6.4.7 *FEZ1* mRNA expression at 21 PCW

Expression appeared strong in the cortical plate right up to the oldest stage studied (21 PCW; Figure 6.14 A, E), particularly in the pyramidal layer of the hippocampus (Figure 6.14 D). Expression in the cortical plate was strongest at the boundary between the cortical plate and the marginal zone. This may partially reflect a higher density of cells at this location, but also reflects higher levels of expression per individual cell. These neurons are the most recent cells to have stopped migrating to the cortical plate at this stage, and this may suggest a role for FEZ1 in cell migration. This expression pattern has previously been observed for neurexins (Harkin et al., 2017, Ding et al., 2022), the intracellular transport of which is a mooted role for FEZ1 (see introduction). Intense expression of *FEZ1* by glutamatergic pyramidal neurons was a feature of the hippocampus; however, there was low expression in the stratum oriens, which contains predominantly GABAergic neurons of various phenotypes (Figure 6.14 A) (Freund and Buzsáki, 1996). Similarly, the caudal ganglionic eminence, containing GABAergic progenitor cells, showed relatively high expression compared to the overlying caudate nucleus, which is principally composed of post-mitotic GABAergic neurons. Relatively high levels of expression of FEZ1 were still observed in the cortical VZ and SVZ, although by this stage neurogenesis is ending and gliogenesis beginning (Cadwell et al., 2019). The VZ evidenced reduced levels of cell division at this stage (Nowakowski et al., 2016).

FEZ1 mRNA expression was maintained in the forebrain throughout the period of development, and this increased in the post-mitotic glutamatergic neurons of the thalamus. Different levels of expression were observed in different thalamic nuclei, with the lateral geniculate nucleus (LGN) showing higher levels of expression than the pulvinar (Figure 6.14 A, C). However, this at least partially reflects a higher cell density in the LGN. Nevertheless, distinct thalamic nuclei are identifiable at this age, differing from the earlier stages of development shown in Figure 6.5 and 6.6.

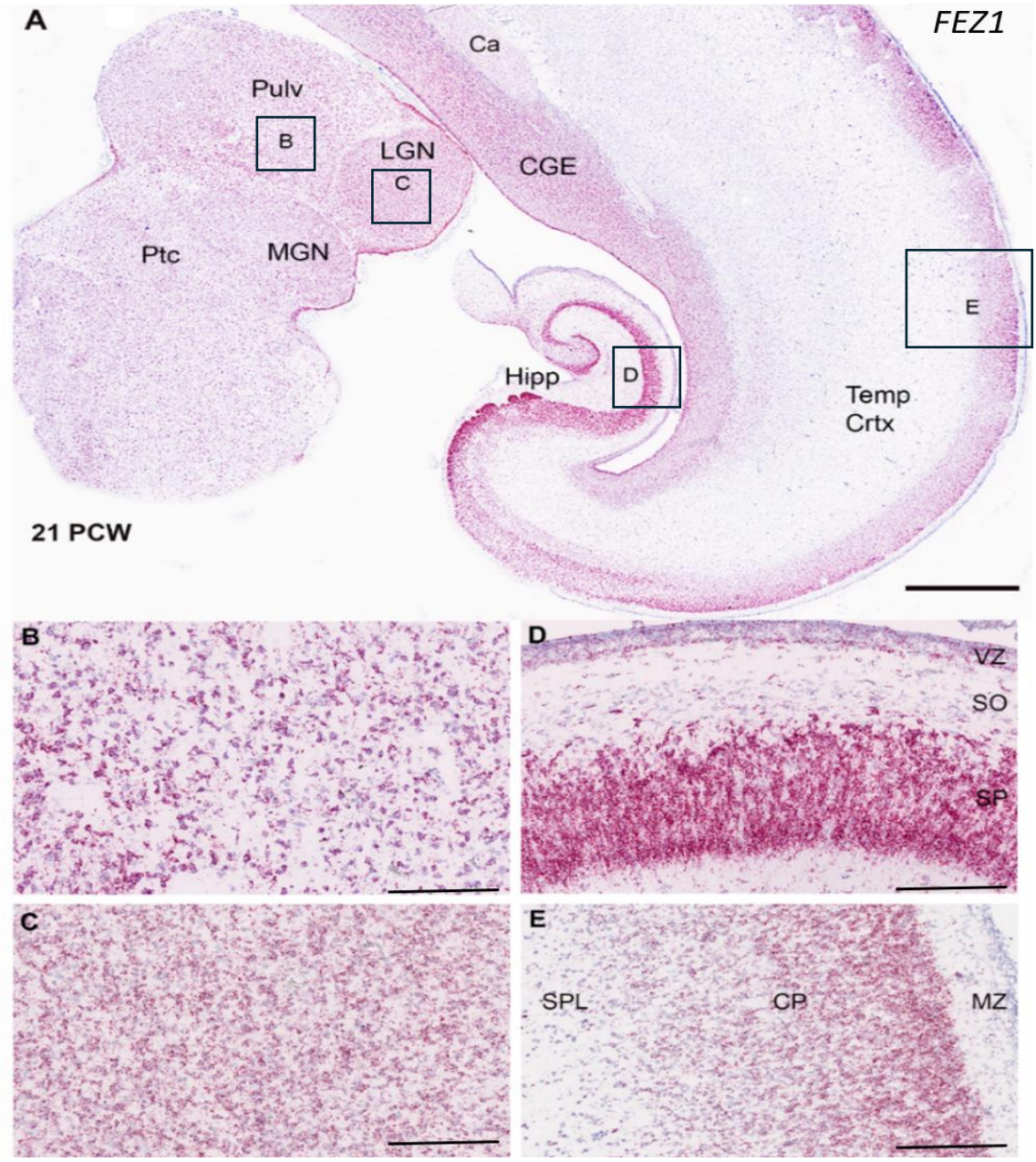

Figure 6.14. *FEZ1* expression: RNAscope at 21 PCW. (A) Coronal section showing temporal cortex, caudal ganglionic eminence and thalamus (Pulv, MGN and LGN). At low magnification, expression was present in both progenitor and postmitotic cell, and was positively correlated with cell density. However, expression appeared particularly dense in the hippocampus in the pyramidal cell layer. Higher magnification images of thalamus showed that the pulvinar region (pulv; B) has a lower cell density but similar density of staining per cell compared to the Lateral Geniculate Nucleus (LGN; C). However, in cortical areas the hippocampal stratum pyramidalis which contains predominantly glutamatergic neurons there was very high expression per cell compared to the stratum oriens which contains predominantly GABAergic neurons (D). In the neocortex (E), expression was highest in the outer layers of the cortical plate. Abbreviations: temporal cortex (Temp Crtx); caudal ganglionic eminence (CGE); lateral geniculate nucleus (LGN); medial geniculate nucleus (MGN); pulvinar (pulv); pretectum (Ptc); hippocampus (Hipp); subplate (SPL); Lateral Geniculate Nucleus (LGN); ventricular zone (VZ); stratum oriens (SO); stratum pyramidalis (SP); Scale bars; A, 1 mm; B–E, 200 μm.

6.5 Discussion

Transcriptomic analysis indicated that FEZ1 is significantly expressed in several cell types within the developing human forebrain, encompassing progenitor cells and post-mitotic neurones. Histological investigations have substantiated this finding, demonstrating that FEZ1 is prominently expressed in cortical glutamatergic neurones and minimally expressed in their progenitors. Conversely, in the ventral telencephalon and diencephalon during early developmental stages, expression is significantly greater in progenitor cells compared to post-mitotic cells. FEZ1 is primarily suggested to function in axon outgrowth. FEZ1 was prominently expressed in the cell bodies of certain neuronal groups and in the axons of other neurones. This indicates that FEZ1 has delineated roles specific to certain cell types in development. Our transcriptomic analysis strongly suggested *FEZ1* expression is closely coupled to the expression of genes associated with the SNARE complex and implicated in neurodevelopmental disorders (Figure 6.15). FEZ1 may play a significant role in transporting proteins, such as NRXN1 (Chapter 5) and STXBP1, to sites of exocytosis in the developing cortex (Figure 6.1). SNARE mediated exocytosis is not only significant in early synapse function, disruption of which could alter the forebrain's developmental trajectory (Molnár et al., 2020a), but also in adding plasma membrane to growing neurites at growth cones (Urbina and Gupton, 2020), another vital process intrinsic to early development. FEZ1 mRNA in humans is highly expressed in the brain; specifically in the thalamus and hippocampus (Gunaseelan et al., 2021). Recent studies using human cerebral organoids have highlighted the involvement of FEZ1 in early cortical brain development, noting that FEZ1 is detectable in both neuroprogenitor subtypes and immature neurons, and that FEZ1 deletion interferes with the expression of genes present in neuronal and synaptic development (Qu et al., 2023).

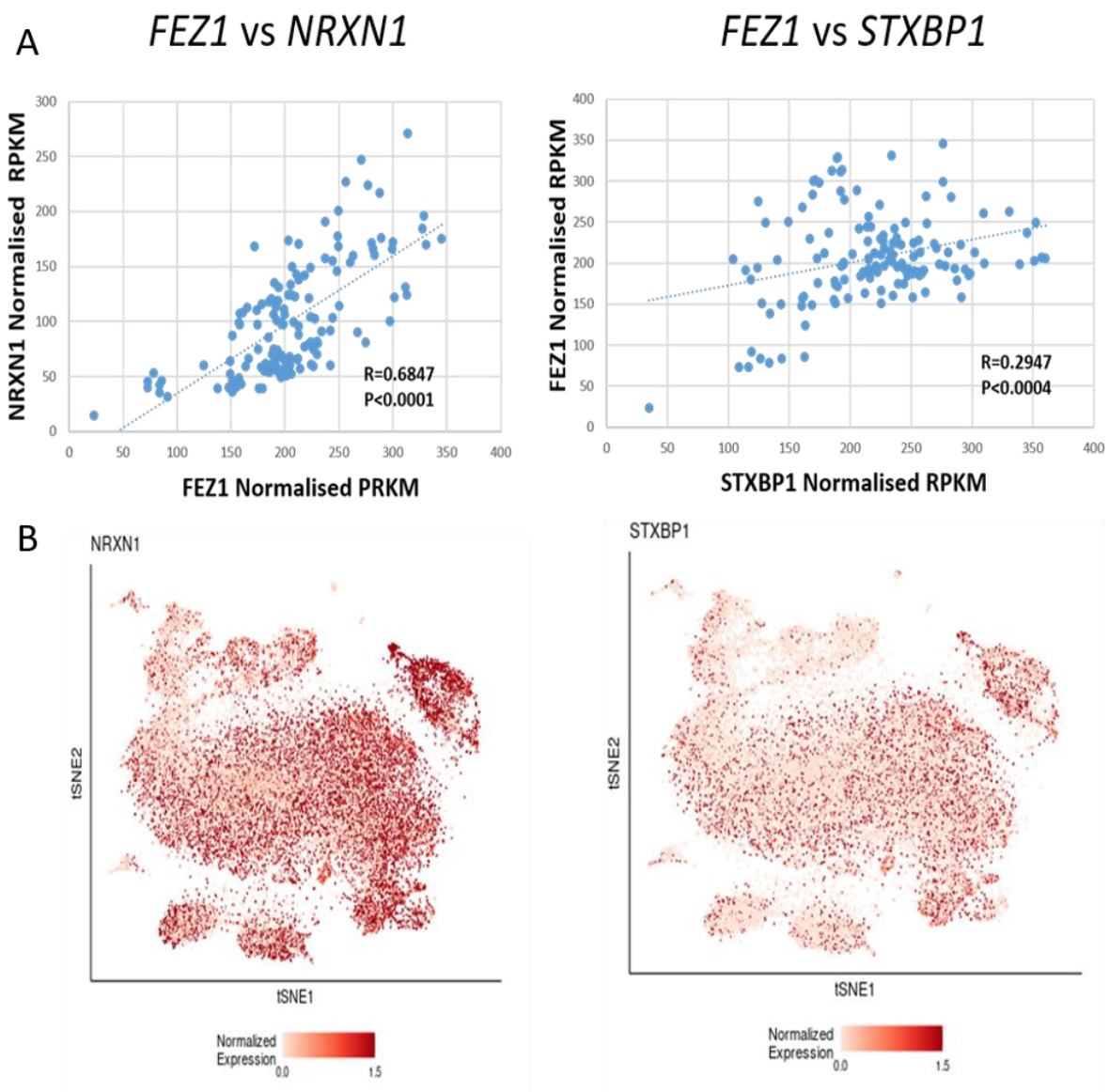

Figure 6.15. Whole tissue RNAseq performed on 138 cortical samples at various developmental stages (PCW). Expression levels given as normalised RPKM. Expression of FEZ1 was shown to increase significantly with age, and was highly correlated with the expression of both NRXN1 and STXBP1. Single cell RNAseq data for the cerebral cortex at 17/18 PCW was taken from solo.bmap.ucla.edu/shiny/webapp/, which shows FEZ1 expression is highly correlated with NRXN1, and STXBP1 susceptibility gene expression in the developing human cerebral cortex.

6.5.1 Telencephalic expression

In the cortex, *FEZ1* mRNA expression in the early stage of development (8-10 PCW) was greater in the cortical plate, which contains post-mitotic neurons. Furthermore, it only showed weak expression in the progenitor cells. It is also expressed in the proliferative zone and within post-mitotic neurons of ganglionic eminences. At 10 PCW, *FEZ1* mRNA showed stronger expression in the progenitor cells of the medial ganglionic eminences (Figure 6.6) than in lateral ganglionic eminences. In a different section, the FEZ1 protein expression seemed stronger in the lateral ganglionic eminence at 10 PCW (Figure 6.8). There is evidence that some ganglionic eminence derived cells may migrate to the cortex while retaining the capacity to undergo cell division, and that the human cerebral cortex itself may produce some GABAergic neuron specific progenitors (Radonjić et al., 2014, Alzu'bi et al., 2017, Delgado et al., 2022). FEZ1 expression in the later stages was more restricted to post-mitotic glutamatergic neurons and the cellular rather than the axonal compartment (with the exception of hippocampal fornix projections). *FEZ1* mRNA weakens in the progenitor cells and continues to be more restricted in post-mitotic cells in the cortical plate at 14, 16 and 19 PCW. However, in the cortical areas, FEZ1 mRNA showed strong staining in the hippocampal stratum pyramidale (SP), which contains predominantly glutamatergic neurons. Additionally, there was very high expression per cell compared to the stratum oriens (SO), which contains predominantly GABAergic neurons (Figure 6.14). However, it has been previously reported that FEZ1 shows high expression in GABAergic cells, which is contrary to our results (Sakae et al., 2008).

6.5.2 Axonal expression of FEZ1

Proper development of neuronal networks in the developing brain requires precise guidance when extending neuronal processes to their targets (Chua et al., 2021). Demonstrably, the FEZ1 protein has critical involvement in axon and dendrite development and plays a role as a common effector in the integration of guidance cue pathways to advance the development of axons and dendrites during the generation of neuronal networks, as has been previously highlighted (Chua et al., 2021). Our findings show FEZ1 is expressed in the thalamocortical axons at 16 PCW but is absent at 10-12 PCW (Figure 6.12-6.13). Moreover, FEZ1 was expressed in axons in the subplate and in the corpus callosum and the fornix (Figure 6.13) implicating it in axonal development (Maturana et al., 2010).

6.5.3 Thalamic expression

In the thalamus, *FEZ1* mRNA showed strong expression in the progenitor cells in the early stage of development of the human brain and weak expression in the post-mitotic cells. FEZ1 was expressed in the dividing cells, as evidenced by co-expression of FEZ1 with KI67 in the ventricular cells. FEZ1 mRNA at 14 PCW was expressed in a different nucleus, and there was co-expression with GAD67, which provides evidence of the presence of FEZ1 in the GABAergic neurons of the thalamus. The FEZ1 protein was expressed in the thalamic axons at 14 PCW and 16 PCW. Previously, disrupted thalamo-cortical-thalamic interactions have been strongly implicated in schizophrenia (Woodward and Heckers, 2016, Anticevic and Halassa, 2023). Altered FEZ1 expression in thalamic progenitors may similarly affect the differentiation of thalamic neurons. We also provide evidence for FEZ1 expression in post-mitotic thalamic neurons and their axons in the later stages of development, suggesting thalamic axon outgrowth and synapse formation may be affected. At 21 PCW, *FEZ1* mRNA started to become regionalized in specific nuclei, such as the pulvinar, which are classified as higher order nuclei associated with neurodevelopmental disorders (Homman-Ludiye and Bourne, 2019). This indicates that FEZ1 is implicated in the development of the human thalamus.

6.5.4 Implications of FEZ1 in schizophrenia

Characteristic symptoms of schizophrenia such as psychosis are exhibited in adolescence, although other symptoms, such as deficits in working memory, are present from childhood**.** Therefore, it is conceivable that the failures of cortical circuit formation in the earlier stages of development, including *in utero*, result in susceptibility to later disease manifestations as the brain matures. FEZ1 is implicated during initial neuronal development, and earlier loss of FEZ1 has been hypothesized to produce more acute developmental abnormalities (Chua et al., 2021). One of the genes related to schizophrenia encodes the protein Disrupted-In-Schizophrenia 1 (DISC1), and this was identified as an interactant with FEZ1 using a two-hybrid assay (Miyoshi et al., 2003). Specifically, the C-terminal of both proteins was required for this interaction. In addition, this interaction process was further confirmed by experiments in mammalian cells (Teixeira et al., 2019). Several converging lines of evidence have suggested that DISC1 Ser704Cys is of particular importance as a tool to increase the risk of schizophrenia through modifying DISC1 protein interactions (Burdick et al., 2008, DeRosse et al., 2007, Callicott et

al., 2005, Lipska et al., 2006). FEZ1 may play a role in dendrite and dendritic spine formation in cortical post-mitotic glutamatergic neurons (Glausier and Lewis, 2013). Hypofunctionality of pyramidal (glutamatergic) neurons in the cortex due to decreased dendritic spine and synapse formation has also been implicated in schizophrenia (Glausier and Lewis, 2013) at least in certain cortical regions, such as the dorsal prefrontal cortex. Cortical GABAergic interneurons are a group of cells implicated in schizophrenia (Sakae et al., 2008, Glausier and Lewis, 2013). For instance, in mice the schizophrenia susceptibility gene ErbB4 is exclusively expressed by GABAergic neurons in the cerebral cortex (Bean et al., 2014). It is thought that altered FEZ1 expression/activity in the progenitor cells of the ganglionic eminences may subtly alter the subsequent gene expression and differentiation of these cell types.

We conclude that FEZ1 is expressed in multiple classes of forebrain neuron and neural progenitors, and so may play a number of roles dependent on timing and the spatial and cellular localisation of expression. This may need to be studied further in human cell derived disease models to clarify the potential role FEZ1 plays in human neurodevelopment.

7 Chapter 7. General Discussion

In this thesis, beginning with the analyses of scRNAseq data, we demonstrated that it is possible to cluster different classes of cells in the thalamus at 16 PCW, as confirmed by immunohistochemistry or in situ hybridisation. A critical insight provided concerned the perhaps unexpected high proportion of dividing cells observed, as cell proliferation was previously believed to be complete before 16 PCW in the thalamus. This suggests neurogenesis, or at least gliogenesis, continues to occur at this developmental time point. The data also shows, a relatively high proportion of GABAergic neurons and their precursors were present. This may reflect the inclusion of the prethalamic structures in the sample, and indicate extensive invasion of the thalamus by GABAergic neurons of mid-brain origin, as well as possibly forebrain origin by 16 PCW. This study not only enhances our understanding of thalamic development, but also sets the stage for further investigations into the functional implications of associated cellular dynamics. Future research could also explore how the ongoing proliferation of specific cell types influences thalamic connectivity and the establishment of sensory pathways. Additionally, the role of neurosusceptibility genes, like *FEZ1* and *NRXN1*, in this context may provide valuable insights into the molecular mechanisms underlying neurodevelopmental disorders. Overall, these initial studies, and the ensuing findings, underscore the dynamic nature of thalamic development at 16 PCW, suggesting both neurogenesis and extensive cellular migration are pivotal processes that occur during this crucial period. A detailed exploration of these phenomena using live imaging and time-lapse microscopy as well as genetic fate mapping and lineage tracing, to unravel the complexities of thalamic function and its contribution to overall brain development, is therefore recommended as essential.

Further, we observed a relatively rapid transition from largely homogenous gene expression patterns in the thalamic mantle at 8 PCW to evidence of differentiated patterns of expression by 10 PCW and recognizable thalamic nuclei by 14 PCW. This suggests a combinatorial protomap of transcription factor expression guides the specification of thalamic neurons. It was anticipated that we would observe higher PAX6 expression in the VZ posteriorly and dorsally, but that it would be absent from the ZLI. However, PAX6 was expressed strongly in the prethalamus of p3, which would be expected to receive a relatively high dose of SHH,

indicating co-expression and regulation of specific receptors and regulators of SHH signalling pathways in target cells is critical. We observed a different gradient of expression of NR2F2 in thalamic VZ, with expression being highest posteriorly and ventrally. We also identified four zones to the human thalamic progenitor zone; anterior/ventral which is NR2F2+/PAX6-; anterior dorsal which is NR2F2-/PAX6-; posterior/ventral which is NR2F2+/PAX6- and posterior/dorsal which is NR2F2+/PAX6+. We further observed very weak expression of OLIG2 immunoreactivity in or near the VZ, although unfortunately, we only looked at this at 8 PCW and 14 PCW.

To investigate the emergence of thalamic nuclei in the foetal brain, we studied the expression patterns of a variety of transcription factors which display universal expression in thalamic post-mitotic neurons but show restricted expression to specific nuclei as development proceeds. GBX2 immunoreactivity was evident in the thalamus medially, and excluded from the ventricular zone at 8 PCW, being restricted to the medial and posterior regions of the thalamus as early as 10 PCW, and by 14 PCW confined to medial locations and the medial geniculate nucleus. We have also observed FOXP2 expression change from being homogenous across the thalamus at 8 PCW, to widespread but stronger medially and posterior at 10 PCW, to being strongly expressed only in specific nuclei (e.g. centromedian, medial geniculate nucleus, paraventricular thalamus) and absent from anterior nuclei by 14 PCW. *ZIC4* expression was widespread in the human thalamus at 8 PCW and expressed in the epithalamus as well, maintaining expression laterally where FOXP2 expression was weaker, but then showing expression confined to anterior and medial structures, and the lateral geniculate nucleus, by 14 PCW. Importantly, the detection of high SP8 immunoreactivity in the thalamus was a surprising finding. We provided evidence for a potential novel role for SP8 in thalamic development, which may be human specific, as it has not been previously reported in other studies in other species. Our findings also demonstrated that *SOX14*, OTX2 and GAD67 expressing cells appear in the posterior two thirds of the thalamus by 14 PCW. Our observations concur that the appearance of interneurons in the thalamus proceeds posterior to anterior, and is co-incident with the emergence of thalamic nuclei. This finding underscores the point that human thalamic development is taking place relatively earlier than might be expected**.** Future studies into SP8 and *SOX14* expression and functional role in the thalamus is warranted.

Next, we explored the expression of NRXN1 in foetal human forebrain development. Transcriptomic data analysis demonstrated that *NRXN1* was highly expressed by diverse cell types in the developing human forebrain, including progenitor cells and post-mitotic neurons.

Histological experiments also confirmed this, revealing that while NRXN1 (mRNA and protein) was strongly expressed by cortical glutamatergic neurons and weakly expressed by their progenitors, the opposite was the case for the GABAergic cells of the ganglionic eminences in the early stages of development, where expression is much stronger in progenitor cells than post-mitotic cells. In the diencephalon, NRXN1 was highly prominent in the glutamatergic neurons and intermediate progenitor cells, and weakly expressed by progenitor cells in the ventricular zone in the early stages (8, 10 PCW). At 12-14 PCW, *NRXN1* mRNA in the thalamus and epithalamus was expressed in quiescent progenitor cells in the ventricular zone and post-mitotic neurons. Additionally, telencephalic and thalamic expression of NRXN1 were studied. When examined at 8-10 PCW, *NRXN1* showed a strong expression pattern in the cortical plate, aligning with the findings of (Harkin et al., 2017) where the cortical plate showed the highest expression, as well as the apical ventricular zone of the cortex. Therefore, mutations in *NRXN1*α in early cortical development may potentially cause subtle alterations in rates and quantity of neuroblast production from radial glia CELLS (Harkin et al., 2017). PAX6 identifies radial glial cells in the proliferative ventricular (VZ) and subventricular (SVZ) zones. At 10 PCW, NRXN1 showed co-localisation with PAX6 in the proliferative zones, confirming that NRXN1 is expressed in radial glial cells as reported by (Harkin et al., 2017). However, expression of NRXN1 in the apical ventricular cells was higher in the ganglionic eminences than in the cortex. It was observed in the ventral but not dorsal LGE, LGE-like CGE, and MGE. This is the major site of GABAergic neuron production in the forebrain.

Potentially, NRXN1 mutations expressed in progenitor cells of the ganglionic eminences are the most likely cause of alterations to the production of cortical interneurons, and the neurons of the basal ganglia. Aside from the individual expression of the *NRXN1* gene, the study also unveiled the co-expression of *NRXN1* with suitable markers, elucidating its association with MKI67 (cell division), PAX6 (progenitor cells) in the ventricular zone of the thalamus and the cortex, *FOXP2* (postmitotic cells) at 14 PCW in the thalamus post-mitotic cells, and at 14 and 16 PCW with GAD67 (GABAergic neurons), respectively; thereby, emphasizing its multifaceted role in neurodevelopment throughout the gestational stages. We also observed that NRXN1 was highly expressed in the ventral pallium at 8 PCW. This was confirmed by demonstrating co-expression with NR2F1, which is present in the ventral pallium. These results suggest *NRXN1* is also a marker gene for the ventral pallium given its strong expression. Based on its expression patterns, we could also infer that NRXN1 expression plays a role in the developmental trajectories of both glutamatergic and GABAergic neurons. To summarize, our

findings suggest NRXN1 is involved in the human forebrain development, and we have shown the expression patterns at different stages of development of the human foetal forebrain. *NRXN1* is expressed in the earliest stages of human cortical development, showing distinct expression patterns. These findings could potentially pave the way for future diagnostic and therapeutic purposes associated with neurodevelopmental disorders involving *NRXN1*. Future functional experiments using live imaging and time-lapse microscopy in organotypic human brain slice cultures should be designed as a way to probe the potential roles of NRXN1 in cell migration and axon guidance, axon outgrowth, regulation of neuronal proliferation, and the early development of subplate circuitry. For example, using viral vector labelling, the migration of cells can be tracked and/or CRISPR-based fate-mapping techniques can be used to track specific cell populations. However, given the differences in anatomical organization, non-human animal models may not be ideal to study human thalamic development.

Next, we explored FEZ1 in the developing human forebrain. An analysis of transcriptomics data suggested FEZ1 is highly expressed in the developing human forebrain by a variety of cell types, including progenitor cells and post-mitotic neurons. Histological studies confirmed this, revealing that while FEZ1 was strongly expressed by cortical glutamatergic neurons and weakly expressed by their progenitors, the opposite was true in the ventral telencephalon and diencephalon in the early stages of development, where expression is much stronger in progenitor cells than in post-mitotic cells. Our transcriptomic analysis strongly suggested FEZ1 expression is closely coupled to the expression of proteins associated with the SNARE complex, which are also implicated in neurodevelopmental disorders. FEZ1 may also play a significant role in transporting proteins such as NRXN1 and STXBP1 to sites of exocytosis in the developing cortex. Notably, NRXN1 shares similarities with FEZ1 expression, in that both proteins interact with the SNARE complex, and both NRXN1 and FEZ1 are highly expressed in cortical glutamatergic neurons and GABAergic progenitor cells, although both proteins have low expression in cortical progenitor cells and GABAergic neurons (Alhesain et al., 2023).
In addition, we studied the telencephalic, thalamic and axonal expression of FEZ1. In the cortex, *FEZ1* mRNA expression in the early stage (8-10 PCW) showed marked expression in the cortical plate, which contains postmitotic neurons, but only weak expression in the progenitor cells. It is also expressed in the proliferative zone and in the postmitotic neurons of ganglionic eminences. At 10 PCW, in the ganglionic eminences, *FEZ1* mRNA showed strong expression in the progenitor cells of the medial ganglionic eminences compared with lateral ganglionic eminences. In a different section, FEZ1 protein expression appeared strong in the

lateral ganglionic eminence at 10 PCW. In the cortical areas, *FEZ1* mRNA showed strong staining in the hippocampal stratum pyramidale (SP), which contains predominantly glutamatergic neurons; there was also very high expression per cell compared to the stratum oriens (SO), which contains predominantly GABAergic neurons.

Our findings further showed that FEZ1 is expressed in thalamocortical axons. Furthermore, FEZ1 is expressed in axons in the subplate and in the corpus callosum, and in the fornix, meaning it is implicated in axonal development. In the thalamic region, *FEZ1* mRNA showed strong expression in the progenitor cells at early stage of the developing human brain and weak expression in the postmitotic cells. FEZ1 is also expressed in dividing cells, as evidenced by co-expression of FEZ1 with KI67 in the ventricular cells. *FEZ1* mRNA at 14 PCW showed co-expression with GAD67, providing evidence for FEZ1 in GABAergic neurons in the thalamus. The FEZ1 protein was expressed in the thalamic axons at 14 PCW and 16 PCW. We also provide evidence for FEZ1 expression in postmitotic thalamic neurons and their axons in the later stages of development, suggesting that thalamic axon outgrowth and synapse formation may be affected. At 21 PCW, *FEZ1* mRNA starts to become regionalized in specific nuclei, such as the pulvinar which are classified as higher order nuclei associated with neurodevelopmental disorders. This indicates FEZ1 is implicated in the development of the human thalamus. We conclude FEZ1 is expressed in multiple classes of forebrain neurons such as glutamatergic neurons, dividing cells and GABAergic neurons and neural progenitors, and fill a number of roles dependent on timing, and the spatial and cellular localisation of its expression.

7.1 Conclusion

In summary, this thesis aimed to explore the genes involved in human foetal forebrain development. We also outlined a protomap of transcription factor expression to guide the specification of thalamic neurons, considering the molecular players involved in the emergence of thalamic nuclei in the foetal brain. Further, we explored in great detail the expression patterns of the neurosusceptibility genes, *NRXN1* and *FEZ1*. We also elucidated the spatial and temporal expression profiles of these genes as they present in forebrain development. While providing critical insights into neurodevelopment itself, the findings also underscore the need for further human cell derived disease models to fully understand the potential roles of these genes in human neurodevelopment and neurodevelopmental disorders.

References

Acampora, D., Mazan, S., Lallemand, Y., Avantaggiato, V., Maury, M., Simeone, A. & Brûlet, P. 1995. Forebrain and midbrain regions are deleted in Otx2−/− mutants due to a defective anterior neuroectoderm specification during gastrulation. *Development,* 121**,** 3279-3290.

Acampora, D. & Simeone, A. 1999. The TINS lecture: Understanding the roles of Otx1 and Otx2 in the control of brain morphogenesis. *Trends in Neurosciences,* 22**,** 116-122.

Alhesain, M., Alzu'bi, A., Sankar, N., Smith, C., Kerwin, J., Laws, R., Lindsay, S. & Clowry, G. J. 2025. Development of the early fetal human thalamus: from a protomap to emergent thalamic nuclei. *Frontiers in Neuroanatomy,* 19**,** 1530236.

Alhesain, M., Ronan, H., LeBeau, F. E. & Clowry, G. J. 2023. Expression of the schizophrenia associated gene FEZ1 in the early developing fetal human forebrain. *Frontiers in Neuroscience,* 17**,** 1249973.

Alzu'bi, A. & Clowry, G. J. 2019. Expression of ventral telencephalon transcription factors ASCL1 and DLX2 in the early fetal human cerebral cortex. *Journal of Anatomy,* 235**,** 555-568.

Alzu'bi, A., Lindsay, S. J., Harkin, L. F., McIntyre, J., Lisgo, S. N. & Clowry, G. J. 2017. The transcription factors COUP-TFI and COUP-TFII have distinct roles in arealisation and GABAergic interneuron specification in the early human fetal telencephalon. *Cerebral Cortex,* 27**,** 4971-4987.

Alzu'bi, A. & Clowry, G. J. 2020. Multiple origins of secretagogin expressing cortical GABAergic neuron precursors in the early human fetal telencephalon. *Frontiers in Neuroanatomy,* 14**,** 61.

Alzu'bi, A., Homman-Ludiye, J., Bourne, J. A. & Clowry, G. J. 2019. Thalamocortical afferents innervate the cortical subplate much earlier in development in primate than in rodent. *Cerebral Cortex,* 29**,** 1706-1718.

Alzu'bi, A., Lindsay, S., Kerwin, J., Looi, S. J., Khalil, F. & Clowry, G. J. 2017. Distinct cortical and sub-cortical neurogenic domains for GABAergic interneuron precursor transcription factors NKX2. 1, OLIG2 and COUP-TFII in early fetal human telencephalon. *Brain Structure and Function,* 222**,** 2309-2328.

Anderson, S. A., Marín, O., Horn, C., Jennings, K. & Rubenstein, J. L. 2001. Distinct cortical migrations from the medial and lateral ganglionic eminences. *Development,* 128**,** 353-363.

Anderson, S. A., Qiu, M., Bulfone, A., Eisenstat, D. D., Meneses, J., Pedersen, R. & Rubenstein, J. L. 1997. Mutations of the homeobox genes Dlx-1 and Dlx-2 disrupt the striatal subventricular zone and differentiation of late born striatal neurons. *Neuron,* 19**,** 27-37.

Angevine Jr, J. B. 1970. Time of neuron origin in the diencephalon of the mouse. An autoradiographic study. *Journal of Comparative Neurology,* 139**,** 129-187.

Anholt, R. R. 2014. Olfactomedin proteins: central players in development and disease. *Frontiers in Cell and Developmental Biology,* 2**,** 6.

Anticevic, A. & Halassa, M. M. 2023. The thalamus in psychosis spectrum disorder. *Frontiers in Neuroscience,* 17**,** 1163600.

Arai, Y., Funatsu, N., Numayama-Tsuruta, K., Nomura, T., Nakamura, S. & Osumi, N. 2005. Role of Fabp7, a downstream gene of Pax6, in the maintenance of neuroepithelial cells during early embryonic development of the rat cortex. *Journal of Neuroscience,* 25**,** 9752-9761.

Arcelli, P., Frassoni, C., Regondi, M., De Biasi, S. & Spreafico, R. 1997. GABAergic neurons in mammalian thalamus: a marker of thalamic complexity? *Brain Research Bulletin,* 42**,** 27-37.

Areas, H.-O. V. 2013. Geniculocortical Input Drives Genetic Distinctions Between Primary. *science,* 1232806**,** 340.

Arellano, J. I., Morozov, Y. M., Micali, N. & Rakic, P. 2021. Radial glial cells: new views on old questions. *Neurochemical Research,* 46**,** 2512-2524.

Armentano, M., Filosa, A., Andolfi, G. & Studer, M. 2006. COUP-TFI is required for the formation of commissural projections in the forebrain by regulating axonal growth.

Aruga, J., Nagai, T., Tokuyama, T., Hayashizaki, Y., Okazaki, Y., Chapman, V. M. & Mikoshiba, K. 1996. The Mouse Zic Gene Family: HOMOLOGUES OF THE DROSOPHILA PAIR-RULE GENE odd-paired (∗). *Journal of Biological Chemistry,* 271**,** 1043-1047.

Asada, H., Kawamura, Y., Maruyama, K., Kume, H., Ding, R.-G., Kanbara, N., Kuzume, H., Sanbo, M., Yagi, T. & Obata, K. 1997. Cleft palate and decreased brain γ-aminobutyric acid in mice lacking the 67-kDa isoform of glutamic acid decarboxylase. *Proceedings of the National Academy of Sciences,* 94**,** 6496-6499.

Asede, D., Joseph, A. & Bolton, M. M. 2020. Deletion of NRXN1α impairs long-range and local connectivity in amygdala fear circuit. *Translational Psychiatry,* 10**,** 242.

Ashrafizadeh, M., Zarrabi, A., Orouei, S., Zabolian, A., Saleki, H., Azami, N., Bejandi, A. K., Mirzaei, S., Janaghard, M. N. & Hushmandi, K. 2021. Interplay between SOX9 transcription factor and microRNAs in cancer. *International Journal of Biological Macromolecules,* 183**,** 681-694.

Aslam, M., Ahmad, N., Srivastava, R. & Hemmer, B. 2012. TNF-alpha induced NFκB signaling and p65 (RelA) overexpression repress Cldn5 promoter in mouse brain endothelial cells. *Cytokine,* 57**,** 269-275.

Assaf, M., Calhoun, V. D., Kuzu, C. H., Kraut, M. A., Rivkin, P. R., Hart Jr, J. & Pearlson, G. D. 2006. Neural correlates of the object-recall process in semantic memory. *Psychiatry Research: Neuroimaging,* 147**,** 115-126.

Avazzadeh, S., Quinlan, L. R., Reilly, J., McDonagh, K., Jalali, A., Wang, Y., McInerney, V., Krawczyk, J., Ding, Y. & Fitzgerald, J. 2021. NRXN1α+/-is associated with increased excitability in ASD iPSC-derived neurons. *BMC Neuroscience,* 22**,** 1-14.

B Hughes, R., Whittingham-Dowd, J., Simmons, R. E., Clapcote, S. J., Broughton, S. J. & Dawson, N. 2020. Ketamine restores thalamic-prefrontal cortex functional connectivity in a mouse model of neurodevelopmental disorder-associated 2p16. 3 deletion. *Cerebral Cortex,* 30**,** 2358-2371.

Baek, S.-H., Maiorino, E., Kim, H., Glass, K., Raby, B. A. & Yuan, K. 2022. Single cell transcriptomic analysis reveals organ specific pericyte markers and identities. *Frontiers in Cardiovascular Medicine,* 9**,** 876591.

Bakken, T. E., van Velthoven, C. T., Menon, V., Hodge, R. D., Yao, Z., Nguyen, T. N., Graybuck, L. T., Horwitz, G. D., Bertagnolli, D. & Goldy, J. 2020. Single-cell RNA-seq uncovers shared and distinct axes of variation in dorsal LGN neurons in mice, non-human primates and humans. *bioRxiv***,** 2020.11. 05.367482.

Bakken, T. E., van Velthoven, C. T., Menon, V., Hodge, R. D., Yao, Z., Nguyen, T. N., Graybuck, L. T., Horwitz, G. D., Bertagnolli, D. & Goldy, J. 2021. Single-cell and single-nucleus RNA-seq uncovers shared and distinct axes of variation in dorsal LGN neurons in mice, non-human primates, and humans. *Elife,* 10**,** e64875.

Baldwin, M. K., Balaram, P. & Kaas, J. H. 2017. The evolution and functions of nuclei of the visual pulvinar in primates. *Journal of Comparative Neurology,* 525**,** 3207-3226.

Bandiera, S. & Molnár, Z. 2022. Development of the thalamocortical systems. *The Thalamus; Cambridge University Press: Cambridge, UK***,** 139-162.

Barch, D. M. 2014. Cerebellar-thalamic connectivity in schizophrenia. Oxford University Press US.

Bayatti, N., Moss, J. A., Sun, L., Ambrose, P., Ward, J. F., Lindsay, S. & Clowry, G. J. 2008. A molecular neuroanatomical study of the developing human neocortex from 8 to 17 postconceptional weeks revealing the early differentiation of the subplate and subventricular zone. *Cerebral Cortex,* 18**,** 1536-1548.

Bean, J. C., Lin, T. W., Sathyamurthy, A., Liu, F., Yin, D.-M., Xiong, W.-C. & Mei, L. 2014. Genetic labeling reveals novel cellular targets of schizophrenia susceptibility gene: distribution of GABA and non-GABA ErbB4-positive cells in adult mouse brain. *Journal of Neuroscience,* 34**,** 13549-13566.

Becker, L. M., Chen, S.-H., Rodor, J., de Rooij, L. P., Baker, A. H. & Carmeliet, P. 2023. Deciphering endothelial heterogeneity in health and disease at single-cell resolution: progress and perspectives. *Cardiovascular Research,* 119**,** 6-27.

Bell, S. M., Schreiner, C. M., Waclaw, R. R., Campbell, K., Potter, S. S. & Scott, W. J. 2003. Sp8 is crucial for limb outgrowth and neuropore closure. *Proceedings of the National Academy of Sciences,* 100**,** 12195-12200.

Benarroch, E. E. 2015. Pulvinar: associative role in cortical function and clinical correlations. *Neurology,* 84**,** 738-747.

Benowitz, L. I. & Routtenberg, A. 1997. GAP-43: an intrinsic determinant of neuronal development and plasticity. *Trends in Neurosciences,* 20**,** 84-91.

Bergamo, A., Gerdol, M., Pallavicini, A., Greco, S., Schepens, I., Hamelin, R., Armand, F., Dyson, P. J. & Sava, G. 2019. Lysozyme-Induced Transcriptional Regulation of TNF-α Pathway Genes in Cells of the Monocyte Lineage. *Int J Mol Sci,* 20.

Bertacchi, M., Parisot, J. & Studer, M. 2019. The pleiotropic transcriptional regulator COUP-TFI plays multiple roles in neural development and disease. *Brain Research,* 1705**,** 75-94.

Bertini Teixeira, M., Figueira, A. C. M., Furlan, A. S., Aquino, B., Alborghetti, M. R., Paes Leme, A. F., Wei, L. N. & Kobarg, J. 2018. Fasciculation and elongation zeta-1 protein (FEZ1) interacts with the retinoic acid receptor and participates in transcriptional regulation of the Hoxb4 gene. *FEBS Open Bio,* 8**,** 4-14.

Bertrand, N., Castro, D. S. & Guillemot, F. 2002. Proneural genes and the specification of neural cell types. *Nature Reviews Neuroscience,* 3**,** 517-530.

Bilgic, M., Wu, Q., Suetsugu, T., Shitamukai, A., Tsunekawa, Y., Shimogori, T., Kadota, M., Nishimura, O., Kuraku, S. & Kiyonari, H. 2023. Truncated radial glia as a common precursor in the late corticogenesis of gyrencephalic mammals. *Elife,* 12**,** RP91406.

Bluske, K. K., Kawakami, Y., Koyano-Nakagawa, N. & Nakagawa, Y. 2009. Differential activity of Wnt/β-catenin signaling in the embryonic mouse thalamus. *Developmental Dynamics,* 238**,** 3297-3309.

Boucard, A. A., Chubykin, A. A., Comoletti, D., Taylor, P. & Südhof, T. C. 2005. A splice code for trans-synaptic cell adhesion mediated by binding of neuroligin 1 to α-and β-neurexins. *Neuron,* 48**,** 229-236.

Braun, M. M., Etheridge, A., Bernard, A., Robertson, C. P. & Roelink, H. 2003. Wnt signaling is required at distinct stages of development for the induction of the posterior forebrain.

Broccoli, V., Boncinelli, E. & Wurst, W. 1999. The caudal limit of Otx2 expression positions the isthmic organizer. *Nature,* 401**,** 164-168.

Bruno, S., Ghelli Luserna di Rorà, A., Napolitano, R., Soverini, S., Martinelli, G. & Simonetti, G. 2022. CDC20 in and out of mitosis: a prognostic factor and therapeutic target in hematological malignancies. *Journal of Experimental & Clinical Cancer Research,* 41**,** 159.

Bryant, D. T., Landles, C., Papadopoulou, A. S., Benjamin, A. C., Duckworth, J. K., Rosahl, T., Benn, C. L. & Bates, G. P. 2017. Disruption to schizophrenia-associated gene Fez1 in the hippocampus of HDAC11 knockout mice. *Scientific Reports,* 7**,** 11900.

Bu, D.-F., Erlander, M. G., Hitz, B. C., Tillakaratne, N., Kaufman, D. L., Wagner-McPherson, C. B., Evans, G. A. & Tobin, A. J. 1992. Two human glutamate decarboxylases, 65-kDa GAD and 67-kDa GAD, are each encoded by a single gene. *Proceedings of the National Academy of Sciences,* 89**,** 2115-2119.

Buchmann, A., Dentico, D., Peterson, M. J., Riedner, B. A., Sarasso, S., Massimini, M., Tononi, G. & Ferrarelli, F. 2014. Reduced mediodorsal thalamic volume and prefrontal cortical spindle activity in schizophrenia. *Neuroimage,* 102**,** 540-547.

Bulfone, A., Puelles, L., Porteus, M., Frohman, M., Martin, G. & Rubenstein, J. 1993. Spatially restricted expression of Dlx-1, Dlx-2 (Tes-1), Gbx-2, and Wnt-3 in the embryonic day 12.5 mouse forebrain defines potential transverse and longitudinal segmental boundaries. *Journal of Neuroscience,* 13**,** 3155-3172.

Burdick, K. E., Kamiya, A., Hodgkinson, C. A., Lencz, T., DeRosse, P., Ishizuka, K., Elashvili, S., Arai, H., Goldman, D. & Sawa, A. 2008. Elucidating the relationship between DISC1, NDEL1 and NDE1 and the risk for schizophrenia: evidence of epistasis and competitive binding. *Human Molecular Genetics,* 17**,** 2462-2473.

Burger, P. C., Shibata, T. & Kleihues, P. 1986. The use of the monoclonal antibody Ki-67 in the identification of proliferating cells: application to surgical neuropathology. *The American Journal of Surgical Pathology,* 10**,** 611-617.

Butkevich, E., Härtig, W., Nikolov, M., Erck, C., Grosche, J., Urlaub, H., Schmidt, C. F., Klopfenstein, D. R. & Chua, J. J. E. 2016. Phosphorylation of FEZ1 by microtubule affinity regulating kinases regulates its function in presynaptic protein trafficking. *Scientific Reports,* 6**,** 26965.

Byne, W., Hazlett, E. A., Buchsbaum, M. S. & Kemether, E. 2009. The thalamus and schizophrenia: current status of research. *Acta Neuropathologica,* 117**,** 347-368.

Bystron, I., Blakemore, C. & Rakic, P. 2008. Development of the human cerebral cortex: Boulder Committee revisited. *Nature Reviews Neuroscience,* 9**,** 110-122.

C Yuen, R. K., Merico, D., Bookman, M., L Howe, J., Thiruvahindrapuram, B., Patel, R. V., Whitney, J., Deflaux, N., Bingham, J. & Wang, Z. 2017. Whole genome sequencing resource identifies 18 new candidate genes for autism spectrum disorder. *Nature Neuroscience,* 20**,** 602-611.

Caballero, I. M., Manuel, M. N., Molinek, M., Quintana-Urzainqui, I., Mi, D., Shimogori, T. & Price, D. J. 2014. Cell-autonomous repression of Shh by transcription factor Pax6 regulates diencephalic patterning by controlling the central diencephalic organizer. *Cell Reports,* 8**,** 1405-1418.

Cadwell, C. R., Bhaduri, A., Mostajo-Radji, M. A., Keefe, M. G. & Nowakowski, T. J. 2019. Development and arealization of the cerebral cortex. *Neuron,* 103**,** 980-1004.

Callicott, J. H., Straub, R. E., Pezawas, L., Egan, M. F., Mattay, V. S., Hariri, A. R., Verchinski, B. A., Meyer-Lindenberg, A., Balkissoon, R. & Kolachana, B. 2005. Variation in DISC1 affects hippocampal structure and function and increases risk for schizophrenia. *Proceedings of the National Academy of Sciences,* 102**,** 8627-8632.

Cao, S., Zhou, K., Zhang, Z., Luger, K. & Straight, A. F. 2018. Constitutive centromere-associated network contacts confer differential stability on CENP-A nucleosomes in vitro and in the cell. *Molecular Biology of The Cell,* 29**,** 751-762.

Carachi, R. & Doss, S. H. E. 2019. *Clinical embryology: an atlas of congenital malformations*, Springer.

Carballo, G. B., Honorato, J. R., de Lopes, G. P. F. & Spohr, T. C. L. d. S. e. 2018. A highlight on Sonic hedgehog pathway. *Cell Communication and Signaling,* 16**,** 1-15.

Carić, D., Gooday, D., Hill, R. E., McConnell, S. K. & Price, D. J. 1997. Determination of the migratory capacity of embryonic cortical cells lacking the transcription factor Pax-6. *Development,* 124**,** 5087-5096.

Chatterjee, M., Li, K., Chen, L., Maisano, X., Guo, Q., Gan, L. & Li, J. Y. 2012. Gbx2 regulates thalamocortical axon guidance by modifying the LIM and Robo codes. *Development,* 139**,** 4633-4643.

Chen, B., Schaevitz, L. R. & McConnell, S. K. 2005a. Fezl regulates the differentiation and axon targeting of layer 5 subcortical projection neurons in cerebral cortex. *Proceedings of the National Academy of Sciences,* 102**,** 17184-17189.

Chen, F., Venugopal, V., Murray, B. & Rudenko, G. 2011. The structure of neurexin 1α reveals features promoting a role as synaptic organizer. *Structure,* 19**,** 779-789.

Chen, J.-G., Rašin, M.-R., Kwan, K. Y. & Šestan, N. 2005b. Zfp312 is required for subcortical axonal projections and dendritic morphology of deep-layer pyramidal neurons of the cerebral cortex. *Proceedings of the National Academy of Sciences,* 102**,** 17792-17797.

Chen, L., Guo, Q. & Li, J. Y. 2009. Transcription factor Gbx2 acts cell-nonautonomously to regulate the formation of lineage-restriction boundaries of the thalamus.

Chen, S. X., Tari, P. K., She, K. & Haas, K. 2010. Neurexin-neuroligin cell adhesion complexes contribute to synaptotropic dendritogenesis via growth stabilization mechanisms in vivo. *Neuron,* 67**,** 967-983.

Cheng, H., Zhang, N. & Pati, D. 2020. Cohesin subunit RAD21: From biology to disease. *Gene,* 758**,** 144966.

Chih, B., Gollan, L. & Scheiffele, P. 2006. Alternative splicing controls selective trans-synaptic interactions of the neuroligin-neurexin complex. *Neuron,* 51**,** 171-178.

Child, N. D. & Benarroch, E. E. 2013. Anterior nucleus of the thalamus: functional organization and clinical implications. *Neurology,* 81**,** 1869-1876.

Ching, M. S., Shen, Y., Tan, W. H., Jeste, S. S., Morrow, E. M., Chen, X., Mukaddes, N. M., Yoo, S. Y., Hanson, E. & Hundley, R. 2010. Deletions of NRXN1 (neurexin-1) predispose to a wide spectrum of developmental disorders. *American Journal of Medical Genetics Part B: Neuropsychiatric Genetics,* 153**,** 937-947.

Choe, Y.-G., Yoon, J.-H., Joo, J., Kim, B., Hong, S. P., Koh, G. Y., Lee, D.-S., Oh, W.-Y. & Jeong, Y. 2022. Pericyte loss leads to capillary stalling through increased leukocyte-endothelial cell interaction in the brain. *Frontiers in Cellular Neuroscience,* 16**,** 92.

Chua, J. J. E., Butkevich, E., Worseck, J. M., Kittelmann, M., Grønborg, M., Behrmann, E., Stelzl, U., Pavlos, N. J., Lalowski, M. M. & Eimer, S. 2012. Phosphorylation-regulated axonal dependent transport of syntaxin 1 is mediated by a Kinesin-1 adapter. *Proceedings of the National Academy of Sciences,* 109**,** 5862-5867.

Chua, J. Y., Ng, S. J., Yagensky, O., Wanker, E. E. & Chua, J. J. E. 2021. FEZ1 forms complexes with CRMP1 and DCC to regulate axon and dendrite development. *Eneuro,* 8.

Chui, R. & Dorovini-Zis, K. 2010. Regulation of CCL2 and CCL3 expression in human brain endothelial cells by cytokines and lipopolysaccharide. *Journal of Neuroinflammation,* 7**,** 1-12.

Clegg, J. M., Li, Z., Molinek, M., Caballero, I. M., Manuel, M. N. & Price, D. J. 2015. Pax6 is required intrinsically by thalamic progenitors for the normal molecular patterning of thalamic neurons but not the growth and guidance of their axons. *Neural Development,* 10**,** 1-12.

Clowry, G. J., Alzu'bi, A., Harkin, L. F., Sarma, S., Kerwin, J. & Lindsay, S. J. Charting the protomap of the human telencephalon. Seminars in Cell & Developmental Biology, 2018. Elsevier, 3-14.

Colas, J. F. & Schoenwolf, G. C. 2001. Towards a cellular and molecular understanding of neurulation. *Developmental Dynamics: an Official Publication of the American Association of Anatomists,* 221**,** 117-145.

Colmers, W. F. 1990. Modulation of synaptic transmission in hippocampus by neuropeptide Y: presynaptic actions. *Ann NY Acad Sci,* 611**,** 206-218.

Comoletti, D., Flynn, R. E., Boucard, A. A., Demeler, B., Schirf, V., Shi, J., Jennings, L. L., Newlin, H. R., Südhof, T. C. & Taylor, P. 2006. Gene selection, alternative splicing, and post-translational processing regulate neuroligin selectivity for β-neurexins. *Biochemistry,* 45**,** 12816-12827.

Condie, B. G., Bain, G., Gottlieb, D. I. & Capecchi, M. R. 1997. Cleft palate in mice with a targeted mutation in the γ-aminobutyric acid-producing enzyme glutamic acid decarboxylase 67. *Proceedings of the National Academy of Sciences,* 94**,** 11451-11455.

Copp, A. J., Greene, N. D. & Murdoch, J. N. 2003. The genetic basis of mammalian neurulation. *Nature Reviews Genetics,* 4**,** 784-793.

Corbin, J. G., Rutlin, M., Gaiano, N. & Fishell, G. 2003. Combinatorial function of the homeodomain proteins Nkx2. 1 and Gsh2 in ventral telencephalic patterning.

Cotrufo, T., Pérez-Brangulí, F., Muhaisen, A., Ros, O., Andrés, R., Baeriswyl, T., Fuschini, G., Tarrago, T., Pascual, M. & Urena, J. 2011. A signaling mechanism coupling netrin-1/deleted in colorectal cancer chemoattraction to SNARE-mediated exocytosis in axonal growth cones. *Journal of Neuroscience,* 31**,** 14463-14480.

Covington, B. P. & Al Khalili, Y. 2019. Neuroanatomy, nucleus lateral geniculate.

Davatolhagh, M. F. & Fuccillo, M. V. 2021. Neurexin1α differentially regulates synaptic efficacy within striatal circuits. *Cell Reports,* 34.

De Rosa, A., Pellegatta, S., Rossi, M., Tunici, P., Magnoni, L., Speranza, M. C., Malusa, F., Miragliotta, V., Mori, E. & Finocchiaro, G. 2012. A radial glia gene marker, fatty acid binding protein 7 (FABP7), is involved in proliferation and invasion of glioblastoma cells. *PloS One,* 7**,** e52113.

Dean, C., Scholl, F. G., Choih, J., DeMaria, S., Berger, J., Isacoff, E. & Scheiffele, P. 2003. Neurexin mediates the assembly of presynaptic terminals. *Nature Neuroscience,* 6**,** 708-716.

Delgado, R. N., Allen, D. E., Keefe, M. G., Mancia Leon, W. R., Ziffra, R. S., Crouch, E. E., Alvarez-Buylla, A. & Nowakowski, T. J. 2022. Individual human cortical progenitors can produce excitatory and inhibitory neurons. *Nature,* 601**,** 397-403.

Delvecchio, G., Sugranyes, G. & Frangou, S. 2013. Evidence of diagnostic specificity in the neural correlates of facial affect processing in bipolar disorder and schizophrenia: a meta-analysis of functional imaging studies. *Psychological Medicine,* 43**,** 553-569.

DeRosse, P., Hodgkinson, C. A., Lencz, T., Burdick, K. E., Kane, J. M., Goldman, D. & Malhotra, A. K. 2007. Disrupted in schizophrenia 1 genotype and positive symptoms in schizophrenia. *Biological Psychiatry,* 61**,** 1208-1210.

Dessaud, E., McMahon, A. P. & Briscoe, J. 2008. Pattern formation in the vertebrate neural tube: a sonic hedgehog morphogen-regulated transcriptional network.

Dharmapal, D., Jyothy, A., Mohan, A., Balagopal, P., George, N. A., Sebastian, P., Maliekal, T. T. & Sengupta, S. 2021. β-Tubulin Isotype, TUBB4B, Regulates The Maintenance of Cancer Stem Cells. *Frontiers in Oncology,* 11**,** 788024.

Ding, S. L., Royall, J. J., Lesnar, P., Facer, B. A., Smith, K. A., Wei, Y., Brouner, K., Dalley, R. A., Dee, N. & Dolbeare, T. A. 2022. Cellular resolution anatomical and molecular atlases for prenatal human brains. *Journal of Comparative Neurology,* 530**,** 6-503.

Dixon, G. & Harper, C. G. 2001. Quantitative analysis of glutamic acid decarboxylase-immunoreactive neurons in the anterior thalamus of the human brain. *Brain Research,* 923**,** 39-44.

Domin, H. 2021. Neuropeptide Y Y2 and Y5 receptors as potential targets for neuroprotective and antidepressant therapies: Evidence from preclinical studies. *Progress in Neuro-Psychopharmacology and Biological Psychiatry,* 111**,** 110349.

Domin, H., Kajta, M. & Smialowska, M. 2006. Neuroprotective effects of MTEP, a selective mGluR5 antagonist and neuropeptide Y on the kainate-induced toxicity in primary neuronal cultures. *Pharmacological Reports,* 58**,** 846.

Donnelly, L. 2011. The brain: functional divisions. *Anaesthesia & Intensive Care Medicine,* 12**,** 208-213.

Dorph-Petersen, K.-A. & Lewis, D. A. 2017. Postmortem structural studies of the thalamus in schizophrenia. *Schizophrenia Research,* 180**,** 28-35.

Duan, D., Fu, Y., Paxinos, G. & Watson, C. 2013. Spatiotemporal expression patterns of Pax6 in the brain of embryonic, newborn, and adult mice. *Brain Structure and Function,* 218**,** 353-372.

Duque, A., Krsnik, Z., Kostović, I. & Rakic, P. 2016. Secondary expansion of the transient subplate zone in the developing cerebrum of human and nonhuman primates. *Proceedings of the National Academy of Sciences,* 113**,** 9892-9897.

Džaja, D., Hladnik, A., Bičanić, I., Baković, M. & Petanjek, Z. 2014. Neocortical calretinin neurons in primates: increase in proportion and microcircuitry structure. *Frontiers in Neuroanatomy,* 8**,** 103.

Ebisu, H., Iwai-Takekoshi, L., Fujita-Jimbo, E., Momoi, T. & Kawasaki, H. 2017. Foxp2 regulates identities and projection patterns of thalamic nuclei during development. *Cerebral Cortex,* 27**,** 3648-3659.

Englund, C., Fink, A., Lau, C., Pham, D., Daza, R. A., Bulfone, A., Kowalczyk, T. & Hevner, R. F. 2005. Pax6, Tbr2, and Tbr1 are expressed sequentially by radial glia, intermediate progenitor cells, and postmitotic neurons in developing neocortex. *Journal of Neuroscience,* 25**,** 247-251.

Ericson, J., Rashbass, P., Schedl, A., Brenner-Morton, S., Kawakami, A., Van Heyningen, V., Jessell, T. & Briscoe, J. 1997. Pax6 controls progenitor cell identity and neuronal fate in response to graded Shh signaling. *Cell,* 90**,** 169-180.

Erlander, M. G., Tillakaratne, N. J., Feldblum, S., Patel, N. & Tobin, A. J. 1991. Two genes encode distinct glutamate decarboxylases. *Neuron,* 7**,** 91-100.

Esclassan, F., Francois, J., Phillips, K. G., Loomis, S. & Gilmour, G. 2015. Phenotypic characterization of nonsocial behavioral impairment in neurexin 1α knockout rats. *Behavioral Neuroscience,* 129**,** 74.

Etherton, M. R., Blaiss, C. A., Powell, C. M. & Südhof, T. C. 2009. Mouse neurexin-1α deletion causes correlated electrophysiological and behavioral changes consistent with cognitive impairments. *Proceedings of the National Academy of Sciences,* 106**,** 17998-18003.

Euiseok J. Kim, C. T. L., Randall R. Reed and Jane E. Johnson 2007. In Vivo Analysis of Ascl1 Defined Progenitors Reveals Distinct Developmental Dynamics during Adult Neurogenesis and Gliogenesis. *The Journal of Neuroscience,* 27**,** 12764-12774.

Evans, A. E., Kelly, C., Precious, S. V. & Rosser, A. E. 2012. Molecular regulation of striatal development: a review. *Anatomy research international,* 2012**,** 106529.

Eze, U. C., Bhaduri, A., Haeussler, M., Nowakowski, T. J. & Kriegstein, A. R. 2021. Single-cell atlas of early human brain development highlights heterogeneity of human neuroepithelial cells and early radial glia. *Nature Neuroscience,* 24**,** 584-594.

Falcone, C., Penna, E., Hong, T., Tarantal, A. F., Hof, P. R., Hopkins, W. D., Sherwood, C. C., Noctor, S. C. & Martínez-Cerdeño, V. 2021. Cortical interlaminar astrocytes are generated prenatally, mature postnatally, and express unique markers in human and nonhuman primates. *Cerebral Cortex,* 31**,** 379-395.

Feng, J., Schroer, R., Yan, J., Song, W., Yang, C., Bockholt, A., Cook Jr, E. H., Skinner, C., Schwartz, C. E. & Sommer, S. S. 2006. High frequency of neurexin 1β signal peptide structural variants in patients with autism. *Neuroscience letters,* 409**,** 10-13.

Ferland, R. J., Cherry, T. J., Preware, P. O., Morrisey, E. E. & Walsh, C. A. 2003. Characterization of Foxp2 and Foxp1 mRNA and protein in the developing and mature brain. *Journal of comparative Neurology,* 460**,** 266-279.

Filser, M., Gardie, B., Wemeau, M., Aguilar-Martinez, P., Giansily-Blaizot, M. & Girodon, F. 2022. Importance of sequencing HBA1, HBA2 and HBB genes to confirm the diagnosis of high oxygen affinity hemoglobin. *Genes,* 13**,** 132.

Flaherty, E., Zhu, S., Barretto, N., Cheng, E., Deans, P. M., Fernando, M. B., Schrode, N., Francoeur, N., Antoine, A. & Alganem, K. 2019. Neuronal impact of patient-specific aberrant NRXN1α splicing. *Nature Genetics,* 51**,** 1679-1690.

Flames, N., Pla, R., Gelman, D. M., Rubenstein, J. L., Puelles, L. & Marín, O. 2007. Delineation of multiple subpallial progenitor domains by the combinatorial expression of transcriptional codes. *Journal of Neuroscience,* 27**,** 9682-9695.

Fode, C., Ma, Q., Casarosa, S., Ang, S.-L., Anderson, D. J. & Guillemot, F. 2000. A role for neural determination genes in specifying the dorsoventral identity of telencephalic neurons. *Genes & Development,* 14**,** 67-80.

Forsingdal, A., Jørgensen, T. N., Olsen, L., Werge, T., Didriksen, M. & Nielsen, J. 2019. Can animal models of copy number variants that predispose to schizophrenia elucidate underlying biology? *Biological Psychiatry,* 85**,** 13-24.

Frantz, G. D., Weimann, J. M., Levin, M. E. & McConnell, S. K. 1994. Otx1 and Otx2 define layers and regions in developing cerebral cortex and cerebellum. *Journal of Neuroscience,* 14**,** 5725-5740.

Freund, T. F. & Buzsáki, G. 1996. Interneurons of the hippocampus. *Hippocampus,* 6**,** 347-470.

Friedman, J., Baross, Á., Delaney, A. D., Ally, A., Arbour, L., Asano, J., Bailey, D. K., Barber, S., Birch, P. & Brown-John, M. 2006. Oligonucleotide microarray analysis of genomic imbalance in children with mental retardation. *The American Journal of Human Genetics,* 79**,** 500-513.

Fung, S. J., Joshi, D., Allen, K. M., Sivagnanasundaram, S., Rothmond, D. A., Saunders, R., Noble, P. L., Webster, M. J. & Shannon Weickert, C. 2011. Developmental patterns of doublecortin expression and white matter neuron density in the postnatal primate prefrontal cortex and schizophrenia. *PloS One,* 6**,** e25194.

Gabbott, P., Somogyi, J., Stewart, M. & Hamori, J. 1988. The orientation of interneurones in the dorsal lateral geniculate nucleus of the rat: a quantitative study. *Brain Research,* 438**,** 379-384.

Gargareta, V.-I., Reuschenbach, J., Siems, S. B., Sun, T., Piepkorn, L., Mangana, C., Späte, E., Goebbels, S., Huitinga, I. & Möbius, W. 2022. Conservation and divergence of

myelin proteome and oligodendrocyte transcriptome profiles between humans and mice. *Elife,* 11**,** e77019.

Gaspard, N. 2020. How much GAD65 do you have? High levels of GAD65 antibodies in autoimmune encephalitis. *Epilepsy Currents,* 20**,** 267-270.

Gaston-Massuet, C., Henderson, D. J., Greene, N. D. & Copp, A. J. 2005. Zic4, a zinc-finger transcription factor, is expressed in the developing mouse nervous system. *Developmental Dynamics: an Official Publication of the American Association of Anatomists,* 233**,** 1110-1115.

Gauthier, J., Siddiqui, T. J., Huashan, P., Yokomaku, D., Hamdan, F. F., Champagne, N., Lapointe, M., Spiegelman, D., Noreau, A. & Lafrenière, R. G. 2011. Truncating mutations in NRXN2 and NRXN1 in autism spectrum disorders and schizophrenia. *Human Genetics,* 130**,** 563-573.

Gavin, D. P., Sharma, R. P., Chase, K. A., Matrisciano, F., Dong, E. & Guidotti, A. 2012. Growth arrest and DNA-damage-inducible, beta (GADD45b)-mediated DNA demethylation in major psychosis. *Neuropsychopharmacology,* 37**,** 531-542.

Gerstner, J. R., Flores, C. C., Lefton, M., Rogers, B. & Davis, C. J. 2023. FABP7: a glial integrator of sleep, circadian rhythms, plasticity, and metabolic function. *Frontiers in Systems Neuroscience,* 17**,** 1212213.

Gezelius, H., Moreno-Juan, V., Mezzera, C., Thakurela, S., Rodríguez-Malmierca, L. M., Pistolic, J., Benes, V., Tiwari, V. K. & López-Bendito, G. 2017. Genetic labeling of nuclei-specific thalamocortical neurons reveals putative sensory-modality specific genes. *Cerebral Cortex,* 27**,** 5054-5069.

Giraldo-Chica, M. & Woodward, N. D. 2017. Review of thalamocortical resting-state fMRI studies in schizophrenia. *Schizophrenia Research,* 180**,** 58-63.

Glausier, J. R. & Lewis, D. A. 2013. Dendritic spine pathology in schizophrenia. *Neuroscience,* 251**,** 90-107.

Gleeson, J. G., Lin, P. T., Flanagan, L. A. & Walsh, C. A. 1999. Doublecortin is a microtubule-associated protein and is expressed widely by migrating neurons. *Neuron,* 23**,** 257-271.

Glessner, J. T., Wang, K., Cai, G., Korvatska, O., Kim, C. E., Wood, S., Zhang, H., Estes, A., Brune, C. W. & Bradfield, J. P. 2009. Autism genome-wide copy number variation reveals ubiquitin and neuronal genes. *Nature,* 459**,** 569-573.

Golding, B., Pouchelon, G., Bellone, C., Murthy, S., Di Nardo, A. A., Govindan, S., Ogawa, M., Shimogori, T., Lüscher, C. & Dayer, A. 2014. Retinal input directs the recruitment of inhibitory interneurons into thalamic visual circuits. *Neuron,* 81**,** 1057-1069.

González-Maya, M. & González-Barrios, J. A. 2021. Single-nucleotide polymorphisms and cerebral palsy. *Factors Affecting Neurodevelopment.* Elsevier.

Götz, M. 2013. Radial glial cells. *Neuroglia. Oxford University Press, New York***,** 50-61.

Götz, M., Sirko, S., Beckers, J. & Irmler, M. 2015. Reactive astrocytes as neural stem or progenitor cells: in vivo lineage, in vitro potential, and genome-wide expression analysis. *Glia,* 63**,** 1452-1468.

Götz, M., Stoykova, A. & Gruss, P. 1998. Pax6 controls radial glia differentiation in the cerebral cortex. *Neuron,* 21**,** 1031-1044.

Graf, E. R., Zhang, X., Jin, S.-X., Linhoff, M. W. & Craig, A. M. 2004. Neurexins induce differentiation of GABA and glutamate postsynaptic specializations via neuroligins. *Cell,* 119**,** 1013-1026.

Grant, E., Hoerder-Suabedissen, A. & Molnár, Z. 2012. Development of the corticothalamic projections. *Frontiers in Neuroscience,* 6**,** 53.

Gray, T. S. & Morley, J. E. 1986. Neuropeptide Y: anatomical distribution and possible function in mammalian nervous system. *Life Sciences,* 38**,** 389-401.

Grayton, H. M., Missler, M., Collier, D. A. & Fernandes, C. 2013. Altered social behaviours in neurexin 1α knockout mice resemble core symptoms in neurodevelopmental disorders. *PloS One,* 8**,** e67114.

Graziano, A., Liu, X. B., Murray, K. D. & Jones, E. G. 2008. Vesicular glutamate transporters define two sets of glutamatergic afferents to the somatosensory thalamus and two thalamocortical projections in the mouse. *Journal of Comparative Neurology,* 507**,** 1258-1276.

Greber, S., Schwarzer, C. & Sperk, G. 1994. Neuropeptide Y inhibits potassium-stimulated glutamate release through Y2 receptors in rat hippocampal slices in vitro. *British Journal of Pharmacology,* 113**,** 737-740.

Greenbaum, D., Colangelo, C., Williams, K. & Gerstein, M. 2003. Comparing protein abundance and mRNA expression levels on a genomic scale. *Genome Biology,* 4**,** 1-8.

Grimm, J., Sachs, M., Britsch, S., Di Cesare, S., Schwarz-Romond, T., Alitalo, K. & Birchmeier, W. 2001. Novel p62dok family members, dok-4 and dok-5, are substrates of the c-Ret receptor tyrosine kinase and mediate neuronal differentiation. *The Journal of Cell Biology,* 154**,** 345-354.

Grindley, J. C., Hargett, L. K., Hill, R. E., Ross, A. & Hogan, B. L. 1997. Disruption of PAX6 function in mice homozygous for the Pax6Sey-1Neu mutation produces abnormalities in the early development and regionalization of the diencephalon. *Mechanisms of Development,* 64**,** 111-126.

Guillery, R. & Harting, J. K. 2003. Structure and connections of the thalamic reticular nucleus: advancing views over half a century. *Journal of Comparative Neurology,* 463**,** 360-371.

Gunaseelan, S., Wang, Z., Tong, V. K. J., Ming, S. W. S., Razar, R. B. B. A., Srimasorn, S., Ong, W.-Y., Lim, K.-L. & Chua, J. J. E. 2021. Loss of FEZ1, a gene deleted in Jacobsen syndrome, causes locomotion defects and early mortality by impairing motor neuron development. *Human Molecular Genetics,* 30**,** 5-20.

Guo, Q. & Li, J. Y. 2019. Defining developmental diversification of diencephalon neurons through single cell gene expression profiling. *Development,* 146**,** dev174284.

Hagemann, A. I. & Scholpp, S. 2012. The tale of the three brothers–Shh, Wnt, and Fgf during development of the thalamus. *Frontiers in Neuroscience,* 6**,** 76.

Hara, T., Umaru, B. A., Sharifi, K., Yoshikawa, T., Owada, Y. & Kagawa, Y. 2020. Fatty acid binding protein 7 is involved in the proliferation of reactive astrocytes, but not in cell migration and polarity. *Acta Histochemica et Cytochemica,* 53**,** 73-81.

Harkin, L. F., Lindsay, S. J., Xu, Y., Alzu'bi, A., Ferrara, A., Gullon, E. A., James, O. G. & Clowry, G. J. 2017. Neurexins 1–3 each have a distinct pattern of expression in the early developing human cerebral cortex. *Cerebral Cortex,* 27**,** 216-232.

Hata, Y., Butz, S. & Sudhof, T. C. 1996. CASK: a novel dlg/PSD95 homolog with an N-terminal calmodulin-dependent protein kinase domain identified by interaction with neurexins. *Journal of Neuroscience,* 16**,** 2488-2494.

Hébert, J. M. 2011. FGFs: neurodevelopment's Jack-of-all-trades–how do they do it? *Frontiers in Neuroscience,* 5**,** 133.

Hébert, J. M. & Fishell, G. 2008. The genetics of early telencephalon patterning: some assembly required. *Nature Reviews Neuroscience,* 9**,** 678-685.

HERN, W. M. 1984. Correlation of fetal age and measurements between 10 and 26 weeks of gestation. *Obstetrics & Gynecology,* 63**,** 26-32.

Herrick, C. J. 1910. The morphology of the forebrain in amphibia and reptilia. *Journal of comparative Neurology and Psychology,* 20**,** 413-547.

Hevner, R. F., Miyashita-Lin, E. & Rubenstein, J. L. 2002. Cortical and thalamic axon pathfinding defects in Tbr1, Gbx2, and Pax6 mutant mice: evidence that cortical and thalamic axons interact and guide each other. *Journal of Comparative Neurology,* 447**,** 8-17.

Hikosaka, O. 2010. The habenula: from stress evasion to value-based decision-making. *Nature Reviews Neuroscience,* 11**,** 503-513.

Hill, M. A. 2018. Developing the digital Kyoto collection in education and research. *The Anatomical Record,* 301**,** 998-1003.

Hirata, T., Nakazawa, M., Yoshihara, S.-i., Miyachi, H., Kitamura, K., Yoshihara, Y. & Hibi, M. 2006. Zinc-finger gene Fez in the olfactory sensory neurons regulates development of the olfactory bulb non-cell-autonomously.

Hirata, T., Suda, Y., Nakao, K., Narimatsu, M., Hirano, T. & Hibi, M. 2004. Zinc finger gene fez-like functions in the formation of subplate neurons and thalamocortical axons. *Developmental dynamics: an official publication of the American Association of Anatomists,* 230**,** 546-556.

Hirokawa, N. & Noda, Y. 2008. Intracellular transport and kinesin superfamily proteins, KIFs: structure, function, and dynamics. *Physiological Reviews,* 88**,** 1089-1118.

Hirokawa, N., Noda, Y., Tanaka, Y. & Niwa, S. 2009. Kinesin superfamily motor proteins and intracellular transport. *Nature reviews Molecular Cell Biology,* 10**,** 682-696.

Hitchcock, P. F. & Hickey, T. 1980. Prenatal development of the human lateral geniculate nucleus. *Journal of Comparative Neurology,* 194**,** 395-411.

Hoch, R. V., Rubenstein, J. L. & Pleasure, S. Genes and signaling events that establish regional patterning of the mammalian forebrain. Seminars in Cell & Developmental Biology, 2009. Elsevier, 378-386.

Hodgkinson, C. A., Goldman, D., Ducci, F., DeRosse, P., Caycedo, D. A., Newman, E. R., Kane, J. M., Roy, A. & Malhotra, A. K. 2007. The FEZ1 gene shows no association to schizophrenia in Caucasian or African American populations. *Neuropsychopharmacology,* 32**,** 190-196.

Höflich, A., Hahn, A., Küblböck, M., Kranz, G. S., Vanicek, T., Windischberger, C., Saria, A., Kasper, S., Winkler, D. & Lanzenberger, R. 2015. Ketamine-induced modulation of the thalamo-cortical network in healthy volunteers as a model for schizophrenia. *International Journal of Neuropsychopharmacology,* 18**,** pyv040.

Hogan, B. L., Horsburgh, G., Cohen, J., Hetherington, C. M., Fisher, G. & Lyon, M. F. 1986. Small eyes (Sey): a homozygous lethal mutation on chromosome 2 which affects the differentiation of both lens and nasal placodes in the mouse. *Development,* 97**,** 95-110.

Hol, E. M. & Pekny, M. 2015. Glial fibrillary acidic protein (GFAP) and the astrocyte intermediate filament system in diseases of the central nervous system. *Current Opinion in Cell Biology,* 32**,** 121-130.

Holst, C. B., Brøchner, C. B., Vitting-Seerup, K. & Møllgård, K. 2023. The HOPX and BLBP landscape and gliogenic regions in developing human brain. *Journal of Anatomy*.

Homman-Ludiye, J. & Bourne, J. A. 2019. The medial pulvinar: function, origin and association with neurodevelopmental disorders. *Journal of Anatomy,* 235**,** 507-520.

Horng, S., Kreiman, G., Ellsworth, C., Page, D., Blank, M., Millen, K. & Sur, M. 2009. Differential gene expression in the developing lateral geniculate nucleus and medial geniculate nucleus reveals novel roles for Zic4 and Foxp2 in visual and auditory pathway development. *Journal of Neuroscience,* 29**,** 13672-13683.

Hu, C., Tao, L., Cao, X. & Chen, L. 2020. The solute carrier transporters and the brain: Physiological and pharmacological implications. *Asian Journal of Pharmaceutical Sciences,* 15**,** 131-144.

Hu, Z., Xiao, X., Zhang, Z. & Li, M. 2019. Genetic insights and neurobiological implications from NRXN1 in neuropsychiatric disorders. *Molecular Psychiatry,* 24**,** 1400-1414.

Hunt, C., Pang, D. & Jones, E. 1991. Distribution and density of GABA cells in intralaminar and adjacent nuclei of monkey thalamus. *Neuroscience,* 43**,** 185-196.

Huttner, W. B. 2023. Neocortical neurogenesis in development and evolution.

Ichtchenko, K., Hata, Y., Nguyen, T., Ullrich, B., Missler, M., Moomaw, C. & Südhof, T. C. 1995. Neuroligin 1: a splice site-specific ligand for β-neurexins. *Cell,* 81**,** 435-443.

Ichtchenko, K., Nguyen, T. & Südhof, T. C. 1996. Structures, alternative splicing, and neurexin binding of multiple neuroligins. *Journal of Biological Chemistry,* 271**,** 2676-2682.

Ikeda, M., Aleksic, B., Kirov, G., Kinoshita, Y., Yamanouchi, Y., Kitajima, T., Kawashima, K., Okochi, T., Kishi, T. & Zaharieva, I. 2010. Copy number variation in schizophrenia in the Japanese population. *Biological Psychiatry,* 67**,** 283-286.

Ilyas, A., Pizarro, D., Romeo, A. K., Riley, K. O. & Pati, S. 2019. The centromedian nucleus: anatomy, physiology, and clinical implications. *Journal of Clinical Neuroscience,* 63**,** 1-7.

Inoue, T., Nakamura, S. & Osumi, N. 2000. Fate mapping of the mouse prosencephalic neural plate. *Developmental Biology,* 219**,** 373-383.

Inverardi, F., Beolchi, M. S., Ortino, B., Moroni, R., Regondi, M., Amadeo, A. & Frassoni, C. 2007. GABA immunoreactivity in the developing rat thalamus and Otx2 homeoprotein expression in migrating neurons. *Brain Research Bulletin,* 73**,** 64-74.

Ishibashi, M. & Mcmahon, A. P. 2002. A sonic hedgehog-dependent signaling relay regulates growth of diencephalic and mesencephalic primordia in the early mouse embryo.

Jaffe, A. E., Straub, R. E., Shin, J. H., Tao, R., Gao, Y., Collado-Torres, L., Kam-Thong, T., Xi, H. S., Quan, J. & Chen, Q. 2018. Developmental and genetic regulation of the human cortex transcriptome illuminate schizophrenia pathogenesis. *Nature Neuroscience,* 21**,** 1117-1125.

Jager, P., Moore, G., Calpin, P., Durmishi, X., Salgarella, I., Menage, L., Kita, Y., Wang, Y., Kim, D. W. & Blackshaw, S. 2021. Dual midbrain and forebrain origins of thalamic inhibitory interneurons. *Elife,* 10**,** e59272.

Jager, P., Ye, Z., Yu, X., Zagoraiou, L., Prekop, H.-T., Partanen, J., Jessell, T. M., Wisden, W., Brickley, S. G. & Delogu, A. 2016. Tectal-derived interneurons contribute to phasic and tonic inhibition in the visual thalamus. *Nature Communications,* 7**,** 13579.

Jakovcevski, I., Filipovic, R., Mo, Z., Rakic, S. & Zecevic, N. 2009. Oligodendrocyte development and the onset of myelination in the human fetal brain. *Frontiers in Neuroanatomy,* 3**,** 665.

Jakovcevski, I. & Zecevic, N. 2005. Olig transcription factors are expressed in oligodendrocyte and neuronal cells in human fetal CNS. *Journal of Neuroscience,* 25**,** 10064-10073.

Jang, S. H., Lim, H. W. & Yeo, S. S. 2014. The neural connectivity of the intralaminar thalamic nuclei in the human brain: a diffusion tensor tractography study. *Neuroscience letters,* 579**,** 140-144.

Janz, P., Bainier, M., Marashli, S., Schoenenberger, P., Valencia, M. & Redondo, R. L. 2022. Neurexin1α knockout rats display oscillatory abnormalities and sensory processing

deficits back-translating key endophenotypes of psychiatric disorders. *Translational Psychiatry,* 12**,** 455.

Jenkins, A. K., Paterson, C., Wang, Y., Hyde, T. M., Kleinman, J. E. & Law, A. J. 2016. Neurexin 1 (NRXN1) splice isoform expression during human neocortical development and aging. *Molecular Psychiatry,* 21**,** 701-706.

Jeong, Y., Dolson, D. K., Waclaw, R. R., Matise, M. P., Sussel, L., Campbell, K., Kaestner, K. H. & Epstein, D. J. 2011. Spatial and temporal requirements for sonic hedgehog in the regulation of thalamic interneuron identity. *Development,* 138**,** 531-541.

Jessell, T. M. & Sanes, J. R. 2000. Development: The decade of the developing brain. *Current Opinion in Neurobiology,* 10**,** 599-611.

Jiang, M., Zhuang, H., Xia, R., Gan, L., Wu, Y., Ma, J., Sun, Y. & Zhuang, Z. 2017. KIF11 is required for proliferation and self-renewal of docetaxel resistant triple negative breast cancer cells. *Oncotarget,* 8**,** 92106.

Jiang, Y., Patton, M. H. & Zakharenko, S. S. 2021. A case for thalamic mechanisms of schizophrenia: perspective from modeling 22q11. 2 deletion syndrome. *Frontiers in Neural Circuits,* 15**,** 769969.

Jin, Y., Murakumo, Y., Ueno, K., Hashimoto, M., Watanabe, T., Shimoyama, Y., Ichihara, M. & Takahashi, M. 2004. Identification of a mouse cytoskeleton-associated protein, CKAP2, with microtubule-stabilizing properties. *Cancer Science,* 95**,** 815-821.

Jonas, P., Bischofberger, J., Fricker, D. & Miles, R. 2004. Interneuron Diversity series: Fast in, fast out–temporal and spatial signal processing in hippocampal interneurons. *Trends in Neurosciences,* 27**,** 30-40.

Jones, E. 2002. Dichronous appearance and unusual origins of GABA neurons during development of the mammalian thalamus. *Thalamus & Related Systems,* 1**,** 283-288.

Jones, E. & Hendry, S. 1989. Differential calcium binding protein immunoreactivity distinguishes classes of relay neurons in monkey thalamic nuclei. *European Journal of Neuroscience,* 1**,** 222-246.

Jones, E. G. 2007. Descriptions of the Thalamus in Representative Mammals. *The Thalamus.* Springer.

Jones, E. G. & Rubenstein, J. L. 2004. Expression of regulatory genes during differentiation of thalamic nuclei in mouse and monkey. *Journal of Comparative Neurology,* 477**,** 55-80.

Jones, L., López-Bendito, G., Gruss, P., Stoykova, A. & Molnár, Z. 2002. Pax6 is required for the normal development of the forebrain axonal connections.

Joppé, S. E., Cochard, L. M., Levros, L.-C., Hamilton, L. K., Ameslon, P., Aumont, A., Barnabé-Heider, F. & Fernandes, K. J. 2020. Genetic targeting of neurogenic precursors in the adult forebrain ventricular epithelium. *Life Science Alliance,* 3.

Jun, H., Hussaini, S. M. Q., Cho, C. H., Welby, J. & Jang, M.-H. 2015. Gadd45b mediates electroconvulsive shock induced proliferation of hippocampal neural stem cells. *Brain Stimulation,* 8**,** 1021-1024.

Kageyama, R., Ohtsuka, T. & Kobayashi, T. 2007. The Hes gene family: repressors and oscillators that orchestrate embryogenesis.

Kang, E., Burdick, K. E., Kim, J. Y., Duan, X., Guo, J. U., Sailor, K. A., Jung, D.-E., Ganesan, S., Choi, S. & Pradhan, D. 2011. Interaction between FEZ1 and DISC1 in regulation of neuronal development and risk for schizophrenia. *Neuron,* 72**,** 559-571.

Kang, Y., Zhang, X., Dobie, F., Wu, H. & Craig, A. M. 2008. Induction of GABAergic postsynaptic differentiation by α-neurexins. *Journal of Biological Chemistry,* 283**,** 2323-2334.

Kasem, E., Kurihara, T. & Tabuchi, K. 2018. Neurexins and neuropsychiatric disorders. *Neuroscience Research,* 127**,** 53-60.

Kast, R. J., Lanjewar, A. L., Smith, C. D. & Levitt, P. 2019. FOXP2 exhibits projection neuron class specific expression, but is not required for multiple aspects of cortical histogenesis. *Elife,* 8**,** e42012.

Kataoka, A. & Shimogori, T. 2008. Fgf8 controls regional identity in the developing thalamus.

Kaufman, D. L., Houser, C. R. & Tobin, A. J. 1991. Two forms of the γ-aminobutyric acid synthetic enzyme glutamate decarboxylase have distinct intraneuronal distributions and cofactor interactions. *Journal of neurochemistry,* 56**,** 720-723.

Kawano, H., Fukuda, T., Kubo, K., Horie, M., Uyemura, K., Takeuchi, K., Osumi, N., Eto, K. & Kawamura, K. 1999. Pax-6 is required for thalamocortical pathway formation in fetal rats. *Journal of Comparative Neurology,* 408**,** 147-160.

Kebir, O., Chaumette, B., Fatjo-Vilas, M., Ambalavanan, A., Ramoz, N., Xiong, L., Mouaffak, F., Millet, B., Jaafari, N. & DeLisi, L. E. 2014. Family-based association study of common variants, rare mutation study and epistatic interaction detection in HDAC genes in schizophrenia. *Schizophrenia Research,* 160**,** 97-103.

Kepecs, A. & Fishell, G. 2014. Interneuron cell types are fit to function. *Nature,* 505**,** 318-326.

Keun, J. T. B., van Heese, E. M., Laansma, M. A., Weeland, C. J., de Joode, N. T., van den Heuvel, O. A., Gool, J. K., Kasprzak, S., Bright, J. K. & Vriend, C. 2021. Structural assessment of thalamus morphology in brain disorders: a review and recommendation of thalamic nucleus segmentation and shape analysis. *Neuroscience & Biobehavioral Reviews,* 131**,** 466-478.

Kiecker, C. & Lumsden, A. 2004. Hedgehog signaling from the ZLI regulates diencephalic regional identity. *Nature Neuroscience,* 7**,** 1242-1249.

Kim, C. N., Shin, D., Wang, A. & Nowakowski, T. J. 2023. Spatiotemporal molecular dynamics of the developing human thalamus. *Science,* 382**,** eadf9941.

Kim, H.-G., Kishikawa, S., Higgins, A. W., Seong, I.-S., Donovan, D. J., Shen, Y., Lally, E., Weiss, L. A., Najm, J. & Kutsche, K. 2008. Disruption of neurexin 1 associated with autism spectrum disorder. *The American Journal of Human Genetics,* 82**,** 199-207.

Kinomura, S., Larsson, J., Gulyas, B. & Roland, P. E. 1996. Activation by attention of the human reticular formation and thalamic intralaminar nuclei. *Science,* 271**,** 512-515.

Kiral, F. R., Choe, M. & Park, I.-H. 2023. Diencephalic organoids–A key to unraveling development, connectivity, and pathology of the human diencephalon. *Frontiers in Cellular Neuroscience,* 17**,** 1308479.

Kirov, G., Gumus, D., Chen, W., Norton, N., Georgieva, L., Sari, M., O'Donovan, M. C., Erdogan, F., Owen, M. J. & Ropers, H.-H. 2008. Comparative genome hybridization suggests a role for NRXN1 and APBA2 in schizophrenia. *Human Molecular Genetics,* 17**,** 458-465.

Koehnke, J., Katsamba, P. S., Ahlsen, G., Bahna, F., Vendome, J., Honig, B., Shapiro, L. & Jin, X. 2010. Splice form dependence of β-neurexin/neuroligin binding interactions. *Neuron,* 67**,** 61-74.

Koga, M., Ishiguro, H., Horiuchi, Y., Albalushi, T., Inada, T., Iwata, N., Ozaki, N., Ujike, H., Muratake, T. & Someya, T. 2007. Failure to confirm the association between the FEZ1 gene and schizophrenia in a Japanese population. *Neuroscience letters,* 417**,** 326-329.

Koike, Y., Yin, C., Sato, Y., Nagano, Y., Yamamoto, A., Kitajima, T., Shimura, T., Kawamura, M., Matsushita, K. & Okugawa, Y. 2022. TPX2 is a prognostic marker and promotes cell proliferation in neuroblastoma. *Oncology Letters,* 23**,** 1-9.

Konopka, G., Wexler, E., Rosen, E., Mukamel, Z., Osborn, G. E., Chen, L., Lu, D., Gao, F., Gao, K. & Lowe, J. K. 2012. Modeling the functional genomics of autism using human neurons. *Molecular Psychiatry,* 17**,** 202-214.

Kostovic, I. & Rakic, P. 1990. Developmental history of the transient subplate zone in the visual and somatosensory cortex of the macaque monkey and human brain. *Journal of Comparative Neurology,* 297**,** 441-470.

Kraut, M. A., Calhoun, V., Pitcock, J. A., Cusick, C. & Hart, J. 2003. Neural hybrid model of semantic object memory: implications from event-related timing using fMRI. *Journal of the International Neuropsychological Society,* 9**,** 1031-1040.

Krienen, F. M., Goldman, M., Zhang, Q., CH del Rosario, R., Florio, M., Machold, R., Saunders, A., Levandowski, K., Zaniewski, H. & Schuman, B. 2020. Innovations present in the primate interneuron repertoire. *Nature,* 586**,** 262-269.

Krol, A., Wimmer, R. D., Halassa, M. M. & Feng, G. 2018. Thalamic reticular dysfunction as a circuit endophenotype in neurodevelopmental disorders. *Neuron,* 98**,** 282-295.

Krsnik, Ž., Majić, V., Vasung, L., Huang, H. & Kostović, I. 2017. Growth of thalamocortical fibers to the somatosensory cortex in the human fetal brain. *Frontiers in Neuroscience,* 11**,** 233.

Kuhlenbeck, H. 1937. The ontogenetic development of the diencephalic centers in a bird's brain (chick) and comparison with the reptilian and mammalian diencephalon. *Journal of Comparative Neurology,* 66**,** 23-75.

Kuhlenbeck, H. 1973. The Central Nervous System of Vertebrates: Overall Morphologic.

Kulkarni, N. H., Karavanich, C. A., Atchley, W. R. & Anholt, R. R. 2000. Characterization and differential expression of a human gene family of olfactomedin-related proteins. *Genetics Research,* 76**,** 41-50.

Larsen, K. B., Lutterodt, M. C., Møllgård, K. & Møller, M. 2010. Expression of the homeobox genes OTX2 and OTX1 in the early developing human brain. *Journal of Histochemistry & Cytochemistry,* 58**,** 669-678.

Lau, C. G. & Murthy, V. N. 2012. Activity-dependent regulation of inhibition via GAD67. *Journal of Neuroscience,* 32**,** 8521-8531.

Lavdas, A. A., Grigoriou, M., Pachnis, V. & Parnavelas, J. G. 1999. The medial ganglionic eminence gives rise to a population of early neurons in the developing cerebral cortex. *Journal of Neuroscience,* 19**,** 7881-7888.

Lee, C. C. 2013. Thalamic and cortical pathways supporting auditory processing. *Brain and language,* 126**,** 22-28.

Lee, S. J., Kwon, S., Gatti, J. R., Korcari, E., Gresser, T. E., Felix, P. C., Keep, S. G., Pasquale, K. C., Bai, T. & Blanchett-Anderson, S. A. 2017. Large-scale identification of human cerebrovascular proteins: Inter-tissue and intracerebral vascular protein diversity. *PloS One,* 12**,** e0188540.

Letinić, K. & Kostović, I. 1997. Transient fetal structure, the gangliothalamic body, connects telencephalic germinal zone with all thalamic regions in the developing human brain. *Journal of Comparative Neurology,* 384**,** 373-395.

Letinic, K. & Rakic, P. 2001. Telencephalic origin of human thalamic GABAergic neurons. *Nature neuroscience,* 4**,** 931-936.

Li, T., Zeng, Z., Zhao, Q., Wang, T., Huang, K., Li, J., Li, Y., Liu, J., Wei, Z. & Wang, Y. 2013. FoxP2 is significantly associated with schizophrenia and major depression in the Chinese Han population. *The World Journal of Biological Psychiatry,* 14**,** 146-150.

Li, Y., Lopez-Huerta, V. G., Adiconis, X., Levandowski, K., Choi, S., Simmons, S. K., Arias-Garcia, M. A., Guo, B., Yao, A. Y. & Blosser, T. R. 2020. Distinct subnetworks of the thalamic reticular nucleus. *Nature,* 583**,** 819-824.

Li, Y., Wu, C., Long, X., Wang, X., Gao, W., Deng, K., Xie, B., Zhang, S., Wu, M. & Qing, L. 2023. Single-Cell Transcriptomics of Glioblastoma Reveals Pericytes Contributing to Blood–Brain Tumor Barrier and Tumor Progression.

Li, Z., Pratt, T. & Price, D. J. 2018. Zic4-lineage cells increase their contribution to visual thalamic nuclei during murine embryogenesis if they are homozygous or heterozygous for loss of Pax6 function. *Eneuro,* 5.

Lindsay, S. J., Xu, Y., Lisgo, S. N., Harkin, L. F., Copp, A. J., Gerrelli, D., Clowry, G. J., Talbot, A., Keogh, M. J. & Coxhead, J. 2016. HDBR expression: a unique resource for global and individual gene expression studies during early human brain development. *Frontiers in neuroanatomy,* 10**,** 86.

Lipiec, M. A., Bem, J., Koziński, K., Chakraborty, C., Urban-Ciećko, J., Zajkowski, T., Dąbrowski, M., Szewczyk, Ł. M., Toval, A. & Ferran, J. L. 2020. TCF7L2 regulates postmitotic differentiation programmes and excitability patterns in the thalamus. *Development,* 147**,** dev190181.

Lipska, B. K., Peters, T., Hyde, T. M., Halim, N., Horowitz, C., Mitkus, S., Weickert, C. S., Matsumoto, M., Sawa, A. & Straub, R. E. 2006. Expression of DISC1 binding partners is reduced in schizophrenia and associated with DISC1 SNPs. *Human Molecular Genetics,* 15**,** 1245-1258.

Liu, Q., Dwyer, N. D. & O'Leary, D. D. 2000. Differential expression of COUP-TFI, CHL1, and two novel genes in developing neocortex identified by differential display PCR. *Journal of Neuroscience,* 20**,** 7682-7690.

Liu, Y., Ouyang, P., Zheng, Y., Mi, L., Zhao, J., Ning, Y. & Guo, W. 2021. A selective review of the excitatory-inhibitory imbalance in schizophrenia: underlying biology, genetics, microcircuits, and symptoms. *Frontiers in Cell and Developmental Biology,* 9**,** 664535.

Lüffe, T. M., D'Orazio, A., Bauer, M., Gioga, Z., Schoeffler, V., Lesch, K.-P., Romanos, M., Drepper, C. & Lillesaar, C. 2021. Increased locomotor activity via regulation of GABAergic signalling in foxp2 mutant zebrafish—implications for neurodevelopmental disorders. *Translational Psychiatry,* 11**,** 529.

Luskin, M., Parnavelas, J. & Barfield, J. 1993. Neurons, astrocytes, and oligodendrocytes of the rat cerebral cortex originate from separate progenitor cells: an ultrastructural analysis of clonally related cells. *Journal of Neuroscience,* 13**,** 1730-1750.

Ma, T., Wang, C., Wang, L., Zhou, X., Tian, M., Zhang, Q., Zhang, Y., Li, J., Liu, Z. & Cai, Y. 2013. Subcortical origins of human and monkey neocortical interneurons. *Nature Neuroscience,* 16**,** 1588-1597.

Makrides, N., Panayiotou, E., Fanis, P., Karaiskos, C., Lapathitis, G. & Malas, S. 2018. Sequential role of SOXB2 factors in GABAergic neuron specification of the dorsal midbrain. *Frontiers in Molecular Neuroscience,* 11**,** 152.

Mallika, C., Guo, Q. & Li, J. Y. 2015. Gbx2 is essential for maintaining thalamic neuron identity and repressing habenular characters in the developing thalamus. *Developmental biology,* 407**,** 26-39.

Malureanu, L., Jeganathan, K. B., Jin, F., Baker, D. J., Van Ree, J. H., Gullon, O., Chen, Z., Henley, J. R. & Van Deursen, J. M. 2010. Cdc20 hypomorphic mice fail to counteract de novo synthesis of cyclin B1 in mitosis. *Journal of Cell Biology,* 191**,** 313-329.

Maness, P. F. & Schachner, M. 2007. Neural recognition molecules of the immunoglobulin superfamily: signaling transducers of axon guidance and neuronal migration. *Nature Neuroscience,* 10**,** 19-26.

Marenco, S., Stein, J. L., Savostyanova, A. A., Sambataro, F., Tan, H.-Y., Goldman, A. L., Verchinski, B. A., Barnett, A. S., Dickinson, D. & Apud, J. A. 2012. Investigation of anatomical thalamo-cortical connectivity and FMRI activation in schizophrenia. *Neuropsychopharmacology,* 37**,** 499-507.

Marshall, C. R., Howrigan, D. P., Merico, D., Thiruvahindrapuram, B., Wu, W., Greer, D. S., Antaki, D., Shetty, A., Holmans, P. A. & Pinto, D. 2017. Contribution of copy number variants to schizophrenia from a genome-wide study of 41,321 subjects. *Nature Genetics,* 49**,** 27-35.

Martinez-Ferre, A. & Martinez, S. 2009. The development of the thalamic motor learning area is regulated by Fgf8 expression. *Journal of Neuroscience,* 29**,** 13389-13400.

Martinez-Ferre, A. & Martinez, S. 2012. Molecular regionalization of the diencephalon. *Frontiers in Neuroscience,* 6**,** 73.

Marucci, G., Morandi, L., Magrini, E., Farnedi, A., Franceschi, E., Miglio, R., Calò, D., Pession, A., Foschini, M. P. & Eusebi, V. 2008. Gene expression profiling in glioblastoma and immunohistochemical evaluation of IGFBP-2 and CDC20. *Virchows Archiv,* 453**,** 599-609.

Mastick, G. S. & Andrews, G. L. 2001. Pax6 regulates the identity of embryonic diencephalic neurons. *Molecular and Cellular Neuroscience,* 17**,** 190-207.

Mastick, G. S., Davis, N. M., Andrews, G. L. & Easter Jr, S. S. 1997. Pax-6 functions in boundary formation and axon guidance in the embryonic mouse forebrain. *Development,* 124**,** 1985-1997.

Matsuda, K. & Yuzaki, M. 2011. Cbln family proteins promote synapse formation by regulating distinct neurexin signaling pathways in various brain regions. *European Journal of Neuroscience,* 33**,** 1447-1461.

Maturana, A. D., Fujita, T. & Kuroda, S. i. 2010. Functions of fasciculation and elongation protein Zeta-1 (FEZ1) in the brain. *The Scientific World Journal,* 10**,** 1646-1654.

McAlear, T. S. & Bechstedt, S. 2022. The mitotic spindle protein CKAP2 potently increases formation and stability of microtubules. *Elife,* 11**,** e72202.

McKeon, A. & Tracy, J. A. 2017. GAD65 neurological autoimmunity. *Muscle & Nerve,* 56**,** 15-27.

McKnight, N. C., Jefferies, H. B., Alemu, E. A., Saunders, R. E., Howell, M., Johansen, T. & Tooze, S. A. 2012. Genome-wide siRNA screen reveals amino acid starvation-induced autophagy requires SCOC and WAC. *The EMBO Journal,* 31**,** 1931-1946.

McLeod, F., Dimtsi, A., Marshall, A. C., Lewis-Smith, D., Thomas, R., Clowry, G. J. & Trevelyan, A. J. 2023. Altered synaptic connectivity in an in vitro human model of STXBP1 encephalopathy. *Brain,* 146**,** 850-857.

Medina, L., Legaz, I., González, G., De Castro, F., Rubenstein, J. L. & Puelles, L. 2004. Expression of Dbx1, Neurogenin 2, Semaphorin 5A, Cadherin 8, and Emx1

distinguish ventral and lateral pallial histogenetic divisions in the developing mouse claustroamygdaloid complex. *Journal of Comparative Neurology,* 474**,** 504-523.

Meiri, K. F., Pfenninger, K. H. & Willard, M. B. 1986. Growth-associated protein, GAP-43, a polypeptide that is induced when neurons extend axons, is a component of growth cones and corresponds to pp46, a major polypeptide of a subcellular fraction enriched in growth cones. *Proceedings of the National Academy of Sciences,* 83**,** 3537-3541.

Mercurio, S., Serra, L. & Nicolis, S. K. 2019. More than just stem cells: functional roles of the transcription factor Sox2 in differentiated glia and neurons. *International Journal of Molecular Sciences,* 20**,** 4540.

Mercurio, S., Serra, L., Pagin, M. & Nicolis, S. K. 2022. Deconstructing Sox2 function in brain development and disease. *Cells,* 11**,** 1604.

Meyer, G. & González-Gómez, M. 2018. The subpial granular layer and transient versus persisting Cajal-Retzius neurons of the fetal human cortex. *Cerebral Cortex,* 28**,** 2043-2058.

Middeldorp, J., Boer, K., Sluijs, J. A., De Filippis, L., Encha-Razavi, F., Vescovi, A. L., Swaab, D. F., Aronica, E. & Hol, E. M. 2010. GFAPδ in radial glia and subventricular zone progenitors in the developing human cortex. *Development,* 137**,** 313-321.

Miller, J. A., Ding, S.-L., Sunkin, S. M., Smith, K. A., Ng, L., Szafer, A., Ebbert, A., Riley, Z. L., Royall, J. J. & Aiona, K. 2014. Transcriptional landscape of the prenatal human brain. *Nature,* 508**,** 199-206.

Millet, S., Campbell, K., Epstein, D. J., Losos, K., Harris, E. & Joyner, A. L. 1999. A role for Gbx2 in repression of Otx2 and positioning the mid/hindbrain organizer. *Nature,* 401**,** 161-164.

Mione, M. C., Danevic, C., Boardman, P., Harris, B. & Parnavelas, J. 1994. Lineage analysis reveals neurotransmitter (GABA or glutamate) but not calcium-binding protein homogeneity in clonally related cortical neurons. *Journal of Neuroscience,* 14**,** 107-123.

Missler, M. & Südhof, T. C. 1998. Neurexins: three genes and 1001 products. *Trends in Genetics,* 14**,** 20-26.

Missler, M., Zhang, W., Rohlmann, A., Kattenstroth, G., Hammer, R. E., Gottmann, K. & Südhof, T. C. 2003. α-Neurexins couple Ca2+ channels to synaptic vesicle exocytosis. *Nature,* 423**,** 939-948.

Miyake, A., Nakayama, Y., Konishi, M. & Itoh, N. 2005. Fgf19 regulated by Hh signaling is required for zebrafish forebrain development. *Developmental Biology,* 288**,** 259-275.

Miyoshi, G., Butt, S. J., Takebayashi, H. & Fishell, G. 2007. Physiologically distinct temporal cohorts of cortical interneurons arise from telencephalic Olig2-expressing precursors. *Journal of Neuroscience,* 27**,** 7786-7798.

Miyoshi, K., Honda, A., Baba, K., Taniguchi, M., Oono, K., Fujita, T., Kuroda, S., Katayama, T. & Tohyama, M. 2003. Disrupted-In-Schizophrenia 1, a candidate gene for schizophrenia, participates in neurite outgrowth. *Molecular Psychiatry,* 8**,** 685-694.

Mo, Z. & Zecevic, N. 2008. Is Pax6 critical for neurogenesis in the human fetal brain? *Cerebral Cortex,* 18**,** 1455-1465.

Molnár, Z., Bandiera, S. & Clowry, G. 2023. Evolution and Development of Thalamocortical Relationships.

Molnár, Z., Clowry, G. J., Šestan, N., Alzu'bi, A., Bakken, T., Hevner, R. F., Hüppi, P. S., Kostović, I., Rakic, P. & Anton, E. 2019. New insights into the development of the human cerebral cortex. *Journal of Anatomy,* 235**,** 432-451.

Molnár, Z., Luhmann, H. & Kanold, P. 2020a. Transient cortical circuits match spontaneous and sensory-driven activity during development. Science 370, eabb2153.

Molnár, Z., Luhmann, H. J. & Kanold, P. O. 2020b. Transient cortical circuits match spontaneous and sensory-driven activity during development. *Science,* 370**,** eabb2153.

Molyneaux, B. J., Arlotta, P., Hirata, T., Hibi, M. & Macklis, J. D. 2005. Fezl is required for the birth and specification of corticospinal motor neurons. *Neuron,* 47**,** 817-831.

Montero, V. & Zempel, J. 1986. The proportion and size of GABA-immunoreactive neurons in the magnocellular and parvocellular layers of the lateral geniculate nucleus of the rhesus monkey. *Experimental Brain Research,* 62**,** 215-223.

Monuki, E. S. 2022. Induction and Patterning in the Telencephalon. *Neuroscience in the 21st Century: From Basic to Clinical.* Springer.

Monuki, E. S., Porter, F. D. & Walsh, C. A. 2001. Patterning of the dorsal telencephalon and cerebral cortex by a roof plate-Lhx2 pathway. *Neuron,* 32**,** 591-604.

Mozhui, K., Wang, X., Chen, J., Mulligan, M., Li, Z., Ingles, J., Chen, X., Lu, L. & Williams, R. 2011. Genetic regulation of Nrnx1 expression: an integrative cross-species analysis of schizophrenia candidate genes. *Translational Psychiatry,* 1**,** e25-e25.

Mussolino, C. & Strouboulis, J. 2021. Recent approaches for manipulating globin gene expression in treating hemoglobinopathies. *Frontiers in Genome Editing,* 3**,** 618111.

Naeve, G. S., Ramakrishnan, M., Kramer, R., Hevroni, D., Citri, Y. & Theill, L. E. 1997a. Neuritin: a gene induced by neural activity and neurotrophins that promotes neuritogenesis. *Proceedings of the National Academy of Sciences,* 94**,** 2648-2653.

Naeve, G. S., Ramakrishnan, M., Kramer, R., Hevroni, D., Citri, Y. & Theill, L. E. 1997b. Neuritin: a gene induced by neural activity and neurotrophins that promotes neuritogenesis. *Proc Natl Acad Sci U S A,* 94**,** 2648-53.

Nakagawa, Y. 2019. Development of the thalamus: From early patterning to regulation of cortical functions. *Wiley Interdisciplinary Reviews: Developmental Biology,* 8**,** e345.

Nakagawa, Y. & O'Leary, D. D. 2001. Combinatorial expression patterns of LIM-homeodomain and other regulatory genes parcellate developing thalamus. *Journal of Neuroscience,* 21**,** 2711-2725.

Nakagawa, Y. & Shimogori, T. 2012. Diversity of thalamic progenitor cells and postmitotic neurons. *European Journal of Neuroscience,* 35**,** 1554-1562.

Nemes, A. D., Ayasoufi, K., Ying, Z., Zhou, Q.-G., Suh, H. & Najm, I. M. 2017. Growth associated protein 43 (GAP-43) as a novel target for the diagnosis, treatment and prevention of epileptogenesis. *Scientific Reports,* 7**,** 17702.

NEMO. 2024. *(The Neuroscience Multi-omic Archive). Single-Cell Sequencing of the Developing Human Brain* [Online]. Available: https://assets.nemoarchive.org/dat-t4xnmho [Accessed].

Nery, S., Fishell, G. & Corbin, J. G. 2002. The caudal ganglionic eminence is a source of distinct cortical and subcortical cell populations. *Nature neuroscience,* 5**,** 1279-1287.

Neyrinck, K., Van Den Daele, J., Vervliet, T., De Smedt, J., Wierda, K., Nijs, M., Vanbokhoven, T., D'hondt, A., Planque, M. & Fendt, S.-M. 2021. SOX9-induced generation of functional astrocytes supporting neuronal maturation in an all-human system. *Stem Cell Reviews and Reports,* 17**,** 1855-1873.

Nicodemus, K. K., Callicott, J. H., Higier, R. G., Luna, A., Nixon, D. C., Lipska, B. K., Vakkalanka, R., Giegling, I., Rujescu, D. & Clair, D. S. 2010. Evidence of statistical epistasis between DISC1, CIT and NDEL1 impacting risk for schizophrenia: biological validation with functional neuroimaging. *Human Genetics,* 127**,** 441-452.

Nowakowski, T. J., Bhaduri, A., Pollen, A. A., Alvarado, B., Mostajo-Radji, M. A., Di Lullo, E., Haeussler, M., Sandoval-Espinosa, C., Liu, S. J. & Velmeshev, D. 2017. Spatiotemporal gene expression trajectories reveal developmental hierarchies of the human cortex. *Science,* 358**,** 1318-1323.

Nowakowski, T. J., Pollen, A. A., Sandoval-Espinosa, C. & Kriegstein, A. R. 2016. Transformation of the radial glia scaffold demarcates two stages of human cerebral cortex development. *Neuron,* 91**,** 1219-1227.

O'Rahilly, R. & Müller, F. 1987. *Development stages in human embryos: including a revision of Streeter's" Horizons" and a survey of the Carnegie Collection*, Carnegie Inst. of Washington.

O'rahilly, R. & Müller, F. 2010. Developmental stages in human embryos: revised and new measurements. *Cells Tissues Organs,* 192**,** 73-84.

Ohara, P., Lieberman, A., Hunt, S. & Wu, J. 1983. Neural elements containing glutamic acid decarboxylase (GAD) in the dorsal lateral geniculate nucleus of the rat; immunohistochemical studies by light and electron microscopy. *Neuroscience,* 8**,** 189-211.

Ohtsuka, T., Sakamoto, M., Guillemot, F. & Kageyama, R. 2001. Roles of the basic helix-loop-helix genes Hes1 and Hes5 in expansion of neural stem cells of the developing brain. *Journal of Biological Chemistry,* 276**,** 30467-30474.

Orvis, J., Gottfried, B., Kancherla, J., Adkins, R. S., Song, Y., Dror, A. A., Olley, D., Rose, K., Chrysostomou, E. & Kelly, M. C. 2021. gEAR: Gene Expression Analysis Resource portal for community-driven, multi-omic data exploration. *Nature Methods,* 18**,** 843-844.

Osumi, N. 2001. The role of Pax6 in brain patterning. *The Tohoku Journal of Experimental Medicine,* 193**,** 163-174.

Ouhaz, Z., Fleming, H. & Mitchell, A. S. 2018. Cognitive functions and neurodevelopmental disorders involving the prefrontal cortex and mediodorsal thalamus. *Frontiers in Neuroscience,* 12**,** 33.

Pabst, O., Herbrand, H., Takuma, N. & Arnold, H.-H. 2000. NKX2 gene expression in neuroectoderm but not in mesendodermally derived structures depends on sonic hedgehog in mouse embryos. *Development genes and evolution,* 210**,** 47-50.

Pak, C., Danko, T., Zhang, Y., Aoto, J., Anderson, G., Maxeiner, S., Yi, F., Wernig, M. & Südhof, T. C. 2015. Human neuropsychiatric disease modeling using conditional deletion reveals synaptic transmission defects caused by heterozygous mutations in NRXN1. *Cell Stem Cell,* 17**,** 316-328.

Pan, Z. Z. 2012. Transcriptional control of Gad2. *Transcription,* 3**,** 68-72.

Papanayotou, C., Mey, A., Birot, A.-M., Saka, Y., Boast, S., Smith, J. C., Samarut, J. & Stern, C. D. 2008. A mechanism regulating the onset of Sox2 expression in the embryonic neural plate. *PLoS Biology,* 6**,** e2.

Parish, E. V., Mason, J. O. & Price, D. J. 2016. Expression of Barhl2 and its relationship with Pax6 expression in the forebrain of the mouse embryo. *BMC Neuroscience,* 17**,** 1-16.

Peñagarikano, O., Abrahams, B. S., Herman, E. I., Winden, K. D., Gdalyahu, A., Dong, H., Sonnenblick, L. I., Gruver, R., Almajano, J. & Bragin, A. 2011. Absence of CNTNAP2 leads to epilepsy, neuronal migration abnormalities, and core autism-related deficits. *Cell,* 147**,** 235-246.

Pergola, G., Danet, L., Pitel, A.-L., Carlesimo, G. A., Segobin, S., Pariente, J., Suchan, B., Mitchell, A. S. & Barbeau, E. J. 2018. The regulatory role of the human mediodorsal thalamus. *Trends in cognitive sciences,* 22**,** 1011-1025.

Pergola, G., Ranft, A., Mathias, K. & Suchan, B. 2013. The role of the thalamic nuclei in recognition memory accompanied by recall during encoding and retrieval: an fMRI study. *Neuroimage,* 74**,** 195-208.

Pergola, G., Selvaggi, P., Trizio, S., Bertolino, A. & Blasi, G. 2015. The role of the thalamus in schizophrenia from a neuroimaging perspective. *Neuroscience & Biobehavioral Reviews,* 54**,** 57-75.

Pergola, G., Trizio, S., Di Carlo, P., Taurisano, P., Mancini, M., Amoroso, N., Nettis, M. A., Andriola, I., Caforio, G. & Popolizio, T. 2017. Grey matter volume patterns in thalamic nuclei are associated with familial risk for schizophrenia. *Schizophrenia Research,* 180**,** 13-20.

Perry, B. A. & Mitchell, A. S. 2019. Considering the evidence for anterior and laterodorsal thalamic nuclei as higher order relays to cortex. *Frontiers in Molecular Neuroscience,* 12**,** 167.

Petrenko, A. G., Ullrich, B., Missler, M., Krasnoperov, V., Rosahl, T. W. & Südhof, T. C. 1996. Structure and evolution of neurexophilin. *Journal of Neuroscience,* 16**,** 4360-4369.

Peukert, D., Weber, S., Lumsden, A. & Scholpp, S. 2011. Lhx2 and Lhx9 determine neuronal differentiation and compartition in the caudal forebrain by regulating Wnt signaling. *PLoS Biology,* 9**,** e1001218.

Pinault, D. 2004. The thalamic reticular nucleus: structure, function and concept. *Brain Research Reviews,* 46**,** 1-31.

Poels, E. M., Kegeles, L. S., Kantrowitz, J. T., Javitt, D. C., Lieberman, J. A., Abi-Dargham, A. & Girgis, R. R. 2014. Glutamatergic abnormalities in schizophrenia: a review of proton MRS findings. *Schizophrenia Research,* 152**,** 325-332.

Polioudakis, D., de la Torre-Ubieta, L., Langerman, J., Elkins, A. G., Shi, X., Stein, J. L., Vuong, C. K., Nichterwitz, S., Gevorgian, M. & Opland, C. K. 2019. A single-cell transcriptomic atlas of human neocortical development during mid-gestation. *Neuron,* 103**,** 785-801. e8.

Pöllänen, P. M., Härkönen, T., Ilonen, J., Toppari, J., Veijola, R., Siljander, H. & Knip, M. 2022. Autoantibodies to N-terminally truncated GAD65 (96-585): HLA associations and predictive value for type 1 diabetes. *The Journal of Clinical Endocrinology & Metabolism,* 107**,** e935-e946.

Popken, G., Leggio, M., Bunney Jr, W. & Jones, E. 2002. Expression of mRNAs related to the GABAergic and glutamatergic neurotransmitter systems in the human thalamus: normal and schizophrenic. *Thalamus & Related Systems,* 1**,** 349-369.

Pratt, T., Quinn, J. C., Simpson, T. I., West, J. D., Mason, J. O. & Price, D. J. 2002. Disruption of early events in thalamocortical tract formation in mice lacking the transcription factors Pax6 or Foxg1. *Journal of Neuroscience,* 22**,** 8523-8531.

Pratt, T., Vitalis, T., Warren, N., Edgar, J. M., Mason, J. O. & Price, D. J. 2000. A role for Pax6 in the normal development of dorsal thalamus and its cortical connections. *Development,* 127**,** 5167-5178.

Puelles, E., Acampora, D., Gogoi, R., Tuorto, F., Papalia, A., Guillemot, F., Ang, S.-L. & Simeone, A. 2006. Otx2 controls identity and fate of glutamatergic progenitors of the thalamus by repressing GABAergic differentiation. *Journal of Neuroscience,* 26**,** 5955-5964.

Puelles, E., Acampora, D., Lacroix, E., Signore, M., Annino, A., Tuorto, F., Filosa, S., Corte, G., Wurst, W. & Ang, S.-L. 2003. Otx dose-dependent integrated control of antero-posterior and dorso-ventral patterning of midbrain. *Nature Neuroscience,* 6**,** 453-460.

Puelles, E., Martínez-de-la-Torre, M., Watson, C. & Puelles, L. 2012a. Midbrain. *The Mouse Nervous System.* Elsevier.

Puelles, L. 2001. Thoughts on the development, structure and evolution of the mammalian and avian telencephalic pallium. *Philosophical Transactions of the Royal Society of London. Series B: Biological Sciences,* 356**,** 1583-1598.

Puelles, L., Harrison, M., Paxinos, G. & Watson, C. 2013. A developmental ontology for the mammalian brain based on the prosomeric model. *Trends in Neurosciences,* 36**,** 570-578.

Puelles, L., Kuwana, E., Puelles, E., Bulfone, A., Shimamura, K., Keleher, J., Smiga, S. & Rubenstein, J. L. 2000. Pallial and subpallial derivatives in the embryonic chick and mouse telencephalon, traced by the expression of the genes Dlx-2, Emx-1, Nkx-2.1, Pax-6, and Tbr-1. *Journal of Comparative Neurology,* 424**,** 409-438.

Puelles, L., Martinez-de-la-Torre, M., Ferran, J.-L. & Watson, C. 2012b. Diencephalon. *The Mouse Nervous System.* Elsevier.

Puelles, L. & Rubenstein, J. L. 1993. Expression patterns of homeobox and other putative regulatory genes in the embryonic mouse forebrain suggest a neuromeric organization. *Trends in Neurosciences,* 16**,** 472-479.

Puelles, L. & Rubenstein, J. L. 2003. Forebrain gene expression domains and the evolving prosomeric model. *Trends in Neurosciences,* 26**,** 469-476.

Puschel, A. & Betz, H. 1995. Neurexins are differentially expressed in the embryonic nervous system of mice. *Journal of Neuroscience,* 15**,** 2849-2856.

Qinlin, F., Bingqiao, W., Linlin, H., Peixia, S., Lexing, X., Lijun, Y. & Qingwu, Y. 2022. miR-129-5p targets FEZ1/SCOC/ULK1/NBR1 complex to restore neuronal function in mice with post-stroke depression. *Bioengineered,* 13**,** 9708-9728.

Qiu, Y., Cooney, A. J., Kuratani, S., DeMayo, F. J., Tsai, S. Y. & Tsai, M.-J. 1994. Spatiotemporal expression patterns of chicken ovalbumin upstream promoter-transcription factors in the developing mouse central nervous system: evidence for a role in segmental patterning of the diencephalon. *Proceedings of the National Academy of Sciences,* 91**,** 4451-4455.

Qu, Y., Lim, J. J.-Y., An, O., Yang, H., Toh, Y.-C. & Chua, J. J. E. 2023. FEZ1 participates in human embryonic brain development by modulating neuronal progenitor subpopulation specification and migrations. *Iscience,* 26.

Quinlan, R., Graf, M., Mason, I., Lumsden, A. & Kiecker, C. 2009. Complex and dynamic patterns of Wnt pathway gene expression in the developing chick forebrain. *Neural Development,* 4**,** 1-27.

Quinn, J. C., West, J. D. & Hill, R. E. 1996. Multiple functions for Pax6 in mouse eye and nasal development. *Genes & Development,* 10**,** 435-446.

Quintana-Urzainqui, I., Hernandez-Malmierca, P., Clegg, J. M., Li, Z., Kozić, Z. & Price, D. J. 2020. The role of the diencephalon in the guidance of thalamocortical axons in mice. *Development,* 147**,** dev184523.

Radonjić, N. V., Ayoub, A. E., Memi, F., Yu, X., Maroof, A., Jakovcevski, I., Anderson, S. A., Rakic, P. & Zecevic, N. 2014. Diversity of cortical interneurons in primates: the role of the dorsal proliferative niche. *Cell Reports,* 9**,** 2139-2151.

Rakic, P., Ayoub, A. E., Breunig, J. J. & Dominguez, M. H. 2009. Decision by division: making cortical maps. *Trends in Neurosciences,* 32**,** 291-301.

Rakic, P. & Sidman, R. L. 1968. Supravital DNA synthesis in the developing human and mouse brain. *Journal of Neuropathology & Experimental Neurology,* 27**,** 240-276.

Rakić, P. & Sidman, R. L. 1969. Telencephalic origin of pulvinar neurons in the fetal human brain. *Zeitschrift für Anatomie und Entwicklungsgeschichte,* 129**,** 53-82.

Rath, M. F., Muñoz, E., Ganguly, S., Morin, F., Shi, Q., Klein, D. C. & Møller, M. 2006. Expression of the Otx2 homeobox gene in the developing mammalian brain: embryonic and adult expression in the pineal gland. *Journal of Neurochemistry,* 97**,** 556-566.

Razar, R. B. A., Qu, Y., Gunaseelan, S. & Chua, J. J. E. 2022. The importance of fasciculation and elongation protein zeta-1 in neural circuit establishment and neurological disorders. *Neural Regeneration Research,* 17**,** 1165-1171.

Redies, C., Hertel, N. & Hübner, C. A. 2012. Cadherins and neuropsychiatric disorders. *Brain Research,* 1470**,** 130-144.

Reichelt, A., Rodgers, R. & Clapcote, S. 2012. The role of neurexins in schizophrenia and autistic spectrum disorder. *Neuropharmacology,* 62**,** 1519-1526.

Reinchisi, G., Ijichi, K., Glidden, N., Jakovcevski, I. & Zecevic, N. 2012. COUP-TFII expressing interneurons in human fetal forebrain. *Cerebral Cortex,* 22**,** 2820-2830.

Reissner, C., Runkel, F. & Missler, M. 2013. Neurexins. *Genome Biology,* 14**,** 1-15.

Rodrigo-Angulo, M. L., Heredero, S., Rodríguez-Veiga, E. & Reinoso-Suárez, F. 2008. GABAergic and non-GABAergic thalamic, hypothalamic and basal forebrain projections to the ventral oral pontine reticular nucleus: their implication in REM sleep modulation. *Brain Research,* 1210**,** 116-125.

Ross, S. E., Greenberg, M. E. & Stiles, C. D. 2003. Basic helix-loop-helix factors in cortical development. *Neuron,* 39**,** 13-25.

Rowen, L., Young, J., Birditt, B., Kaur, A., Madan, A., Philipps, D. L., Qin, S., Minx, P., Wilson, R. K. & Hood, L. 2002. Analysis of the human neurexin genes: alternative splicing and the generation of protein diversity. *Genomics,* 79**,** 587-597.

Rujescu, D., Ingason, A., Cichon, S., Pietiläinen, O. P., Barnes, M. R., Toulopoulou, T., Picchioni, M., Vassos, E., Ettinger, U. & Bramon, E. 2009. Disruption of the neurexin 1 gene is associated with schizophrenia. *Human Molecular Genetics,* 18**,** 988-996.

Sadler, T. Embryology of neural tube development. American Journal of Medical Genetics Part C: Seminars in Medical Genetics, 2005. Wiley Online Library, 2-8.

Sakae, N., Yamasaki, N., Kitaichi, K., Fukuda, T., Yamada, M., Yoshikawa, H., Hiranita, T., Tatsumi, Y., Kira, J.-i. & Yamamoto, T. 2008. Mice lacking the schizophrenia-associated protein FEZ1 manifest hyperactivity and enhanced responsiveness to psychostimulants. *Human Molecular Genetics,* 17**,** 3191-3203.

Sakamoto, T. & Yashima, J. 2022. Prefrontal cortex is necessary for long-term social recognition memory in mice. *Behavioural Brain Research,* 435**,** 114051.

Santana-Bejarano, M. B., Grosso-Martínez, P. R., Puebla-Mora, A. G., Martínez-Silva, M. G., Nava-Villalba, M., Márquez-Aguirre, A. L., Ortuño-Sahagún, D. & Godínez-Rubí, M. 2023. Pleiotrophin and the Expression of Its Receptors during Development of the Human Cerebellar Cortex. *Cells,* 12**,** 1733.

Schaaf, C. P., Boone, P. M., Sampath, S., Williams, C., Bader, P. I., Mueller, J. M., Shchelochkov, O. A., Brown, C. W., Crawford, H. P. & Phalen, J. A. 2012. Phenotypic spectrum and genotype–phenotype correlations of NRXN1 exon deletions. *European Journal of Human Genetics,* 20**,** 1240-1247.

Schmahl, W., Knoedlseder, M., Favor, J. & Davidson, D. 1993. Defects of neuronal migration and the pathogenesis of cortical malformations are associated with Small eye (Sey) in the mouse, a point mutation at the Pax-6-locus. *Acta Neuropathologica,* 86**,** 126-135.

Schmitz, M. T., Sandoval, K., Chen, C. P., Mostajo-Radji, M. A., Seeley, W. W., Nowakowski, T. J., Ye, C. J., Paredes, M. F. & Pollen, A. A. 2022. The development and evolution of inhibitory neurons in primate cerebrum. *Nature,* 603**,** 871-877.

Schoenwolf, G. C. 2021. *Larsen's human embryology*, Philadelphia, PA : Elsevier.

Schoenwolf, G. C., Bleyl, S. B., Brauer, P. R. & Francis-West, P. H. 2014. *Larsen's human embryology*, Elsevier Health Sciences.

Schoenwolf, G. C., Bleyl, S. B., Brauer, P. R. & Francis-West, P. H. 2020. *Larsen's Human Embryology E-Book: Larsen's Human Embryology E-Book*, Elsevier Health Sciences.

Scholpp, S., Foucher, I., Staudt, N., Peukert, D., Lumsden, A. & Houart, C. 2007. Otx1l, Otx2 and Irx1b establish and position the ZLI in the diencephalon.

Schonk, D., Kuijpers, H., Van Drunen, E., Van Dalen, C., Geurts van Kessel, A., Verheijen, R. & Ramaekers, F. 1989. Assignment of the gene (s) involved in the expression of the proliferation-related Ki-67 antigen to human chromosome 10. *Human Genetics,* 83**,** 297-299.

Schreiner, D., Nguyen, T.-M., Russo, G., Heber, S., Patrignani, A., Ahrné, E. & Scheiffele, P. 2014. Targeted combinatorial alternative splicing generates brain region-specific repertoires of neurexins. *Neuron,* 84**,** 386-398.

Schuurmans, C. & Guillemot, F. 2002. Molecular mechanisms underlying cell fate specification in the developing telencephalon. *Current opinion in neurobiology,* 12**,** 26-34.

Sebastian, R., Jin, K., Pavon, N., Bansal, R., Potter, A., Song, Y., Babu, J., Gabriel, R., Sun, Y. & Aronow, B. 2023. Schizophrenia-associated NRXN1 deletions induce

developmental-timing-and cell-type-specific vulnerabilities in human brain organoids. *Nature Communications,* 14**,** 3770.

Serra, L. 2020. Role of the Sox2 and COUP-TF1 transcription factors in the development of the visual system by conditional knock-out in mouse.

Shen, X.-y., Shi, S.-h., Li, H., Wang, C.-c., Zhang, Y., Yu, H., Li, Y.-b. & Liu, B. 2022. The role of Gadd45b in neurologic and neuropsychiatric disorders: An overview. *Frontiers in Molecular Neuroscience,* 15**,** 1021207.

Sherman, S. M. 2012. Thalamocortical interactions. *Current opinion in neurobiology,* 22**,** 575-579.

Sherman, S. M. 2016. Thalamus plays a central role in ongoing cortical functioning. *Nature Neuroscience,* 19**,** 533-541.

Sherman, S. M. & Guillery, R. 2002. The role of the thalamus in the flow of information to the cortex. *Philosophical Transactions of the Royal Society of London. Series B: Biological Sciences,* 357**,** 1695-1708.

Sherman, S. M. & Guillery, R. 2011. Distinct functions for direct and transthalamic corticocortical connections. *Journal of Neurophysiology,* 106**,** 1068-1077.

Sherman, S. M. & Guillery, R. W. 2006. *Exploring the thalamus and its role in cortical function*, MIT press.

Shi, W., Xianyu, A., Han, Z., Tang, X., Li, Z., Zhong, H., Mao, T., Huang, K. & Shi, S.-H. 2017. Ontogenetic establishment of order-specific nuclear organization in the mammalian thalamus. *Nature Neuroscience,* 20**,** 516-528.

Shohayeb, B. & Cooper, H. M. 2023. The ups and downs of Pax6 in neural stem cells. *Journal of Biological Chemistry,* 299.

Siddiqui, T. J., Pancaroglu, R., Kang, Y., Rooyakkers, A. & Craig, A. M. 2010. LRRTMs and neuroligins bind neurexins with a differential code to cooperate in glutamate synapse development. *Journal of Neuroscience,* 30**,** 7495-7506.

Silva, A. P., Xapelli, S., Pinheiro, P. S., Ferreira, R., Lourenço, J., Cristóvão, A., Grouzmann, E., Cavadas, C., Oliveira, C. R. & Malva, J. O. 2005. Up-regulation of neuropeptide Y levels and modulation of glutamate release through neuropeptide Y receptors in the hippocampus of kainate-induced epileptic rats. *Journal of Neurochemistry,* 93**,** 163-170.

Simeone, A., Acampora, D., Gulisano, M., Stornaiuolo, A. & Boncinelli, E. 1992. Nested expression domains of four homeobox genes in developing rostral brain. *Nature,* 358**,** 687-690.

Simeone, A., Acampora, D., Mallamaci, A., Stornaiuolo, A., D'Apice, M. R., Nigro, V. & Boncinelli, E. 1993. A vertebrate gene related to orthodenticle contains a homeodomain of the bicoid class and demarcates anterior neuroectoderm in the gastrulating mouse embryo. *The EMBO Journal,* 12**,** 2735-2747.

Simeone, A., Puelles, E. & Acampora, D. 2002. The otx family. *Current Opinion in Genetics & Development,* 12**,** 409-415.

Simpson, T. I. & Price, D. J. 2002. Pax6; a pleiotropic player in development. *Bioessays,* 24**,** 1041-1051.

Skiba, A., Talarowska, M., Szemraj, J. & Gałecki, P. 2021. Is NRXN1 Gene Expression an Important Marker of Treatment of Depressive Disorders? A Pilot Study. *Journal of Personalized Medicine,* 11**,** 637.

Smitha Karavallil Achuthan, D. S., Paula Argueta, Caroline Vanderburgh, Haley B. Holm, Rajesh K. Kana 2023. Thalamic functional connectivity and sensorimotor processing in neurodevelopmental disorders. *Frontiers in Neuroscience,* 17.

Smoak, E. M., Stein, P., Schultz, R. M., Lampson, M. A. & Black, B. E. 2016. Long-term retention of CENP-A nucleosomes in mammalian oocytes underpins transgenerational inheritance of centromere identity. *Current Biology,* 26**,** 1110-1116.

SOLO. 2024. *Map database* [Online]. Available: http://solo.bmap.ucla.edu/shiny/webapp/ [Accessed].

Stafford, P., Mitra, S., Debot, M., Lutz, P., Stem, A., Hadley, J., Hom, P., Schaid, T. R. & Cohen, M. J. 2022. Astrocytes and pericytes attenuate severely injured patient plasma mediated expression of tight junction proteins in endothelial cells. *Plos One,* 17**,** e0270817.

Stenman, J., Toresson, H. & Campbell, K. 2003. Identification of two distinct progenitor populations in the lateral ganglionic eminence: implications for striatal and olfactory bulb neurogenesis. *Journal of Neuroscience,* 23**,** 167-174.

Stiles, J. 2008. *The fundamentals of brain development: Integrating nature and nurture*, Harvard University Press.

Stiles, J. & Jernigan, T. L. 2010. The basics of brain development. *Neuropsychology Review,* 20**,** 327-348.

Stoykova, A., Fritsch, R., Walther, C. & Gruss, P. 1996. Forebrain patterning defects in Small eye mutant mice. *Development,* 122**,** 3453-3465.

Südhof, T. C. 2008. Neuroligins and neurexins link synaptic function to cognitive disease. *Nature,* 455**,** 903-911.

Sultan, F. A. & Sweatt, J. D. 2013. The role of the Gadd45 family in the nervous system: a focus on neurodevelopment, neuronal injury, and cognitive neuroepigenetics. *Gadd45 Stress Sensor Genes***,** 81-119.

Sun, C., Cheng, M.-C., Qin, R., Liao, D.-L., Chen, T.-T., Koong, F.-J., Chen, G. & Chen, C.-H. 2011. Identification and functional characterization of rare mutations of the neuroligin-2 gene (NLGN2) associated with schizophrenia. *Human Molecular Genetics,* 20**,** 3042-3051.

Sun, W., Cornwell, A., Li, J., Peng, S., Osorio, M. J., Aalling, N., Wang, S., Benraiss, A., Lou, N. & Goldman, S. A. 2017. SOX9 is an astrocyte-specific nuclear marker in the adult brain outside the neurogenic regions. *Journal of Neuroscience,* 37**,** 4493-4507.

Suzuki-Hirano, A., Ogawa, M., Kataoka, A., Yoshida, A. C., Itoh, D., Ueno, M., Blackshaw, S. & Shimogori, T. 2011. Dynamic spatiotemporal gene expression in embryonic mouse thalamus. *Journal of Comparative Neurology,* 519**,** 528-543.

Szu, J., Wojcinski, A., Jiang, P. & Kesari, S. 2021. Impact of the Olig family on neurodevelopmental disorders. *Frontiers in Neuroscience,* 15**,** 659601.

Takebayashi, H., Ohtsuki, T., Uchida, T., Kawamoto, S., Okubo, K., Ikenaka, K., Takeichi, M., Chisaka, O. & Nabeshima, Y.-i. 2002. Non-overlapping expression of Olig3 and Olig2 in the embryonic neural tube. *Mechanisms of Development,* 113**,** 169-174.

Takebayashi, H., Yoshida, S., Sugimori, M., Kosako, H., Kominami, R., Nakafuku, M. & Nabeshima, Y.-i. 2000. Dynamic expression of basic helix-loop-helix Olig family members: implication of Olig2 in neuron and oligodendrocyte differentiation and identification of a new member, Olig3. *Mechanisms of Development,* 99**,** 143-148.

Tang, J., Fan, Y., Li, H., Xiang, Q., Zhang, D.-F., Li, Z., He, Y., Liao, Y., Wang, Y. & He, F. 2017. Whole-genome sequencing of monozygotic twins discordant for schizophrenia indicates multiple genetic risk factors for schizophrenia. *Journal of Genetics and Genomics,* 44**,** 295-306.

Tao, W. & Lai, E. 1992. Telencephalon-restricted expression of BF-1, a new member of the HNF-3/fork head gene family, in the developing rat brain. *Neuron,* 8**,** 957-966.

Tatemoto, K., Carlquist, M. & Mutt, V. 1982. Neuropeptide Y—a novel brain peptide with structural similarities to peptide YY and pancreatic polypeptide. *Nature,* 296**,** 659-660.

Tavazzani, E., Tritto, S., Spaiardi, P., Botta, L., Manca, M., Prigioni, I., Masetto, S. & Russo, G. 2014. Glutamic acid decarboxylase 67 expression by a distinct population of mouse vestibular supporting cells. *Frontiers in Cellular Neuroscience,* 8**,** 428.

Taverna, E. & Huttner, W. B. 2010. Neural progenitor nuclei IN motion. *Neuron,* 67**,** 906-914.

Teixeira, M. B., Alborghetti, M. R. & Kobarg, J. 2019. Fasciculation and elongation zeta proteins 1 and 2: From structural flexibility to functional diversity. *World Journal of Biological Chemistry,* 10**,** 28.

Tekki-Kessaris, N., Woodruff, R., Hall, A. C., Gaffield, W., Kimura, S., Stiles, C. D., Rowitch, D. H. & Richardson, W. D. 2001. Hedgehog-dependent oligodendrocyte lineage specification in the telencephalon.

Thakurela, S., Tiwari, N., Schick, S., Garding, A., Ivanek, R., Berninger, B. & Tiwari, V. K. 2016. Mapping gene regulatory circuitry of Pax6 during neurogenesis. *Cell Discovery,* 2**,** 1-22.

Tian, N., Petersen, C., Kash, S., Baekkeskov, S., Copenhagen, D. & Nicoll, R. 1999. The role of the synthetic enzyme GAD65 in the control of neuronal γ-aminobutyric acid release. *Proceedings of the National Academy of Sciences,* 96**,** 12911-12916.

Toda, H., Mochizuki, H., Flores, R., Josowitz, R., Krasieva, T. B., LaMorte, V. J., Suzuki, E., Gindhart, J. G., Furukubo-Tokunaga, K. & Tomoda, T. 2008. UNC-51/ATG1 kinase regulates axonal transport by mediating motor–cargo assembly. *Genes & Development,* 22**,** 3292-3307.

Tolosa, A., Sanjuán, J., Dagnall, A. M., Moltó, M. D., Herrero, N. & de Frutos, R. 2010. FOXP2 gene and language impairment in schizophrenia: association and epigenetic studies. *BMC Medical Genetics,* 11**,** 1-8.

Torres-Platas, S., Nagy, C., Wakid, M., Turecki, G. & Mechawar, N. 2016. Glial fibrillary acidic protein is differentially expressed across cortical and subcortical regions in healthy brains and downregulated in the thalamus and caudate nucleus of depressed suicides. *Molecular Psychiatry,* 21**,** 509-515.

Treichel, D., Schöck, F., Jäckle, H., Gruss, P. & Mansouri, A. 2003. mBtd is required to maintain signaling during murine limb development. *Genes & Development,* 17**,** 2630-2635.

Treutlein, B., Gokce, O., Quake, S. R. & Südhof, T. C. 2014. Cartography of neurexin alternative splicing mapped by single-molecule long-read mRNA sequencing. *Proceedings of the National Academy of Sciences,* 111**,** E1291-E1299.

Tripodi, M., Filosa, A., Armentano, M. & Studer, M. 2004. The COUP-TF nuclear receptors regulate cell migration in the mammalian basal forebrain.

Uchigashima, M., Konno, K., Demchak, E., Cheung, A., Watanabe, T., Keener, D. G., Abe, M., Le, T., Sakimura, K. & Sasaoka, T. 2020. Specific Neuroligin3–αNeurexin1 signaling regulates GABAergic synaptic function in mouse hippocampus. *Elife,* 9**,** e59545.

Ullrich, B., Ushkaryov, Y. A. & Südhof, T. C. 1995. Cartography of neurexins: more than 1000 isoforms generated by alternative splicing and expressed in distinct subsets of neurons. *Neuron,* 14**,** 497-507.

Ung, K., Huang, T.-W., Lozzi, B., Woo, J., Hanson, E., Pekarek, B., Tepe, B., Sardar, D., Cheng, Y.-T. & Liu, G. 2021. Olfactory bulb astrocytes mediate sensory circuit processing through Sox9 in the mouse brain. *Nature communications,* 12**,** 5230.

Urbina, F. L. & Gupton, S. L. 2020. SNARE-mediated exocytosis in neuronal development. *Frontiers in Molecular Neuroscience,* 13**,** 133.

Ushkaryov, Y. A., Petrenko, A. G., Geppert, M. & Südhof, T. C. 1992. Neurexins: synaptic cell surface proteins related to the α-latrotoxin receptor and laminin. *Science,* 257**,** 50-56.

Vachev, T., Stoyanova, V., Ivanov, H., Minkov, I. & Popov, N. 2015. Investigation of fasciculation and elongation protein ζ-1 (FEZ1) in peripheral blood reveals

differences in gene expression in patients with schizophrenia. *Balkan Journal of Medical Genetics,* 18**,** 31-38.

Van Der Werf, Y. D., Jolles, J., Witter, M. P. & Uylings, H. B. 2003. Contributions of thalamic nuclei to declarative memory functioning. *Cortex,* 39**,** 1047-1062.

Van der Werf, Y. D., Witter, M. P. & Groenewegen, H. J. 2002. The intralaminar and midline nuclei of the thalamus. Anatomical and functional evidence for participation in processes of arousal and awareness. *Brain Research Reviews,* 39**,** 107-140.

Vargha-Khadem, F., Gadian, D. G., Copp, A. & Mishkin, M. 2005. FOXP2 and the neuroanatomy of speech and language. *Nature Reviews Neuroscience,* 6**,** 131-138.

Vathipadiekal, V., Alsultan, A., Baltrusaitis, K., Farrell, J. J., Al-Rubaish, A. M., Al-Muhanna, F., Naserullah, Z., Alsuliman, A., Patra, P. & Milton, J. N. 2016. Homozygosity for a haplotype in the HBG2-OR51B4 region is exclusive to Arab-Indian haplotype sickle cell anemia. *American Journal of Hematology,* 91**,** E308.

Vernes, S. C., Spiteri, E., Nicod, J., Groszer, M., Taylor, J. M., Davies, K. E., Geschwind, D. H. & Fisher, S. E. 2007. High-throughput analysis of promoter occupancy reveals direct neural targets of FOXP2, a gene mutated in speech and language disorders. *The American Journal of Human Genetics,* 81**,** 1232-1250.

Vertes, R. P., Linley, S. B. & Hoover, W. B. 2015. Limbic circuitry of the midline thalamus. *Neuroscience & Biobehavioral Reviews,* 54**,** 89-107.

Vieira, C., Garda, A.-L., Shimamura, K. & Martinez, S. 2005. Thalamic development induced by Shh in the chick embryo. *Developmental Biology,* 284**,** 351-363.

Viñas-Jornet, M., Esteba-Castillo, S., Gabau, E., Ribas-Vidal, N., Baena, N., San, J., Ruiz, A., Coll, M. D., Novell, R. & Guitart, M. 2014. A common cognitive, psychiatric, and dysmorphic phenotype in carriers of NRXN1 deletion. *Molecular Genetics & Genomic Medicine,* 2**,** 512-521.

Vinod Jangir Kumar, E. v. O., Klaus Scheffler, Christian F. Bechmann, Wolfgang Grodd 2017. Functional anatomy of the human thalamus at rest. *NeuroImage,* 147**,** 678-691.

Vogel, J. K. & Wegner, M. 2021. Sox9 in the developing central nervous system: a jack of all trades? *Neural Regeneration Research,* 16**,** 676.

Voigt, T. 1989. Development of glial cells in the cerebral wall of ferrets: direct tracing of their transformation from radial glia into astrocytes. *Journal of Comparative Neurology,* 289**,** 74-88.

Vue, T. Y., Aaker, J., Taniguchi, A., Kazemzadeh, C., Skidmore, J. M., Martin, D. M., Martin, J. F., Treier, M. & Nakagawa, Y. 2007. Characterization of progenitor domains in the developing mouse thalamus. *Journal of Comparative Neurology,* 505**,** 73-91.

Vue, T. Y., Bluske, K., Alishahi, A., Yang, L. L., Koyano-Nakagawa, N., Novitch, B. & Nakagawa, Y. 2009. Sonic hedgehog signaling controls thalamic progenitor identity and nuclei specification in mice. *Journal of Neuroscience,* 29**,** 4484-4497.

Vue, T. Y., Kollipara, R. K., Borromeo, M. D., Smith, T., Mashimo, T., Burns, D. K., Bachoo, R. M. & Johnson, J. E. 2020. ASCL1 regulates neurodevelopmental transcription factors and cell cycle genes in brain tumors of glioma mouse models. *Glia,* 68**,** 2613-2630.

Vuong, C. K., Black, D. L. & Zheng, S. 2016. The neurogenetics of alternative splicing. *Nature Reviews Neuroscience,* 17**,** 265-281.

Waclaw, R. R., Allen, Z. J., Bell, S. M., Erdélyi, F., Szabó, G., Potter, S. S. & Campbell, K. 2006. The zinc finger transcription factor Sp8 regulates the generation and diversity of olfactory bulb interneurons. *Neuron,* 49**,** 503-516.

Walther, C. & Gruss, P. 1991. Pax-6, a murine paired box gene, is expressed in the developing CNS. *Development,* 113**,** 1435-1449.

Wang, H.-L. S., Rau, C.-L., Li, Y.-M., Chen, Y.-P. & Yu, R. 2015. Disrupted thalamic resting-state functional networks in schizophrenia. *Frontiers in behavioral Neuroscience,* 9**,** 45.

Wang, H., Xu, L., Lai, C., Hou, K., Chen, J., Guo, Y., Sambangi, A., Swaminathan, S., Xie, C. & Wu, Z. 2021. Region-specific distribution of Olig2-expressing astrocytes in adult mouse brain and spinal cord. *Molecular Brain,* 14**,** 1-14.

Wang, L., Bluske, K. K., Dickel, L. K. & Nakagawa, Y. 2011. Basal progenitor cells in the embryonic mouse thalamus-their molecular characterization and the role of neurogenins and Pax6. *Neural Development,* 6**,** 1-19.

Wang, P., Hu, Y., Qu, P., Zhao, Y., Liu, J., Zhao, J. & Kong, B. 2020. PTPRZ1 inhibits the cisplatin resistance of ovarian cancer by regulating PI3K/AKT/mTOR signal pathway.

Wang, W. Z., Hoerder-Suabedissen, A., Oeschger, F. M., Bayatti, N., Ip, B. K., Lindsay, S., Supramaniam, V., Srinivasan, L., Rutherford, M. & Møllgård, K. 2010. Subplate in the developing cortex of mouse and human. *Journal of Anatomy,* 217**,** 368-380.

Wang, X., Lai, M., Wang, Y., Chai, R., Li, N., Ou, L., Zheng, K., Li, J., Xu, G., Wang, S., Dong, Y. & Wang, S. 2022. Upregulation of Centromere Proteins as Potential Biomarkers for Esophageal Squamous Cell Carcinoma Diagnosis and Prognosis. *Biomed Res Int,* 2022**,** 3758731.

Warren, A. E., Abbott, D. F., Jackson, G. D. & Archer, J. S. 2017. Thalamocortical functional connectivity in Lennox–Gastaut syndrome is abnormally enhanced in executive-control and default-mode networks. *Epilepsia,* 58**,** 2085-2097.

Warren, R. A., Agmon, A. & Jones, E. G. 1994. Oscillatory synaptic interactions between ventroposterior and reticular neurons in mouse thalamus in vitro. *Journal of Neurophysiology,* 72**,** 1993-2003.

Whittington, M. A. & Traub, R. D. 2003. Interneuron diversity series: inhibitory interneurons and network oscillations in vitro. *Trends in Neurosciences,* 26**,** 676-682.

Wilke, M. & Kagan, I. 2024. VISUOSPATIAL AND MOTOR DEFICITS FOLLO WING PULVINAR LESIONS.

Wilkinson, G., Dennis, D. & Schuurmans, C. 2013. Proneural genes in neocortical development. *Neuroscience,* 253**,** 256-273.

Williams, S. M., An, J. Y., Edson, J., Watts, M., Murigneux, V., Whitehouse, A. J., Jackson, C. J., Bellgrove, M. A., Cristino, A. S. & Claudianos, C. 2019. An integrative analysis of non-coding regulatory DNA variations associated with autism spectrum disorder. *Molecular Psychiatry,* 24**,** 1707-1719.

Wonders, C. P. & Anderson, S. A. 2006. The origin and specification of cortical interneurons. *Nature Reviews Neuroscience,* 7**,** 687-696.

Woodward, N. D. & Heckers, S. 2016. Mapping thalamocortical functional connectivity in chronic and early stages of psychotic disorders. *Biological Psychiatry,* 79**,** 1016-1025.

Workman, A. D., Charvet, C. J., Clancy, B., Darlington, R. B. & Finlay, B. L. 2013. Modeling transformations of neurodevelopmental sequences across mammalian species. *Journal of Neuroscience,* 33**,** 7368-7383.

Wu, D., Zhu, J., You, L., Wang, J., Zhang, S., Liu, Z., Xu, Q., Yuan, X., Yang, L. & Wang, W. 2023. NRXN1 depletion in the medial prefrontal cortex induces anxiety-like behaviors and abnormal social phenotypes along with impaired neurite outgrowth in rat. *Journal of Neurodevelopmental Disorders,* 15**,** 6.

Wulandari, R. D., Lyrawati, D., Fatchiyah, F. & Fitri, L. E. 2020. Thalassemia major and intermedia patients in East Java do not show fetal hemoglobin level difference in relation to XMNI polymorphism. *Medical Archives,* 74**,** 90.

Xu, H., Lin, S., Zhou, Z., Li, D., Zhang, X., Yu, M., Zhao, R., Wang, Y., Qian, J., Li, X., Li, B., Wei, C., Chen, K., Yoshimura, T., Wang, J. M. & Huang, J. 2023. New genetic and epigenetic insights into the chemokine system: the latest discoveries aiding progression toward precision medicine. *Cellular & Molecular Immunology,* 20**,** 739-776.

Yamada, K., Nakamura, K., Minabe, Y., Iwayama-Shigeno, Y., Takao, H., Toyota, T., Hattori, E., Takei, N., Sekine, Y. & Suzuki, K. 2004. Association analysis of FEZ1 variants with schizophrenia in Japanese cohorts. *Biological Psychiatry,* 56**,** 683-690.

Yan, Q., Weyn-Vanhentenryck, S. M., Wu, J., Sloan, S. A., Zhang, Y., Chen, K., Wu, J. Q., Barres, B. A. & Zhang, C. 2015. Systematic discovery of regulated and conserved alternative exons in the mammalian brain reveals NMD modulating chromatin regulators. *Proceedings of the National Academy of Sciences,* 112**,** 3445-3450.

Yeh, C. Y., Wu, K. Y., Huang, G. J. & Verkhratsky, A. 2023. Radial stem astrocytes (aka neural stem cells): identity, development, physio-pathology, and therapeutic potential. *Acta Physiologica,* 238**,** e13967.

Zecevic, N. & Rakic, P. 2001. Development of layer I neurons in the primate cerebral cortex. *Journal of Neuroscience,* 21**,** 5607-5619.

Zembrzycki, A., Griesel, G., Stoykova, A. & Mansouri, A. 2007. Genetic interplay between the transcription factors Sp8 and Emx2 in the patterning of the forebrain. *Neural Development,* 2**,** 1-18.

Zhang, C., Atasoy, D., Araç, D., Yang, X., Fucillo, M. V., Robison, A. J., Ko, J., Brunger, A. T. & Südhof, T. C. 2010. Neurexins physically and functionally interact with GABAA receptors. *Neuron,* 66**,** 403-416.

Zhang, L., Hernández, V. S., Zetter, M. A. & Eiden, L. E. 2020. VGLUT-VGAT expression delineates functionally specialised populations of vasopressin-containing neurones including a glutamatergic perforant path-projecting cell group to the hippocampus in rat and mouse brain. *Journal of Neuroendocrinology,* 32**,** e12831.

Zhang, P., Lu, H., Peixoto, R. T., Pines, M. K., Ge, Y., Oku, S., Siddiqui, T. J., Xie, Y., Wu, W. & Archer-Hartmann, S. 2018. Heparan sulfate organizes neuronal synapses through neurexin partnerships. *Cell,* 174**,** 1450-1464. e23.

Zhang, X., Li, Y., Hu, P., Xu, L. & Qiu, H. 2022. KIF2C is a Biomarker Correlated With Prognosis and Immunosuppressive Microenvironment in Human Tumors. *Frontiers in Genetics,* 13**,** 891408.

Zhao, B. S., Roundtree, I. A. & He, C. 2017. Post-transcriptional gene regulation by mRNA modifications. *Nature reviews Molecular Cell Biology,* 18**,** 31-42.

Zheng, R., Du, Y., Wang, X., Liao, T., Zhang, Z., Wang, N., Li, X., Shen, Y., Shi, L. & Luo, J. 2022. KIF2C regulates synaptic plasticity and cognition in mice through dynamic microtubule depolymerization. *Elife,* 11**,** e72483.

Zhou, C.-J., Pinson, K. I. & Pleasure, S. J. 2004. Severe defects in dorsal thalamic development in low-density lipoprotein receptor-related protein-6 mutants. *Journal of Neuroscience,* 24**,** 7632-7639.

Zhou, C., Qiu, Y., Pereira, F. A., Crair, M. C., Tsai, S. Y. & Tsai, M.-J. 1999. The nuclear orphan receptor COUP-TFI is required for differentiation of subplate neurons and guidance of thalamocortical axons. *Neuron,* 24**,** 847-859.

Zoltan Molnar, G. J. C., Nenad Sestan, Ayman Alzu'bi, Trygve Bakken, Robert F. Hevner, Petra S. Huppi, Ivica Kostovi, Pasko Rakic, E. S. Anton, David Edwards, Patricia Garcez, Anna Hoerder-Suabedissen and Arnold Kriegstein 2019. New insights into the development of the humancerebral cortex. *Journal of Anatomy,* 235**,** 432-451.